U.PORTO

DOUTORAMENTO

PATOLOGIA E GENÉTICA MOLECULAR

Disclosing the role of *Helicobacter pylori* outer membrane vesicles in bacterial pathogenesis

Joana Melo

D

2021

Joana Melo . Disclosing the role of *Helicobacter pylori* outer membrane vesicles in bacterial pathogenesis

D.ICBAS **2021**

Disclosing the role of *Helicobacter pylori* outer membrane vesicles in bacterial pathogenesis

Joana Teixeira Pinto de Melo

INSTITUTO DE CIÊNCIAS BIOMÉDICAS ABEL SALAZAR
FACULDADE DE MEDICINA

Joana Teixeira Pinto de Melo

Disclosing the role of *Helicobacter pylori* outer membrane vesicles in bacterial pathogenesis

Tese de Candidatura ao grau de Doutor em
Patologia e Genética Molecular;
Programa Doutoral da Universidade do Porto
(Instituto de Ciências Biomédicas de Abel Salazar)

Orientador Maria do Céu Fontes Herdeiro Figueiredo
Professora Auxiliar
Faculdade de Medicina da Universidade do Porto (FMUP), Instituto de Patologia e Imunologia Molecular da Universidade do Porto (IPATIMUP) e Instituto de Investigação e Inovação em Saúde, Universidade do Porto (i3S)

Co-orientador Carla Marina Gonçalves Leite
Investigadora Júnior
Instituto de Patologia e Imunologia Molecular da Universidade do Porto (IPATIMUP) e Instituto de Investigação e Inovação em Saúde, Universidade do Porto (i3S)

FINANCIAL SUPPORT

This PhD Thesis was financially supported with a PhD fellowship from Fundação para a Ciência e Tecnologia (FCT; SFRH/BD/116965/2016). This work was supported by Norte Portugal Regional Program (NORTE 2020), under the PORTUGAL 2020 Partnership Agreement, through the European Regional Development Fund (ERDF) (NORTE-01-0145-FEDER-000029).

LIST OF PUBLICATIONS

Ao abrigo do disposto do nº 2, alínea a) do artigo 31° do Decreto-Lei n.° 115/2013 de 7 de Agosto, faz parte integrante desta tese de doutoramento o seguinte trabalho já publicado:

Melo J, Pinto V, Fernandes T, Malheiro AR, Osório H, Figueiredo C, Leite M. Isolation Method and Characterization of Outer Membranes Vesicles of *Helicobacter pylori* Grown in a Chemically Defined Medium. Frontiers in Microbiology 12: 654193, 2021. doi: 10.3389/fmicb.2021.654193.

Outras publicações que não fazem parte integrante desta dissertação, mas foram desenvolvidas durante o período do programa doutoral:

1. Marques MS, **Melo J,** Cavadas B, Mendes N, Pereira L, Carneiro F, Figueiredo C, Leite M. Afadin Downregulation by Helicobacter pylori Induces Epithelial to Mesenchymal Transition in Gastric Cells. Frontiers in Microbiology 2 9:2712, 2018. doi: 10.3389/fmicb.2018.02712.

2. Leite M, Marques MS, **Melo J,** Pinto MT, Cavadas B, Aroso M, Gomez-Lazaro M, Seruca R, Figueiredo C. Helicobacter Pylori Targets the EPHA2 Receptor Tyrosine Kinase in Gastric Cells Modulating Key Cellular Functions. Cells 9(2):513, 2020. doi: 10.3390/cells9020513.

3. Cavadas B, Leite M, Pedro N, Magalhães AC, **Melo J,** Correia M, Máximo V, Camacho R, Fonseca NA, Figueiredo C, Pereira L. Shedding Light on the African Enigma: In Vitro Testing of Homo sapiens-Helicobacter pylori Coevolution. Microorganisms 9(2): 240, 2021. doi: 10.3390/microorganisms9020240.

ACKNOWLEDGEMENTS

Por várias vezes (até demais!) pensei “mas porque é que me meti nisto?!”. E a verdade é que, por mais difíceis e desafiantes que tenham sido estes 5 anos, foram sem dúvida únicos e de muitas conquistas. E esta tese é o culminar de todo este percurso, que, só existe, devido à confiança que depositaram em mim. A todos os que estiveram ao meu lado e me ensinaram algo, e também aos que se cruzaram comigo, um muito obrigada por tornarem tudo mais fácil e memorável. Sem vocês, não teria sido possível!

À minha orientadora Céu, muito obrigada pela oportunidade de fazer parte deste grupo, que tanto cresceu desde que aqui cheguei. Obrigada pela preocupação e pela ajuda, que nunca faltou quando eu precisei. Foi um enorme prazer partilhar esta jornada consigo! Muito obrigada!

À minha co-orientadora Marina, faltam-me as palavras para agradecer tudo o que fizeste por mim… Saiu-me a sorte grande quando te conheci! Foste como uma mãe na loucura que foram estes anos, sempre preocupada e sempre presente. Obrigada por tudo!!!

Ao meu Miguel, um obrigada do tamanho do mundo!! Nem te consigo explicar e agradecer o muito que fizeste, e ainda fazes, por mim. Foste a minha bóia de salvação ao longo destes anos, e o meu cusco preferido, e eu não te podia estar mais agradecida. Continuas a ser a primeira pessoa em quem penso quando quero contar as novidades, if you know what I mean... Obrigada Miguelito :,)

A todos os que passaram pelo grupo da Céu (Cancer Genetics, EPiC e Microbes & Cancer). Um obrigada especial à Tânia e à Vanessa, que muito me ajudaram e apoiaram durante esta jornada. Obrigada meninas :) Patrícia, Joana Marques, Inês, Rui, Cristina, Joana Lima e Deiber, muito obrigada pelo vosso apoio e por todos os bons momentos que partilhámos, tanto no lab como fora. Aliás, devíamos repetir o lab-day out. O que dizem?

Às minha meninas Patrícia, Flávia, Joana, Melissa, Susana, Andreia, Mónica, Ana Margarida, Soraia e Minnie. Foram uns belos serões os que passamos à mesa!! Muito obrigada pelo vosso apoio, disponibilidade e, principalmente, pela vossa amizade. Não tenho palavras... Quer dizer, até tenho: quando repetimos um jantar em casa do Miguel?

À Raquel Seruca e a todo o grupo Cancer Genetics/EPiC, obrigada por me receberem tão bem e por fazerem do laboratório um lugar tão familiar.

À minha Sarocas, a minha Twin! És incrível, sabias? És um dos achados desta jornada. Isto porque és uma peça rara... Ahahah! Obrigada por todas as conversas, desabafos, abraços e sorrisos!

À minha Teresinha, muito muito obrigada por tudo. O teu apoio incondicional e a tua felicidade com os meus achievements deixam-me sem palavras <3 E já agora, quando repetimos o sushi? Prometo que, desta vez, não passámos pela 31 de Janeiro...

À minha Carlita, obrigada pela tua amizade e preocupação. Tenho muitas saudades de te encontrar todos os dias, sabias?

À minha Lau (do Porto, ahahah), obrigada pelas conversas de corredor, pelas cusquices e pela tua amizade!

Ao Bruno, o meu salvador da bioinformática! Nem sei como te agradecer a ajuda incansável, a paciência e os conselhos. Foste, e és, incrível. Obrigada!!!

Às minhas "maminhas" preferias, Babi, Ritinha e Tito, que são a personificação da alegria, no matter what. Obrigada pela sabedoria, pelos abraços, pelos risos, pelas palavras (nem sempre sábias, mas engraçadas), obrigada obrigada obrigada!

Às minha queridas Ana Dias e Peixoto, sem vocês não teria a mesma piada. Muito obrigada por serem um apoio constante! Por falar nisso, temos que marcar o almoço…

Às pessoas que dão abraços no corredor, mesmo em tempos de COVID, a Flávia e a minha Zézinha (ahahah). Meninas, obrigada pelo "colinho" e conforto que me dão sempre que vos vejo. Não imaginam o bem que me faz só de vos ver ao longe!!!

Ao Steeve, o meu companheiro das vesículas, obrigada por todo o brainstorming nos corredores e pela tua disponibilidade!!

Ao querido Nuno Mendes, obrigada pela boa disposição e disponibilidade constantes e por toda a tua amizade.

Às meninas do Molecular Parasitology, Margarida, Filipa e Teresa. Obrigada pela vossa animação e pelos dedinhos de conversa enquanto eu devia estar a escrever a tese. Foi um enorme prazer conhecer-vos!

Aos que me aturaram inúmeras vezes e cuja paciência nunca esgotou, Hugo Osório, Cecília, Rui Fernandes, Rita, Maria Azevedo, Mafalda, Catarina Meireles e Emília. Muito obrigada pela vossa ajuda! Grande parte desta tese deve-se a vocês!

À Zézinha, ao Sr Oliveira, ao Sr Mendes, ao Sr Carlos, à Diana, à Susana e à Alexandra, que me ajudaram sempre que precisei e animaram o meu dia vezes sem conta. Obrigada por tudo!!

Às minhas fofinhas Tânia, Lau, Dani e Ju, que estiveram sempre sempre lá. Obrigada por não se terem cansado de mim, mesmo quando eu não consegui estar presente. Obrigada pela vossa amizade de sempre!

À minha família, obrigada por me terem apoiado e tornado os nosso encontros sempre tão animados e reconfortantes!! Céu, Andréa, Tono, Eduarda e Clarinha, não seria o mesmo sem vocês, nem teria a mesma piada. Raquel, obrigada por todo o apoio que me deste ao longo destes anos e por te teres sido a minha irmã mais velha longe de casa.

Aos meus pais, nem sei como vos agradecer tudo o que fizeram por mim. Nos momentos bons e menos bons, nunca me falharam, principalmente nesta recta final. São o meu maior orgulho <3

Ao Diogo e ao Francisquinho, que animam todos os meus dias, que me enchem de mimos, abraços e beijinhos, e que me dão o melhor colinho que poderia pedir. Diogo, obrigada pela paciência (quase) infinita que tens tido, e por nunca me teres deixado desistir! Francisquinho, nem imaginas como vieste alegrar os meus dias. Tens sido o meu maior balãozinho de oxigénio. Obrigada meu amor!

A todos os que se cruzaram comigo e ajudaram a tornar este percurso memorável, obrigada do fundo do coração!

TABLE OF CONTENTS

INTRODUCTION

HELICOBACTER PYLORI

Helicobacter pylori was described and first isolated in 1982 by Robin Warren and Barry J. Marshall, two Australian researchers in pathology and gastroenterology, respectively. They detected the presence and cultured this Gram-negative bacterium from the stomach of patients with chronic gastritis and with peptic ulcer disease, publishing their observations in 1984 [1]. Their findings challenged the prevailing dogma that the stomach was sterile due to its high acidity. They also confronted the medical concept that ulcers were caused by stress and gastric acidity. More than two decades after their discovery and findings that *H. pylori* is etiologically related to such gastrointestinal disorders, Warren and Marshall were awarded with the Nobel Prize in Physiology or Medicine in 2005.

1. Epidemiology and transmission

H. pylori has been intimately associated with their human host populations for a long time [2]. Simulations indicate that *H. pylori* has spread from Africa approximately 58,000 years ago [2]. Even before the out-of-Africa event, humans may have been infected with *H. pylori* for 88,000-116,000 years [3]. *H. pylori* has co-evolved with humans and the geography of the *H. pylori* populations are a close reflection of the human migrations [4, 5].

In 2015, it was estimated that approximately 4.4 billion individuals were infected with this bacterium worldwide [6]. *H. pylori* is acquired during childhood and, unless treated, it establishes a life-long infection of the host gastric mucosa, representing the most common chronic infection in the world [6]. Despite the infection is present worldwide, the prevalence of *H. pylori* varies between regions. Africa (70%), South America (69%), and Western Asia (67%) present the highest *H. pylori* prevalences, whereas Oceania (24%), Western Europe (34%), and Northern America (37%) have the lowest prevalences [6]. A study conducted in 2013 reported an unsettling 84.2% prevalence of *H. pylori* infection in Portugal, representing one of the highest rates among European countries [7]. While in the past decades the prevalence of the infection has declined in industrialized countries, in developing and newly industrialized ones the prevalence of *H. pylori* has remained high, yet constant [6]. Such dissimilarities in the prevalence rates are related to the socioeconomic status and cultural background, as well as to social, dietary, and environmental factors [8].

The exact mechanisms of *H. pylori* transmission are still not fully understood. The human stomach is the solely recognized reservoir of the bacterium. It is accepted that the acquisition of the infection results from direct human-to-human contact or from environmental contamination [9]. Inter-individual transmission occurs within families, but can also occur between non-related individuals [10, 11]. The faeco-oral, oral-oral, and

gastro-oral routes have been suggested for transmission of *H. pylori* [12-14], and contamination of water and food have also been proposed [15, 16].

2. Colonization of the gastric epithelium

H. pylori is a spiral-shaped bacterium, measuring 2 to 4 µm in length and 0.5 to 1 µm in width, and having 2 to 6 unipolar flagella of approximately 3 µm in length (**Figure 1**) [17]. When faced with adverse environmental conditions, *H. pylori* modifies its morphology to a coccoid form and enters a reversible viable but non-culturable state, retaining its active virulence factors with minimal metabolic activity [18].

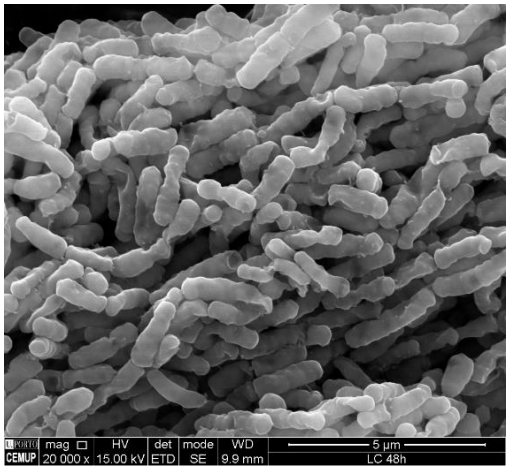

Figure 1. Scanning electron microscopy (SEM) micrograph of spiral-shaped *H. pylori* grown in F12-cholesterol liquid medium. Scale bar: 5 µm; 20,000x original magnification. [Melo J, unpublished].

H. pylori has a predilection for the gastric mucosa. In the stomach, *H. pylori* can be found within 25 µm of the epithelial surface. However, while the majority of them is free-swimming in the mucus layer, only 20% are adherent to gastric epithelial cells, localized at the cell surface, at the intercellular junctions, and on the basolateral side of epithelial cells [19, 20]. Some reports also detected *H. pylori* inside epithelial cells and underlying the epithelium lamina propria [20]. Outside the stomach, *H. pylori* has been identified in the duodenum of patients who had developed gastric metaplasia [21].

In order to survive to the gastric harsh environment characterized by an acidic lumen (pH 2), *H. pylori* developed several strategies. One important mechanism to protect itself from the highly acidic environment is the production of the urease enzyme, which hydrolyses urea into NH_3 and CO_2, establishing a neutral pH directly around the bacterium [22]. Urease enzyme constitutes up to 10% of total bacterial proteins and is fundamental for the successful colonization of the stomach, as urease-defective *H. pylori* mutants cannot colonize the gastric environment [23]. In addition to its role in acid neutralization, urease activity may also cause damage to the host cells through the production of ammonia, that

reacts with neutrophil metabolites to form carcinogenic agents, increasing the risk for the development of *H. pylori*-associated gastric malignancies [24].

Regardless of being able to survive for a brief period of time in an acidic pH, *H. pylori* is a neutralophilic bacterium and can only grow within a pH range of 5.5 to 8.0 [17]. To reach such a pH range, the bacterium has to move towards the gastric mucosa and pass through the mucus layer, a viscous gel layer that protects epithelial cells and preserves a near-neutral pH. Such movement is guided by chemotactic factors, which include urea, amino acids and metals as attractants, and is facilitated by the bacterial helical shape and flagellar motility [22]. As soon as *H. pylori* reaches the gastric epithelium, it is protected from discharge by peristaltic movements and mucus turnover, and can adhere to gastric cells [24].

Adhesion to the gastric epithelium is an essential step for *H. pylori* colonization and persistence, giving bacteria access to nutrients and the opportunity to deliver bacterial factors to host cells. The *H. pylori* genome encodes more than 30 outer membrane proteins (OMPs) that have been divided into Hop (*Helicobacter* OMPs) and Hor (hop-related proteins) subgroups [25]. BabA (blood group antigen-binding adhesion) and SabA (sialic acid-binding adhesion) are two of the best described Hop adhesion molecules. BabA, the first *H. pylori* adhesin discovered, mediates the binding of *H. pylori* to fucosylated Lewis^{b} (Le^{b}) blood group antigens and to terminal fucose residues on blood groups A, B, and O that are expressed on the gastric mucosa [26, 27]. This interaction enhances the type IV secretion system (T4SS)-dependent bacterial pathogenicity by triggering a proinflammatory cytokine response [28]. Analysis of clinical isolates from patients with gastric disorders revealed that expression of *babA* is associated with a higher risk of gastric cancer development [29]. BabA is of outmost importance in bacterial adherence during the early stages of infection. However, upon infection and with the increase of inflammation, there is an upregulation in the expression of sialyl-dimeric-Lewis^{x} glycosphingolipid by gastric cells, which is the receptor for the *H. pylori* SabA adhesin. In the inflamed gastric mucosa, the SabA adhesion plays a critical role in *H. pylori* adherence [30].

3. Clinical consequences of *H. pylori* infection

H. pylori persists throughout the lifespan of its human host and, though the majority of the infected individuals remain asymptomatic, infection causes chronic gastritis in all of them [17]. Upon infection, epithelial cells are the first to respond to *H. pylori*. After recognizing bacterial products via a number of pattern-recognition molecules (toll-like receptors – TLRs – and the intracellular nucleotide-binding oligomerization domain-containing protein 1 – NOD1), epithelial cells secrete cytokines and chemokines, including interleukin (IL)-8, IL-6,

tumor necrosis factor (TNF)-α, and CCL20 [31, 32]. These factors recruit neutrophils, dendritic cells, lymphocytes, and other immune cells to the infection site, which will produce more pro-inflammatory cytokines, as well as reactive oxygen species (ROS) and reactive nitrogen species (RNS), leading to further inflammation and immune cell recruitment [33-35].

Despite inducing gastric inflammation and recruiting immune cells, it is currently accepted that bacterial persistence in the gastric mucosa is only possible due to the sophisticated mechanisms *H. pylori* has developed in order to escape and manipulate the host immune response [36]. One of the strategies adopted by *H. pylori* to evade recognition by the immune system is the alteration of flagellin and lipopolysaccharides (LPS) to trigger a weak TLR response, and thus a low-level inflammatory response [37]. Also, *H. pylori* protects itself against the harmful effects of ROS and RNS by secreting catalase and arginase [38, 39]. In order to modulate the host immune response, *H. pylori* possesses antigens that are structurally similar with host antigens, a mechanism designated as molecular mimicry, which leads to the secretion of antibodies that will react with both bacteria and host antigens [40]. These autoreactive antibodies contribute to inflammation and tissue damage [40].

In addition, *H. pylori* infection recruits $CD4^+$ T lymphocytes, particularly the pro-inflammatory T helper 1 (Th1) and Th17 subsets, and also the anti-inflammatory regulatory T (Treg) subset [41-44]. While the pro-inflammatory T cells contribute to tissue damage and recruitment of more immune cells to the infection site, Tregs are important to create a tolerogenic environment that allows *H. pylori* to persist [36]. The interplay between the bacterium and the host immune response results in the perpetuation of inflammation and in the exacerbation of tissue damage, which rarely results in bacterial clearance. Instead, the balance between *H. pylori* and the host contributes to the establishment of chronic gastritis [17, 36].

Chronic *H. pylori*-mediated gastritis may remain for the lifetime of the host, or more severe disease may follow. Accordingly, about 10% to 15% of *H. pylori*-infected individuals develop peptic ulcer disease. In fact, *H. pylori* infection is closely associated with a high risk of developing peptic ulceration, being the causative agent in 95% of duodenal ulcer cases and in 70% of gastric ulcer cases [45]. *H. pylori* eradication in peptic ulcer disease patients, not only treats peptic ulcers, but also reduces the risk of disease relapse [46, 47].

It is estimated that about 1% to 3% of *H. pylori*-infected patients will end up developing gastric carcinoma [48]. Infection with *H. pylori* is considered as the major risk factor for the development of gastric carcinoma, and approximately 90% of all non-cardia gastric carcinomas are attributable to chronic *H. pylori* infection [49, 50]. In 1994 *H. pylori* was recognized as a type I carcinogen by the International Agency for Research on Cancer [51]. There are two main types of gastric carcinoma, both strongly associated with the presence

of *H. pylori*: gastric carcinoma of the intestinal type, which is associated with atrophic gastritis and intestinal metaplasia of the stomach, and gastric carcinoma of the diffuse type, characterized by the presence of isolated or poorly cohesive neoplastic cells [52]. While the pathway leading to the diffuse-type gastric carcinoma remains unclear, a histological model for the role of *H. pylori* in the development of the intestinal-type gastric carcinoma was proposed by Correa [53, 54]. According to this model, *H. pylori* infection leads to a multistep change of the gastric mucosa involving superficial gastritis, atrophic gastritis, intestinal metaplasia, dysplasia, and finally gastric carcinoma. Progression to gastric carcinoma occurs only in a very small proportion of *H. pylori*-infected patients and the molecular mechanisms underlying malignant transformation are associated with ROS/RNS-mediated DNA damage, with silencing of tumor suppressor genes, and with epithelial-mesenchymal transition, amongst other factors [17, 36, 55]. Interestingly, *H. pylori* eradication decreases the gastric carcinoma risk, at least in patients who have not yet developed cancer precursor conditions like intestinal metaplasia [56].

Approximately 0.1% of subjects with *H. pylori*-associated chronic gastritis may ultimately develop gastric mucosa-associated lymphoid tissue (MALT) lymphoma [48]. Gastric MALT lymphoma is characterized by the presence of lymphoid follicles in the gastric mucosa, with uncontrolled expansion of B cells [48]. *H. pylori* can be found in more than 90% of gastric MALT lymphoma patients [57]. Interestingly, eradication of *H. pylori* in patients with early-stage disease, results in complete remission of the lymphoma in 60%-80% of the cases, making this the only malignancy for which antibiotic-based therapy is the first choice of therapy with curative intent [57-59].

H. pylori infection has also been positively associated with a number of extra-gastric diseases, including unexplained iron deficiency anemia and idiopathic thrombocytopenic purpura, conditions which can be improved by *H. pylori* eradication [60, 61]. Associations with atherosclerosis and various neurological conditions have also been postulated, but the causality has not been proven [62-64]. On the other hand, there is evidence suggesting that the presence of *H. pylori* may be beneficial for the host by conferring protection against asthma and other allergies, esophageal disorders, and inflammatory bowel disease [65-67]. It is proposed that *H. pylori* immunomodulatory effects on immune cells, mainly dendritic cells (DCs) and Tregs, account for its beneficial effects [68].

As described above, while all *H. pylori*-infected individuals develop chronic gastritis, the consequences of the chronic infection may be substantially different. This diversity of clinical outcomes of *H. pylori* infection may be explained by inter-individual variation on factors from the host, including the type and extent of immune response to the bacterium and genetic susceptibility to infection, factors from the environment, such as smoking and diet, and

factors from the bacteria, including differences that exist on specific virulence factors [52, 55, 69, 70].

4. Virulence factors associated with *H. pylori* pathogenicity

Once established on the gastric epithelium, *H. pylori* has to promote its survival. This occurs by the manipulation of the host cell pathways and functions and through the activity of a number of bacterial virulence factors. CagA (cytotoxin-associated gene A), VacA (vacuolating cytotoxin A), HtrA (high-temperature requirement A protein), urease and the protease PqqE are some of the most studied *H. pylori* virulence factors.

4.1. CagA oncoprotein

CagA is the most extensively studied *H. pylori* virulence factor. It is considered as the *H. pylori* oncoprotein because it was demonstrated that transgenic mice expressing CagA had gastric epithelial hyperplasia, and some of the animals developed gastric polyps and carcinoma [71].

This highly immunogenic protein is encoded by the *cagA* gene that is located in a specific 40 kb region of the chromosomal DNA. This region, designated by *cag* pathogenicity island (*cag*PAI), encodes about 27 to 31 proteins, depending on the *H. pylori* strain [72]. Seventeen of those proteins form the T4SS apparatus, a syringe-like structure protruding from the bacterial surface that penetrates gastric epithelial cells and translocates CagA and fragments of peptidoglycan (PG) into their cytoplasm [32, 73]. The interaction of T4SS with epithelial cells occurs through the binding of the *H. pylori* CagL protein with the host cell integrin-α5β1 [74]. Once inside host cells, CagA can interact with about 20 host cell proteins and modulate host signaling pathways in a phosphorylated-dependent and -independent manner [75].

Phosphorylation of CagA occurs on tyrosine residues within the Glu-Pro-Ile-Tyr-Ala (EPIYA) amino acid sequence, at the C-terminal region, by host cell Src and Abl family kinases [76, 77]. Four distinct EPIYA motifs (EPIYA-A, -B, -C and -D) have been defined, depending on the amino acid sequence surrounding the EPIYA motif [78]. *H. pylori* from different geographic regions contains CagA with different EPIYA motifs. While EPIYA-A and EPIYA-B motifs are common to strains throughout the world, EPIYA-C is mainly present in strains from Western countries and EPIYA-D in strains from the far East Asia [75]. Upon phosphorylation of EPIYA motifs, CagA induces the cytoskeleton rearrangement in epithelial cells *in vitro*, with cell elongation and scattering, described as the hummingbird phenotype [79]. On the other hand, non-phosphorylated CagA exerts important effects on

disrupting cell-cell junctions, altering cell polarity, and inducing pro-inflammatory responses and cell proliferation [75].

Not all *H. pylori* strains, however, contain the *cag*PAI (and CagA), being the prevalence of *cag*PAI-positive strains of 70% in Western countries and over 90% in East Asian countries [80]. The presence of CagA and variation in its phosphorylation motifs are associated with disease. Compared to CagA-negative strains, *H. pylori* strains that are CagA-positive are associated with higher levels of gastric inflammation and increased risk of peptic ulcer disease and of gastric carcinoma [70, 81-84]. Furthermore, infection with CagA strains containing higher numbers of EPIYA-C motifs is associated with higher risk for intestinal metaplasia and gastric carcinoma [80, 85].

4.2. VacA cytotoxin

VacA is a cytotoxin produced by virtually all *H. pylori* strains that plays an important role in pathogenicity by eliciting multiple effects on host cells [86-90]. This toxin can be secreted by *H. pylori* or remain associated with the outer membrane (OM), where it exerts its effects upon bacterial contact with host cells [91]. After binding to the epithelial cell membrane, VacA may induce the formation of membrane channels and large acidic vacuoles, triggering apoptosis mediated by cytochrome c release from mitochondria [86-89]. VacA can also have immunomodulatory properties, such as inhibition of T and B lymphocytes proliferation [90].

Although the *vacA* gene is present in all *H. pylori* strains, it displays different polymorphic rearrangements and, consequently, variation in the VacA toxin capacity to induce vacuolization in epithelial cells [92, 93]. Three main polymorphic regions have been described, each with two main forms: the signal (s)-region, which encodes the signal peptide; the middle (m)-region, responsible for the cell binding domain; and the intermediate (i)-region, located between the s- and m-regions [94]. The mosaic combination of these different regions determines different vacuolating activities: *H. pylori vacA* s1/m1 strains have a higher vacuolating activity, whereas strains with *vacA* s2/m2 genotypes present no detectable activity [92, 95]. Also, *H. pylori* harboring s1, m1 or i1 *vacA* regions are associated with higher levels of inflammation and epithelial damage of the gastric mucosa, as well as increased risk for gastric carcinoma development, when compared with *H. pylori* strains with *vacA* s2 or m2 [70, 83, 92].

4.3. HtrA protease

The high-temperature requirement A (HtrA) protein is a serine protease secreted by *H. pylori* to the extracellular space [96]. This protease was described to cleave the extracellular

domain of the cell-cell adhesion molecule E-cadherin, leading to disrupted inter-cellular adhesion [97, 98]. More recently, and in addition to cleaving E-cadherin, HtrA was found to cleave also the extracellular domains of the tight junctional molecules occludin and claudin-8, resulting in the disruption of the epithelial barrier [99]. Interestingly, HtrA-mediated opening of cell junctions was required for paracellular transmigration of *H. pylori* and for the activation of the T4SS pilus, thus allowing the bacterium to reach basolaterally-located integrins and to inject CagA into the host cells [99]. The *htrA* gene is highly conserved across *H. pylori* strains worldwide and is an essential gene for bacterial survival [100]. Evidence has shown that HtrA is highly stable and active under stress conditions (extreme pH values, high temperature or salt conditions), reinforcing its importance for *H. pylori* colonization [101].

4.4. PqqE protease

PqqE is a metalloprotease identified in the extracellular proteome of *H. pylori* at multiple phases of bacterial growth [102]. This protein is codified by the *HP1012* gene, which appears to be an essential gene in *H. pylori* [103]. Very recently, Marques *et al* assigned a novel substrate and function for PqqE. They have shown that *H. pylori* PqqE cleaves the cytoplasmic C-terminus of the tight junctional protein JAM-A [104]. Cleavage of the cytoplasmic domain of JAM-A resulted in altered gastric epithelial barrier and impaired cell-cell adhesion [104]. PqqE reached maximum proteolytic activity when combined with YmxG, another metalloprotease [104]. Noteworthy, PqqE cleaves JAM-A independently of the *H. pylori* T4SS [104], suggesting alternative paths for the PqqE protease to reach the host cell cytoplasm.

5. Treatment of *H. pylori* infection

There are multiple regimens for the treatment of *H. pylori* infection [105]. An optimal *H. pylori* eradication regimen is currently defined as one that achieves a cure rate of at least 90%, and efficacies <90% are considered as unacceptable [106]. The first-line treatment of *H. pylori* consisted on the standard triple therapy that combined a proton pump inhibitor (PPI) with two antibiotics (clarithromycin and amoxicillin or metronidazole). Nowadays, the standard triple therapy achieves eradication rates of about 70%. Besides the poor patient compliance to therapy, one of the main reasons for such low success is the worldwide increase in clarithromycin resistance, which in many regions of the world reaches values between 30% and 50% [107]. Consequently, the clarithromycin-based triple therapy is currently only recommended in regions with low resistance rates to this antibiotic [59]. The increase in the duration of therapy from 7 or 10 days, to 14 days is associated with higher

eradication rates, even in face of clarithromycin resistance [108]. In addition to resistance to clarithromycin, there are also generalized high levels of resistance to metronidazole and dual resistance to both antibiotics [107]. Therefore, alternative regimens that vary between different regions of the world have been introduced into the clinics. Current guidelines recommend for areas of high clarithromycin resistance, bismuth quadruple or non-bismuth quadruple, concomitant (PPI, amoxicillin, clarithromycin and nitroimidazole) therapies. For areas where the resistance to both clarithromycin and metronidazole is high, the bismuth quadruple therapy is the recommended first-line treatment [59]. In addition to the rising *H. pylori* resistance to antibiotics, the success of the treatment is dependent on multiple other aspects, including the choice of antibiotics and anti-secretory drugs used and the respective doses, the duration of therapy, and the number of administrations per day [106].

Considering the numerous factors that influence the ability to eradicate *H. pylori*, alternative options of treatment are in demand. Theoretically, vaccination appears to be the most effective option in young children to prevent infection and its chronic consequences. However, the development of an *H. pylori* vaccine has been challenging and there is still no effective vaccine available in the market [6, 109].

OUTER MEMBRANE VESICLES (OMVS)

All forms of life constitutively release extracellular vesicles (EVs) as part of their normal growth [110]. EVs were first described in Gram-negative bacteria as products excreted by cultures of lysine-requiring *Escherichia coli* grown under lysine-limiting conditions [111]. These products were thought to be related with the bacterial cell wall, based on their chemical composition and on their immunological properties [111]. At that time, authors observed the presence of numerous blebs attached to the cell wall of the bacteria and the presence of extracellular globules with triple-layered membranes, which suggested that these spherical structures originated from the bacterial OM. As the composition of these vesicles had similarities with that of the OM, and since secretion occurred through blebbing of the OM, EVs from Gram-negative bacteria were therefore designated as outer membrane vesicles (OMVs). Despite their thick cell-wall, Gram-positive bacteria also secrete EVs, denominated as membrane vesicles [112, 113]. Additionally, there are other types of EVs, including exosomes, microvesicles, and outer-inner membranes, secreted by eukaryotes, prokaryotes, and archaea and formed through different routes [113]. OMVs are the only type of EVs secreted by *H. pylori* described so far [110].

1. Structure and composition of OMVs

OMVs have a spherical structure ranging from 20 to 500 nm in size. They enclose membrane, periplasmic and cytoplasmic components, such as proteins, lipids, LPS, PG, and genetic material, derived from their parental bacterium (**Figure 2**) [114]. Despite the fact that all OMVs are predominantly composed of OM components, certain constituents can be enriched or depleted in comparison to their frequency in the parental bacterium, and subpopulations of OMVs within the same bacterial culture may present distinct cargo, which is translated into vesicles with distinct physical properties, namely size and density [115, 116]. Such cargo selectivity suggests that OMVs biogenesis is a deliberated process beneficial to the bacterial community [115, 116].

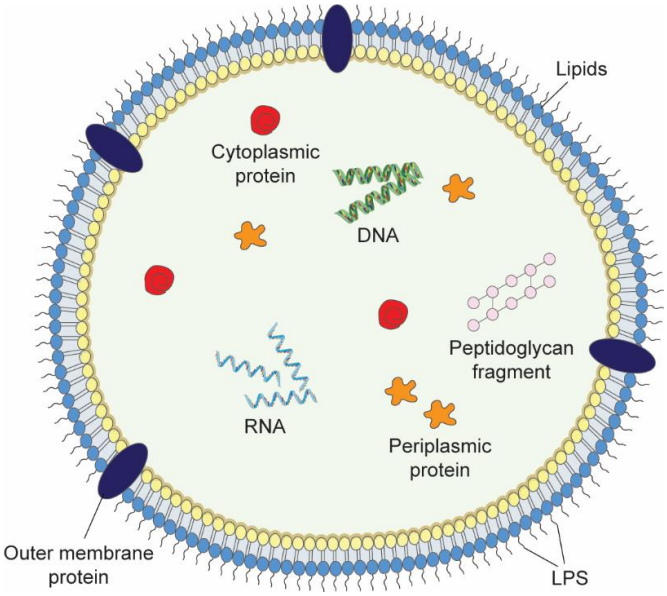

Figure 2. Diagram representation of the structure and content of OMVs secreted by Gram-negative bacteria. OMVs are composed by outer membrane components (outer membrane proteins, lipids, and lipopolysaccharides – LPS), periplasmic content (proteins and peptidoglycan fragments), and cytoplasmic material (proteins and nucleic acids – DNA and RNA).

1.1. Composition of *H. pylori* OMVs

As other OMVs, *H. pylori* OMVs carry a diversified content that is dependent on the bacterial strain, bacterial growth stage, and environmental conditions [117-119].

LPS, PG, and several lipids have been identified in *H. pylori* OMVs, including phosphatidylethanolamine and cardiolipin PG [119-121]. DNA and small noncoding RNA (sncRNA) have also been detected in *H. pylori* OMVs, the latter being associated with a reduced IL-8 secretion and suggestive of a bacterial escape mechanism from the host immune response [122, 123]. Regarding the protein content, published proteomic analysis of OMVs isolated from different *H. pylori* strains show an enrichment in OMPs and in

uncharacterized proteins. The presence of various known *H. pylori* virulence factors, namely BabA, SabA, and OipA adhesins, lipoprotein (Lpp) 20, VacA, CagA, urease, and HtrA has also been detected in H. *pylori* OMVs [118, 119, 124]. Interestingly, and in contrast with others, Keenan *et al* did not detect CagA in OMVs secreted by *H. pylori* strain 60190, which is a CagA positive strain [125]. The authors suggest this may be related with the different techniques followed by different groups for the growth of *H. pylori*, for the isolation of OMVs, and for the detection of CagA [125]. Recent findings from Turner *et al* also revealed that the protein composition of OMVs is determined by the size of the vesicles [126]. Despite the relatively low number of proteins identified in OMVs, they showed that larger OMVs contained a significantly higher number and a more diverse protein content than smaller OMVs, and small and large vesicles each had unique and common proteins. *H. pylori* adhesins SabA, BabA, and OMPs were exclusive to large OMVs; proteins associated with metabolism were exclusive to small OMVs; and *H. pylori* survival- and virulence-associated proteins like UreA and UreB, NapA, and VacA were common to small and large OMVs, suggesting that vesicles of both sizes play a role in pathogenesis [126].

2. Models for OMVs biogenesis

The formation of OMVs results from the liberation of the OM from the underlying PG, which bulges outwards and detaches from the bacterial cell without compromising membrane integrity. Evidence suggests there are multiple mechanisms through which the vesiculation process occurs (**Figure 3**). Still, there is one aspect that appears to be common to all vesiculation mechanisms, which is the alteration of the envelope stability. The stability of the envelop is maintained by different crosslinks established between the PG and different components of the outer and inner membranes, such as the Braun's Lpp, the outer membrane protein A (OmpA), and the Tol-Pal system [115]. Thus, it is proposed that areas of the envelope that present decreased abundance or displacement of crosslinks have increased vesicle production [115, 127]. This association has been emphasized by the observation of hypervesiculation in bacterial mutants that lack OmpA [128-130]. Similarly, the overall number of Lpp-PG and Tol-Pal-PG crosslinks inversely correlates with vesiculation [131, 132]. The influence of the Tol-Pal system in the vesiculation process has been demonstrated in *H. pylori,* in which a *tolB* mutant had significantly increased production of OMVs in comparison with the wild-type strain [133].

The lipid content of the OM dictates membrane fluidity and curvature, hence the plausibility for their involvement in the biogenesis of OMVs [115]. It was hypothesized that areas enriched in LPS, specific LPS-associated molecules or phospholipids, have increased membrane flexibility and have increased susceptibility for vesiculation [115]. In fact, the

hydrophobic LPS-binding protein *Pseudomonas* quinolone signal (PQS), a quorum sensing molecule used by *Pseudomonas* for cell-cell communication, was shown to enhance the production of OMVs by incorporating it into the OM and inducing membrane curvature [134, 135]. The importance of these proteins in the biogenesis of OMVs has been demonstrated in *Pseudomonas* spp, but also in other bacterial species, such as *E. coli, Burkholderia* spp, and Gram-positive bacteria [134, 136].

Vesicle formation has also been shown to occur as a consequence of the accumulation of misfolded proteins or envelope components in nanoterritories localized in the OM, leading to an increased turgor pressure, and forcing the OM to bulge outwards and bud off [137]. This mechanism could represent an immediate protective bacterial response to stressful and harmful environments, such as temperature, pH, nutrient deprivation, or exposure to antimicrobial agents, in order to remove undesirable components and to increase bacterial fitness [138]. For instance, *E. coli* subjected to a temperature of 55 ºC for 10 minutes (min) showed an increase in the production of OMVs [139]. Hypervesiculation was also described under iron-limiting conditions, where OMVs from *Mycobacterium tuberculosis* were enriched in a siderophore mycobactin and able to support the growth of iron-starved mycobacteria [140].

The discussed mechanisms for OMVs biogenesis are not exclusive and more than one mechanism can occur in the same bacterial species, explaining the great variety of OMVs of different sizes and cargo.

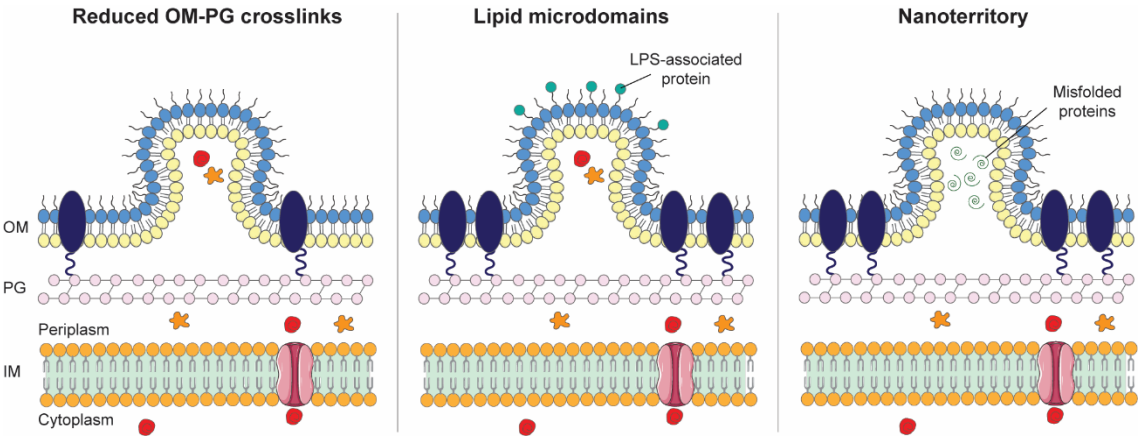

Figure 3. Models for OMVs biogenesis. Several factors influence the formation of OMVs, including the modulation of crosslinks between the PG layer and the OM, the lipid composition of specific regions of the OM that dictate membrane fluidity, and the presence of nanoterritories formed by the accumulation of misfolded proteins or envelope components. OM: outer membrane; PG: peptidoglycan; IM: inner membrane.

2.1. *H. pylori* vesiculation

H. pylori can exist in different morphological shapes, including the bacillary, U-shaped and coccoid forms, which represent a mechanism of bacterial adaptation to adverse environmental conditions [18, 141]. The morphological shape transition from bacillary to a coccoid bacterial cell has been also associated with bacterial growth [119, 141]. It was observed that as bacterial growth progressed, OMVs increased in number and became less heterogeneous in size [118, 119].

In the case of *H. pylori*, it has also been shown that vesiculation is affected by environmental factors. Under iron-limiting conditions, there was an increase in the number of secreted OMVs, despite the inhibition of *H. pylori* growth [142]. In addition, the composition of OMVs was also affected by the limitation in iron, as there was a reduction in VacA levels in these vesicles, and the detection of two new proteolytic enzymes [142].

3. Entry of OMVs into host cells

Despite the abundant evidence that OMVs can enter into host cells, the specific mechanism underlying their entry is still not fully elucidated [143]. There are five possible endocytic pathways that can mediate the entry of OMVs into a non-phagocytic host cell (**Figure 4**): macropinocytosis, clathrin-mediated endocytosis, caveolin-mediated endocytosis, lipid raft-mediated endocytosis, and membrane fusion (not depicted in the figure) [143].

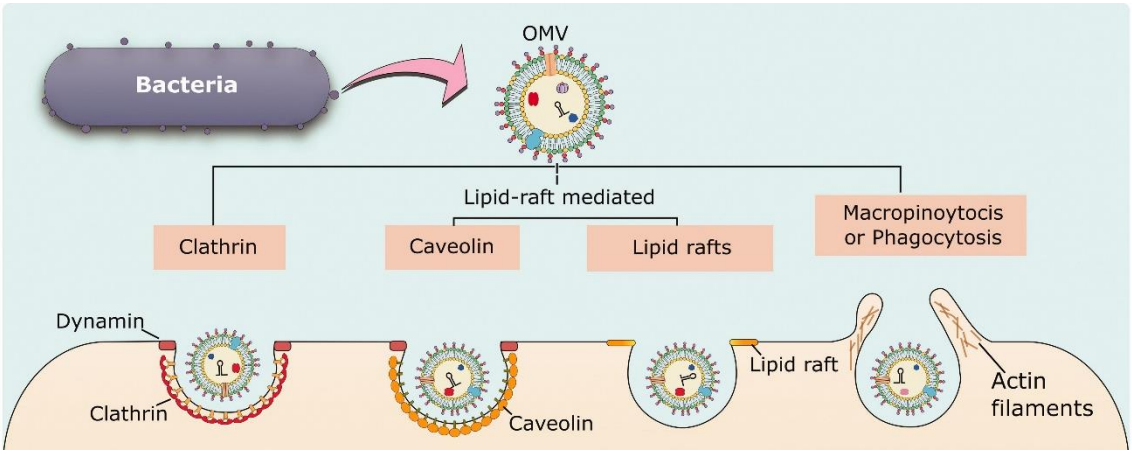

Figure 4. Endocytic pathways for the entry of OMVs into host cells. OMVs can entry non-phagocytic host cells via clathrin-mediated endocytosis, caveolin-mediated endocytosis, lipid raft-mediated endocytosis, or macropinocytosis. Adapted from [144].

Macropinocytosis is characterized by the actin-driven formation of a membrane protrusion that eventually closes to engulf a portion of the extracellular space, resulting in the formation of large endocytic vesicles (< 1 µm) [143, 145]. Usually, macropinocytosis is not cargo-

induced and it is likely that the entry of OMVs by this route occurs involuntarily [145]. Nonetheless, data support the uptake of OMVs from *P. aeruginosa* and *Porphyromonas gingivalis* through this mechanism [146, 147].

Clathrin-mediated endocytosis is triggered by ligand binding to cell surface receptors, leading to the formation of clathrin coated pits that mature into 200 nm vesicles, in a dynamin-dependent manner [143, 145]. This was shown to be the route of entry for OMVs from *H. pylori*, *Brucella abortus*, and *E. coli* [148-150].

Caveolin-mediated endocytosis involves membrane lipid raft domains that are enriched in cholesterol, caveolins, and sphingolipids. These regions form membrane invaginations, the caveolae, with around 80 nm, which are also internalized in a dynamin-dependent manner [143, 145]. Caveolae have been suggested as the preferred entry route for many pathogens and there are now multiple examples of OMVs that use this mechanism to enter host cells, as there is no fusion with lysosomes and subsequent degradation, in contrast to what happens with clathrin-coated vesicles [145].

Lipid rafts are also used as an endocytic mechanism in a caveolin-independent manner. Their enriched composition in cholesterol and sphingolipids provides this region with a more ordered and compact structure than the surrounding membrane, allowing the curvature and invagination of the membrane [145]. OMVs from *P. gingivalis*, *P aeruginosa*, and *Vibrio vulnificus* have been shown to require lipid rafts for their entry and for the delivery of cargo into the host cells [147, 151, 152].

Finally, and despite the structural differences between the membrane of OMVs and that of the host eukaryotic cells, direct membrane fusion can occur between them, preferentially at lipid raft domains [145]. This was demonstrated for *P. aeruginosa*, *Aggregatibacter actinomycetemcomitans*, and *Legionella pneumophila* [146, 153, 154].

It is now clear that OMVs from the same bacterial species use multiple endocytic pathways to enter host cells [146, 147, 151]. This fact can be explained by the differences in size and cargo composition of OMVs, which may direct them to specific uptake routes.

3.1. Entry of *H. pylori* OMVs into host cells

The entry of *H. pylori* OMVs into host cells has been demonstrated to occur through different routes. In 2010, Kaparakis *et al* and Parker *et al* described different endocytic pathways for the uptake of OMVs [121, 148]. Kaparakis *et al* reported that *H. pylori* OMVs enter AGS epithelial cells through lipid rafts, as pharmacological inhibition of sphingomyelin and cholesterol prevented both the entry and immunostimulatory capacities of OMVs [121]. Conversely, Parker *et al* determined that the uptake of *H. pylori* OMVs by AGS cells was not cholesterol-dependent, but required clathrin-dependent endocytosis [148]. In addition,

the presence of VacA on the surface of OMVs enhanced the vesicle uptake and the results of this investigation suggested that VacA-containing OMVs could still be internalized when the clathrin-mediated pathway was inhibited, though via a different route [148]. Later, Olofsson *et al* confirmed that *H. pylori* OMVs enter AGS cells by both clathrin- and dynamin-dependent pathways and that the uptake of OMVs decreased after depletion of cholesterol from the epithelial cell membrane [155]. In fact, *H. pylori* OMVs can enter epithelial cells through different pathways, which is determined by their size [126]. Small OMVs (20 to 100 nm in size) preferentially entered AGS cells via caveolin-dependent endocytosis, whereas larger OMVs (90 to 450 nm) entered cells via the clathrin- and dynamin-mediated pathways [126]. Nevertheless, the authors did not assess the entry of OMVs with different sizes via lipid rafts domains, and the opposing results from Kaparakis *et al* and Parker *et al* could not be confirmed.

4. Biological roles of OMVs

As a result of their physical properties and their capacity to disseminate and reach areas otherwise inaccessible to the bacterial cell, OMVs were described to play multiple roles in intra- and inter-species communication, as well as in bacterial defense [116, 138].

One important role of OMVs is the nutrient acquisition in bacterial communities [115]. As discussed above, bacteria starvation induces the production of OMVs that contain a specialized cargo of glycosidases, proteases, and proteins, capable of adsorbing and carrying essential nutrients for the benefit of the bacterial community within their niche [156]. This OMVs' function was demonstrated for the acquisition of multiple essential nutrients, including iron, cysteine, sulfate, and carbon, in bacterial populations of *M. tuberculosis*, *Neisseria meningitides,* and *Prochlorococcus* [140, 157-159].

OMVs are also key players in bacterial and bacteria-host communication. Mashburn *et al* showed that removal of PQS-containing vesicles from *P. aeruginosa* cultures interfered in cell-cell communication and inhibited PQS-controlled group behavior [134]. Bacterial communication can also occur through horizontal gene transfer. It has been shown that DNA encoding antibiotic resistance genes can be carried by OMVs, representing an important defense strategy for the bacterial cell and also for the bacterial community [160, 161]. More recently, a role for OMVs as mediators of transfer of nucleic acids between bacteria and host cells have been described. Koeppen *et al* showed that *P. aeruginosa* OMVs transferred small RNAs (sRNAs) into human epithelial airway cells, which resulted in the reduction of IL-8 secretion [162]. *P. aeruginosa* OMVs were also shown to carry DNA that was internalized by lung epithelial cells and detected in the nuclear fraction of those cells [163].

The similar composition between the bacterial OM and OMVs provides bacteria with another effective defensive mechanism. When faced with antimicrobial agents and bacteriophages, bacteria hypervesiculate and OMVs may act as decoys to adsorb such agents, thus protecting the surrounding bacterial cells [164, 165].

Bacteria also benefit from producing OMVs, since they constitute a regulated secretion system of specific and highly-concentrated groups of compounds, protected from physical and biochemical stressors, which can be delivered into host cells without the need for bacterial contact [116]. In pathogenic bacterial infections, such system may be important in the shape of the host immune response, as well as in the trigger of disease pathogenesis. Indeed, several studies have identified OMVs in a range of infected host tissues. For example, OMVs from *Neisseria meningitidis* have been identified in the cerebrospinal fluid of infected infants [166]; *H. pylori* OMVs have been detected in the gastric samples of infected individuals [125, 167]; and OMVs from *Moraxella catarrhalis* have been observed in the sinuses of a child [168].

Altogether, these observations suggest that OMVs are important for the onset and progression of disease.

4.1. Biological roles of *H. pylori* OMVs

Even though there are descriptions of the content of *H. pylori* OMVs, the functional consequences of their delivery into host cells are still far from understood.

Regarding the biological roles attributed to *H. pylori* OMVs, one important feature is their ability to elicit an inflammatory response in the host, contributing to chronic inflammation, a hallmark of *H. pylori* infection. For example, the PG present in OMVs was shown to upregulate NF-kB and NOD1-dependent immune responses [121]. In addition, *H. pylori* OMVs can induce the secretion of pro- and anti-inflammatory cytokines, including IL-8, IL-6, IL-1β, IL-17, TNF-α, IFN-γ, IL-4 and IL-10, both *in vitro* and *in vivo* [169-172]. More specifically, OMVs induced the secretion of IL-8 by AGS cells, independently of the T4SS and in a dose-dependent manner [169, 171]. Conversely, sncRNA carried in *H. pylori* OMVs were associated with a reduced IL-8 secretion by AGS cells, after the observation that OMVs isolated from specific sncRNA *H. pylori* mutants stimulated a higher cytokine secretion [123]. In the *in vivo* setting, *H. pylori* OMVs led to the production of a specific serum immunoglobulin G (IgG) against Lpp20, and elicited Th1 and Th17 immune responses [171, 173].

The VacA toxin was found to be membrane-associated in OMVs that were either isolated from the *H. pylori* strain 60190 or identified in biopsies from infected patients [125, 167]. Studies showed that VacA-containing OMVs induced vacuolization of HEp2 and AGS cells,

while the incubation of RK13 cells with OMVs from a *vacA* mutant strain only induced vacuolation at a basal level [125, 169, 170, 174]. Moreover, the presence of VacA associated to OMVs lead to a decrease in the viability of AGS cells through the induction of apoptosis [174].

One mechanism developed by *H. pylori* to counteract the great influx of neutrophils to the gastric mucosa and production of ROS is the expression of the antioxidant enzyme catalase (KatA) at the cell surface [38]. Interestingly, Lekmeechai *et al* found KatA to be enriched at the surface of OMVs, in comparison to bacterial cells, and capable of neutralizing ROS and protect bacteria from lethal oxidative damage [175]. This finding highlights not only the selective packaging and enrichment of OMVs with important components for bacterial survival and colonization, but also their role in bacterial protection from the oxidative stress and the host immune response.

5. Biopharmaceutical applications of OMVs

The physical properties of OMVs and their capacity to serve as long-distance delivery vehicles are some of the advantageous features of OMVs that have been exploited for application in the biomedical field. Furthermore, their large-scale production is relatively easy and cost-effective, and genetic engineering allows tailoring some of the properties of OMVs [176]. Hence, OMVs have been used as vaccines and as carriers of therapeutic compounds.

There is an emerging demand for novel therapeutic strategies to combat bacterial infections, in particular due to the rise in antibiotic-resistant bacteria. The similarity between the membranes of OMVs and their parental bacterium confers OMVs unique immunogenic properties that have been exploited for the development of vaccines. In fact, the use of OMVs secreted by *V. cholera*, *E. coli*, and *Shigella flexneri* as vaccines has proven to not only confer protection to subsequent infections, but also elicit a protective immune response in mice [177-179]. Currently, there are several OMVs-based vaccines that have been licensed for human administration, as is the case of Bexsero® (Novartis) and VA-MENGOC-BC® (Finlay Institute, Cuba) against the serogroup B *N. meningitides* [180, 181].

Genetic engineering of bacteria allows the manipulation of both the secretion and cargo of OMVs. For example, hypervesiculating bacteria are created by mutating genes that encode proteins that connect the OM to the PG layer. This results in an increased yield of OMVs, as demonstrated for the *H. pylori tolB* mutant [133]. Also, inactivation of the *msbB* gene in *E. coli* O157:H7 and in *Salmonella enterica* serovar *typhimurium*, impaired LPS synthesis and resulted in the production of OMVs with reduced endotoxicity [182, 183]. Bacteria can also be engineered to secret OMVs that carry heterologous antigens, which will elicit a

protective immune response in the host. This was demonstrated for *E. coli* OMVs carrying recombinant antigens from both Group A *Streptococcus* and Group B *Streptococcus* that, upon mice immunization, elicited a humoral immune response and protected mice against a subsequent Group A *Streptococcus* infection [184]. In addition, OMVs can carry antimicrobial and chemotherapeutic compounds. *S. flexneri* OMVs produced from parental bacteria that was subjected to a 30 min gentamicin treatment, were able to deliver this non-membrane permeative compound into epithelial cells and to inhibit the growth of *S. flexneri* located inside these cells [185]. Another example is provided by doxorubicin-encapsulated OMVs from an attenuated *Klebsiella pneumonia.* These OMVs were internalized by lung cancer cells and were able to inhibit tumor growth *in vivo* [186].

In the case of *H. pylori*, the development of an effective prophylactic or therapeutic vaccine, predominantly composed of purified or recombinant components of *H. pylori* antigens with an adjuvant, has proven challenging and is, therefore, not yet a reality [187]. Promising data showed that intragastric immunization of C57BL/6 mice with *H. pylori* 7.13 OMVs resulted in the development of humoral and Th2 immune responses, as well as a significant reduction of bacterial load after challenging with *H. pylori* SS1 [188]. These results were later confirmed by Song *et al* that also described the potential of OMVs in enhancing the eradication of *H. pylori* when used in conjugation with OMPs or bacterial lysates [189].

The development of OMVs-based therapeutics for the treatment of several health conditions is a promising field, but it is still in its infancy. Further investigation is needed to overcome issues like the heterogeneity of OMVs between samples and the presence of antigens that induce adverse immune responses in humans [190].

EPITHELIAL CELL-CELL JUNCTIONS

Mucosal epithelia constitute a selective barrier to nutrients between the external environment and the internal organs, while providing a physical barrier against microorganisms. Such structure is composed of polarized cells that are connected through the establishment of cell-cell junctions, which are critical structures for epithelial integrity. Cell-cell junctions are composed by three main adhesive structures, the tight junctions (TJ), the adherens junctions (AJ) and the desmosomes, which are formed by different transmembrane and cytoplasmic molecules and have distinct roles in the maintenance of barrier function (**Figure 5**) [191, 192]. Gap junctions are intercellular channels located below the abovementioned adhesive structures, and mediate the exchange of ions and small molecules between adjacent cells [193].

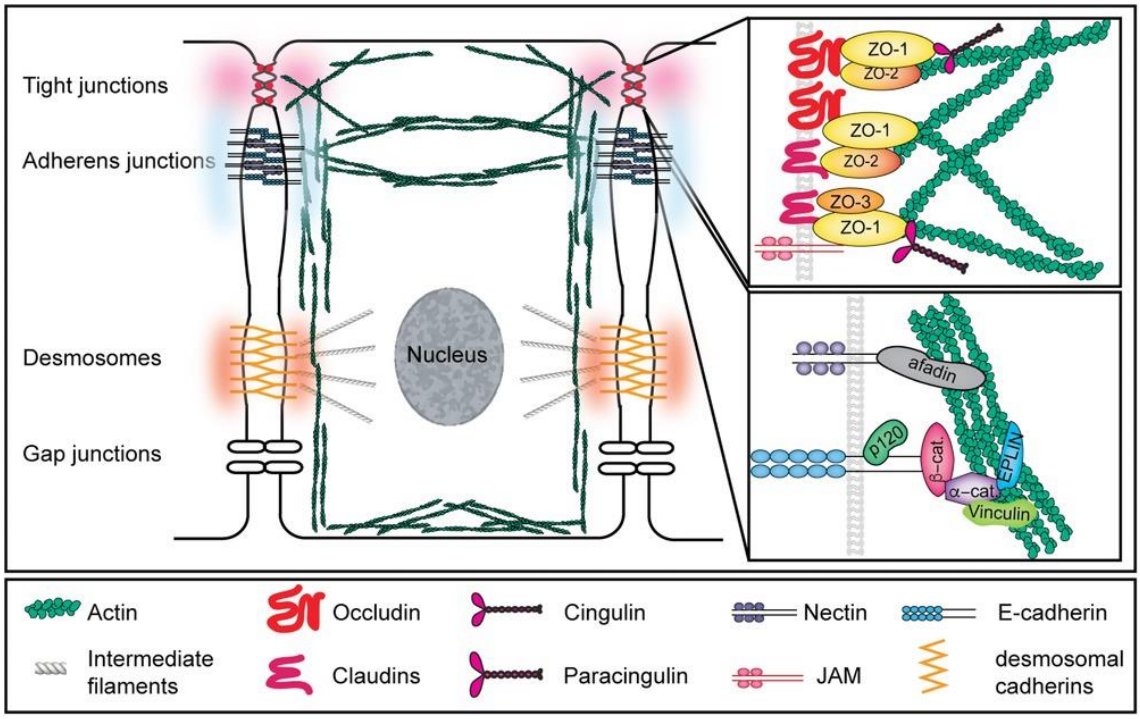

Figure 5. Polarized epithelial cells connect with each other through the establishment of junctional complexes. Tight junctions (TJ) are localized to the most apical side of the lateral membrane, followed by adherens junctions (AJ), desmosomes, and gap junctions. Simplified schemes of the structure of both TJ and AJ are magnified in the right panel, illustrating their composition in transmembrane and cytoplasmic proteins that link to the actin cytoskeleton. TJ (upper right panel) are composed by transmembrane proteins, such as occludin, claudins and JAM, that interact with the cytoplasmic proteins ZO-1, -2, -3 and PAR3 and link to the actin cytoskeleton. The AJ (lower right panel) transmembrane proteins E-cadherin and nectin are linked to the actin cytoskeleton via β-catenin or afadin, respectively. Reproduced with permission from [194].

1. Tight junctions

TJ are the most apical intercellular junctional complex, situated just below the apical membrane. They have two major functions known as gate and fence functions. The gate function regulates paracellular permeability to solutes according to charge and size [195, 196]. The integrity of the junctional gate can be assessed by measuring the transepithelial electrical resistance (TER) of the cell monolayer, as well as by quantifying the passage of large hydrophilic compounds, fluorescently labeled, through the monolayer [195]. The fence function establishes a diffusion barrier that restricts intermixing of apical and basolateral components, thus maintaining the apico-basal cell polarity [195, 196]. This function can be evaluated by labelling the cell membrane with a fluorescent lipid probe in order to visualize its diffusion through the basolateral membrane [195, 196].

Besides the above-mentioned functions, TJ are also linked to multiple signaling mechanisms due to their complex structure that connects with the cell actin cytoskeleton.

They receive signals from the cell to regulate junction assembly, maintenance, and functions, and also signal the cell to regulate cell proliferation, migration, and survival [197-199].

TJ are composed of a set of transmembrane proteins, including claudins, occludin, and junctional adhesion molecules (JAM). Transmembrane proteins are linked to a cytoplasmic plaque composed by zonula occludens (ZO-1, ZO-2, ZO-3), PAR3, and PAR6, among others, which form a network of scaffolding, adaptor, and cytoskeletal proteins that connect TJ to the actin cytoskeleton (**Figure 5**) [196, 199].

TJ transmembrane proteins are important for the connection of adjacent cells. Occludin was the first TJ transmembrane protein identified, in 1993 [200]. However, the role of occludin in TJ remains to be defined, since knockout animals for occludin exhibited normal junctions, both morphologically and functionally, but presented histological abnormalities in several tissues [201].

The claudin family of proteins consists of at least 27 members with different functions and with a tissue specific distribution [202]. Claudin proteins are essential for the formation of a functional barrier, as they participate in Ca^{2+}-independent cell-cell adhesion and mediate paracellular ion selectivity through the formation of aqueous pores [197, 203]. In fact, the permeability properties of a tissue are determined by the claudin composition of TJ. For instance, the absence of claudin 1 is lethal in mice right after birth as it results in water loss across the skin [197].

Other important TJ transmembrane proteins belong to the JAM family. JAMs are part of the immunoglobulin super family and comprise 7 members - JAM-A, -B, -C, -4, -L, CAR and ESAM. JAM proteins were suggested to have a role in the formation of junctional complexes, as well as in the development of cell polarity, due to their interaction with cytoplasmic proteins, such as ZO-1, afadin, and PAR3 [197, 204, 205]. The role of JAM-A in the regulation of epithelial barrier function was demonstrated *in vivo* after the observation that JAM-A deficient mice displayed increased permeability and inflammation [206].

The cytoplasmic plaque is a major structural feature of TJ that forms an interface between the junctional transmembrane proteins and the cell cytoskeleton. It is this interaction that provides cytoplasmic plaque functions to control cell-cell adhesion and paracellular permeability, as well as to transmit signals from the junction to the cell in order to regulate multiple cellular processes [197]. This capability of the cytoplasmic plaque to regulate cellular processes stems from its association with several signaling proteins and from the dual localization of some proteins, at TJ and in the nucleus [197]. One of the most studied TJ cytoplasmic proteins is the adaptor protein ZO-1, belonging to the ZO family. ZO-1 can directly associate with multiple transmembrane (e.g., claudins, occludins and JAM) and cytoplasmic proteins (e.g., ZO-2 and ZO-3), in addition to the actin cytoskeleton, through its

several protein-protein interaction domains [196, 197, 207]. ZO-1 and ZO-2 proteins play an essential role in embryonic development, as deficiencies in these proteins are lethal in developing mice [208, 209].

Other proteins associated with TJ cytoplasmic plaques compose the PAR3/aPKC/PAR6 and Pals1/PATL conserved signaling modules, which are essential for the development of cell polarity [197].

2. Adherens junctions

AJ are localized immediately bellow TJ and physically connect neighboring cells, thus contributing for intercellular adhesion. AJ are composed by two adhesive complexes, the cadherin-catenin and the nectin-afadin (**Figure 5**) [210].

Cadherins are required for cell-cell adhesion. E-cadherin, the prototypical epithelial cadherin, is a transmembrane protein that forms the E-cadherin/catenin core complex by binding directly to the cytoplasmic p120-catenin and β-catenin, which then recruit α-catenin. α-catenin subsequently binds to actin filaments, acting as the bridge between the E-cadherin/catenin complex and the actin cytoskeleton. The association of all these proteins is crucial for the adhesive activity and stability of AJ [207, 211].

The nectin/afadin complex consists on the binding of the transmembrane adhesion molecule nectin to the cytoplasmic actin-binding protein afadin. This complex is essential for the formation and strengthening of AJ, as nectins first establish cell-cell adhesion and only then recruit E-cadherin to the junctional sites [212]. Moreover, there is a link between AJ and TJ that is established through the direct association of afadin with TJ proteins, including α-catenin and vinculin [207].

The strength and adhesive properties of AJ are determined by the tissue-specific expression of cadherins and nectins [210].

3. Cell-cell junctions as targets of *H. pylori*

The gastric mucosal epithelium is one of the first lines of host defense that has evolved to prevent microorganisms from entering the body [213]. However, some pathogens developed mechanisms to breach this barrier and be able to colonize and survive. One of those mechanisms involves the disruption of cell-cell junctions to facilitate cell and/or tissue invasion, or to promote signaling responses to their advantage. For example, the Hepatitis C virus and Reovirus respectively use claudin-1 and JAM-A as receptors for their internalization [198, 214]. Rotavirus is able to alter the localization of claudin-3, ZO-1, and occludin, impairing the epithelial barrier integrity [198, 214]. Bacterial pathogens, such as *Clostridium*, *Shigella*, *Salmonella*, enteropathogenic *E. coli*, *Listeria*, and *Vibrio cholerae*,

use several junctional proteins as receptors for internalization, while also promoting degradation of specific TJ proteins, which leads to the disruption of the epithelial barrier [191, 198].

H. pylori, similarly to other bacteria, exploits cell-cell junctions through a number of mechanisms in order to colonize, extract nutrients from, and replicate at the gastric surface/epithelium [215, 216]. An impairment of the epithelial cell-cell junctions was described to be a consequence of ammonium production by *H. pylori*, as well as the expression of a low molecular weight form of occludin [217]. Accordingly, other reports have shown that the loss of barrier function and occludin internalization upon *H. pylori* infection were consequences of urease activity, and were independent of the T4SS- and of VacA [218].

However, VacA was described to alter the paracellular permeability of polarized MDCK, T84, and epH4 cell monolayers, allowing the passage of low molecular weight molecules and ions, which suggests a role for this virulence factor in the acquisition of nutrients to support *H. pylori* survival and growth [219]. Pelicic *et al* also showed that infection of MDCK cells with VacA-producing *H. pylori* strains resulted in the decrease of TER, while infection with *vacA* mutants did not [220]. Conversely, a number of studies stated that the loss of barrier function was independent of VacA, CagA, or the T4SS [218, 221, 222].

CagA was also reported to be involved in the disruption of the epithelial barrier. Amieva *et al* showed that CagA recruits and associates with ZO-1 and JAM-A at sites of bacterial attachment, thus altering the structure and function of TJ [223]. In addition, they observed altered cell morphology dependent of CagA [223]. Similar data were obtained using primary gastric epithelial cell cultures, reporting the recruitment of ZO-1 to sites of bacterial adhesion, and accumulation of ZO-1 and p120-catenin into small vesicles on the cytoplasm [224]. The involvement of CagA in the disruption of cell-cell junctions, as well as its capacity to induce changes in epithelial cell morphology, was described to be dependent on its phosphorylation state [225]. Another target for CagA is PAR1/MARK kinase, whose interaction promotes junctional and polarity defects, leading to the disorganization of MDCK cell architecture [226]. CagA also binds to the intracellular domain of E-cadherin, impairing the formation of E-cadherin/β-catenin complex and leading to cytoplasmic and nuclear accumulation of β-catenin [227]. The association of CagA with E-cadherin was further studied by Oliveira *et al*, who observed the formation of a CagA/c-Met/E-cadherin/p120-catenin complex in gastric epithelial cell lines, resulting in the suppression of the *H. pylori*-induced cell invasive phenotype [228].

H. pylori-mediated disruption of E-cadherin occurs in a CagA-independent manner as well, as demonstrated using *in vitro* models [229]. This function was later attributed to the disintegrin and metalloprotease ADAM10, that partially abrogated E-cadherin shedding

upon *H. pylori* infection [230]. Very recently, the serine protease HtrA was reported to be involved in the cleavage of the extracellular domain of E-cadherin and of the TJ proteins occludin and claudin-8, thus facilitating the paracellular transmigration of *H. pylori* and the translocation of CagA across integrin-β1 at the basolateral membranes [99]. The *in vivo* evidence of *H. pylori*-induced E-cadherin shedding were sustained by the finding of elevated levels of soluble E-cadherin on serum from infected patients in comparison to uninfected control subjects [231].

In the past few years, our group has unveiled novel cell-cell junction targets of *H. pylori*. In 2018, we have reported a downregulation of afadin protein levels upon *H. pylori* infection both *in vitro* and *in vivo*, which occurred independently of CagA, VacA, and of the T4SS, and led to increased cell motility and invasion [232]. Later, Marques *et al* described that *H. pylori* cleaves the cytoplasmic domain of JAM-A through the action of the bacterial metalloprotease PqqE, resulting in the loss of epithelial barrier and cell-cell adhesion [104]. Although it is well established that *H. pylori* disrupts TJ and AJ, the precise mechanisms and the virulence factors involved are not fully understood, which opens the possibility for the contribution of alternative mechanisms and bacterial factors in the epithelial barrier dysfunction.

Outline and Aims

The general aim of this thesis was to disclose the role of OMVs in *H. pylori* pathogenesis.

Since data on *H. pylori* OMVs are inconsistent, relying on different methods for bacterial growth and isolation of OMVs and hampering the comparison between studies, in **Part I** of this thesis, the aim was to develop and optimize a protocol for the isolation of OMVs suitable for standardization. The chemically defined medium F12-cholesterol was selected for bacterial culture, and the kinetics, viability, and morphology of *H. pylori* grown in this medium were investigated by growth curves, flow cytometry, and transmission electron microscopy (TEM; **Parts I.1** and **I.2** of the Results). The isolation of OMVs from *H. pylori* F12-cholesterol liquid cultures was next optimized, and OMVs were characterized regarding their morphology, size, and yield using TEM and nanoparticle tracking analysis (NTA; **Part I.3**).

Knowing that OMVs carry a diversified cargo, and after having established the isolation protocol of *H. pylori* OMVs, in **Part II** the aim was to analyze the content of OMVs, in terms of their protein and nucleic acids' composition. For protein analysis, nanoscale liquid chromatography coupled to tandem mass spectrometry (nanoLC-MS/MS) was performed using OMVs secreted at different times of *H. pylori* growth (**Part II.1**). For the analysis of the nucleic acid content of OMVs, immunogold labelling and polymerase chain reaction targeting *H. pylori* virulence genes were performed in DNA and RNA isolated from OMVs (**Part II.2**).

Since OMVs play an important role in bacteria-host interactions, in **Part III** the aim was to evaluate the impact of *H. pylori* OMVs on host cell transcriptomics. For that, a human gastric epithelial cell line was challenged with *H. pylori* OMVs, and next-generation sequencing was used to evaluate the gene expression profile of host cells.

Knowing cell-cell junctions are targets of *H. pylori* infection and taking into consideration recent work from our group suggesting that OMVs may constitute an alternative mechanism of virulence factor delivery, in **Part IV** the aim was to evaluate the influence of *H. pylori* OMVs in intercellular junction disruption. In **Part IV.1**, the entry of OMVs into gastric epithelial cells was evaluated by immunofluorescence. Then, the influence of OMVs on cell-cell junctions was addressed using two gastric epithelial cell line models challenged with *H. pylori* OMVs. The structure of epithelial cell-cell junctions was evaluated by immunofluorescence and western blot analysis, and the functions were evaluated by transepithelial electrical resistance (TER) and paracellular permeability assays (**Part IV.2** and **IV.3**). Finally, in **Part IV.4**, the involvement of OMVs in the recently described *H. pylori*-mediated JAM-A cleavage was evaluated by nanoLC-MS/MS.

The great majority of data presented in **Part I** and **Part II** of the Results are compiled in **Paper I**. Data in **Parts III** and **IV** have not yet been published.

MATERIALS AND METHODS

H. pylori strains and growth conditions in TSA plates

H. pylori strains 26695 (ATCC® 700392, *cagA*+, *vacA* s1/m1), 60190 (ATCC® 49503, *cagA*+, *vacA* s1/m1), and Tx30a (ATCC® 51932; *cagA*-, *vacA* s2/m2) were routinely cultured in Trypticase™ Soy Agar (TSA) supplemented with 5% Sheep Blood (Becton, Dickinson and Company, Franklin Lakes, NJ, USA) and incubated in a sealed jar with a microaerophilic atmosphere (GENBox microaer; bioMérieux S.A., Marcy l'Etoile, France) at 37 °C for 48 hours (h). Bacteria were sub-cultured for a maximum of 12 passages.

H. pylori growth in liquid cultures

H. pylori previously grown in TSA plates for 48 h was collected with 1 mL of either sterile Ham's F12 with L-glutamine medium (#L0135-500; Biowest, Nuaillé, France) supplemented with 1x cholesterol (Gibco®, Thermo Fisher Scientific, Waltham, MA, USA) (hereafter designated as F12-cholesterol), or BBL™ Brucella broth (BB; #211088; BD Biosciences, San Jose, CA, USA) supplemented with 5% fetal bovine serum (FBS; HyClone™, GE Healthcare Life Sciences, USA) (abbreviated as BB-FBS). The optical density of 600 nm (OD_{600}) was measured using a spectrophotometer (Genesys20; Thermo Fisher Scientific), in polystyrene cuvettes (Thermo Fisher Scientific). The culture medium of the corresponding bacterial culture was used as the blank solution to calibrate the spectrophotometer to 100% absorbance.

The initial OD_{600} of the bacterial suspension was adjusted to 0.02 (~6×10^6 colony forming units-CFUs/mL) in 200 mL of F12-cholesterol or BB-FBS. Bacteria were grown in a 500 mL Schott flask, placed in a sealed jar, under microaerophilic conditions, at 37 °C, and with a constant rotation of 100 rpm (SI600 Large Shaking Incubator; Stuart, Staffordshire, UK) for the defined periods of time, 24 h, 48 h, 64 h, or 72 h. Bacterial growth was monitored at the referred time points by measuring the OD_{600} of the liquid bacterial cultures.

Bacterial viability

The viability of *H. pylori* grown in liquid media was assessed by two methods: colony forming units (CFUs) counting and flow cytometry using the LIVE/DEAD BacLight Bacterial Viability Kit (Thermo Fisher Scientific), according to the manufacturers' instructions.

For the CFUs counting, at the referred time points, 100 µL of bacterial suspension were collected, serially diluted by 10-fold in BB, and 10 µL of each dilution were plated on TSA plates, in quadruplicates. Plates were incubated in a sealed jar with a microaerophilic atmosphere, at 37 °C for 48 h. At this time, colonies were counted and the number of CFUs/mL was calculated (CFUs/mL = number of colonies ÷ inoculum × dilution factor × 1000 µL).

For the LIVE/DEAD assay, a bacterial suspension of 2×10^6 cells was filtered through a 10 µm CellTrics® filter (Sysmex Partec, Göerlitz, Germany) to remove aggregates. Bacteria were then stained with 0.5 nM SYTO9, a cell-permeant green fluorescent nucleic acid stain that labels both live and dead cells, and with 2 µg/mL Propidium Iodide (PI), a nucleic acid red-fluorescent dye that labels non-viable cells with damaged membranes, for 15 min at room temperature (RT) and in the dark. Data acquisition was immediately performed on a FACSCanto II cytometer (BD Biosciences), and analyzed using the FlowJo™ version 10 software (BD Biosciences). $SYTO9^+$ stained bacterial cells were defined as $SYTO9^+PI^-$ (live) or $SYTO9^+PI^+$ (dead) and results are shown as the frequency of gated cells. SYTO9 and PI single stainings and unstained samples were used as controls.

Isolation of OMVs from bacterial liquid cultures

Isolation of *H. pylori*-derived OMVs was performed from the supernatant of the liquid bacterial cultures. At the specified time points of bacterial growth, 200 mL of bacterial cultures were subjected to low-speed centrifugation at 15,000 x g, for 15 minutes (min) at 4 °C, in a JA25-50 rotor (Avanti J-25; Beckman Coulter, Fullerton, CA, USA), to pellet bacteria. The bacteria-free supernatant was filtered through a 0.45 µm cellulose acetate bottle-top filter unit (Corning, NY, USA), and then OMVs were pelleted by ultracentrifugation at 200,000 x g, for 90 min at 4 °C, in a 70Ti rotor (Optima XE-100; Beckman Coulter). OMVs from the different centrifuge tubes were pooled and washed once in 20 mL sterile 0.9% NaCl solution (saline; Braun; Kronberg im Taunus, German) (200,000 x g, 90 min, 4 °C), resuspended in 100 µL saline and frozen at -80 °C until use.

Transmission Electron Microscopy

The morphology and purity of *H. pylori* cultures grown in F12-cholesterol and of *H. pylori*-derived OMVs were confirmed by transmission electron microscopy (TEM). The presence of protein aggregates in the liquid media was also evaluated by TEM. For negative staining, 7 µL of sample (bacterial suspensions, OMVs or liquid medium) was mounted in Formvar/carbon film-coated mesh nickel grids (Electron Microscopy Sciences, Hatfield, PA, USA), and after the excess liquid was removed, 2 µL of aqueous 1% uranyl acetated solution (#22400; Electron Microscopy Sciences) were added onto the grids. For the ultrastructure analysis, OMVs samples were fixed in a solution of 2% glutaraldehyde (#16316; Electron Microscopy sciences) with 2.5% formaldehyde (#15713; Electron Microscopy sciences) in 0.1 M sodium cacodylate buffer (pH 7.4) for 1 h, at RT, and post fixed in 1% osmium tetroxide (#19190; Electron Microscopy Sciences) diluted in 0.1 M sodium cacodylate buffer. After ultracentrifugation (200,000 x g, 90 min, 4 °C), the pellet was resuspended in Histogel™ (HG-4000-012, Thermo Fisher Scientific) and then stained

with aqueous 1% uranyl acetate solution (Electron Microscopy sciences) overnight, dehydrated and embedded in Embed-812 resin (#14120; Electron Microscopy sciences). Ultra-thin sections (50 nm thickness) were cut on a RMC Ultramicrotome (PowerTome, USA) using Diatome diamond knifes (DDK, Wilmington, DE, USA), mounted on mesh nickel grids (Electron Microscopy Sciences), and stained with uranyl acetate substitute (#11000; Electron Microscopy Sciences) and lead citrate (#11300; Electron Microscopy Sciences) for 5 min each. Negative staining samples and thin sections were examined under a JEOL JEM 1400 transmission electron microscope (JEOL, Tokyo, Japan) and images were digitally recorded using a CCD digital camera Orius 1100W (Tokyo, Japan).

Scanning Electron Microscopy

For scanning electron microscopy (SEM) analysis, 5 mL of bacterial suspension from F12-cholesterol cultures were pre-fixed in 2.5% glutaraldehyde solution, diluted in 0.2 M sodium phosphate buffer (0.2 M Na_2HPO_4•$2H_2O$ and 0.2 M NaH_2PO_4•H_2O in H_2O; PB; pH 7.3), for 24 h at RT. After two washes in PB, samples were post-fixed in 2% osmium tetroxide for 48 h at RT, rinsed in distilled water, and dehydrated in graded ethanol solutions of 50%, 70%, 80%, and 95%, with two final 100% ethanol changes, for 10 min in each dilution. Samples were chemically dried in Hexamethyldisilazane (HMDS) (Sigma-Aldrich Co., St. Louis, MO, USA) by a first incubation in 50% HMDS diluted in absolute ethanol for 24 h, followed by a 15 min incubation in 100% HMDS. Samples were left to air-dry in a fume hood at RT. Dried samples were mounted on an aluminum stub with double-sided adhesive carbon tape and sputter-coated with a thin film of Au/Pd, to improve the electrically conducting properties of the sample surface. Image acquisition was performed using a High resolution (Schottky) Environmental Scanning Electron Microscope with X-Ray Microanalysis and Electron Backscattered Diffraction analysis (FEI Quanta 400 FEG ESEM/EDAX Genesis X4M; Thermo Fisher Scientific).

Nanoparticle Tracking Analysis of OMVs

The quantification and sizing of the OMVs were determined using a NS300 particle-size tracker with the Nanosight NTA 3.0 software (Malvern, Worcestershire, UK). Samples were diluted (1:40,000) in saline to achieve a concentration of 10^7 to 10^9 particles/mL for the analysis. Under controlled fluid flow, three measurements (videos of 30 seconds each) of each sample were acquired as technical replicates and results were averaged. Reads were performed using the camera level adjusted to a value between 14 and 16, and a detection threshold fixed at five. The sample chamber was flushed with sterile PBS between samples, to avoid cross-contamination.

Protein quantification of OMVs

A total of 10^{11} OMVs were diluted in 4x Laemmli buffer (Bio-Rad Laboratories Inc.) with β-mercaptoethanol (Sigma-Aldrich Co.), denaturated at 95 °C for 5 min and loaded onto 7.5% sodium dodecyl sulfate–polyacrylamide gels (SDS-PAGE). After electrophoresis, gels were stained with 25 mL of BlueSafe (NZYTech, Lisbon, Portugal), for 1 h at RT with gentle rotation, washed with distilled water for 10 min three times, and visualized in a GS-800 Calibrated Densitometer (Bio-Rad Laboratories Inc.). Bands were quantified by densitometry using the Quantity One® 1-D version 4.6.8 software (Bio-Rad Laboratories Inc.). Bovine serum albumin (BSA; #05482, Sigma-Aldrich Co.) was used as a protein standard to draw a calibration curve, following the same procedure as OMVs samples. The protein concentration of the OMVs samples was determined by interpolation from the standard curve. This protocol was optimized by Steeve Lima and Paulo Oliveira at i3S (unpublished).

Proteomics analysis

A pellet of 5×10^{11} *H. pylori* 26695 OMVs isolated from liquid bacterial cultures at 48 h, 64 h and 72 h of growth was lysed in cold lysis buffer (1% NP-40, 1% Triton X-100 diluted in PBS, pH7.4) containing 1x Bacterial Protease Arrest™ (GBiosciences, St. Louis, MO, USA) and 6 mg/mL lysozyme (PanReac AppliChem S. L. U., Barcelona, Spain), for 1 h on ice. Upon centrifugation (21,000 x g for 15 min at 4 °C), the cleared lysate was recovered and solubilized in a solution of 100 mM Tris pH 8.5, 1% sodium deoxycholate, 10 mM tris(2-carboxyethyl)phosphine (TCEP), 40 mM chloroacetamide and 1x cOmplete™ protease inhibitor cocktail (Roche Applied Science, Mannheim, Germany), for 10 min, at 95 ºC, with a constant rotation of 1000 rpm (Thermomixer, Eppendorf, Hamburg, Germany). Samples were processed for proteomics following the solid-phase-enhanced sample-preparation (SP3) protocol as described in Hughes *et al* [233]. Briefly, enzymatic digestion was achieved by adding 2 µg Trypsin/LysC to each sample and incubated overnight at 37 ºC with constant rotation (1000 rpm). Protein identification and quantitation was performed by nanoLC-MS/MS using an Ultimate 3000 liquid chromatography system coupled to a Q-Exactive Hybrid Quadrupole-Orbitrap mass spectrometer (Thermo Fisher Scientific). Samples were loaded onto a trapping cartridge (Acclaim PepMap C18 100Å, 5 mm x 300 µm i.d., 160454, Thermo Fisher Scientific) in a mobile phase of 2% acetonitrile (ACN), 0.1% formic acid (FA) at 10 µL/min. After 3 min loading, the trap column was switched in-line to a 50 cm by 75 µm inner diameter EASY-Spray column (ES803, PepMap RSLC, C18, 2 µm, Thermo Fisher Scientific), at 300 nL/min. Separation was generated by gradient mixing A (0.1% FA) and B (80% ACN, 0.1% FA) as follows: 5 min (2.5% B to 10% B), 120 min (10% B to 30% B), 20 min (30% B to 50% B), 5 min (50% B to 99% B), and 10 min (hold 99% B). Subsequently,

the column was equilibrated with 2.5% B for 17 min. Data acquisition was controlled by Xcalibur 4.0 and Tune 2.9 software (Thermo Fisher Scientific). The mass spectrometer was operated in data-dependent (dd) positive acquisition mode alternating between a full scan (m/z 380-1580) and subsequent HCD MS/MS of the 10 most intense peaks from full scan (normalized collision energy of 27%). ESI spray voltage was 1.9 kV. Global settings: use lock masses best (m/z 445.12003), lock mass injection Full MS, chrom. peak width (FWHM) 15s. Full scan settings: 70k resolution (m/z 200), AGC target 3×10^6, maximum injection time 120 ms. dd settings: minimum AGC target 8×10^3, intensity threshold 7.3×10^4, charge exclusion: unassigned, 1, 8, >8, peptide match preferred, exclude isotopes on, dynamic exclusion 45 s. MS2 settings: microscans 1, resolution 35k (m/z 200), AGC target 2×10^5, maximum injection time 110 ms, isolation window 2.0 m/z, isolation offset 0.0 m/z, spectrum data type profile. Three biological replicates were used for each time point and the LC-MS acquisition of each sample was performed in triplicate.

The protease activity of OMVs against the cytoplasmic domain of JAM-A was also detected by nanoLC-MS/MS. For that, a synthetic 40-amino acid cytoplasmic domain peptide of JAM-A (^{260}AYSRGHFDRTKKGTSSKKVIYSQPSARSEGEFKQTSSFLV^{299}) was incubated with *H. pylori* 26695 OMVs or with *H. pylori* 26695 sonicate for 15 min. Samples were then loaded onto a trapping cartridge in a mobile phase of 2% ACN, 0.1% FA at 30 µL/min. After 1 min loading, the trap column was switched in-line to a 10 µm inner diameter transfer line (ES993, PepMap RSLC, C18, 2 µm, Thermo Fisher Scientific), at 1 µL/min. Separation was generated by gradient mixing A (0.1% FA) and B (80% ACN, 0.1% FA) as follows: 2 min (2.5% B), 3 min (99% B). Subsequently, the system was equilibrated with 2.5% B. Data acquisition was controlled by Xcalibur 4.0 and Tune 2.9 software (Thermo Fisher Scientific). The mass spectrometer was operated in dd positive acquisition mode alternating between a full scan (m/z 380-1300) and subsequent HCD MS/MS of the 5 most intense peaks from full scan (normalized collision energy of 27%). ESI spray voltage was 1.9 kV. Global settings: use lock masses best (m/z 445.12003), lock mass injection Full MS, chrom. peak width (FWHM) 15s. Full scan settings: 70k resolution (m/z 200), AGC target 3×106, maximum injection time 120 ms. dd settings: minimum AGC target 8×10^3, intensity threshold 7.3×10^4, charge exclusion: unassigned, 1, 8, >8, peptide match preferred, exclude isotopes on, dynamic exclusion 5 s. MS2 settings: microscans 1, resolution 35k (m/z 200), AGC target 2×10^5, maximum injection time 110 ms, isolation window 4.0 m/z, isolation offset 0.0 m/z, spectrum data type profile. Data analysis was performed with the Proteome Discoverer software v2.5.0.400 (Thermo Scientific).

Database searching, protein identification and classification

Raw data regarding OMVs samples was processed using the Proteome Discoverer 2.5.0.400 software (Thermo Fisher Scientific) and searched against the UniProt (www.uniprot.org) database for the *Helicobacter pylori* 26695 Proteome 2021_01 release, 1552 entries, and a common contaminant database from MaxQuant (version 1.6.2.6, Max Planck Institute of Biochemistry, Munich, Germany). The Sequest HT and the MS Amanda 2.0 search engines, together with the Inferys PSM rescoring node, were used to identify tryptic peptides. The ion mass tolerance was 10 ppm for precursor ions and 0.02 Da for fragment ions. Maximum allowed missing cleavage sites was set to 2. Cysteine carbamidomethylation was defined as constant modification. Methionine oxidation, asparagine and glutamine deamidation, peptide N-terminus glutamine to pyro-glutamine, and protein N-terminus acetylation, methionine loss, and methionine loss plus acetylation, were defined as variable modifications. Peptide confidence was set to high. The processing node Percolator was enabled with the following settings: maximum delta Cn 0.05; decoy database search target false discovery rate (FDR) 1%, validation based on q-value. Protein label free quantitation was performed with the Minora feature detector node at the processing step. Precursor ions quantification was performed at the processing step with the following parameters: unique plus razor peptides were used for quantification, precursor abundance based on intensity and normalization based on total peptide amount. Common contaminants were excluded from data analysis. The ANOVA hypothesis test (individual proteins) for *p*-value calculation was performed for the three bacterial growth periods. Differentially expressed proteins were identified using the following parameters: fold change ratios ± 2.00 and $p < 0.05$. The total abundance of the predicted groups was calculated by the sum of the abundance of proteins classified for each group. Prediction of proteins cellular localization, biological process, and molecular function was obtained from the gene ontology (GO) UniProt database (www.uniprot.org). The mass spectrometry proteomics data have been deposited to the ProteomeXchange Consortium via the PRIDE [234] partner repository with the dataset identifier PXD025393.

Immunogold labelling of dsDNA in *H. pylori* OMVs

OMVs samples were treated with DNase I (5 µg/µL, 30 min at 37 °C; Roche Diagnostics GmbH, Mannheim, Germany) and heat-inactivated at 60 °C for 10 min. Samples were washed in saline (200,000 x g, 90 min, 4 °C), fixed in a solution of 2.5% glutaraldehyde (Electron Microscopy sciences) with 2% formaldehyde (Electron Microscopy sciences) in 0.1 M sodium cacodylate buffer (pH 7.4) for 1 h, at RT, and post fixed in 1% osmium tetroxide (Electron Microscopy sciences) overnight at 4 °C. After ultracentrifugation (200,000 x g, 90 min, 4 °C), the pellet was resuspended in Histogel™ (Thermo Fisher

Scientific), stained with aqueous 1% uranyl acetate solution (Electron Microscopy sciences), dehydrated and embedded in Embed-812 resin (Electron Microscopy sciences). Ultra-thin sections (50 nm thickness) were cut, mounted on mesh nickel grids previously treated with DNase I (Roche Diagnostics GmbH), and incubated with the antigen retrieval solution 14.4% sodium metaperiodate (#311448, Sigma-Aldrich Co.) for 1h. After blocking in tris-buffered saline (TBS) with 2% BSA for 30 min, sections were incubated with the primary antibody mouse monoclonal anti-dsDNA (1:25 dilution; Bioporto, Hellerup, Denmark) overnight, washed four times in TBS with 0.1% BSA and incubated with the secondary antibody goat anti-mouse IgG (#AB39614, 1:20 dilution; Abcam, Cambridge, UK) conjugated with 15 nm gold particles for 45 min. Prior to washes, sections were fixed in 1% glutaraldehyde for 5 min, washed six times with MilliQ water (Millipore, Billerica, MA, USA) for 10 min, air-dried and contrasted with 1% uranyl acetate (saturated aqueous solution) for 5 min. Sections were examined under a JEOL JEM 1400 transmission electron microscope (JEOL) and images were digitally recorded using a CCD digital camera Orius 1100W.
To confirm the specificity of the primary antibody, a negative control was included, which was incubated only with the secondary antibody.

DNA and RNA extraction from *H. pylori* OMVs, and cDNA synthesis

DNA was extracted from the parental *H. pylori* 26695 and Tx30a strains, and from OMVs derived from *H. pylori* 26695 and Tx30a, using the QIAamp® DNA Mini Kit (Qiagen, Hilden, Germany), following the manufacturer's instructions. RNA was extracted from OMVs secreted by *H. pylori* 26695 and Tx30a using the PureLink® RNA Mini Kit (Ambion, Thermo Fisher Scientific), following the manufacturer's instructions.
Prior to DNA and RNA extraction, extracellular DNA and RNA were removed from the surface of OMVs. For that, samples were subjected to a sequential treatment with RNase A (0.5 µg/µL, 20 min at 37 °C; PureLink™, Thermo Fisher Scientific), NZY Ribonuclease inhibitor (4U/µL; NZYtech), DNase I (5 µg/µL; 30 min at 37 °C; Roche Diagnostics GmbH), and DNase I heat-inactivation at 60 °C for 10 min. Concentration and quality of DNA and RNA were assessed by measuring the absorbance at 260 nm and 280 nm in a NanoDrop® 1000 Spectrophotometer (Thermo Fisher Scientific).
RNA (500 ng) was reversed transcribed to cDNA using the NZY M-MuLV Reverse Transcriptase (200 U/µL; NZYTech), random hexamer mix (50ng/µL; NZYTech), dNTPs NZYMix (0.5 mM; NZYTech), NZY Ribonuclease inhibitor (4U/µL; NZYtech), DTT (1 mM; Thermo Fisher Scientific), 10x Reaction Buffer (NZYtech), and nuclease free-water, in a final volume of 20 µL. Reaction was carried on a T100™ Thermal Cycler (Bio-Rad Laboratories Inc.) with the following conditions: 10 min at 25 °C, 1 h at 37 °C and 10 min at 70 °C.

cagA, *vacA* and *ureB* amplification

DNA and cDNA were used for *cagA*, *vacA* and *ureB* amplification by polymerase chain reaction (PCR), using the primers shown in **Table 1**. PCR mixtures were prepared to a final volume of 25 µL containing 1 µL DNA or cDNA, AmpliTaq Gold DNA polymerase (0.5 U; Applied Biosystems, Thermo Fisher Scientific), $MgCl_2$ (2.5 µM; Applied Biosystems), PCR buffer II (1x; Applied Biosystems), dNTPs NZYMix (0.5 mM; NZYTech) and 0.4 µM of forward and reverse primers, in nuclease free-water. Reactions were incubated for 9 min at 95 °C (pre-denaturation), followed by 35 cycles of 30 s at 95 °C (denaturation), 1 min at 60 °C (annealing), and 45 s at 72 °C (extension), and a final step of 10 min at 72 °C (final extension). PCR amplification was performed on a T100™ Thermal Cycler (Bio-Rad Laboratories Inc.). Reaction products were visualized in GreenSafe (NZYTech) stained 2% agarose gels in a Gel Doc XR+ System (Bio-Rad Laboratories Inc.).

Genomic DNA extracted from *H. pylori* 26695 and Tx30a were used as positive controls. PCR negative controls containing nuclease-free water, saline, DNase I-treated DNA or cDNA obtained from RNase A-treated RNA, instead of genetic material, were processed as described.

Table 1. Primers used for PCR amplification.

Primer	Sequence (5'-3')	Amplicon size (bp)
cagFN1	GATAAGAAYGATAGGGATAA	190
cagRN1	AATACTGATTCTTTTTGG	
Va1F *	ATGGAAATACAACAAACACAC	s1: 176; s2: 203
Va1XR *	CCTGARACCGTTCCTACAGC	
UreB_RT_F	CTATGGCAGCTATTGCCGGA	230
UreB_RT_R	GTTTGAGGGCGGATCCTTGA	

* van Doorn *et al*., Journal of Clinical Microbiology 1998 [235]

Cell culture

The human gastric adenocarcinoma cell lines MKN74 (a gift from Carla Oliveira, University of Porto) and NCI-N87 (ATCC® CRL-5822™; ATCC, Manassas, VA, USA) were cultured in RPMI medium (Gibco®), supplemented with 10% of heat inactivated FBS (HyClone™, GE Healthcare Life Sciences, Logan, UT, USA) and 100 U-100 µg/mL penicillin G-streptomycin sulfate (Gibco®), at 37 °C under a 5% CO_2 humidified atmosphere.

For *in vitro* experiments with *H. pylori* and OMVs, cells to be challenged were seeded and maintained in antibiotic-free culture medium until the end of the experiment. Medium was changed every other day and immediately before co-culture.

Challenge of gastric cell lines with OMVs and *H. pylori*

Unless stated otherwise, *H. pylori* OMVs were added daily to gastric epithelial cells at a defined number of $2x10^6$ vesicles per cell, for the time points specified. Infection experiments were performed with *H. pylori* grown on TSA plates for 48 h. At this time point, bacteria were collected in 1 mL of saline and the OD_{600} of the bacterial suspension was determined. Bacteria were added to gastric cell monolayers at a multiplicity of infection (MOI) of 100 bacteria per gastric cell and the co-culture was maintained for 24 h, unless stated otherwise. Uninfected control cells were treated similarly, with the addition of saline instead of OMVs or *H. pylori*. Co-cultures were maintained at 37 °C under a 5% CO_2 humidified atmosphere.

Human RNA Processing and AmpliSeq Expression Profiling

MKN74 cells (200,000 cells) were seeded on 4 cm^2 12-well plates and maintained for 24 h. Then, cells were challenged with saline (control), with $5x10^{11}$ *H. pylori* OMVs (~ 20 µg protein) or with *H. pylori* at MOI 100 for 24 h. mRNA was extracted from MKN74 co-cultures using the PureLink® RNA Mini Kit (Ambion, Thermo Fisher Scientific), following the manufacturer's instructions.

Ion Torrent sequencing libraries were prepared according to the Ampliseq Library prep kit protocol as published in [236]. Briefly, 100 ng of total RNA was reverse transcribed followed by a cDNA amplification using the AmpliSeq human transcriptome gene expression primer pool which is composed by 18,574 protein-coding mRNAs and 2,228 ncRNA. Amplicons were digested and barcoded to the target amplicons followed by a ligation to magnetic beads. Templating was performed with an Ion Chef (Thermo-Fisher) followed by sequencing on an Ion AmpliSeq™ Transcriptome Human Gene Expression panel (Thermo-Fisher). AmpliSeq sequencing data was analysed within the Ion Torrent Suite using the Ion Torrent mapping alignment program (TMAP). TMAP implements a two-stage mapping approach using four different algorithms tow achieve better specificity and sensitivity.

Differential expression analysis for OMVs- and *H. pylori*-infected samples was performed against the non-infected controls by DESeq2 package, which applied a negative binomial distribution test to model gene counts and test for differential expression. Only genes with a *p* value adjusted for multiple testing (Benjamini-Hochberg method) below 0.05 were considered as statistically significant.

All analysis and representations were performed in R version 4.0.5 (R Foundation for Statistical Computing, Vienna, Austria). Quality control of the expression profiles of all experimental conditions were investigated through Principal Component Analysis (PCA). Venn diagrams with the common up-regulated and downregulated genes were generated with the VennDiagram R package.

The list of the genes involved in each of the analyzed pathways were extracted from Kyoto encyclopedia of genes and genomes (KEGG) website for the cell cycle (hsa04110) and DNA repair (hsa03430 for mismatch repair; hsa03410 for base excision repair; hsa03440 for homologous recombination). To allow for a better representation of up and downregulation of genes between the different experimental conditions, these values were converted into a fold-change format. This was accomplished by subtracting the $\log_2$ of the mean values of the non-infected triplicates by the $\log_2$ value of each infected samples, OMVs and *H. pylori*.

Gene-set enrichment analysis

Pre-ranked pairwise gene-set enrichment analysis (GSEA) was conducted in the GSEA tool for the Gene Ontology (Biological Processes, BP) and KEGG pathway databases. Only the top 10 pathways with the highest normalized enrichment score (NES) and a FDR below 0.25, as per the GSEA recommendation, were considered.

Fluorescent labelling of OMVs

OMVs were labeled with 1 µM Vybrant® DiD Cell-Labeling solution (#V22887; LifeTechnologies) for 1 h at 37 °C, protected from light and under agitation. Excess dye was removed by dialysis using Pur-A-Lyzer™ Midi Dialysis 3500 tubes (Sigma-Aldrich Co.), for 1 h at RT, using saline as the dialysis buffer and performing saline renewal every 15 min, according to the manufacturer's instructions. DiD-labelled OMVs were collected from the Pur-A-Lyzer™ tube, washed once in 20 mL saline (200,000 x *g*, 90 min, 4 °C) and resuspended in saline. Saline was submitted to the same protocol and used as a negative control.

Internalization of OMVs

To visualize the internalization of *H. pylori* OMVs, MKN74 cells were previously transfected with a fluorescence reporter plasmid, either expressing a constitutively active Rab5 (Rab5Q79L-GFP mutant forming large vacuoles) as an early endosome marker [237], or LAMP1-GFP, as a marker for late endosome/lysosome. Cells (70,000 cells) were plated on 2 cm^2 24-well plate with 1 mL of growth medium without antibiotics, on the day before transfection. Cell transfections were performed using Rab5Q79L-GFP and LAMP1-GFP DNA plasmids (kindly donated by Prof. Allan I. Levey from Emory University, Atlanta, GA, USA), in a final volume of 200 µL of serum- and antibiotics-free Opti-MEM™ (Gibco™, Thermo Fisher Scientific), using Lipofectamine™ 2000 Transfection Reagent (Invitrogen, Thermo Fisher Scientific), and following the manufacturer's protocol. Plasmids (400 ng in 25 µL) and Lipofectamine (1 µL in 25 µL) were diluted in Gibco™ Opti-MEM™, before

complexing at 1:1 ratio (final volume of 50 µL). After overnight incubation with the transfection mixture, at 37 °C in a CO_2 incubator, cells were washed and cultured in fresh Opti-MEM™ medium for 24 h. Rab5Q79L-GFP and LAMP-1-GFP transfected cells were then pulsed with DiD-labelled saline (control) or with 2.5×10^{12} DiD-labelled OMVs (~100 µg protein) for 3 or 15 min, respectively. After the challenge, cells were washed twice with saline, fixed in 4% paraformaldehyde for 1 h, and mounted with ProLong™ Gold Antifade Mountant (Thermo Fisher Scientific). Confocal images were acquired using an Abberior Instruments Expert-Line Quadscan confocal microscope coupled to a Nikon Ti stand equipped with autofocus (PFS) and a piezo stage for z-scans. An oil-immersion 60× 1.4 NA Plan-Apo objective lens (Nikon, Lambda Series, Tokyo, Japan) and a 0.8 Airy-unit pinhole were used in all acquisitions. High-sensitivity (low dynamic-range) avalanche photo-diode detectors were used in photon-counting mode with dwell times in the 5-20 micro-second range.

Immunofluorescence

MKN74 and NCI-N87 gastric epithelial cells were seeded on glass coverslips (Paul Marienfeld GmbH & Co. KG, Lauda-Königshofen, Germany) on 2 cm^2 24-well plates, and grown at 100% confluence for 5 days. Challenge with 1×10^{12} OMVs (~ 40 µg protein) or with *H. pylori* (MOI 100) were performed as described above. Cells treated with saline were used as controls. At the specified time-points of 24 h (control, OMVs and *H. pylori*) and 72 h (OMVs), cells were washed with saline and fixed in ice-cold methanol for 10 min on ice. Upon blocking with 5% goat serum-0.3% Triton X-100 in saline, for 1 h at RT, cells were incubated with the primary antibodies, for 2 h at RT, washed and incubated with the respective fluorochrome-conjugated secondary antibodies, for 1 h at RT, in the dark. Coverslips were mounted on slides with Vectashield®-DAPI (Vector Laboratories, Burlingame, CA, USA) and fluorescence was monitored in a Zeiss Axio Imager Z1 upright fluorescence microscope (Carl Zeiss, Oberkochen, Germany). Image processing and analysis were performed using the Fiji (ImageJ) version 1.52 software.

Antibodies were as follows: goat polyclonal anti-JAM-A (#AF1103, 1:300; dilution, R&D Systems), rabbit monoclonal anti-E-Cadherin (#3195, 1:150 dilution; Cell Signaling), mouse monoclonal anti-ZO1 (#33-9100, 1:300 dilution; Thermo Fisher Scientific), goat anti-mouse IgG Alexa Fluor 594 (#A-11032, 1:500; dilution, Thermo Fisher Scientific), goat anti-rabbit IgG Alexa Fluor 488 (#A-11034, 1:500 dilution; Thermo Fisher Scientific), and donkey anti-goat IgG Alexa Fluor 594 (#A-11055, 1:500 dilution; Thermo Fisher Scientific).

Western blotting

MKN74 and NCI-N87 epithelial cells were seeded and grown at 100% confluence for 5 days on 2 cm^2 24-well plates, and treated with saline (control), with 1×10^{12} OMVs (~ 40 µg protein) or with *H. pylori* (MOI 100), as described above. Co-cultures were washed with saline and total cell lysates were prepared in cold lysis buffer (1% NP-40, 1% Triton X-100 in PBS, pH7.4) containing a cocktail of proteases (Roche Applied Science) and phosphatases (Sigma-Aldrich Co.) inhibitors. The protein concentration of the cleared lysate, recovered upon centrifugation, was assessed using the DC protein assay (Bio-Rad Laboratories Inc., Hercules, CA, USA), according to the manufacturer's instructions. Samples containing 10 µg of protein were diluted in 4x Laemmli buffer (Bio-Rad Laboratories Inc.) with β-mercaptoethanol (Sigma-Aldrich Co.), denaturated at 95 °C for 5 min, and loaded onto 7.5% sodium dodecyl sulfate–polyacrylamide gels (SDS-PAGE). After electrophoresis, proteins were transferred onto a 0.45 µm pore-size nitrocellulose membrane (Bio-Rad). Membranes were blocked with 5% fat-free milk in TBS with 0.1% Tween 20, for 1 h at RT, and further blotted with the appropriate unconjugated primary antibody, overnight at 4 °C. Prior to washes with TBS-0.1% Tween 20, membranes were incubated with the respective horseradish peroxidase (HRP)-conjugated secondary antibodies for 1 h at RT, and signal detection was performed with Clarity Western ECL Substrate (Bio-Rad). Bands were quantified by densitometry using the Quantity One® 1-D version 4.6.8 software (Bio-Rad Laboratories Inc.).

Antibodies were as follows: rabbit monoclonal anti-JAM-A (#ab52647, 1:300 dilution; Abcam), mouse monoclonal anti E-Cadherin (clone 24E10, #3195, 1:1000 dilution; Cell Signaling Technology), mouse monoclonal anti-ZO1 (#33-9100, 1:500 dilution; Thermo Fisher Scientific), mouse monoclonal anti-GAPDH (#sc-47724, 1:5000 dilution; Santa Cruz Biotechnology), and HRP conjugated ECL™ donkey anti-rabbit IgG (#NA934V, 1:5000 dilution; GE Healthcare) and ECL™ sheep anti-mouse IgG (#NA931V, 1:5000 dilution; GE Healthcare).

Transepithelial electrical resistance (TER) and fluorescein isothiocyanate (FITC)-dextran permeability assay

Gastric epithelial cells were seeded and grown at 100% confluence for 5 days in 6.5mm Transwell® with 3.0 µm Pore Polyester Membrane Insert (Corning). The integrity of the epithelial monolayer was monitored by measuring the transepithelial electrical resistance (TER) using a Millicell ERS Voltohmmeter (EMDMillipore, Germany) and the procedures, equilibration and decontamination of the electrode were performed according to the manufacturer's instructions, and as previously described [232]. To avoid temperature influence, plate was allowed to reach RT for 15 min before measurement. TER was

measured every 24 h, and, after each measurement, media at both upper and lower compartments were changed. Cells were challenged daily with 1×10^{11} OMVs (~ 4 µg protein) and in the beginning of the experiment with *H. pylori* (MOI 100), during 72 h. At the end of the experiment, paracellular permeability was assessed by measuring the diffusion of 4 KDa FITC-dextran molecules (FD4, Sigma-Aldrich Co.) across the cell monolayer. Upon TER measurement, media was changed and allowed to equilibrate for 1 h at 37 °C. FITC-dextran was added to the upper compartment, at a final concentration of 1 mg/mL, and incubated at 37 °C for another hour. The presence of FITC-dextran in the bottom compartment was measured by fluorescence at $485_{Ex}/544_{Em}$, on a Synergy Mx 96-well. Media without FITC-dextran was used as blank.

Statistical analyses

Data were analyzed using the GraphPad Prism version 9.1.0 software (San Diego, CA, USA). For the comparison of two groups, the unpaired Student's t-test was used. The one-way, the two-way and the Brown-Forsythe ANOVA, with post-hoc tests (Tukey's, Dunnett's or Sidak's) for paired comparisons, were applied for comparisons between three independent groups. Statistical significance was set at *p*-values ≤ 0.05 (* $p \leq 0.05$, ** $p \leq 0.01$, $^{\#\#}$ $p \leq 0.01$, *** $p \leq 0.001$, $^{\#\#\#}$ $p \leq 0.001$, **** $p \leq 0.0001$, $^{\#\#\#\#}$ $p \leq 0.0001$).

RESULTS

PART I: Isolation method and characterization of outer membranes vesicles of *Helicobacter pylori* grown in a chemically defined medium

The current methods described for the isolation of *H. pylori*-derived OMVs are diverse and time-consuming. They include several ultracentrifugation and/or density gradient centrifugation steps to purify and recover OMVs, after an initial low-speed centrifugation and culture medium filtration intended to remove the bacteria [238, 239]. Besides being laborious, the existing methods rely on complex and chemically undefined media for bacterial growth, such as Brucella broth (BB) or Brain Heart Infusion (BHI), owing to the widely held notion that *H. pylori* is a fastidious organism and requires such enriched media to grow [118, 121, 124, 125]. Nonetheless, Testerman and colleagues have demonstrated that *H. pylori* has few nutritional requirements and can grow in the chemically defined Ham's-F12 (F12) liquid medium. Furthermore, they have shown that supplementation of F12 with cholesterol, bovine seum albumin (BSA), or fetal bovine serum (FBS), can further enhance *H. pylori* growth [240, 241]. Therefore, we aimed to develop a simpler and faster method to isolate OMVs from *H. pylori*, based on a chemically defined medium for bacterial growth. This enables the standardization of the isolation method, which is pivotal for downstream applications.

1. *H. pylori* growth and viability in F12 liquid medium supplemented with cholesterol

Considering our goal to isolate OMVs from *H. pylori* cultures grown in a chemically defined medium, we started by characterizing the bacterial growth and viability in the Ham's F-12 liquid medium supplemented with cholesterol, previously reported to support *H. pylori* growth [240].

The bacterial growth of *H. pylori* 26695 was monitored by measuring the optical density at 600 nm (OD_{600}) of the bacterial liquid cultures at 24 h, 48 h, 64 h, and 72 h, starting with an inoculum density of 0.02 per mL at OD_{600} (~6 x 10^6 CFUs/mL) in 200 mL of F12-cholesterol medium (**Figure 6A**). The growth curve was predicted using the Gompertz model [242] fitted to our data. *H. pylori* presented an exponential growth during the first 32 h of culture, after which it reached a stationary phase that lasted nearly until the endpoint of 72 h. The experimental OD_{600} values at 24 h, 48 h, 64 h, and 72 h were, respectively, 0.127 ± 0.004, 0.147 ± 0.003, 0.148 ± 0.004, and 0.139 ± 0.003, decreasing 6.1% from 64 h to 72 h, although not statistically significant (p = 0.3528; one-way ANOVA with post-hoc Tukey's test), indicating that bacterial growth might become limited by nutrient availability. The growth kinetics of *H. pylori* 26695 in the chemically defined F12-cholesterol medium and in the complex BB medium supplemented with 5% FBS was compared, under the same

experimental conditions (**Figure 6A)**. The growth curve was similar for both media, although bacteria grew faster in BB-FBS, with bacterial cultures reaching higher densities (OD_{600} at 24h: 0.160 ± 0.010; 48h: 0.199 ± 0.004; 64h: 0.206 ± 0.011; and 72h: 0.209 ± 0.005).

To assess the viability of *H. pylori* 26695 strain in F12-cholesterol, we determined the number of colony forming units (CFUs) and performed the LIVE/DEAD BacLight Bacterial Viability assay using flow cytometry. The number of CFUs increased until 48 h of bacterial growth (24 h: 9.46 ± 0.96 $\times 10^7$ CFUs/mL; 48 h: 1.12 ± 0.06 $\times 10^8$ CFUs/mL), and decreased slightly at 64 h, although not statistically significantly (64 h: 9.11 ± 0.71 $\times 10^7$ CFUs/mL; 48 h *vs* 64 h: $p = 0.2080$), and until 72 h (6.38 ± 0.66 $\times 10^7$ CFUs/mL,48 h *vs* 72 h: $p = 0.0082$; 64 h *vs* 72 h: $p = 0.0571$) (**Figure 6B**). For comparative purposes, we also evaluated the number of CFUs in BB-FBS bacterial cultures (**Figure 6B**). The number of CFUs was similar at 24 h of growth in both media (24 h: 8.47 ± 0.38 $\times 10^7$ CFUs/mL; $p = 0.8217$), and significantly lower in BB-FBS at 48 h (6.88 ± 0.44 $\times 10^7$ CFUs/mL; $p < 0.0001$), 64 h (4.58 ± 0.71 $\times 10^7$ CFUs/mL; $p < 0.0001$) and 72 h (3.00 ± 0.70 $\times 10^7$ CFUs/mL; $p = 0.0030$). These results show that F12-cholesterol medium sustains the growth and a higher number of viable *H. pylori*, although at a slower rate than BB-FBS medium. The viability of *H. pylori* 26695 grown in F12-cholesterol was also evaluated by another method, using the LIVE/DEAD BacLight assay. This assay relies on the simultaneous staining with two fluorescent nucleic acids dyes to distinguish between live and dead bacteria: SYTO9 (green) that enters in all bacterial cells, staining both live and dead cells, and propidium iodide (PI; red) that enters in cells with a disrupted membrane, labelling only dead bacteria. Using SYTO9 to define the bacterial cell population, the percentage of live ($SYTO9^+PI^-$) and dead ($SYTO9^+PI^+$) bacteria was then calculated for each sample. No statistically significant differences in the percentage of live (48 h: 93.3 ± 1.8%; 64 h: 92.8 ± 1.6%; 72 h: 91.0 ± 1.7%) and dead (48 h: 6.7 ± 1.8%; 64 h: 7.1 ± 1.6%; 72 h: 8.7 ± 1.7%) bacteria were found between the experimental time points (**Figure 6B**). This shows that bacteria remained viable until 72 h, despite the above-mentioned decrease in the number of CFUs.

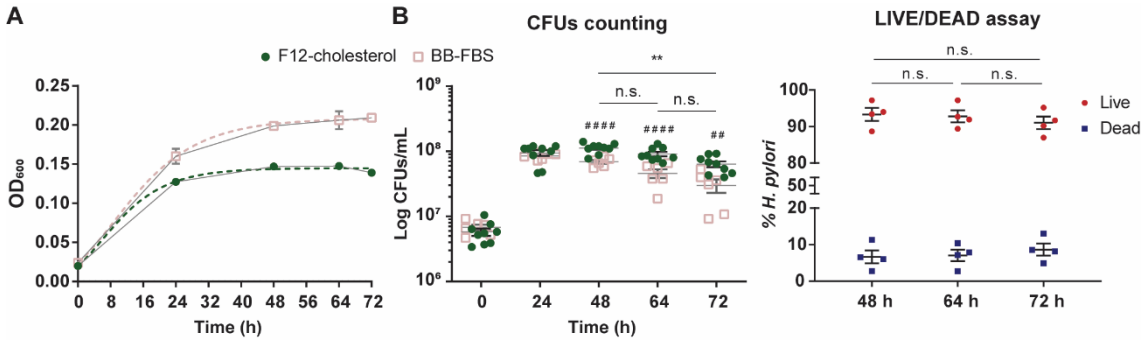

Figure 6. Kinetics and viability of *H. pylori* growth in liquid F-12-cholesterol.

(A) Growth curve of *H. pylori* 26695 grown in F12 liquid medium supplemented with 1x cholesterol (F12-cholesterol; continuous line defined by the green circles) or in BB liquid medium supplemented with 5x FBS (BB-FBS; continuous line defined by the red squares), modeled using the Gompertz growth equation model (dotted lines), calculated with GraphPad Prism, and based on the optical density measurements of the bacterial suspension at 600 nm (OD_{600}) at 24 h, 48 h, 64 h, and 72 h of culture. Data are shown as mean ± SEM of 16 (F12-cholesterol) or 6 (BB-FBS) biological replicates. **(B)** Bacterial viability evaluated by colony-forming units (CFUs) counting (left graph) and the LIVE/DEAD BacLight Bacterial Viability assay (right graph). The number of CFUs was determined at the referred time points, represented as CFUs/mL. Each dot represents a biological replicate (n=9 for F12-cholesterol or n=6 for BB-FBS) and data are shown as mean ± SEM. Statistical significance was evaluated using the one-way ANOVA with post-hoc Tukey's test, comparing all F12-cholesterol datasets with each other; only comparisons between 48 h, 64 h and 72 h were illustrated for the sake of simplicity; ** $p \leq 0.01$, n.s. – not significant. Statistical significance between F12-cholesterol and BB-FBS datasets at each time point was evaluated using the two-way ANOVA with post-hoc Sidak's test. $^{\#\#}p \leq 0.01$, $^{\#\#\#\#}p \leq 0.0001$. LIVE/DEAD BacLight Bacterial Viability assay at 48 h, 64 h, and 72 h of growth, by flow cytometry. After sample staining with SYTO9 and PI dies and acquisition on a FACSCanto II cytometer, live and dead bacteria were gated and defined as $SYTO9^{+}PI^{-}$ and $SYTO9^{+}PI^{+}$, respectively. Each dot represents a biological replicate (n=4) and data are shown as mean ± SEM of the frequency of gated $SYTO9^{+}PI^{-}$ and $SYTO9^{+}PI^{+}$ bacteria. Statistical significance was evaluated using the two-way ANOVA with post-hoc Tukey's test; n.s. – not significant.

2. Morphology of *H. pylori* grown in liquid F12-cholesterol

Knowing that *H. pylori* morphology changes from a bacillary to a coccoid structure in response to nutrient deprivation and other adverse environmental conditions [243, 244], which could explain the differences between CFUs counts and LIVE/DEAD assay results, we evaluated the morphological alterations during the bacterial growth in F12-cholesterol. Bacillary, U-shaped, and coccoid bacteria were manually counted from negative stain transmission electron microscopy (TEM) micrographs taken from 48 h, 64 h, and 72 h-bacterial liquid cultures (**Figure 7A**). No statistically significant differences were found

regarding the frequency of each morphological shape between samples collected at 48 h and 64 h, and between 64 h- and 72 h-samples (**Figure 7B**). However, a significant decrease in the number of bacillary (p = 0.003) and an increase in the number of coccoid *H. pylori* (p = 0.012) were observed in samples collected at 72 h when compared to those obtained at 48 h. This observation suggests that coccoid forms are viable but non-culturable [18], as there was no alteration in the frequency of viable bacteria, assessed by the LIVE/DEAD assay, at this time point. As an ancillary analysis, we checked the morphology of *H. pylori* grown in F12-cholesterol by scanning electron microscopy (SEM) (**Figure 7C**), which confirmed that the bacillary shape was predominant at all time points, with the U-shape and coccoid bacteria becoming noticeable in the 72 h cultures.

Altogether, these results show that the F12-cholesterol medium is capable of nutritionally support *H. pylori* growth, preserving its typical bacillary morphology and viability.

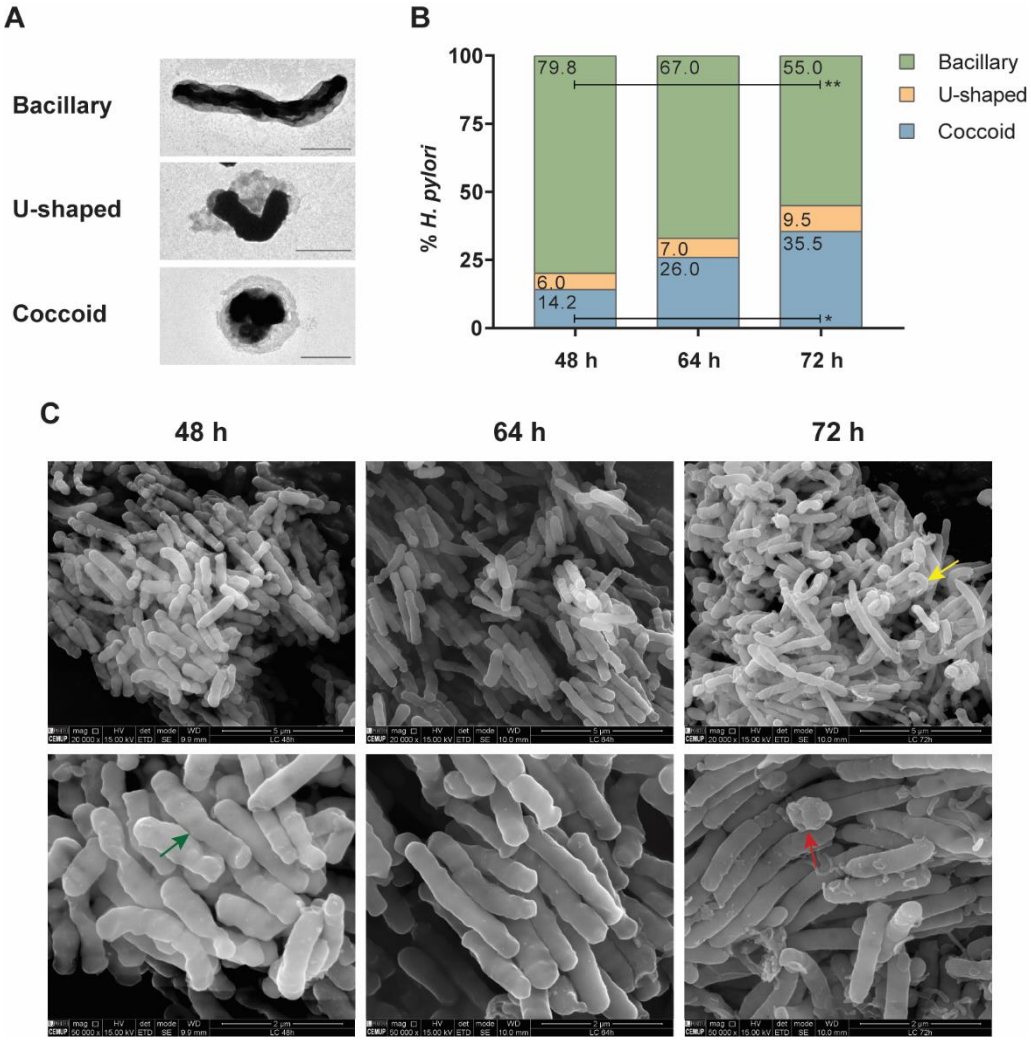

Figure 7. Morphology of *H. pylori* grown in liquid F-12-cholesterol.

(A) Representative negative stain transmission electron microscopy (TEM) micrographs of bacillary, U-shaped, and coccoid forms of *H. pylori* from a 64 h F12-cholesterol liquid culture. Scale bars: 1 µm; 80,000x (bacillary and coccoid) and 8,000x (U-shaped) original magnifications. **(B)**

Quantification of bacillary, U-shaped, and coccoid forms of *H. pylori* present in F12-cholesterol liquid cultures at 48 h, 64 h, and 72 h from negative stained TEM micrographs, using manual counting. The frequency of each bacterial form was calculated considering the total number of bacteria (741, 1215, and 1061) counted in micrographs taken from samples of each time point, 48 h (n=5), 64 h (n=5), and 72h (n=2), respectively. The mean frequency of each form is displayed inside the respective bar. Statistical significance was evaluated using the two-way ANOVA with post-hoc Tukey's test, comparing all datasets with each other; statistical significance was only observed between 72 h and 48 h for bacillary and coccoid forms; * $p \leq 0.05$, ** $p \leq 0.01$. **(C)** Representative scanning electron micrographs of 48 h, 64 h, and 72 h *H. pylori* liquid cultures. Bacillary (green arrow), U-shapped (yellow arrow) and coccoid (red arrow) forms of *H. pylori* are represented. Top images: scale bars: 5 µm; 20,000x original magnification. Bottom images: scale bars: 2 µm; 50,000x original magnification.

3. Quantification and morphological characterization of OMVs secreted by *H. pylori* grown in F12-cholesterol medium

After ensuring that the F12-cholesterol medium supports both growth and viability of *H. pylori* 26695 under our experimental settings, we optimized the OMVs' isolation protocol to be fast and simple, while reliable. This protocol comprises one low-speed centrifugation followed by a 0.45 µm-filtration to deplete both bacterial cells and debris, one ultracentrifugation to recover OMVs, and a final ultracentrifugation to wash the OMVs fraction (**Figure 8**). The overall duration of the protocol is of approximately 4 h, distributed in 60 min of hands-on and 195 min of hands-off time. This protocol is substantially shorter than those published, which report the hands-off time between 335 min to 1170 min [119, 124].

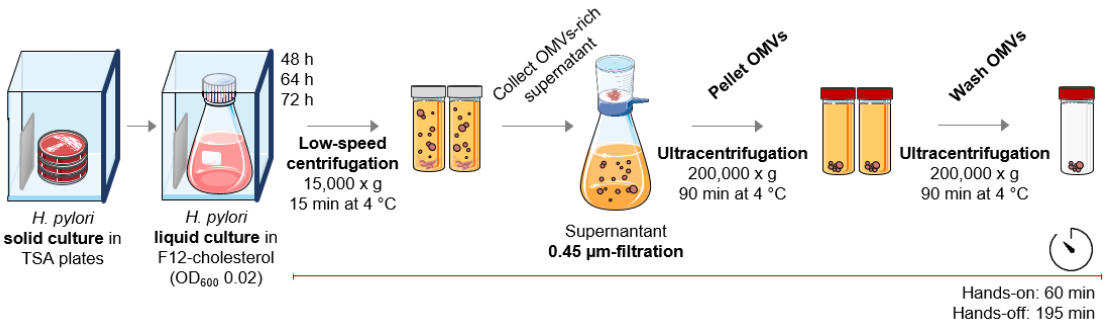

Figure 8. Outline of the OMVs isolation method from *H. pylori* cultures in F12-cholesterol medium.

Schematic representation of the method to isolate OMVs from *H. pylori* liquid cultures based on F12-cholesterol medium. The isolation protocol comprises a hands-on period of 60 min and a hands-off period of 195 min.

The OMVs recovered following this protocol exhibited a spherical shape with a central depression and a heterogeneous size, as visualized by negative staining followed by TEM (**Figure 9A**), matching the OMVs' prototypical morphology and size distribution [245]. Moreover, ultrastructural analysis enabled validation of the vesicles as OMVs, since they are delimited by a single lipid bilayer (**Figure 9B**). TEM analysis revealed the absence of bacterial debris, flagella, and proteins, showing that OMVs preparations were highly pure. The comparative analysis of the negative staining images of OMVs isolated from *H. pylori* 26695 grown in F12-cholesterol and in complex BB-FBS medium, and between the respective culture media alone, highlighted the importance of using the synthetic medium for the recovery of highly pure OMVs. F12-cholesterol medium and OMVs isolated from F12-cholesterol bacterial cultures had a clear background, without protein aggregates (**Figures 9A** and **9C**), distinctly from BB-FBS medium and the respective OMVs samples, in which the presence of proteins was detected (**Figures 9D** and **9E**).

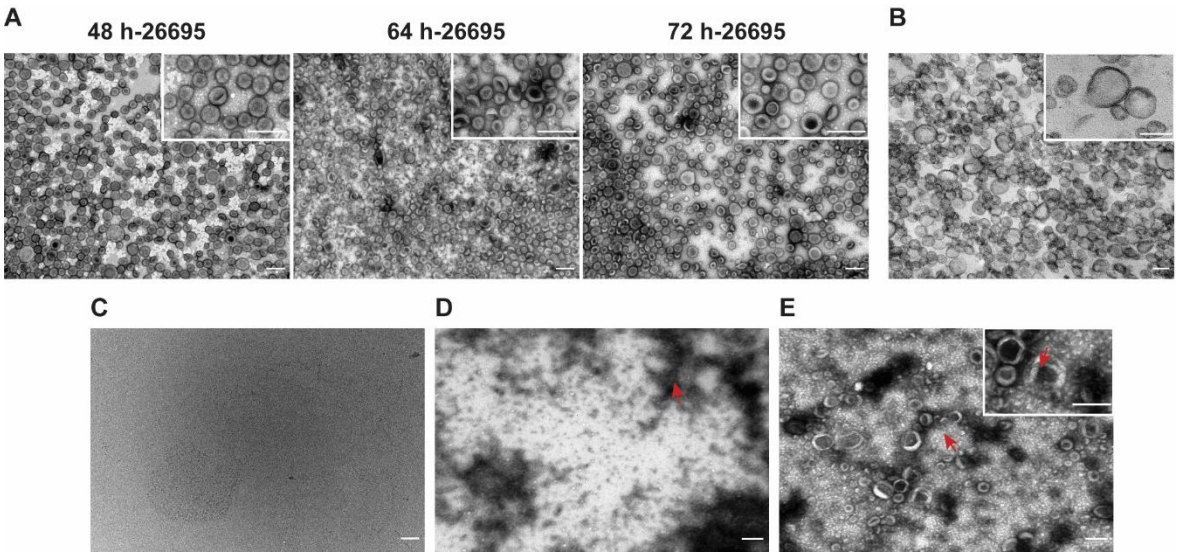

Figure 9. Morphological characterization of OMVs secreted by H. pylori 26695 grown in F12-cholesterol medium.

(A) Negative staining of OMVs isolated from *H. pylori* 26695 F12-cholesterol liquid cultures at 48 h, 64 h, and 72 h of growth, and **(B)** ultrastructure section of OMVs from 64 h *H. pylori* cultures. Representative negative stain TEM micrographs of **(C)** F12-cholesterol liquid medium, **(D)** BB-FBS medium, **(E)** OMVs isolated from *H. pylori* BB-FBS liquid cultures. Red arrows point to proteins present in BB medium and in OMVs preparations from BB liquid cultures. Scale bars: 200 nm; 50,000x, 100,000x (inset in **A** and **E**) and 200,000x (inset in **B**) original magnifications.

We next characterized the size distribution and number of OMVs recovered from the 48 h, 64 h, and 72 h *H. pylori* cultures by NTA (**Figure 10A**). More than 99% of all OMVs presented a size range between 20 to 200 nm, regardless of the culture time, and 0.66% of vesicles were detected above the 200 nm. The presence of OMVs higher than 450 nm was

negligible, which matched the exclusion filter pore-size and demonstrated the absence of vesicle aggregates. From the NTA data, we also identified that the mode sizes of OMVs isolated from the 48 h, 64 h, and 72 h liquid cultures were, respectively, 84.3 ± 1.7, 79.8 ± 6.4 and 83.3 ± 5.0 nm. Despite the fact that OMVs isolated from 48 h bacterial cultures were more heterogeneous in size than OMVs from 64 h and 72 h cultures, presenting a distinctive population of smaller OMVs with a diameter ranging from 15 to 60 nm, the size distribution of OMVs from the three time points presented no statistically significant differences between them.

Concerning the yield of OMVs, an average of 1.68 ± 0.24 $\times 10^{10}$, 3.37 ± 0.31 $\times 10^{10}$, and 3.59 ± 0.91 $\times 10^{10}$ OMVs per mL of liquid culture was recovered from the 48 h, 64 h, and 72 h bacterial cultures, respectively (**Figure 10B**). The 64 h-bacterial cultures produced a significantly higher number of OMVs/mL when compared to the 48 h-culture (p = 0.014), but not significantly different from the 72h-cultures. Although we cannot exclude some loss of OMVs during the isolation procedure, we assume that the number of secreted vesicles is likely near the recovered ones, given that no vesicles were detected in the supernatant collected after the first ultracentrifugation, both in F12-cholesterol and in BB-FBS, when analyzed by TEM (**Figures 10C** and **10D**). As so, the shorter number of steps and the recovery of a high yield of vesicles emphasize the efficacy of our protocol, even when different culture media are used.

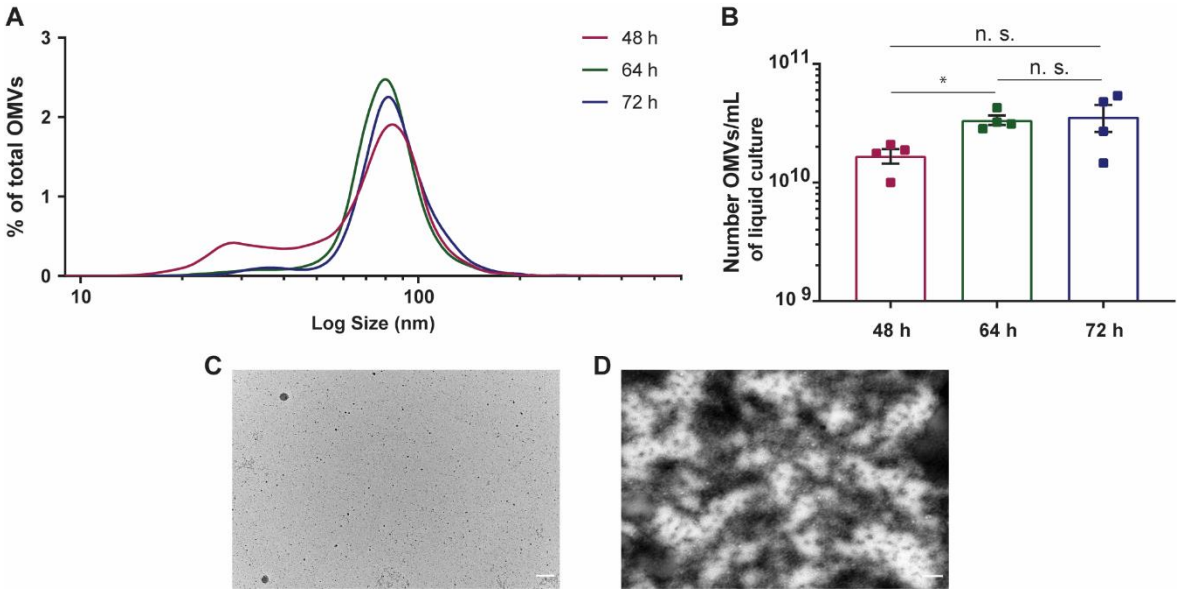

Figure 10. Size distribution and yield of OMVs secreted by H. pylori 26695 grown in F12-cholesterol medium.

(A) Size distribution of OMVs isolated from *H. pylori* 26695 F12-cholesterol liquid cultures at 48 h, 64 h, and 72 h of growth, represented as percentage of the total number of isolated OMVs. Data are shown as mean ± SEM of 4 biological replicates and statistical significance was evaluated using the one-way ANOVA with post-hoc Tukey's test; * $p \leq 0.05$ and n.s. – not significant. **(B)** Number of

recovered OMVs per mL of bacterial culture, determined using Nanoparticle Tracking Analysis (NTA) at 48 h, 64 h, and 72 h periods of bacterial growth. Data are shown as mean ± SEM of 4 biological replicates and statistical significance was evaluated using the one-way ANOVA with post-hoc Tukey's test; * $p \leq 0.05$, n.s. – not significant. Supernatants collected after the first ultracentrifugation from **(C)** F12-cholesterol and **(D)** BB-FBS *H. pylori* 26695 liquid cultures. Scale bars: 200 nm; 50,000x original magnification

To ascertain the applicability of this protocol to *H. pylori* strains other than 26695, we selected two additional *H. pylori* reference strains, 60190 and Tx30a. These strains were grown in F12-cholesterol medium, under the same conditions as strain 26695, and their OMVs were isolated and characterized by TEM and NTA, in the 64 h bacterial cultures. OMVs recovered from *H. pylori* 60190 and TX30a were highly pure and with the same size heterogeneity as 26695-OMVs (**Figures 11A and 11B**). The number of OMVs recovered per mL of bacterial culture was similar between the three strains at 64 h of bacterial growth (26695: 3.37 ± 0.31×10^{10}; 60190: 3.09 ± 0.74×10^{10}; Tx30a: 2.45 ± 0.58×10^{10} OMVs/mL) (**Figure 11C**).

In summary, these results show that OMVs recovered from *H. pylori* grown in F12-cholesterol cultures are *bona fide*, presenting the same morphology and ultrastructure as those isolated from complex media [126, 245]. Furthermore, our abridged protocol provided a good yield and a highly pure population of OMVs from various *H. pylori* strains and in different phases of bacterial growth.

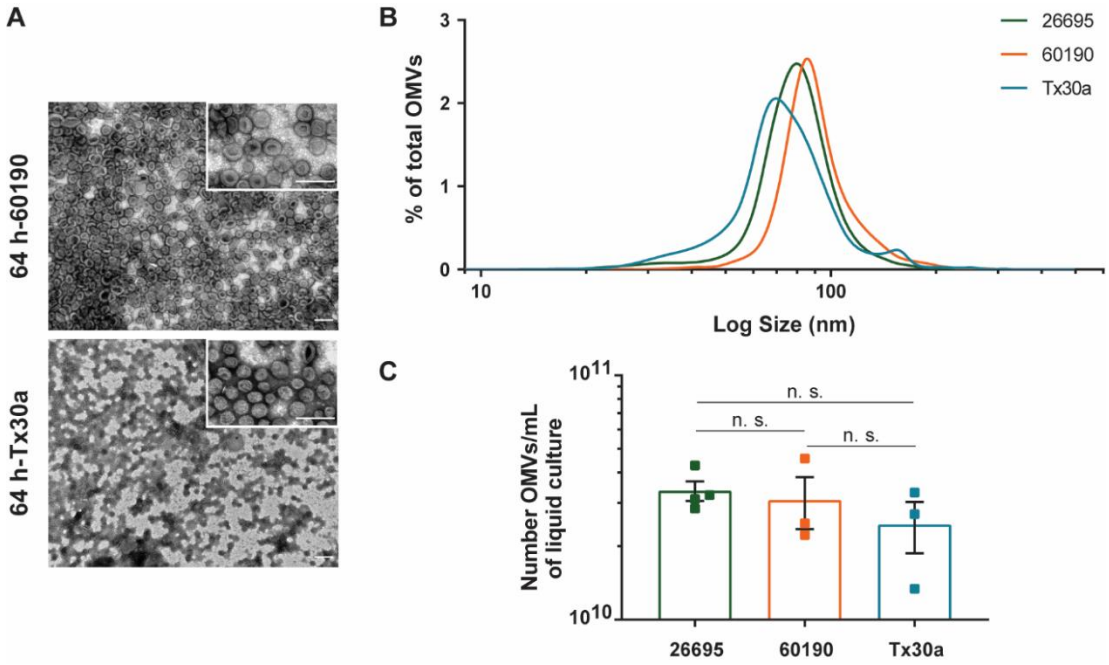

Figure 11. Morphological characterization, size distribution, and yield of *H. pylori* 60190 and Tx30a OMVs.

(A) Representative negative stain TEM micrographs of *H. pylori* 60190 and Tx30a-OMVs generated from 64 h F12-cholesterol bacterial cultures. Scale bars: 200 nm; 50,000x and 100,000x (insets) original magnification. **(B)** Size distribution, represented as percentage of the total number of isolated OMVs at 64 h of liquid culture, and **(C)** number of recovered OMVs per mL of bacterial culture determined by NTA. Data are shown as mean ± SEM of 4 (for 26695) or 3 (for 60190 and Tx30a*)* biological replicates and statistical significance was evaluated using the Brown-Forsythe and Welch ANOVA with post-hoc Dunnett's test; n.s. – not significant.

PART II: Content analysis of *H. pylori* OMVs

H. pylori OMVs carry a diversified content of proteins, lipids, LPS, PG, and genetic material, derived from the parental bacterium [118-126]. This OMVs composition is dependent on and varies with the parental bacterial strain, the bacterial growth stage, and the environmental conditions bacteria are faced with [117-119]. Analysis of OMVs produced by *H. pylori* at different phases of growth revealed that, as bacterial growth progressed, there was an increase in vesiculation, and large variability in the protein composition of OMVs isolated at different time points [118]. Furthermore, not much is known regarding the nucleic acid composition of *H. pylori* OMVs. Therefore, we aimed to analyze the content of OMVs, in terms of proteins and nucleic acids, isolated from *H. pylori* 26695 chemically defined liquid cultures, and compare it with previous reports available on the literature.

1. Proteomic content and proteomic analysis of *H. pylori* 26695 OMVs

Knowing that the cargo of OMVs is influenced by both bacterial growth conditions and bacterial growth stage [118, 142], our approach was to use a chemically defined medium for the growth of *H. pylori* and to compare the proteome of OMVs isolated at different stages of bacterial growth.

Thus, we characterized and compared the protein cargo of OMVs secreted by *H. pylori* grown in the medium and culture/isolation conditions described in Part I of the Results at different time points of bacterial growth.

The total protein amount from OMVs was assessed by SDS-PAGE and gel staining with BlueSafe, using 10^{11} OMVs (**Figure 12**). OMVs isolated from 48 h-, 64 h- and 72 h-bacterial cultures presented an identical protein profile (**Figure 12A**) and similar total protein amounts (48 h: 3.55 ± 1.16; 64 h: 4.02 ± 0.95; 72 h: 4.25 ± 1.42 μg of protein per 10^{11} OMVs) (**Figure 12B**).

Next, we applied nanoscale liquid chromatography coupled to tandem mass spectrometry (nanoLC-MS/MS) to 5×10^{11} OMVs of each time point of bacterial growth, and analyzed the differential expression of proteins between each of them. A total of 267, 268, and 269 proteins from *H. pylori* 26695 were identified on 48 h-, 64 h-, and 72 h-OMVs, respectively. Of these, 233, 231, and 232 proteins, with a false discovery rate (FDR) of 1%, were further classified according to their predicted cellular localization, biological process and molecular function, using the gene ontology (GO) UniProt database resource and manual curation (**Supplementary Table 1** in Appendix). All proteins identified in 64 h-OMVs (n = 231) were common to 48 h- and 72 h-samples. Pyruvate ferredoxin oxidoreductase was identified only in 48 h- and 72 h-samples, whereas flagellar P-ring protein was detected exclusively in 48 h-OMVs.

In terms of cellular localization (**Figure 12C**), the most diverse and abundant group of proteins identified in OMVs from all time points analyzed was predicted to be associated with the bacterial membrane, and within this group outer membrane proteins (OMPs) are the most frequent (48 h: n = 50, abundance = 5.67 ± 0.41×10^9; 64 h: n = 49, abundance = 5.73 ± 1.25×10^9; 72 h: n = 49, abundance = 6.52 ± 0.74×10^9). Periplasmic, cytoplasmic and extracellular region-associated proteins were also detected. In addition, 3 flagellar proteins were identified in 48 h-samples, while only 2 were detected in 64 h- and 72 h-OMVs.

Concerning the biological process analysis, proteins were distributed into 8 groups (**Figure 12D**). Proteins involved in cellular processes constituted the most numerous and abundant group, followed by proteins involved in metabolic processes, localization proteins, response to stimulus, biological regulation, and interspecies interaction proteins. Detoxification and cell motility proteins were the less abundant.

Regarding the molecular functions (**Figure 12E**), the majority of the classified proteins was predicted to have catalytic, binding and/or transporter activities, followed by proteins with antioxidant and structural molecular activities, enzyme activators, a toxin, and a translation elongation factor. Besides the above-mentioned molecular functions, several of the identified proteins are also involved in processes related with *H. pylori* colonization, survival, and pathogenesis. These include urease α/β, BabA, OipA, β-lactamases HcpA, HcpC, HcpD, and HcpE, HtrA, VacA, GGT, HP-NAP, catalase, superoxide dismutase, and a bacterial non-heme ferritin. The presence of these virulence factors in *H. pylori* OMVs isolated from F12-cholesterol indicates that some proteins may be preferably loaded onto OMVs, and suggests the importance of OMVs for the success of *H. pylori* infection. Seventy of the 233 identified proteins were uncharacterized and approximately half of them did not have a predicted cellular localization or molecular function.

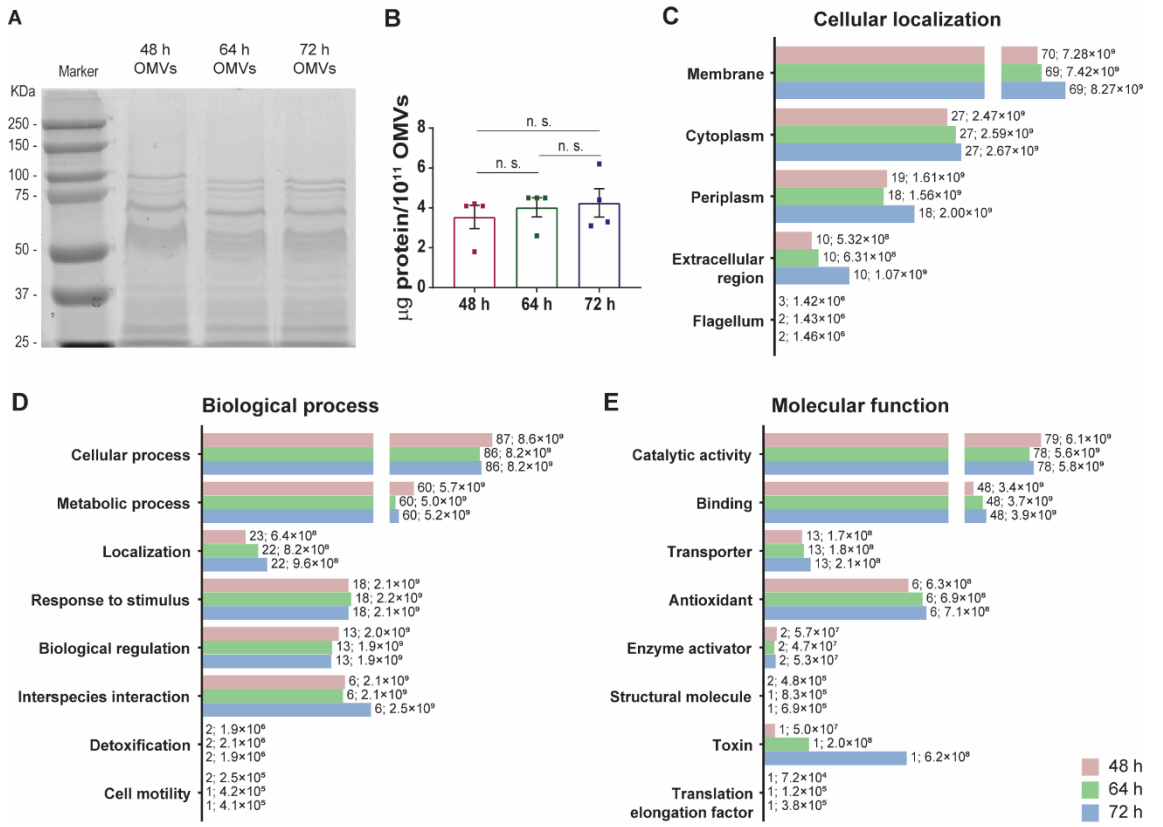

Figure 12. Protein profile and proteomic analysis of OMVs secreted by *H. pylori* grown in F12-cholesterol medium.

(A) Protein profile of 10^{11} OMVs isolated from 48 h-, 64 h- and 72 h-*H. pylori* 26695 bacterial cultures, after staining a SDS-PAGE with BlueSafe, and corresponding **(B)** protein quantification. Data are shown as mean ± SEM of 4 biological replicates and statistical significance was evaluated using the one-way ANOVA with post-hoc Tukey's test; n.s. – not significant. Proteomic analysis of 48 h-, 64 h- and 72 h-OMVs isolated from *H. pylori* 26695 F12-cholesterol liquid cultures by nanoLC-MS/MS and prediction of the **(C)** cellular localization, **(D)** biological process and **(E)** molecular function of the identified proteins using the gene ontology UniProt database. Data are shown as the abundance of proteins in each group; for each bar, the number of proteins and respective abundance is indicated.

Although OMVs isolated from 48 h-, 64 h-, and 72 h-bacterial cultures had a similar protein content, some of the proteins were differentially expressed (**Table 2** for the comparison between 48 h and 64 h; **Table 3** for the comparison between 48 h and 72 h; and **Table 4** for the comparison between 64 h and 72 h). These include VacA, TRXR, FrpB, and FecA, which were significantly more abundant in 64 h- and 72 h-OMVs, in comparison to 48 h-samples.

Overall, our proteomic analysis supports the selective sorting of protein cargo into OMVs, as only a fraction of the total bacterial proteins is represented in the cargo of OMVs. In addition, it confirms the reliability of F12-cholesterol as the bacterial culture medium, by

showing that OMVs contain proteins from the membrane, periplasmic, and cytoplasmic bacterial compartments, as previously described for chemically undefined media.

Table 2. Differentially expressed proteins identified in OMVs isolated from 48 h and 64 h *H. pylori* strain 26695 F12-cholesterol liquid cultures.

Accession number	Protein names	Abundance Ratio 64 h/48 h	*p*-value
P56463	Purine nucleoside phosphorylase DeoD-type (PNP)	12.269	3.96×10^{-5}
O25325	Uroporphyrinogen decarboxylase (UPD)	4.794	0.001
O25573	Iron-regulated outer membrane protein (FrpB)	4.486	0.012
P55981	Vacuolating cytotoxin autotransporter (VacA)	3.946	0.012
O25218	Outer membrane protein (Omp11)	2.777	0.003
P48285	Enolase	2.454	0.013
O25436	Uncharacterized aminotransferase HP_0736	2.129	0.046
O25401	Uncharacterized protein	2.098	0.031
O25395	Iron(III) dicitrate transport protein (FecA)	2.074	0.014
O25972	Ribosomal RNA small subunit methyltransferase A	2.004	0.047
O25410	Outer membrane protein (Omp15)	1.927	0.031
P56431	Thioredoxin reductase (TRXR)	1.920	0.038
O25509	Uncharacterized protein	1.852	0.013
P56089	Serine hydroxymethyltransferase	1.821	0.040
O25884	YtkA domain-containing protein	1.784	0.032
O25713	Uncharacterized protein	1.529	0.019
O24863	Uncharacterized protein	1.343	0.016
O25423	Uncharacterized protein	0.918	0.050
O25717	Uncharacterized protein	0.892	0.031
O25270	Cag pathogenicity island protein (Cag16; CagM)	0.850	0.006
O25728	Putative beta-lactamase HcpC	0.841	0.048
O24996	Uncharacterized protein	0.812	0.001
O25872	Conserved hypothetical secreted protein	0.796	0.046
O25873	Conserved hypothetical secreted protein	0.784	0.001
P55969	Neuraminyllactose-binding hemagglutinin	0.782	0.024
O24943	Uncharacterized protein	0.778	0.042
O25271	Cag pathogenicity island protein (Cag17; CagN)	0.771	0.005
O25038	Conserved hypothetical secreted protein	0.754	0.028
O25137	Uncharacterized protein	0.736	0.001
O25696	Uncharacterized protein	0.718	0.017
P56112	Putative peptidyl-prolyl cis-trans isomerase	0.683	0.042
O24938	Uncharacterized protein	0.623	0.001
O25403	N-methylhydantoinase	0.069	0.019
O25402	Hydantoin utilization protein A (HyuA)	0.049	0.016
O25404	Uncharacterized protein	0.025	0.025

Table 3. Differentially expressed proteins identified in OMVs isolated from 48 h and 72 h *H. pylori* strain 26695 F12-cholesterol liquid cultures.

Accession number	Protein names	Abundance Ratio 72 h/48 h	*p*-value
P56463	Purine nucleoside phosphorylase DeoD-type (PNP)	16.491	1.59×10^{-5}
P55981	Vacuolating cytotoxin autotransporter (VacA)	12.376	0.002
O25325	Uroporphyrinogen decarboxylase (UPD)	6.148	2.83×10^{-4}
O25573	Iron-regulated outer membrane protein (FrpB)	5.620	0.015
P56003	Elongation factor Tu (EF-Tu)	5.317	0.030
O25349	Quinone-reactive Ni/Fe hydrogenase (HydB)	3.725	0.018
O25218	Outer membrane protein (Omp11)	3.113	0.003
O25329	Uncharacterized protein	3.064	0.032
Q48252	CAG pathogenicity island protein 23 (CagE)	2.926	0.042
O25477	Uncharacterized protein	2.727	0.048
O26003	Uncharacterized protein	2.666	0.022
O25230	Uncharacterized protein	2.629	0.034
O25395	Iron(III) dicitrate transport protein (FecA)	2.492	0.005
O25410	Outer membrane protein (Omp15)	2.327	0.008
O25401	Uncharacterized protein	2.100	0.008
O25713	Uncharacterized protein	1.997	0.006
P48285	Enolase	1.989	0.019
O25735	Outer membrane protein (Omp23)	1.915	0.007
P56089	Serine hydroxymethyltransferase	1.785	0.031
P50610	Flagellar hook protein FlgE	1.662	0.049
O25509	Uncharacterized protein	1.628	0.018
P56431	Thioredoxin reductase (TRXR)	1.617	0.035
O25580	Outer membrane protein (Omp22)	1.528	0.030
O24863	Uncharacterized protein	1.329	0.043
O25075	Alginate_lyase domain-containing protein	1.314	0.034
O25442	Uncharacterized protein	1.219	0.040
O25270	Cag pathogenicity island protein (Cag16; CagM)	0.819	0.002
P55969	Neuraminyllactose-binding hemagglutinin	0.805	0.017
O25728	Putative beta-lactamase HcpC	0.800	0.010
O25076	YceI domain-containing protein	0.787	0.030
O24943	Uncharacterized protein	0.772	0.043
O25140	Thiol:disulfide interchange protein (DsbC)	0.767	0.037
O25872	Conserved hypothetical secreted protein	0.742	0.011
O25271	Cag pathogenicity island protein (Cag17; CagN)	0.728	0.002
O25696	Uncharacterized protein	0.718	0.019
O25905	Protease	0.707	0.025
O25873	Conserved hypothetical secreted protein	0.697	8.98×10^{-5}
P56112	Putative peptidyl-prolyl cis-trans isomerase	0.675	0.019
O24996	Uncharacterized protein	0.663	7.69×10^{-6}
O25018	UPF0323 lipoprotein	0.638	0.031
O25052	ATP-dependent nuclease (AddB)	0.629	0.018
O24938	Uncharacterized protein	0.577	4.35×10^{-4}
O25256	Beta-lactamase	0.417	0.004
O25403	N-methylhydantoinase	0.085	0.018
O25402	Hydantoin utilization protein A (HyuA)	0.068	0.021
O25404	Uncharacterized protein	0.038	0.022

Table 4. Differentially expressed proteins identified in OMVs isolated from 64 h and 72 h *H. pylori* strain 26695 F12-cholesterol liquid cultures.

Accession number	Protein names	Abundance Ratio 72 h/64 h	*p*-value
O26055	Uncharacterized protein	1.408	0.015
O25137	Uncharacterized protein	1.205	0.024
O25495	Uncharacterized protein	1.137	0.036
O25945	Outer membrane protein (Omp30)	1.118	0.050
O25423	Uncharacterized protein	1.106	0.023
O25873	Conserved hypothetical secreted protein	0.889	0.020
O24996	Uncharacterized protein	0.816	3.08×10^{-4}
O25256	Beta-lactamase	0.511	0.009

2. Nucleic acids detection in OMVs isolated from *H. pylori* 26695

Knowing that OMVs from Gram-negative bacteria, in addition to proteins, may carry cytoplasmic contents, including nucleic acids from the parental bacteria [159, 246, 247], we next investigated whether *H. pylori* OMVs would also contain nucleic acids. Since previous reports have shown that the majority of DNA from OMVs of Gram-negative pathogens was present on the external surfaces of OMVs [163], and that this DNA may result from lysed bacterial cells, we aimed for the detection of internal nucleic acids.

For that, OMVs were isolated from strain *H. pylori* 26695 using the growth medium and optimized protocol conditions described in Part I of the Results. Then, and in order to remove possible DNA and RNA associated with the outside of vesicles, *H. pylori* OMVs were treated with DNase I and RNase A before analyses.

The presence of internal DNA in OMVs was first confirmed by TEM. Thin-sections of DNase-treated OMVs were incubated with an antibody specific for double-stranded DNA (dsDNA) and a secondary antibody coupled to 15 nm gold particles. Immunogold labelling of *H. pylori* 26695 OMVs detected DNA within the vesicle lumen and close to the vesicle surface, as can be observed in the images of **Figure 13A**. The specificity of the anti-dsDNA antibody was confirmed by incubating thin sections with the gold-coupled secondary antibody alone, which showed no signal (**Figure 13B**).

Next, we isolated DNA and RNA from 10^{12} DNase I- and RNase A-treated *H. pylori* OMVs and determined internal DNA and RNA amounts using a NanoDrop Spectrophotometer. As shown in **Figure 13C**, we were able to identify and quantify both DNA and RNA within *H. pylori* OMVs, and the results indicate that these OMVs carry a higher amount (2-fold) of RNA (210.0 ± 27.8 ng) than DNA (108.7 ± 10.4 ng; $p = 0.0270$).

In *P. aeruginosa*, the internal DNA of OMVs was mapped to genes encoding virulence-related products [163]. Therefore, we selected three genes that encode *H. pylori* virulence factors associated with pathogenicity (CagA and VacA), and bacterial survival (Ureaseβ).

For these analyses, we selected two different *H. pylori* strains, namely strain 26695 and Tx30a. Both strains contain the Ureaseβ and the VacA-encoding genes. However, and concerning *vacA*, the strains present a different polymorphic combination, being *H. pylori* 26695 *vacA* s1/m1 and Tx30a *vacA* s2/m2. Regarding *cagA*, the gene is present in *H. pylori* 26695 and not in *H. pylori* Tx30a.

DNA and RNA were extracted from DNase- and RNase-treated *H. pylori* OMVs. In parallel, we extracted DNA from the two parental strains. RNA was transcribed to cDNA. Next, we performed PCR in DNA and in cDNA amplifying *cagA, vacA,* and *ureB* genes.

As expected, we were able to amplify all three genes in the genomic DNA (gDNA) of strain 26695, and the *vacA* and *ureB* genes in strain Tx30a, which is a *cagA*-negative strain (**Figure 13D**). As shown in this figure, *vacA* gene has a size-difference between the two strains, due to the polymorphism mentioned above. In DNA isolated from OMVs, and similarly to the control experiments with the gDNA from the parental bacteria, we could detect all three genes in OMVs from strain 26695, and *vacA* and *ureB* in strain Tx30a (**Figure 13E**). Likewise, when PCR was performed in cDNA obtained from the RNA isolated from OMVs, we could amplify *cagA, vacA,* and *ureB* in accordance with their presence in each of the parental strains (**Figure 13F**), showing that transcripts from these genes are present in the content of OMVs.

The enzymatic activity of DNase I and RNase A was evaluated by treating DNA and RNA isolated from *H. pylori* 26695 OMVs with these enzymes, respectively. RNase-treated RNA was then transcribed to cDNA. Next, DNase-treated DNA and cDNA transcribed from RNase-treated RNA were subjected to PCR amplification of *cagA, vacA,* and *ureB* genes. As shown in **Figure 13G**, there was no observable amplification of any of the referred genes. Similarly, PCR amplification using nuclease free-water or saline (solution used for the elution of OMVs) as substitutes of the genetic material, and used as PCR negative controls, resulted in any visible bands (**Figure 13G**).

Taken together, our results show the presence of nucleic acids, namely DNA and RNA, as internal contents of *H. pylori* OMVs. The detection of genes and of the respective gene transcripts that encode for known *H. pylori* virulence factors, suggest a mechanism of transfer of nucleic acids from the cytoplasm of the parental bacterium to their OMVs, which may help bacteria in the modulation of the host cell response.

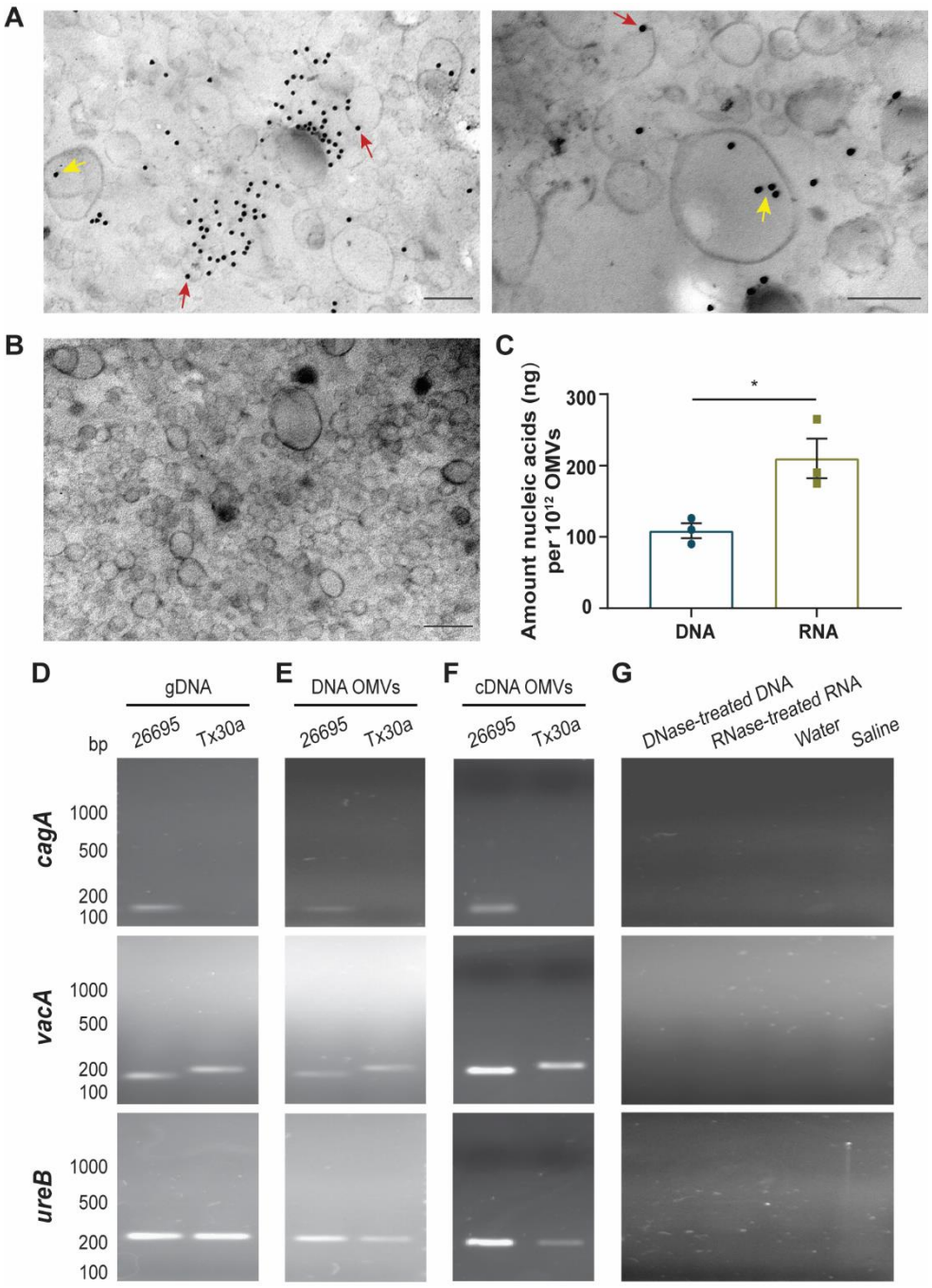

Figure 13. Detection of DNA and RNA in *H. pylori* OMVs.

(A) Representative micrographs of TEM immunogold labelling for dsDNA on DNase-treated OMVs isolated from *H. pylori* 26695 F12-cholesterol liquid cultures at 64 h of growth. Thin sections were incubated with an antibody anti-dsDNA and a secondary antibody coupled to 15 nm gold particles or **(B)** the secondary antibody alone. Grids were DNase-treated before thin sections attachment. Yellow arrows point to gold-associated dsDNA present within OMVs lumen and red arrows point to dsDNA close to the vesicle surface. Scale bars: 200 nm; 100,000x (**A** left image and **B**) and 150,000x (**A** right image) original magnifications. **(C)** Quantification of DNA and RNA extracted from 10^{12} DNase- and RNase-treated OMVs using a NanoDrop Spectrophotometer. Data are shown as mean ± SEM of 3 biological replicates and statistical significance was evaluated using the unpaired Student's t-

test; * $p \leq 0.05$. PCR amplification of *cagA*, *vacA*, and *ureB* genes from **(D)** genomic DNA extracted from *H. pylori* 26695 and Tx30a (reference control), **(E)** DNA extracted from DNase- and RNase-treated *H. pylori* 26695 and Tx30a OMVs, **(F)** cDNA synthesized from RNA extracted from DNase- and RNase-treated *H. pylori* 26695 and Tx30a OMVs, **(G)** DNase-treated DNA and cDNA transcribed from RNase-treated RNA isolated from *H. pylori* 26695 OMVs, nuclease free-water and saline (negative controls). The base pair markers (bp) are shown in the left. Amplicons size: *cagA* 190 bp; *vacA* s1: 176 bp; *vacA* s2: 203 bp; *ureB*: 230 bp.

PART III: Transcriptomic analysis of gastric epithelial cells challenged with *H. pylori* OMVs

1. Global expression profile analysis

To address the influence of *H. pylori* OMVs on the host cell transcriptomic profile, we treated the MKN74 gastric epithelial cell line with saline (control), with *H. pylori* OMVs, or with the parental bacteria *H. pylori* 26695, for 24 h. Then, we performed human targeted transcriptome sequencing using the Ion AmpliSeq™ Transcriptome Human Gene Expression Kit, and compared the expression profiles of cells treated with OMVs with both the control and *H. pylori*-infected conditions.

To have a global and unsupervised overview of the gene expression profile variation, we performed principal component analysis (PCA). As can be observed in **Figure 14**, PCA analysis shows that samples from the same experimental group clustered together, reflecting similar gene expression profiles. It also shows that each experimental condition forms distinct clusters representing different gene expression profiles. The highest variation in the transcriptional profiles, corresponding to principal component 1 (PC1), was observed between *H. pylori*-infected cells and the other experimental conditions, OMVs-challenged and control cells. The smallest variation, corresponding to PC2, was observed between OMVs-treated and control samples (**Figure 14**). Overall, PCA analysis revealed that OMVs induce a unique gene expression profile on MKN74 cells that is different from those of the control and of the *H. pylori*-infected cells.

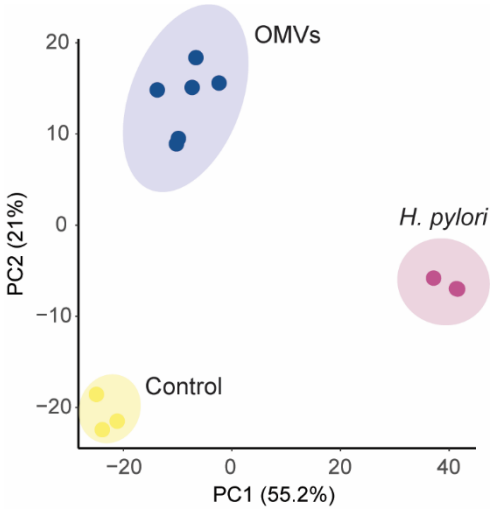

Figure 14. Gastric epithelial gene expression profile variation after treatment with *H. pylori* OMVs.

Principal component analysis (PCA) of the transcriptomic profile of MKN74 cells treated for 24 h with saline (control; n=3), with *H. pylori* OMVs, at a multiplicity of $2x10^6$ OMVs per cell (n=6), or with the parental *H. pylori* 26695 strain, at a multiplicity of infection (MOI) of 100 bacteria per cell (n=3).

Differential expression analysis between OMVs- or *H. pylori*-challenged cells against non-challenged control cells is shown in **Supplementary Table 2** (for OMVs vs control) and in **Supplementary Table 3** (for *H. pylori* vs control), in Appendix. In comparison with unchallenged control cells, OMVs and *H. pylori* upregulated 646 and 2222 genes, respectively, 389 of which were common to both challenged conditions (**Figure 15A**). OMVs and *H. pylori* respectively downregulated 635 and 1949 genes, 423 of which were common (**Figure 15B**).

Next, we used the g:Profiler to gather information about gene functions resorting to gene ontology (GO) and KEGG (Kyoto encyclopedia of genes and genomes) pathway databases [248]. Considering genes common to OMVs- and *H. pylori*-challenge, upregulated genes were associated with cellular responses to various stimulus, namely external stimuli, nutrient levels, presence of unfolded proteins, or stress, and to genes involved in autophagy and pathways related with cytokine and MAPK signaling. Downregulated genes were mainly involved in different DNA repair systems and cell cycle pathways.

Upregulated genes uniquely induced by OMVs were mainly associated with the host immune response and metabolic pathways, whereas downregulated genes were involved in cell cycle- and DNA repair-related pathways, in HIF-1 signaling, and in glycolytic processes.

Upregulated genes uniquely induced by *H. pylori* were related with cellular responses to external stimulus, autophagy, and lymphocyte signaling pathways, and downregulated genes were associated with diverse cellular metabolic processes.

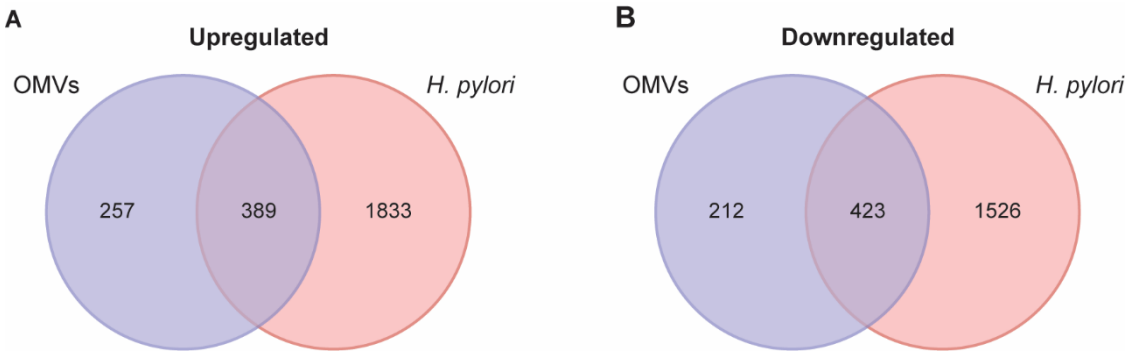

Figure 15. Gene expression analysis of OMVs- and *H. pylori*-challenged gastric epithelial cells.

Venn diagrams for **(A)** upregulated and **(B)** downregulated genes in *H. pylori* OMVs- and *H. pylori*-challenged cells, with a log2 fold change > 1 in expression when compared to control cells (*p*FDR < 0.05). Non-intersected areas of the circles show the number of unique differentially expressed genes for each condition and intersected area shows the number of common differentially expressed genes to both conditions.

Next, to better dissect the host genes and respective pathways that were significantly enriched (upregulated) or diminished (downregulated), we performed gene set enrichment analysis (GSEA), using gene ontology – biological process (GO-BP) and KEGG pathways databases. GSEA assembles together differentially expressed genes between pairwise comparisons, according to their involvement in the same biological pathway, identifying pathways otherwise unperceived in traditional differential expression analysis.

The top enriched pathways in OMVs-treated cells were associated with RNA transcription, endocytosis, cellular stress, ion transport, and apoptotic signaling, and the top diminished pathways were mainly related with cell cycle, DNA replication and repair, and metabolic processes (**Figure 16A**).

In the *H. pylori* setting, the top enriched pathways were related with regulation of autophagy, host immune response, and epithelial signaling pathways, while cell cycle, DNA repair, and multiple metabolic pathways were amongst the top downregulated (**Figure 16B**).

Lastly, the comparison between challenges with OMVs and *H. pylori* revealed that treatment with OMVs induced downregulation of cell cycle-related pathways, glycolysis and gluconeogenesis metabolic pathways, and upregulation of DNA base excision repair (BER) mechanism, and metabolic pathways (lipids/fatty acids, amino acid, vitamins, glutathione, and pyrimidine) (**Figure 16C**).

Taken together, these results show that OMVs secreted by *H. pylori* modify host gene expression, affecting important host biological pathways. They further show common host cell pathways and functions targeted by OMVs and the bacterium, besides unique signatures of differentially expressed genes induced by either OMVs or *H. pylori*. Moreover, and although cell cycle-related pathways are downregulated by both OMVs and the bacterium, there is downregulation of this pathway in OMVs in comparison with *H. pylori*.

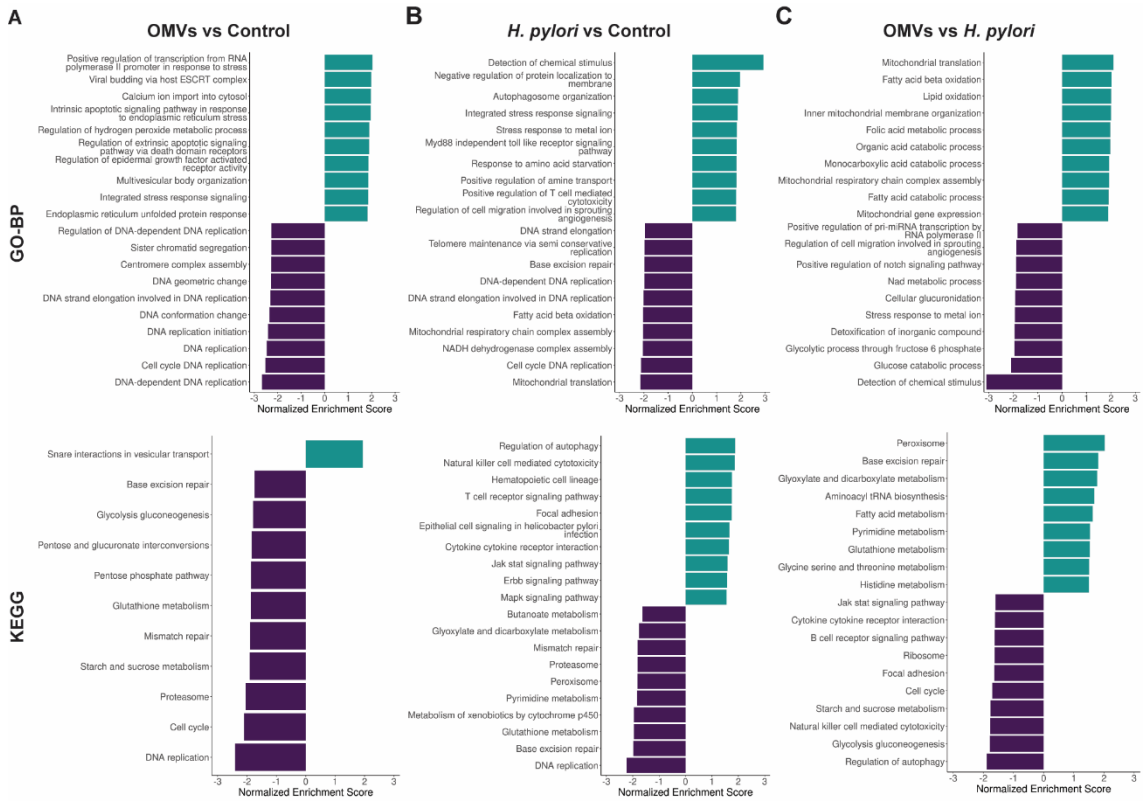

Figure 16. Identification of enriched pathways in *H. pylori* OMVs- and *H. pylori*-challenged gastric epithelial cells.

Identification of enriched pathways between OMVs-, *H. pylori*-treated and control cells, using Gene set enrichment analysis (GSEA) for Gene Ontology (GO) and Kyoto Encyclopedia of Genes and Genomes (KEGG). Top 10 terms of Biological Processes (GO-BP, upper graphs) and KEGG pathways (bottom graphs) for the pairwise comparisons (**A**) OMVs-treated vs control, (**B**) *H. pylori*-treated vs control, and (**C**) OMVs vs *H. pylori* challenges. Scale reports the normalized enrichment score values.

The analyses of the molecular pathways in the next sections will be focused on cell cycle and DNA repair pathways, since these were shown to be important for *H. pylori* infection [249-257].

2. Enriched molecular pathways – Cell cycle

Cell cycle is a tightly controlled process that involves numerous signaling pathways, ultimately determining whether cells proliferate, remain quiescent, arrest for DNA repair, or undergo apoptosis. Challenge of MKN74 cells with both *H. pylori* OMVs and the parental bacteria induced downregulation of multiple cell cycle-related genes. To explore the cell cycle-related genes affected by OMVs or by *H. pylori*, we retrieved the genes annotated to the cell cycle pathway (hsa04110) from the KEGG database. The pathway includes genes that encode cyclins (*CCNs*), cyclin-dependent kinases (*CDKs*), and CDK inhibitors (*CDKN*), which are the major players in cell cycle progression between G0, G1, S, G2, and M phases. It also includes genes that encode downstream targets of CDKs, namely the transcription factor *E2F* and its regulator *Rb*, genes associated with checkpoints arrest, DNA repair, and structural maintenance of chromosomes. Of the 124 genes ascribed to this pathway, we found 103 to have a statistically significantly different expression in at least one challenged condition, when compared to the control (**Figure 17** and **Supplementary Table 4** in Appendix). OMVs and *H. pylori* induced downregulation of, respectively, 57 and 45 genes and upregulation of 14 and 45 genes.

In particular, OMVs upregulated G1 phase-related genes *CCND2* and *CDK6*, while downregulating G1/S phase transition genes, *CCNE1*, *CCNE2*, and *CDK2*. In addition, the expression of the CDK inhibitors, *CDKN2B* (*p15*) and *CDKN1A* (*p21*) genes, that control the activity of G1 cyclin D/CDK6 and cyclin E/CDK2 complexes, respectively, and induce cell cycle G1 phase arrest, were also upregulated by OMVs. Moreover, p21 activity in the induction of cell cycle arrest is regulated by p53 (*TP53*), which we found to be upregulated by OMVs.

Concerning *H. pylori*, besides downregulating *CCNE1*, *CCNE2*, and *CDK2*, and upregulating *p15, p21*, and *TP53*, also upregulated M phase-related *CCNH* and *CDK7* genes. Expression of the G1 phase-related gene *CCND2* was not affected by *H. pylori* infection. In addition, genes associated with spindle assembly checkpoint arrest during the M phase of the cell cycle, namely *WEE1* (negative regulator of G2/M phase transition), *BUB1* and *BUB3* (protein kinases that activate members of the mitotic checkpoint), and *RAD21* (important for the correct sister chromatid cohesion), were upregulated by *H. pylori*, and downregulated by OMVs.

G2 and M phases *CCNA* and *CCNB* were downregulated in both OMVs- and *H. pylori*-challenged cells.

In conclusion, expression analysis of cell cycle-related genes highlighted that OMVs downregulated a higher number of cell cycle-related genes than *H. pylori* infection, confirming the results of g:Profiler and GSEA functional enrichment analyses. Moreover,

our results suggest that, while *H. pylori* upregulated genes involved in the cell cycle M phase, *H. pylori* OMVs induced a cell cycle arrest at the transition between G1 and S phases, pointing to a different temporal regulation of host cell cycle.

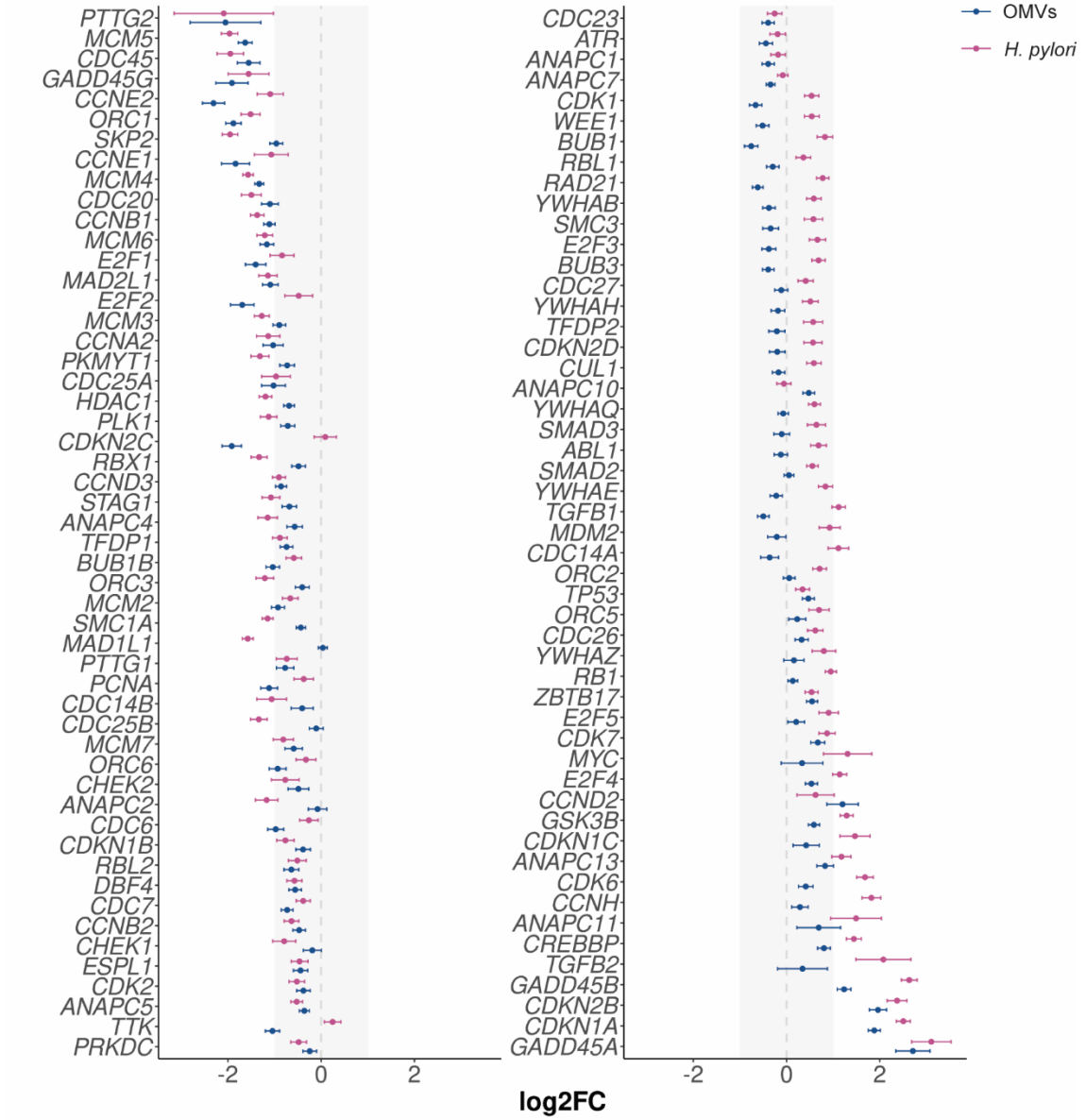

Figure 17. **Expression profiles for cell cycle-related genes in *H. pylori* OMVs- and *H. pylori*-challenged gastric epithelial cells.**

Expression profiles for cell cycle-related genes based on the KEGG database (hsa04110). Barplot representation of the $\log_2$ fold changes ($\log_2$FC) in gene expression between OMVs- (in blue) or *H. pylori*-challenged (in pink) MKN74 cells with untreated control cells.

3. Enriched molecular pathways – DNA repair

Eukaryotic host cells have distinct DNA repair systems as part of the DNA damage response mechanism to endogenous and exogenous insults, including pathogens, to protect cells from detrimental lesions. The GSEA analysis revealed that the treatment of MKN74 cells with OMVs or with *H. pylori* also resulted in the downregulation of DNA repair pathways. So, we explored more deeply which DNA repair-related genes were differentially expressed in our experimental conditions. For that, we retrieved the annotated genes of different DNA repair mechanisms from the KEGG database: mismatch repair (MMR; hsa03430), base excision repair (BER; hsa03410), and homologous recombination (HR; hsa03440). Of 99 genes, we found 62 to have a statistically significantly different expression in at least one challenged condition, when compared to the control (**Figure 18** and **Supplementary Table 5** in Appendix). OMVs and *H. pylori* induced downregulation of, respectively, 38 and 40 genes and upregulation of 10 and 9 genes.

Evaluation of the expression of genes involved in each of the analyzed DNA repair pathways revealed that genes involved in BER, namely *XRCC1*, *NEIL1*, *MUTYH*, and *APEX1*, were the ones that displayed the greatest differences in expression between treated conditions. This observation is in agreement with GSEA result of upregulation of the BER pathway in the presence of OMVs, when compared to *H. pylori*-challenged cells. In addition, while all of these genes were downregulated by *H. pylori* infection, *MUTYH* and *APEX1* were upregulated after treatment with OMVs. Interestingly, these genes are involved in the repair of damaged DNA during G1 phase that was originated from oxidative stress [258].

Regarding the MMR mechanism, which is extremely important during the S phase of the cell cycle for the repair of mismatched bases [258], our results showed that OMVs downregulated the expression of *MSH2* and *MSH6*, and upregulated *MLH3* expression, and *H. pylori* downregulated all the above mentioned genes. In addition, infection with the parental bacteria also downregulated *MLH1* and *PMS2*.

Finally, in relation to HR, a mechanism for repair of DNA double strand breaks, acting mainly during S and G2 phases of the cell cycle after DNA replication [258], we observed that *BRCA2* and *RAD51C*, which encode important players in HR repair of damaged DNA [259], were upregulated by *H. pylori* and not affected by OMVs. Conversely, the expression of *RAD52* was only affected by and upregulated in the presence of OMVs. Both challenged conditions downregulated *RAD54L* and *BLM*.

Taken together, analysis of the expression profile of DNA repair-related genes confirms the downregulation of the overall DNA repair pathways by both OMVs and *H. pylori*, observed in GSEA results. In addition, upregulation of the BER-related genes *MUTYH* and *APEX1*

suggests that OMVs induce oxidative stress to the epithelial cells and consequent DNA damage, thus activating DNA BER mechanisms.

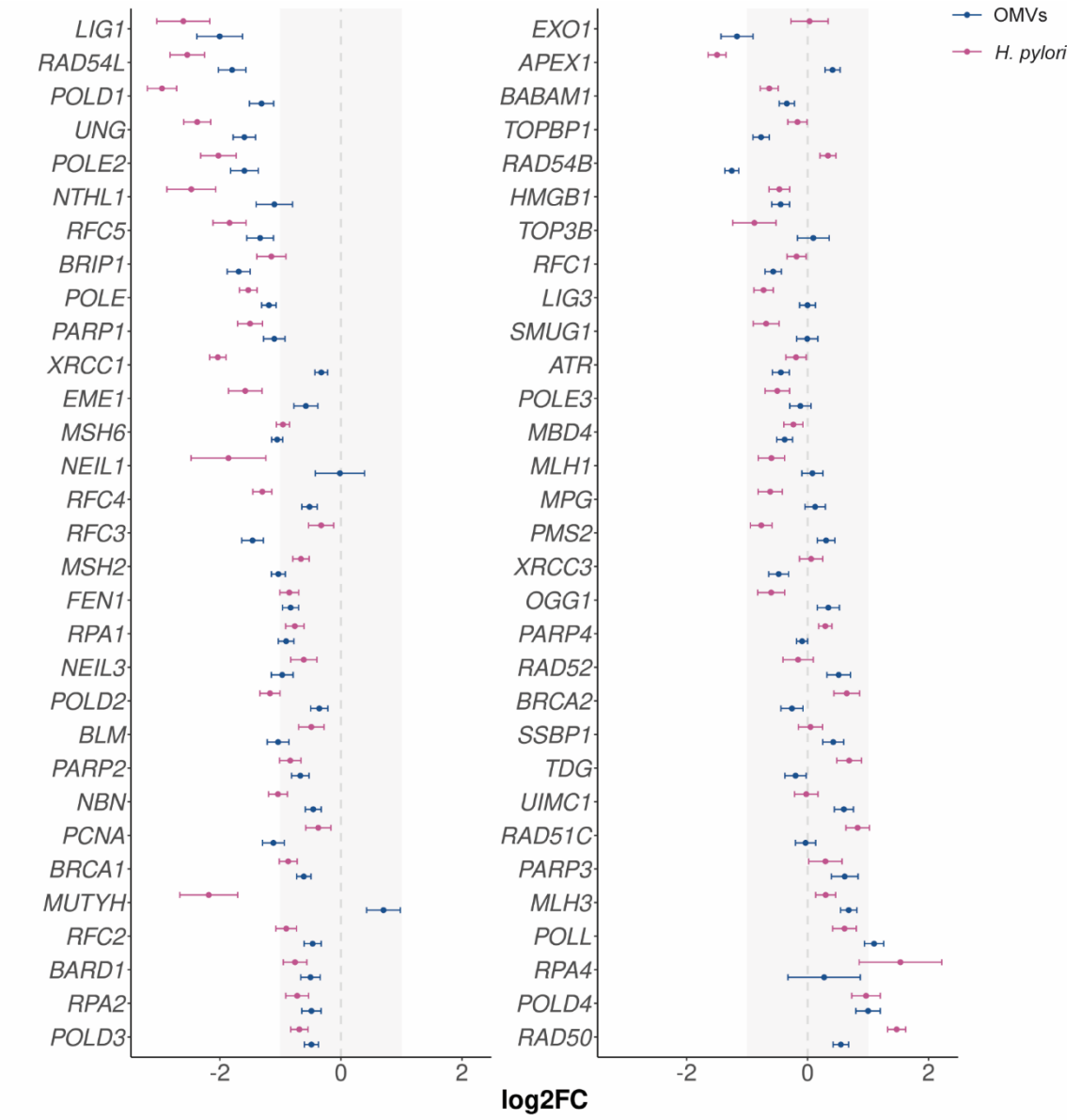

Figure 18. **Expression profiles for DNA repair-related genes in *H. pylori* OMVs- and *H. pylori*-challenged gastric epithelial cells.**

Expression profiles for DNA repair-related genes based on the KEGG database (mismatch repair - hsa03430, base excision repair - hsa03410, and homologous recombination - hsa03440). Barplot representation of the $\log_2$ fold changes ($\log_2$FC) in gene expression between OMVs- (in blue) or *H. pylori*-challenged (in pink) MKN74 cells with untreated control cells.

PART IV: Effect of *H. pylori* OMVs on gastric epithelial cell-cell junctions

H. pylori had developed a number of mechanisms in order to colonize and survive in the gastric mucosal epithelium, being cell-cell junctions one of the targets of this bacterium. Although it is well stablished that *H. pylori* disrupts TJ and AJ, the precise mechanisms involved are still largely unknown. Recent work from our group unraveled a new mechanism through which *H. pylori* alters epithelial cell integrity. Marques *et al* found that the bacterial metalloprotease PqqE cleaved the cytoplasmic domain of JAM-A, leading to the loss of epithelial barrier and cell-cell adhesion [104]. Since this protease is not secreted by the T4SS, but is part of the OMVs proteome, along with other factors known to target cell-cell junction proteins, we evaluated the involvement of *H. pylori* OMVs in the disruption of the epithelial barrier.

1. Entry of OMVs secreted by *H. pylori* into gastric epithelial cells

H. pylori OMVs are known to enter host cells, both *in vitro* and *in vivo*, through different endocytic pathways [125, 148, 155, 167]. The clathrin-dependent endocytosis was described as the preferential route of entry for small vesicles, measuring between 20 to 100 nm in diameter [126]. Considering that the majority of OMVs isolated from liquid cultures of *H. pylori* grown in F12-cholesterol are within this size range, we investigated whether these vesicles would be internalized by gastric epithelial cells.

For that, we used as model the MKN74 cell line. Cells were transfected with fluorescence reporter plasmids either expressing a mutant form of Rab5 (Rab5Q79L-GFP), which produces enlarged vacuoles and is an early endosome marker, or of the late endosome/lysosome marker LAMP-1 (LAMP1-GFP). Next, Rab5Q79L-GFP and LAMP1-GFP transfected MKN74 cells were treated with DiD-labelled saline, or challenged with DiD-OMVs and the association of OMVs with Rab5Q79L and LAMP1 vesicles was evaluated by confocal microscopy. Fluorescence analysis showed colocalization of DiD-OMVs with the early endosome marker Rab5Q79L, 3 min after challenge (**Figure 19A**), whereas after 15 min, DiD-OMVs associated with the late endosome/lysosomal marker LAMP1 (**Figure 19B**). These results clearly demonstrate that *H. pylori* 26695 OMVs are uptaken by MKN74 gastric epithelial cells.

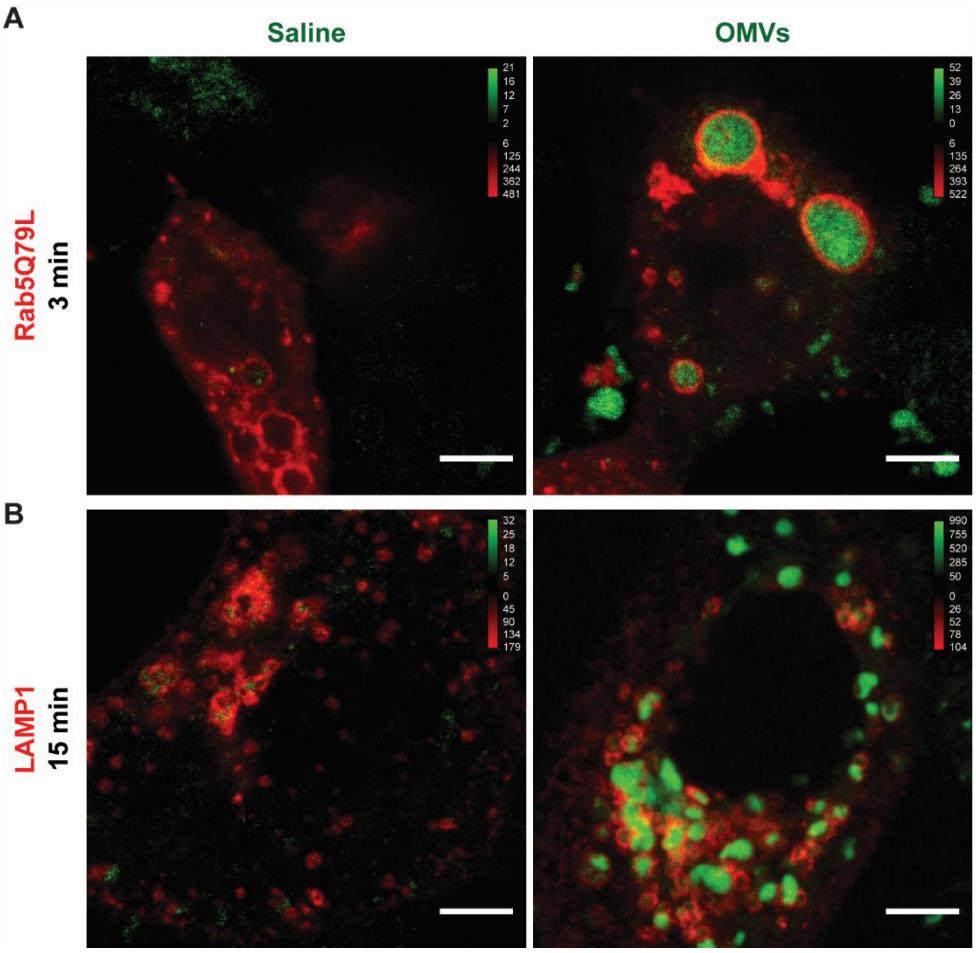

Figure 19. Internalization of *H. pylori* OMVs by MKN74 cells.

Confocal analysis of **(A)** Rab5Q79L-GFP and **(B)** LAMP1-GFP transfected MKN74 cells after treatment with DiD-saline (control), or with 2.5×10^{12} DiD-*H. pylori* OMVs, for 3 and 15 min, respectively. Calibration bar was used to map extremes in fluorescence intensity. Scale bars: 5 µm.

2. Effects of *H. pylori* OMVs on cell-cell junction proteins

Infection of gastric epithelial cells with *H. pylori* induces alterations in several TJ and AJ proteins. This may involve junctional protein delocalization from the cell membrane, decreased protein expression, and/or cleavage of junctional protein components [99, 104, 232].

To address whether OMVs from *H. pylori* had an impact on cell-cell junctional complexes, similar to what has been observed for the bacterium, we used two different cell line models. The MKN74 and the NCI-N87 cell lines, which were shown to establish competent tight and adherens junctions, were challenged with *H. pylori* OMVs for 24 h and 72 h. In parallel, the same cell lines were infected with *H. pylori*. Analysis of the localization of junctional proteins by immunofluorescence revealed that, similarly to *H. pylori*, OMVs induced the membrane displacement, from the membrane to the cytoplasm, or disorganization, of the TJ proteins

JAM-A and ZO-1, and the AJ protein E-cadherin, after 24 h and 72 h of challenge, in both MKN74 (**Figure 20**) and NCI-N87 (**Figure 21**) cell lines.

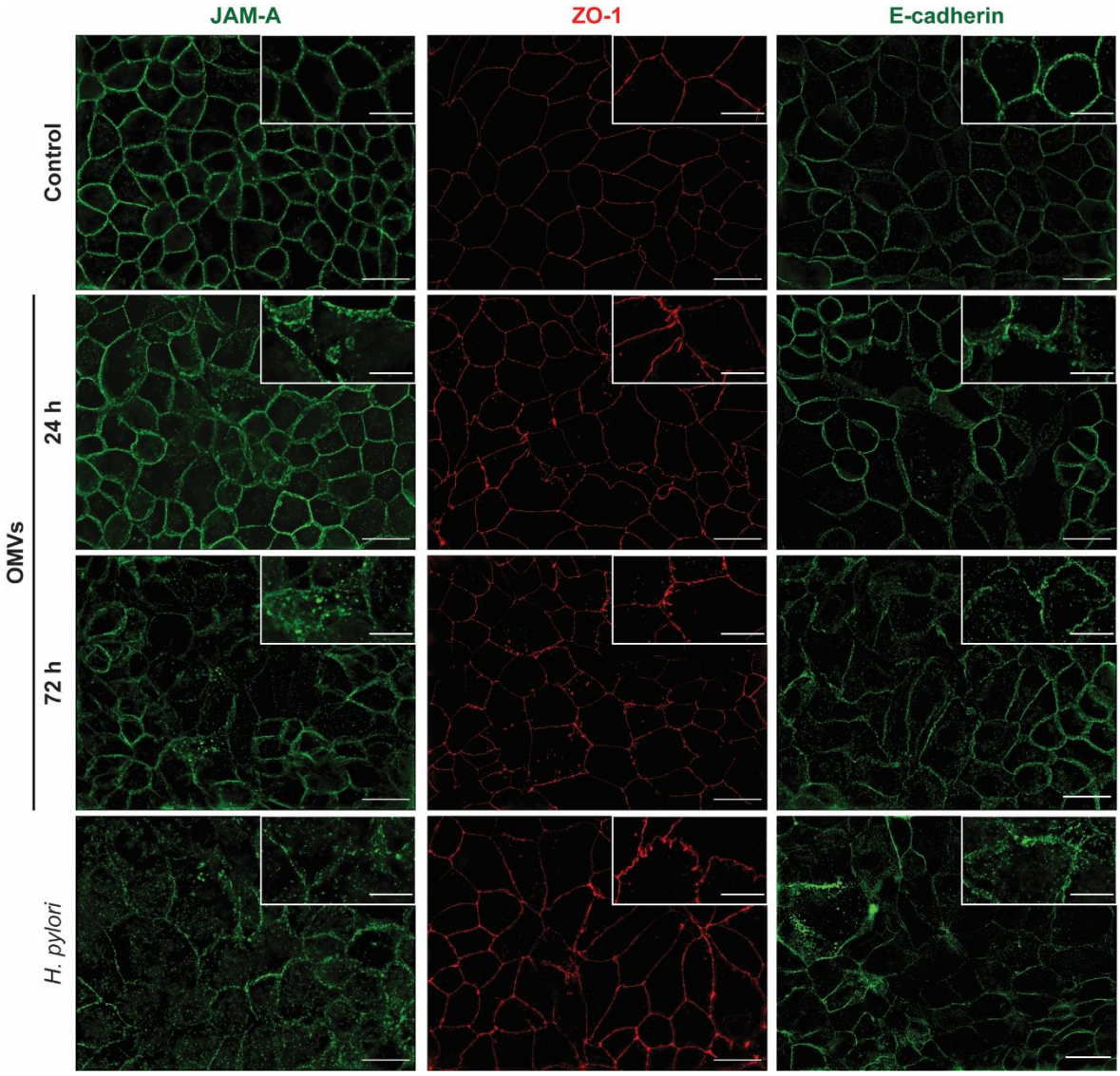

Figure 20. *H. pylori* OMVs induce the membrane delocalization of several apical junctional complex proteins, in gastric epithelial cells.

Immunofluorescence of the TJ proteins JAM-A (green) and ZO-1 (red), and the AJ protein E-cadherin (green) in confluent MKN74 cells treated with saline (control), challenged with a multiplicity of $2x10^6$ OMVs per cell, or infected with *H. pylori* at a MOI of 100. OMVs were added daily for a maximum of 72 h. Co-culture with *H. pylori* was maintained for 24 h. Scale bars: 20 µm and 10 µm (insets); 63x original magnification.

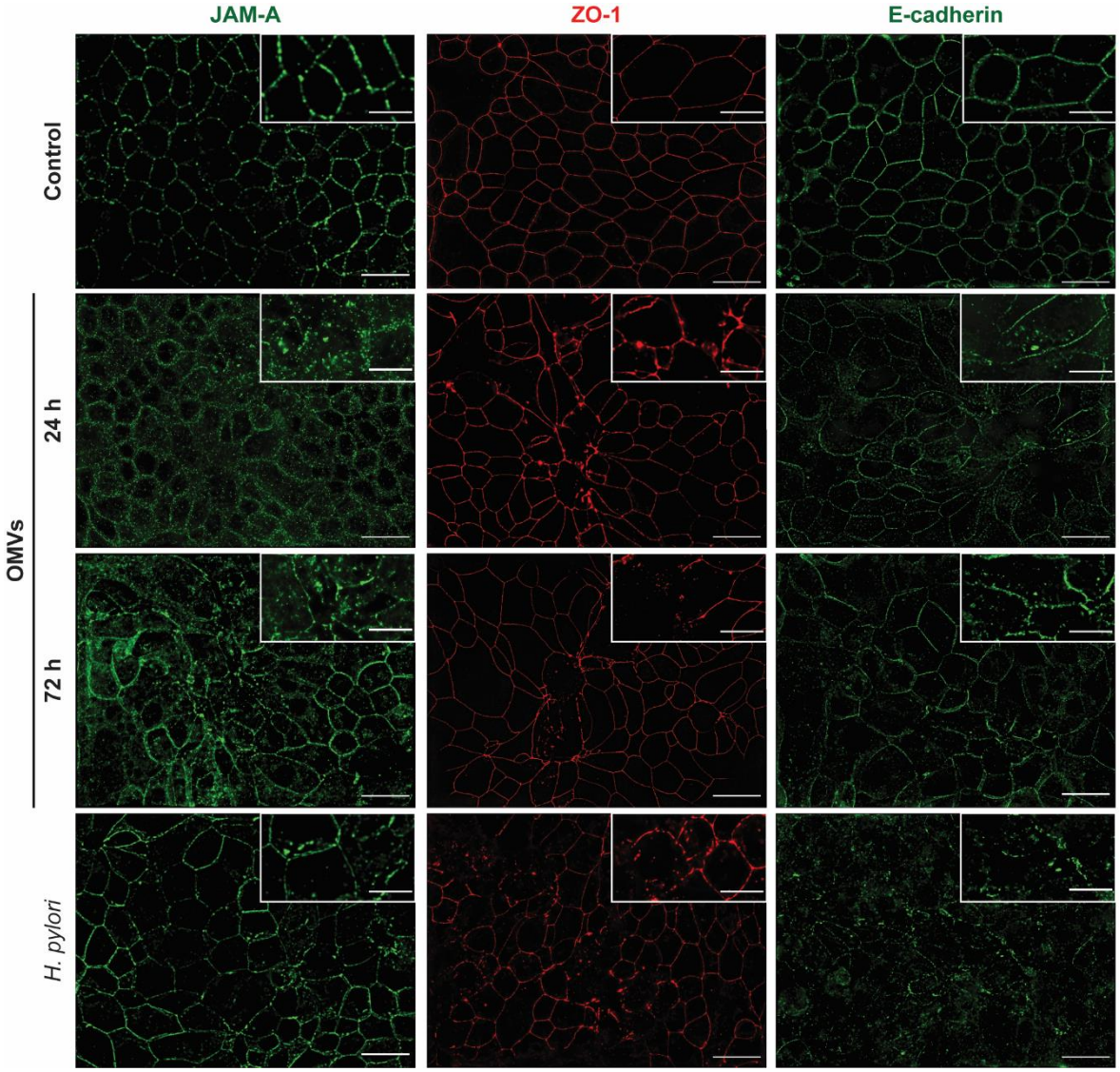

Figure 21. *H. pylori* OMVs induce the membrane delocalization of several apical junctional complex proteins, in gastric epithelial cells.

Immunofluorescence of the TJ proteins JAM-A (green) and ZO-1 (red), and the AJ protein E-cadherin (green) in confluent NCI-N87 cells treated with saline (control), challenged with a multiplicity of $2x10^6$ OMVs per cell, or infected with *H. pylori* at a MOI of 100. OMVs were added daily for a maximum of 72 h. Co-culture with *H. pylori* was maintained for 24 h. Scale bars: 20 µm and 10 µm (insets); 63x original magnification.

The quantification of the protein levels of the referred TJ and AJ proteins, however, showed no significantly differences after challenged with OMVs, whereas infection with *H. pylori* significantly decreased those values, when compared to control cells (**Figures 22A** and **22B**).

Overall, these results suggest that *H. pylori* OMVs are able to alter the structure of cell-cell junctions by inducing the delocalization of several TJ and AJ proteins, without disturbing their expression.

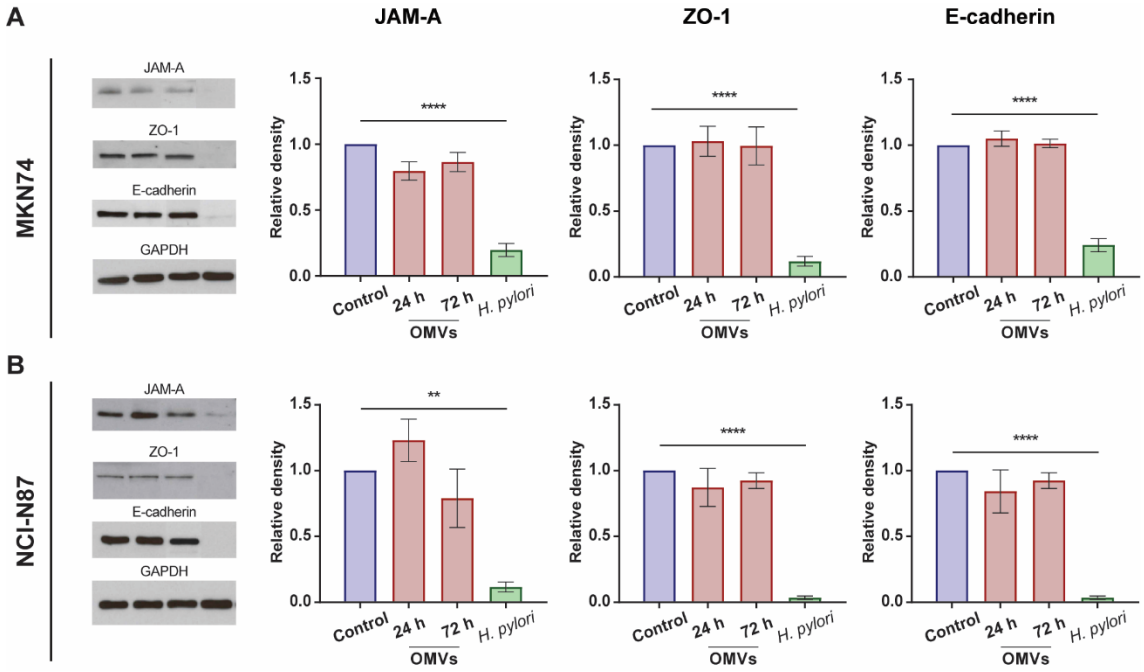

Figure 22. Challenge of gastric epithelial cells with *H. pylori* OMVs does not alter the expression of cell-cell junctional proteins.

Western blot analysis and respective quantifications of the protein levels of JAM-A, ZO-1, and E-cadherin in **(A)** MKN74 and **(B)** NCI-N87 cells treated with saline, challenged with *H. pylori* OMVs or infected with *H. pylori*. GAPDH was used as loading control. Data are shown as mean ± SEM of 3 biological replicates. Statistical significance was evaluated using the one-way ANOVA with post-hoc Dunnett's test; ** $p \leq 0.01$, **** $p \leq 0.0001$.

3. Effects of *H. pylori* OMVs on cell-cell junction functions

Having shown that *H. pylori* OMVs alter the localization of junctional proteins, we addressed the functional consequences of their misplacement by evaluating TJ integrity and monolayer permeability to macromolecules. For that, confluent polarized MKN74 and NCI-N87 epithelial cells were challenged daily with OMVs, or were infected in the beginning of the experiment with *H. pylori*. During 72 h, the transepithelial electrical resistance (TER) of the cell monolayers was measured daily. Both OMVs and *H. pylori* significantly decreased the electrical resistance of MKN74 cell monolayers over time, in comparison to control cells (OMVs – 24 h: $p = 0.0166$, 48 h: $p = 0.0001$, 72 h: $p = 0.0002$; *H. pylori* – 24 h, 48 h and 72 h: $p < 0.0001$) (**Figure 23A**). Similar results were observed when the NCI-N87 cell line was used (OMVs – 24 h: $p = 0.0177$, 48 h: $p = 0.0167$, 72 h: $p = 0.0166$; *H. pylori* – 24 h: $p = 0.0005$, 48 h: $p = 0.0010$, 72 h: $p = 0.0042$) (**Figure 23A**).

After 72 h of culture, the permeability of the gastric monolayers to the 4 KDa high molecular weight FITC-Dextran was also evaluated. Both OMVs ($p = 0.0284$) and *H. pylori* ($p = 0.0128$) increased MKN74 permeability to FITC-Dextran (**Figure 23B**). On the opposite, NCI-N87

permeability showed no statistically significant alteration upon treatment with OMVs (p = 0.2151), but increased in the presence of *H. pylori* (p = 0.0413) (**Figure 23B**).

Altogether, these results support a role for *H. pylori* OMVs in the disruption of epithelial barrier integrity and function.

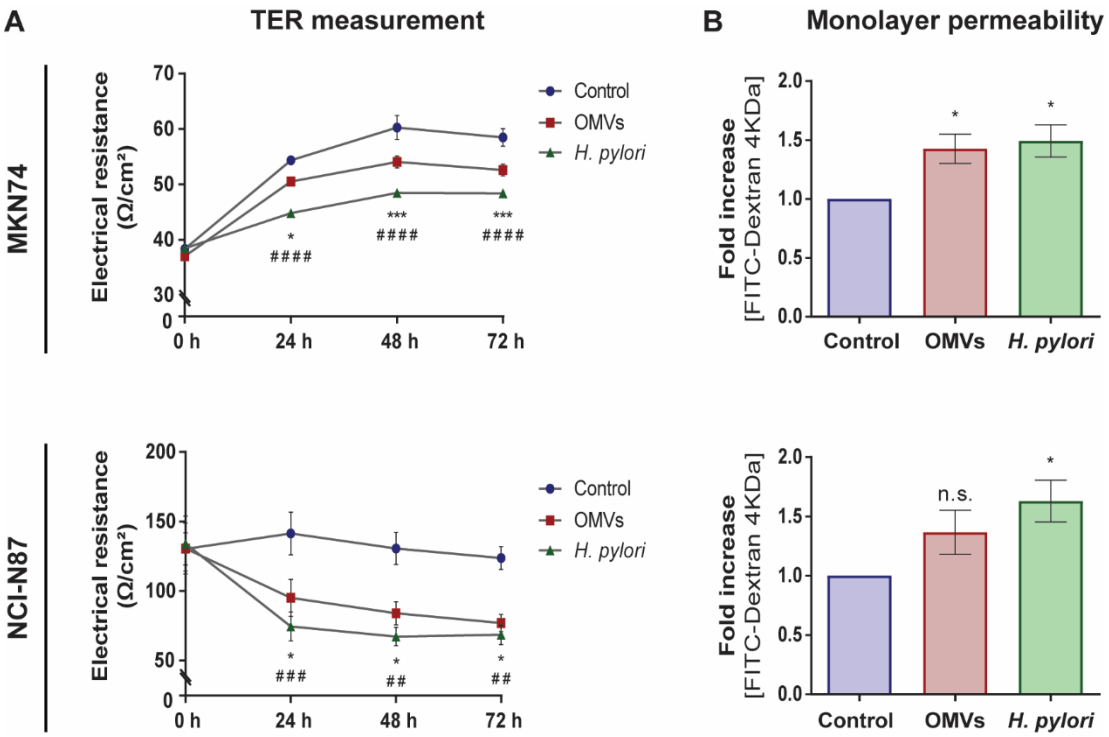

Figure 23. *H. pylori*-derived OMVs alter the epithelial barrier function in gastric epithelial cell monolayers.

MKN74 (upper panel) and NCI-N87 (lower panel) cells were left in confluence for 5 days before treatment with saline or challenge with *H. pylori* OMVs or *H. pylori*. **(A)** Transepithelial electrical resistance (TER) of gastric cells was measured before challenge and every 24 h, during 72 h. OMVs were added daily at a multiplicity of $2x10^6$ OMVs per gastric cell, while *H. pylori* was added only in the beginning of the experiment, at a MOI of 100. Data are shown as the mean ± SEM of 5 (MKN74) or 6 (NCI-N87) biological replicates. Statistical significance was evaluated using the two-way ANOVA with the post-hoc Dunnett's test. Comparison between OMVs and control datasets: * $p \leq 0.05$, *** $p \leq 0.001$. Comparison between *H. pylori* and control datasets: $^{\#\#}$ $p \leq 0.01$, $^{\#\#\#}$ $p \leq 0.001$, $^{\#\#\#\#}$ $p \leq 0.0001$. **(B)** Cell monolayer permeability to the 4 kDa FITC-Dextran molecule after 72 h of co-culture. TER results are shown as the mean ± SEM of 5 (MKN74) or 3 (NCI-N87) biological replicates. Statistical significance was evaluated using the one-way ANOVA with the post-hoc Dunnett's test. * $p \leq 0.05$, n.s. – not significant.

4. Effects of *H. pylori* OMVs on JAM-A cleavage

Our group recently reported a new mechanism through which *H. pylori* disrupts epithelial barrier function [104]. In this study, it was found that *H. pylori* cleaves the cytoplasmic domain of the TJ protein JAM-A. By performing a range of functional assays, it was demonstrated that the region cleaved by *H. pylori* is critical to the maintenance of the epithelial barrier and of cell-cell adhesion [104]. Moreover, the *H. pylori* PqqE, encoded by the *HP1012* gene, was identified as the protease that cleaved the cytoplasmic domain of JAM-A. Additionally, the activity of the recombinant *H. pylori* PqqE in cleaving a peptide mimicking the 40-amino acids of the cytoplasmic domain of JAM-A, was enhanced when PqqE was simultaneously expressed with the *H. pylori* metalloprotease homologue, YmxG, encoded by the *HP0657* gene [104]. Noteworthy, when in search for the *H. pylori* factors involved in JAM-A cleavage, it was shown that the bacterial T4SS was not involved [104]. Taken together, the abovementioned data raised the hypothesis that OMVs act as vehicles of the JAM-A proteases into the host cell cytoplasm.

To test this hypothesis, we first evaluated whether PqqE and YmxG were present in the proteome of *H. pylori* OMVs. Proteomics analysis of *H. pylori* OMVs from strain 26695 described in Part II.1 revealed that both PqqE and YmxG are present in the proteome of OMVs (**Supplementary Table 1** in Appendix). Importantly, they are at the top 19% of the most abundant proteins; of the total 231 proteins identified in OMVs from *H. pylori* 26695, PqqE and YmxG are respectively the 34th and the 45th most abundant proteins.

Thus, we next evaluated whether *H. pylori* OMVs would have the same effect as the parental bacteria on the cleavage of JAM-A. For that, we performed an *in vitro* cleavage assay using the 40-amino acid cytoplasmic domain peptide of JAM-A (cJAMA), corresponding to amino acids 260 to 299 in the human JAM-A (UniProtKB Q9Y624), followed by nanoLC-MS/MS analysis.

The incubation of *H. pylori* 26695 OMVs with the cJAMA peptide (^{260}AYSRGHFDRTKKGTSSKKVIYSQPSARSEGEFKQTSSFLV^{299}), for 15 min, resulted in the cleavage of the cJAMA into two smaller fragments: a larger peptide composed by 26 amino acids (1-26), ^{260}AYSRGHFDRTKKGTSSKKVIYSQPSA^{285} (m/z 580.9), and a smaller peptide with 14 amino acids (27-40), ^{286}RSEGEFKQTSSFLV^{299} (m/z 538.9) (**Figure 24A**). Similar results were observed when the cJAMA peptide was incubated with sonicates of the parental *H. pylori* 26695 strain (**Figure 24B**). These results show that, similarly to the data obtained with *H. pylori,* and with PqqE and PqqE-YmxG recombinants [104], *H. pylori* OMVs cleave JAM-A in the same position, which is after Ala^{285}.

In conclusion, our results suggest that *H. pylori* OMVs transport PqqE and YmxG into the gastric epithelial cells' cytoplasm, where the proteases are then able to access JAM-A's cytoplasmic domain and to cleave it.

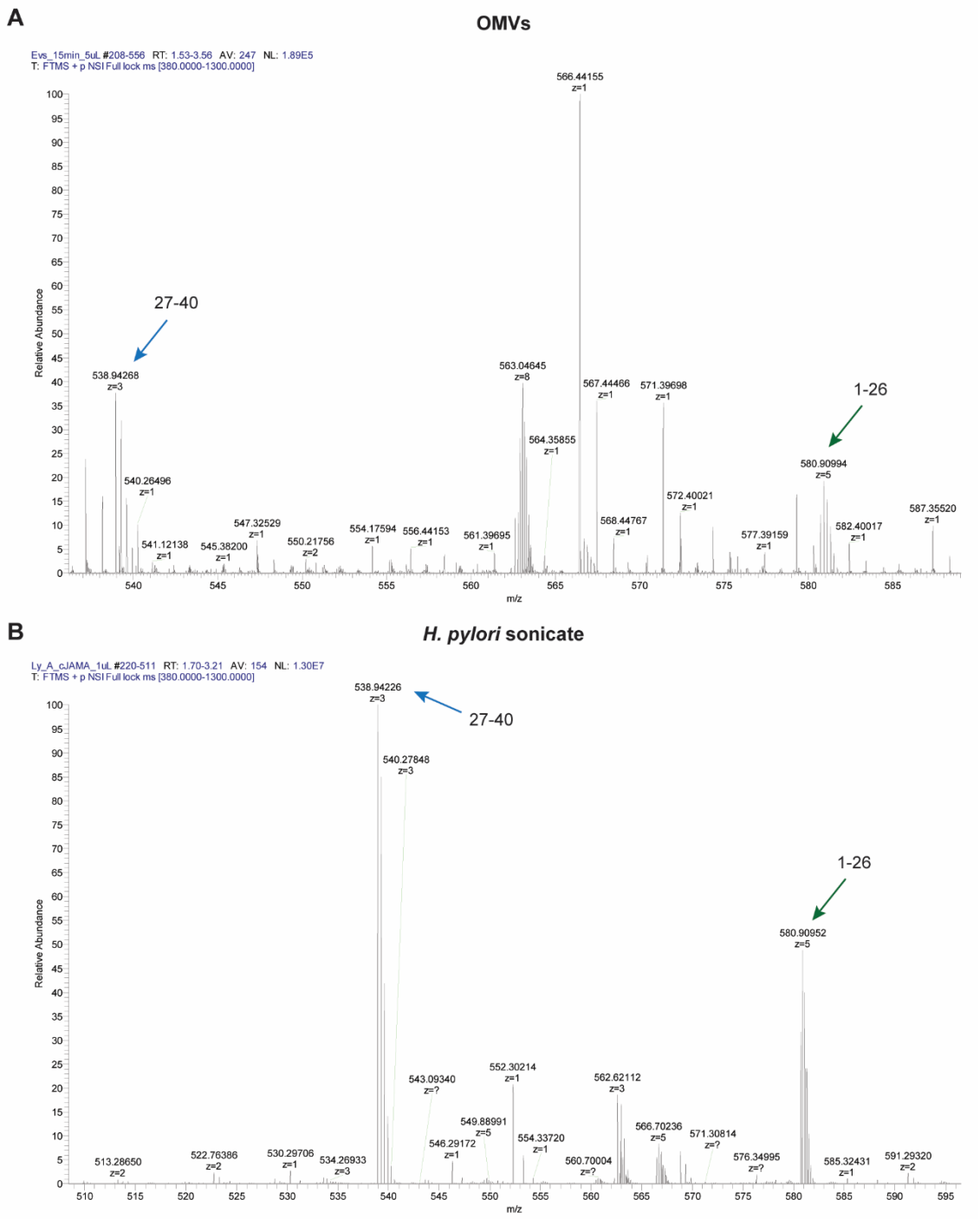

Figure 24. *H. pylori* OMVs cleave the cytoplasmic domain of JAM-A.

NanoLC-MS/MS analysis of the 40-amino acid synthetic cytoplasmic domain peptide of JAM-A after incubation with **(A)** *H. pylori* 26695 OMVs or with **(B)** the parental bacteria sonicate, for 15 min. Arrows indicate the peaks obtained after cleavage. Green arrows indicate the larger peptide: 1-26 = ^{260}AYSRGHFDRTKKGTSSKKVIYSQPSA^{285} (m/z 580.9). Blue arrows indicate the smaller peptides: 27-40 = ^{286}RSEGEFKQTSSFLV^{299} (m/z 538.9).

DISCUSSION

PART I: Isolation method and characterization of outer membranes vesicles of *Helicobacter pylori* grown in a chemically defined medium

OMVs have emerged as an important delivery system of bacterial components with an impact on bacteria-bacteria and bacteria-host interactions. In addition, OMVs are increasingly used for diverse therapeutic applications, namely vaccine development, taking advantage of their flexibility to genetic manipulation and nanosized structure for dissemination throughout the body, besides their easy production at large-scale and reduced costs [190].

The prevailing methods for the isolation of *H. pylori* OMVs are time-consuming and diverse, hampering the standardization of a suitable protocol for OMVs isolation, which is essential for downstream research and biomedical applications, namely the assessment of the functional roles of OMVs *in vitro* and *in vivo*, and large-scale production. The current published protocols have various disadvantages. First, they rely on the use of complex undefined media that contain yeast and animal tissue extracts, thus affecting the purity, content, and variability of OMVs between samples [119, 260]. Second, they have a lengthy duration due to the multiple centrifugation steps, which might compromise the final yield of OMVs [245]. Finally, the high variability of procedures and diversity of protocols weakens the comparison between studies, as the recovered fractions of OMVs can be different.

To overcome these drawbacks, in **Part I** we developed an isolation method of *H. pylori* OMVs trimming nonessential steps, after selecting the chemically defined medium F12 supplemented with cholesterol, as the bacterial culture medium for *H. pylori* growth. The final layout of this method included one low-speed centrifugation followed by supernatant 0.45 µm-filtration to remove bacteria and debris from the culture medium and to collect all range of OMVs sizes, and finally two ultracentrifugations for the recovery and washing of the OMVs.

Our results showed that F12-cholesterol medium was effective in sustaining bacterial growth, while achieving higher viability than the complex BB-FBS medium. Like previously described for several bacterial culture media [119, 243, 261], we observed a morphological change of *H. pylori* from the bacillary to the coccoid forms throughout the bacterial growth. The significantly decrease in CFUs counts at 72 h was not mirrored by the loss of bacterial viability using the LIVE/DEAD assay, likely due to the fact that coccoid forms are viable but non-culturable bacteria, with minimal metabolic activity and preserved membrane and genetic material integrities [18, 261].

Associated with the bacterial growth was the increased number of secreted OMVs, in accordance with descriptions of OMVs isolated from complex liquid cultures [118, 119]. Over 99% of OMVs measured between 20 and 200 nm, with mode of nearly 80 nm, which

is distinct from the reported enrichment in 100 to 200 nm sized OMVs isolated from *H. pylori* grown in BHI supplemented with 0.2% β-cyclodextrin [118]. This difference might be related with the distinct medium used, as well as with the effect of β-cyclodextrin, which chelates cholesterol that is essential for *H. pylori* growth [262, 263], highlighting how bacterial growth conditions impact on the properties of OMVs. Our findings also demonstrated the reproducibility of our OMVs' isolation protocol, as OMVs isolated from different *H. pylori* strains presented a similar size heterogeneity and were equally pure.

OMVs isolated from F12-cholesterol medium using our shorter protocol were highly pure, free from protein aggregates, flagella, and other bacterial contaminants, while requiring significantly less hands-on/hands-off time. Of relevance was also the high yield of OMVs, with around 10^{10} OMVs per mL of bacterial culture.

Considering the therapeutic potential of bacterial OMVs, it is of uttermost importance that the harvest of OMVs occurs from a chemically defined bacterial culture without animal-derived components that hinder the purification process and ultimately interfere with the host immune response [264]. Our method overcomes this issue and, by having increased time-efficiency in comparison to previous protocols, is a suitable approach for application in the biomedical field. Still, the yield and purity of *H. pylori* OMVs on a large-scale implementation of the protocol, and its application for the isolation of OMVs from other bacteria species, needs further evaluation.

PART II: Content analysis of *H. pylori* OMVs

In **Part II** of the results, we analyzed the content of *H. pylori* OMVs isolated from chemically defined bacterial liquid cultures following the protocol described in **Part I**. Knowing that OMVs transport a variety of contents derived from the parental bacterium [118-126], we focused the analyses on their protein and nucleic acids composition.

In **Part II.1**, the proteomic analysis of *H. pylori* OMVs showed that their cargo contained proteins from the membrane bacterial compartment. In fact, the most abundant group of proteins was associated with the bacterial membrane, being OMPs the most frequent. This finding was consistent throughout the different time points analyzed. Considering that OMVs originate from the blebbing of the OM, a high abundance of membrane-associated proteins was expected to be present as vesicle cargo [115, 118]. Our data is also in agreement with previous proteomic data from OMVs isolated from *H. pylori* 26695 [118]. Nevertheless, proteins from other bacterial compartments, including the periplasm and the cytoplasm were also part of the OMVs' content.

The proteins in *H. pylori* OMVs could be allocated to different biological processes and molecular functions. Of particular interest were proteins related with *H. pylori* colonization, survival, and pathogenesis, which were consistently present in OMVs isolated at the different time points. As examples, urease α/β neutralizes the acidic environment of the gastric mucosa [265], which together with outer membrane proteins (BabA, OipA) contribute to *H. pylori* colonization [28, 266]; β-lactamase (HcpA, HcpC, HcpD, HcpE) provides resistance to amoxicillin [267]; HtrA disrupts the epithelial cell-cell junctions, enabling transmigration of *H. pylori* across the gastric epithelium [99]; VacA and GGT induce vacuolization and apoptosis [268, 269]; HP-NAP, OipA, and urease β act as immune modulators by inducing pro-inflammatory responses [270-272]; catalase, superoxide dismutase, and thioredoxin protect *H. pylori* from the oxidative stress [273-275]; HP-NAP and bacterial non-heme ferritin are iron storage proteins, a key element for bacterial survival [276]. The presence of these virulence factors in *H. pylori* OMVs isolated from F12-cholesterol and from other complex liquid cultures [118, 119, 124] suggests that some proteins may be preferably loaded onto OMVs, independently of the culture media or bacterial strain, and highlights the importance of OMVs for the success of *H. pylori* infection.

Besides the common proteins identified in *H. pylori* OMVs between our study and those published by others [118, 119, 124], there were also unique proteins ascribed to each one. For example, the presence of the CagA protein in OMVs samples is not unanimous. In our study, we could not confidently identify CagA in OMVs derived from the CagA-positive *H. pylori* 26695, while several studies identified this protein as part of the proteome of OMVs of different *H. pylori* strains, namely J99, 26695, and P12 [118, 119, 124]. Our finding

regarding CagA is in agreement with that of Keenan *et al,* who also did not identify CagA in OMVs secreted by *H. pylori* 60190 [125]. Although we cannot exclude that these opposing data may arise from differences in the parental bacterial strains, they could also be related with differences in the methodology to grow *H. pylori* and to isolate OMVs from liquid cultures.

Our analysis also revealed that, even though the protein content of OMVs was similar throughout bacterial growth, some of these proteins were differentially expressed. For example, the virulence factor VacA was significantly more abundant in OMVs from later than from earlier time points of culture. These results contrast with those reported by Zavan *et al.*, who showed an enrichment of VacA in 16 h-OMVs in comparison to vesicles isolated from 48 h and 72 h bacterial cultures [118]. Additionally, the thioredoxin reductase, which protects *H. pylori* from the oxidative stress [275], and two proteins involved in iron acquisition and transport across the membrane, which is an essential micronutrient for bacterial survival, FrpB [277] and FecA, presented a significantly higher expression in OMVs from later than from earlier time points of culture. As discussed above, such differences in OMVs protein cargo might be related to the underlying growth conditions (bacterial strain, culture media, and initial bacterial density), which influence bacterial growth and the vesiculation process, in addition to technical issues (isolation method and proteomic analysis).

In **Part II.2**, the analysis of the nucleic acids' content of *H. pylori* OMVs confirmed the presence of both DNA and RNA. Because data from other Gram-negative pathogens showed that DNA from OMVs was associated with the external surface of vesicles [163], suggesting it resulted from bacterial lysis rather from a controlled process [278], our analysis was directed towards the detection of nucleic acids inside OMVs.

Our results showed *H. pylori* OMVs contain double-stranded DNA within the vesicle lumen and close to the vesicle surface, as identified by TEM and immunogold labelling. Furthermore, both DNA and RNA could be isolated from OMVs from distinct parental *H. pylori* strains that were subjected to external treatment with DNase and RNase. The characterization of these nucleic acids based on the amplification of genes associated with *H. pylori* colonization and virulence, revealed that *cagA*, *vacA*, and *ureB* genes and gene transcripts are present inside *H. pylori* OMVs.

Various studies have reported the presence of DNA inside OMVs secreted by Gram-negative bacteria, including *P. aeruginosa*, *E. coli*, *Acinetobacter baumannii*, and also *H. pylori* [122, 123, 162, 163, 247, 278-280]. OMVs act as vehicles for gene transfer between the same and between different bacterial species, in which the transfer of antibiotic resistant genes and of virulence genes has been demonstrated [161, 279, 281]. The transmission of

bacterial DNA mediated by OMVs into eukaryotic cells has also been shown [163]. Both fluorescent labelling and PCR analysis of the DNA within *P. aeruginosa* OMVs revealed that OMVs could deliver DNA into lung epithelial cells, where DNA was detected at the nucleus or the perinuclear space [163]. The influence of the delivery of DNA into host cells has, however, not been elucidated. It has been suggested that bacteria-human somatic cell lateral gene transfer can occur, in particular in cancer samples [282]. One of the examples was *Pseudomonas* spp. DNA integration found in gastric carcinoma samples. However, these analyses have been done using bioinformatics in human whole-genome and whole-transcriptome sequencing data of samples from The Cancer Genome Atlas (TCGA), which have been sequenced disregarding good practices for microbiome analyses. In fact, it has been shown that the microbiome of various TCGA batches of gastric carcinoma contained almost exclusively *Pseudomonas*, which may suggest that *Pseudomonas* spp. DNA integration in gastric carcinoma was an artifact [283].

The presence of RNA within bacteria OMVs has gained increasing attention recently, raising the hypothesis this cargo represents a mechanism that influences gene expression of host cells and/or host immune response [284, 285]. Indeed, the RNA repertoire of OMVs from various bacteria comprises a range of RNA species, including rRNA, tRNAs, sRNAs, RNA from coding and from intergenic regions, and full-length protein-encoding mRNAs [162, 278, 286-290]. Still, not many studies have reported their biological effects on host cells. The first example that RNAs within OMVs directly interact with host cell targets comes from the study of *P. aeruginosa* [162]. The authors speculated that bacterial sRNAs may act like eukaryotic microRNAs and bind to host cell mRNA targets to repress translation. Indeed, they showed that specific sRNAs in *P. aeruginosa* OMVs were predicted to form stable secondary structures and to target human immune mRNAs. The transfer of one of those sRNAs to primary human airway epithelial cells led to a reduction in LPS- and OMVs-induced IL-8 expression/secretion by those cells. The authors also provided *in vivo* evidence of decreased OMV-induced secretion of the IL-8 mouse cytokine homologue and attenuated neutrophilic infiltration in the mouse lung, mediated by this sRNA contained in OMVs [162]. A similar report identified sncRNAs in *H. pylori* OMVs and showed their transfer to gastric carcinoma cells, reducing LPS-stimulated induction of IL-8 secretion from cultured gastric cells [123]. Yet another study provided evidence for the cytoplasmic delivery and host cell activity of sRNAs contained in OMVs of *Aggregatibacter actinomycetemcomitans* [290]. The RNA cargo of OMVs from this periodontal pathogen was associated with TNF-α production via the TLR-8 and NF-κB signaling pathways. In contrast with the aforementioned studies, the transcriptional immune response pathways of bladder cells treated with the RNA cargo of OMVs from uropathogenic *E. coli* could not be differentiated from those of OMVs' LPS alone [291]. The authors noticed when purifying RNA from OMVs, there was also LPS that

co-purified with the vesicle RNA, highlighting technical factors that need to be considered in studies that evaluate the functional role of bacterial RNA.

Taken together with our results, these studies support a role for the nucleic acid cargo of *H. pylori* OMVs in influencing host cell gene expression and in modulating the host immune response, together with other bacterial components.

Considering OMVs originate from the bacterial OM, the presence of cytoplasmic components inside OMVs remains poorly understood and, for many years, it was considered that their detection derived from contamination due to bacterial cell lysis. It was described in *P. aeruginosa* the explosive cell lysis of a sub-population of bacteria, which led to the release of membrane fragments that form OMVs and engulf cytoplasmic components, including DNA [292]. However, Kadurugamuwa and Beveridge proposed a vesiculation mechanism that explains how cytoplasmic material is exported via OMVs [293]. In their model, the PG layer of the bacterial cell directly beneath the OM bleb is transiently disrupted, and allows the passage of cytoplasmic components into OMVs [293]. This localized and transient breach in the PG ensures that the bacterial cell does not dye and lysis does not occur. This mechanism of OMVs biogenesis further supports the notion that vesiculation is a selective and deliberated process, with increasing benefits for the bacterial community.

PART III: Transcriptomic analysis of gastric epithelial cells challenged with *H. pylori* OMVs

In **Part III** of the results we analyzed the effect of *H. pylori* OMVs on the transcriptomic profile of MKN74 gastric epithelial cell line by evaluating which host cell genes and biological pathways were affected after treatment. In addition, we compared the transcriptomic profile of OMVs-treated cells with the one of cells treated with *H. pylori*. For that, we used the Ion AmpliSeq™ Transcriptome Human Gene Expression that enables the simultaneous measurement of the expression levels of over 20,000 human genes.

In **Part III.1**, our results showed that the challenge of MKN74 cells with OMVs induced a unique gene expression profile that was different from the one of the *H. pylori*-infected cells and the one of the unchallenged control cells. However, and regardless of the different number of differentially expressed genes obtained for each experimental condition, OMVs- and *H. pylori*-treated cells shared a common signature of altered genes and of host cell functions and pathways that were affected by the challenge. Interestingly, OMVs had a greater effect than the parental bacteria in the alteration of some of those functions/pathways. This shows the competence of OMVs *per se* on modulating the host cell gene expression, which represents an important mechanism for *H. pylori* pathogenesis without the need for direct contact between bacteria and host.

Among the altered pathways, we observed that challenge with both OMVs and *H. pylori* induced the upregulation of, for example, host cell immune responses and apoptosis mechanisms, while downregulating mainly cell cycle and DNA repair pathways. In fact, despite both OMVs and *H. pylori* lead to the alteration of common pathways, GSEA analysis showed that OMVs induced a higher downregulation of cell cycle-associated genes, whereas *H. pylori* induced a higher downregulation of a specific DNA repair mechanism, BER. Taking this into consideration, we further analyzed the expression profile of genes involved in cell cycle and DNA repair.

In **Part III.2**, we focused on the cell cycle pathway. The cell cycle is a biological mechanism characterized by tightly controlled sequences of events that are implicated in cell proliferation, DNA repair and apoptosis. The progression of the cell cycle is dictated and controlled by dynamic interactions among different regulatory proteins. Cyclins and their catalytic subunits, the CDK, form complexes that are activated by cell division cycle proteins [294]. In turn, CDK are negatively regulated by CDK inhibitors in response to signals from the environment or to damage in the DNA [294]. The disturbance of any of these genes may affect the correct function of the cell cycle, resulting in the progressive accumulation of mutations [295]. *In vivo*, infection with *H. pylori* is associated with an increased proliferation

of gastric epithelial cells in both antrum and corpus of infected patients [296]. *In vitro*, the effect of *H. pylori* infection on cell proliferation is still controversial. While some authors reported the increase in proliferation of MKN28 and AGS cells via activation of cyclin E [249, 250], others have shown that infection with *H. pylori* was associated with cell cycle growth arrest at G1/S phase transition in AGS cells [251-253]. Associated to the G1/S arrest was the decrease in the protein levels of cyclins E and A, CDK 4 and 6, and p27, and increase in p21 and p53 proteins expression [251-253]. Our results show that OMVs downregulated the expression of a higher number of host cell cycle-related genes than the parental bacteria. Still, in both treated conditions there was a decrease in the expression of *CDKN1B* (*p27*), *CCNE1*, and *CCNE2*, and an increase in *CDKN1A* (*p21*) and *TP53* expression. These results are in line with the above-mentioned studies referring to G1/S arrest in the presence of *H. pylori* infection [251-253], and suggest a role for OMVs in inducing G1/S cell cycle arrest. Curiously, we found that *H. pylori* upregulated the M phase *CCNH* and *CDK7*, and genes associated with mitotic checkpoint, suggesting a cell cycle arrest at G2/M phase transition of *H. pylori*-treated cells. Nevertheless, it will be important in future studies to evaluate this effect in a cell cycle-synchronized cellular system.

In **Part III.3** we evaluated the effect of *H. pylori* OMVs in the expression of genes related with DNA repair mechanisms. Overall, our results showed that OMVs, similarly to *H. pylori*, downregulated the expression of genes associated with different DNA repair mechanisms. In particular, we detected the downregulation of MMR- and HR-related genes by OMVs. In agreement with these results are studies describing the effects of *H. pylori* infection in the downregulation of MMR-related protein levels and gene expression, and HR-associated gene expression in AGS cell lines and human primary gastric epithelial cells [254, 255, 297]. On the other hand, the expression of BER-related genes was notably different between OMVs-treated cells and *H. pylori*-infected cells. We detected an upregulation of genes involved in the repair of damaged DNA following oxidative stress, in the presence of OMVs. In fact, Futagami *et al* also observed an increase in *APEX1* mRNA levels after incubation of MKN28 cells with protein extracts from clinical isolates of *H. pylori* [298]. This upregulation in BER-associated genes may be associated with the suggested cell cycle arrest at G1/S induced by *H. pylori* OMVs.

PART IV: Effects of *H. pylori* OMVs on gastric epithelial cell-cell junctions

In **Part IV,** we explored the effects of *H. pylori* OMVs on gastric cells, by evaluating their impact on the structure and functions of epithelial intercellular junctions.

We started by demonstrating that MKN74 gastric epithelial cells internalize *H. pylori* OMVs, by showing the presence of fluorescently-labelled OMVs inside Rab5- and LAMP-1-expressing vesicles of the endocytic pathway. Although this is the first reported observation in the MKN74 cell line, others have shown that *H. pylori* OMVs can be uptaken by gastric AGS, MKN45, and KatoIII cell lines [121, 126, 148, 155]. In MKN74 cells, we detected OMVs in early endosomes and late endosomes/lysosomes at 3 and 15 minutes post-challenge. Although we did not perform long-term experiments, others have detected OMVs in lysosomes 1 hour after challenge [155]. OMVs have also been detected inside AGS cells 16 hours post-challenge [121]. Despite *H. pylori* OMVs remain inside cells for at least 16 hours, their fate and the fate of their cargo remain unclear. Bielaszewska *et al* investigated how a number of virulence factors identified on OMVs from the enterohemorrhagic *E. coli* (EHEC) O157 strain contributed to bacterial pathogenesis after internalization. They found that EHEC O157 OMVs entered cells via dynamin-dependent endocytosis and followed the endocytic pathway to lysosomes, where they were degraded. However, during intracellular trafficking, some of their toxin cargo separated from vesicles, while other remained associated with OMVs. The separated toxin cargo targeted different host cell compartments, and was associated with host cell DNA damage and apoptosis [299]. Considering *H. pylori* OMVs partially use dynamin-dependent mechanisms for entry into host cells [126, 155], we may hypothesize that OMVs deliver virulence factors into epithelial cells using a similar mechanism. Further studies are needed to address this hypothesis.

Our analysis on the effects of *H. pylori* OMVs on the cell-cell junctional complexes was performed in two distinct cell lines, which were previously demonstrated to establish competent apical-junctional complexes [104, 228, 232]. In these cell lines, and in confluent conditions, the TJ transmembrane JAM-A and the cytoplasmic plaque adaptor ZO-1, and the AJ transmembrane E-cadherin, were all found located at the cell membrane, in a continuous honeycomb-like pattern. After challenge with *H. pylori* OMVs, there was disorganization and/or displacement of these proteins from the cell membrane to the cytoplasm, and this phenotype was more pronounced with longer times of exposure. These phenotypic alterations were detected in both cell lines, showing that they are cell line-independent. Although this may reflect cell membrane dynamics, it remains to be elucidated whether junctional protein displacement modulates host cell signaling pathways. In keeping with our observations, Turkina *et al* showed that ZO-1 distribution at the membrane of the

colorectal carcinoma Caco-2 cells shifted from a uniform and straight to a disorganized and diffuse pattern upon challenge with OMVs derived from *H. pylori* P12 strain [300].

Interestingly, and contrasting with the infections with the parental *H. pylori* that led to decreased junctional protein expression, we could not detect such variation upon OMVs' exposure. In agreement with our findings, challenging of Caco2 cells with *H. pylori* P12 OMVs caused only very slight changes in the expression levels of junctional proteins ZO-1, occludin, E-cadherin, and β-catenin [300]. The membrane displacement of proteins of the TJ and AJ to the cytoplasm is a similar finding to what others and we have observed upon infection with the parental *H. pylori* strain [104, 218, 232, 301]. However, there is opposing evidence concerning the targeting of intercellular junctions by the bacterium occurring with decreased or without changes in protein expression [104, 218, 224, 232, 301]. For example, Wroblewski *et al* and Krueger *et al* report redistribution of occludin, ZO-1, and p120-catenin in the presence of *H. pylori*, without affecting their protein levels [218, 224].

Concomitantly with junctional protein displacement by *H. pylori* OMVs, there were functional alterations to the integrity of gastric cell monolayers. This was detected by the significantly lower electrical resistance and increased permeability of gastric cell monolayers upon challenge with OMVs in comparison with control unchallenged cells. These observations paralleled the effect of the infection with the parental bacterium.

As shown by our proteomics data and by others, *H. pylori* OMVs contain as part of their cargo factors known to target junctional proteins, namely CagA, VacA, urease, and HtrA [99, 118, 119, 124, 218, 219, 223, 302]. Nevertheless, there is conflicting data concerning the association of such factors with junctional alterations, with results varying depending on the cell line, bacterial strain, culture and co-culture conditions used [191]. Additionally, there are junctional alterations mediated by *H. pylori* infection that cannot be explained by the abovementioned factors [104, 232].

Although in the scope of this Thesis we did not identify the exact factors in the cargo of *H. pylori* OMVs responsible for junctional alterations, after our group identified *H. pylori* PqqE as the protease that cleaves the cytoplasmic domain of JAM-A, independently of the T4SS, it was hypothesized that OMVs constitute the delivery system of the bacterial protease into the host cell [104]. *H. pylori* OMVs were shown to act as vehicles of various bacterial molecules to gastric cells, namely PG and CagA [121, 300]. Our data, in accordance with data published by others, evidenced the presence of PqqE (and YmxG) in the proteome of *H. pylori* OMVs [118, 119]. Noteworthy, and similarly to the bacterium, we demonstrated for the first time that *H. pylori* OMVs cleave the 40-amino acids peptide of the cytoplasmic domain of JAM-A. Cleavage mediated by the OMVs occurred after amino acid 26 of the cytoplasmic domain peptide, which correspond to Ala^{285} of the human JAM-A, having the same cleavage site specificity as the parental *H. pylori* 26695 strain, and PqqE and PqqE-

YmxG recombinant proteins [104]. JAM-A is implicated in a series of functions, namely the regulation of the epithelial barrier, cell polarity, adhesion, and migration [206, 303, 304]. The JAM-A cytoplasmic tail contains a terminal postsynaptic density-95, discs-large, zona occludens 1 (PDZ) domain binding motif (^{296}SFLV^{299}) that can interact with various cytoplasmic adaptor proteins, including afadin, ZO-1, and PAR2 [305]. This domain is important for JAM-A-mediated recruitment of protein scaffolds to specific intercellular adhesion sites and for assembly of signaling complexes at those sites, which are pivotal for JAM-A functions [305]. Since *H. pylori* and *H. pylori*-derived OMVs cleave the cytoplasmic domain of JAM-A before the terminal ^{296}SFLV^{299}, it is highly likely that cellular functions mediated by this motif are lost. Indeed, the comparison of cell line models stably transfected with the full-length JAM-A or with JAM-A lacking the region that encode amino acids 285 to 299 (and consequently lacking ^{296}SFLV^{299}), revealed alterations to the gastric epithelial barrier and to cell adhesion, which could be attributable to the cleaved C-terminus JAM-A upon *H. pylori* infection [104]. In this case, it would also be expected that OMVs would have a similar effect, since they cleave JAM-A at the same site. Although we did not study the effects of OMVs in cell adhesion, in fact we observed decreased TER and increased permeability of gastric cell monolayers when treated with OMVs. Overall, these results favors the hypothesis that OMVs are the means of transport of *H. pylori* PqqE to the inside of the host cell, and may contribute to the disruption of gastric epithelial permeability.

H. pylori infection leads to a series of events that, in particular circumstances may result in severe clinical outcomes. Several virulence factors influence the outcome of *H. pylori* infection. These bacterial virulence factors can be released to the extracellular medium, or influence the host cell by direct contact or by injection. In this context, OMVs released by *H. pylori* may represent an additional means for the bacteria to deliver their factors into epithelial cells. These factors could facilitate bacterial colonization and survival in the gastric mucosa and contribute to bacterial pathogenesis. In accordance with this hypothesis, in this Thesis it was demonstrated that *H. pylori* OMVs carry important factors involved in bacterial survival and pathogenicity. Although the fate of these factors after OMVs entry into epithelial host cells remains unclear, one may consider they are released along the endocytic pathway, before degradation in lysosomes [57].

In this Thesis, it was also demonstrated that *H. pylori* OMVs-mediated alterations to structure and functions of cell-cell junctions. It is likely that alterations to the junctional complexes, namely to TJs, occur early in the infection process, thus creating a favorable replicative niche at the apical surface of the cell, with access to ions essential for bacterial growth and survival [67, 73]. Moreover, *H. pylori* OMVs-mediated alterations to intercellular junctions may result on altered cell polarity, giving bacteria access to host cell receptors

situated basolaterally. The interaction between *H. pylori* and the host receptors activates different signaling pathways important for bacterial pathogenesis and with detrimental consequences for disease development.

Overall, our results support the hypothesis that once reaching the gastric mucosa, *H. pylori* secretes OMVs that will be internalized by epithelial cells. By altering the host cell transcriptomic profile and by affecting the epithelial cell-cell junctional complexes, OMVs will help create a favorable replicative niche at the cell surface with direct access to nutrients, contributing to *H. pylori* colonization, survival, and pathogenesis.

SUMMARY AND CONCLUSIONS

The Gram-negative *Helicobacter pylori* is considered as the most common chronic bacterial infection in the world. Chronic *H. pylori* infection and ensuing gastritis are associated with more severe disease outcomes, like peptic ulcer disease, gastric carcinoma, and gastric mucosa-associated lymphoid tissue (MALT) lymphoma, depending on the interplay between host factors and bacterial virulence factors. Gram-negative bacteria constitutively release outer membrane vesicles (OMVs), which have emerged as intra- and inter-species delivery systems of bacterial components. In the context of *H. pylori* infection, the influence of OMVs in bacterium-host interactions remains largely unexplored. Therefore, the general aim of this thesis was to disclose the role of OMVs in *H. pylori* pathogenesis.

The initial approach consisted on the development and optimization of a protocol for the isolation of *H. pylori* OMVs having as basis a chemically defined medium. Using this approach, a good yield of highly pure bona fide OMVs was recovered from cultures of different *H. pylori* strains and in different periods of bacterial growth, as assessed by nanoparticle tracking analysis, transmission electron microscopy (TEM), and proteomic analyses, confirming the reliability of the protocol.

Next, the cargo of *H. pylori* OMVs was addressed. The evaluation of the proteome of OMVs showed proteins associated with the bacterial membrane, namely outer membrane proteins (OMPs), as the most abundant, despite the presence of proteins from other bacterial compartments. The proteins in OMVs were related to different biological processes and molecular functions, in particular to *H. pylori* colonization, survival, and pathogenesis. The nucleic acids' cargo of OMVs contained both bacterial DNA and RNA inside the vesicles. Targeted analysis revealed the presence of genes and of the respective gene transcripts encoding known *H. pylori* virulence factors.

Since OMVs play an important role in bacteria-host interactions, the effects of *H. pylori* OMVs on host cell gene expression and on the associated molecular pathways were next analyzed. OMVs induced a gene expression profile on gastric epithelial cells that clustered separately from those induced by *H. pylori*-infected and from control cells. Functional gene enrichment analyses identified both shared and unique host cell pathways/functions attributed to OMVs and to the bacterium. In particular, the effects of OMVs and *H. pylori* in cell cycle and DNA repair were shown.

Next, the influence of *H. pylori* OMVs in intercellular junction disruption was evaluated. Challenge of two different gastric cell lines with *H. pylori* OMVs led to the disorganization and/or displacement of tight and adherens junctional proteins from cell-cell contacts, without affecting the respective protein levels. These changes were accompanied by alterations to the electrical resistance and paracellular permeability of cell monolayers, showing that OMVs alter the function of these junctions. Furthermore, the *H. pylori* PqqE protease, known to cleave the cytoplasmic domain of junctional adhesion molecule A (JAM-A), was identified

in the cargo of *H. pylori* OMVs. Notably, OMVs were shown to cleave JAM-A, and to have the same cleavage site specificity as *H. pylori*, suggesting OMVs as a delivery system for PqqE.

In conclusion, *H. pylori* OMVs contain factors associated with bacterial colonization, survival, and pathogenesis, and influence multiple gastric epithelial cell functions. This thesis provides novel evidence for the role of *H. pylori* OMVs in bacteria-host interactions, paving the way for future research on the mechanisms through which the cargo of OMVs directly shapes the host cell programme.

SUMÁRIO E CONCLUSÕES

Helicobacter pylori, bactéria gram-negativa, é considerada como a infeção bacteriana crónica mais comum no mundo. A infeção crónica *de H. pylori* e a gastrite subsequente estão associadas a resultados mais graves da doença, como a doença da úlcera péptica, o carcinoma gástrico e o linfoma do tecido linfóide associado à mucosa gástrica (MALT), dependendo da interação entre os fatores do hospedeiro e os fatores de virulência bacteriana. As bactérias gram-negativas libertam constitutivamente as vesículas da membrana externa (OMVs), que surgiram como sistemas de entrega intra- e inter-espécies de componentes bacterianos. No contexto da infeção por *H. pylori,* a influência das OMVs nas interações bactéria-hospedeiro permanece em grande parte inexplorada. Por conseguinte, o objetivo geral desta tese é o de divulgar o papel das OMVs na patogénese da *H. pylori.*

A abordagem inicial consistiu no desenvolvimento e otimização de um protocolo para o isolamento das OMVs de *H. pylori* tendo como base um meio quimicamente definido. Utilizando esta abordagem, um bom rendimento de OMVs altamente puras foi recuperado de culturas de diferentes estirpes de *H. pylori* e em diferentes períodos de crescimento bacteriano, conforme avaliado pela análise de rastreio de nanopartículas, microscopia electrónica de transmissão (TEM) e análises proteómicas, confirmando a fiabilidade do protocolo.

Em seguida, o conteúdo das OMVs de *H. pylori* foi abordada. A avaliação do proteoma das OMVs mostrou proteínas associadas à membrana bacteriana, nomeadamente proteínas da membrana externa (OMPs), como as mais abundantes, apesar da presença de proteínas de outros compartimentos bacterianos. Observou-se que as proteínas nas OMVs estão relacionadas com diferentes processos biológicos e funções moleculares, em particular com colonização, sobrevivência e patogénese de *H. pylori.* O conteúdo em ácidos nucleicos das OMVs continha ADN bacteriano e ARN dentro das vesículas. A análise direcionada revelou a presença de genes e das respetivas transcrições genéticas que codificam fatores de virulência de *H. pylori* conhecidos.

Uma vez que as OMVs desempenham um papel importante nas interações entre bactérias e hospedeiros, os efeitos das OMVs de *H. pylori* na expressão génica das células hospedeiras e nas vias moleculares associadas foram analisados. As OMVs induzem um perfil de expressão genética em células epiteliais gástricas que se agrupam separadamente dos perfis das células controlo e das células infetadas por *H. pylori*. As análises funcionais de enriquecimento de genes identificaram vias/funções das células hospedeiras que são comuns e únicas ao tratamento com OMVs e com a bactéria. Em particular, foram demonstrados os efeitos das OMVs e de *H. pylori* no ciclo celular e nos mecanismos de reparação do ADN das células hospedeiras.

Em seguida, foi avaliada a influência das OMVs de *H. pylori* na rutura das junções intercelulares. A estimulação de duas linhas celulares gástricas com OMVs de *H. pylori* levou à desorganização e/ou deslocalização de proteínas juncionais oclusivas e aderentes, dos contactos celulares, sem afetar os respetivos níveis proteicos. Estas alterações foram acompanhadas por alterações na resistência elétrica e na permeabilidade paracelular das monocamadas celulares, mostrando que as OMVs alteram o funcionamento destas junções. Além disso, a protease PqqE de *H. pylori*, conhecida por clivar o domínio citoplasmático da molécula de adesão juncional A (JAM-A), foi identificada na carga das OMVs de *H. pylori.* Notavelmente, as OMVs clivaram a JAM-A, tendo a mesma especificidade para o local de clivagem que *H. pylori*, sugerindo que as OMVs funcionam como um sistema de entrega da PqqE.

Em conclusão, as OMVs de *H. pylori* contêm fatores associados à colonização bacteriana, sobrevivência e patogénese, influenciando múltiplas funções epiteliais gástricas. Esta tese fornece novas evidências para o papel das OMVs de *H. pylori* nas interações entre bactérias e hospedeiros, abrindo caminho para futuras pesquisas sobre os mecanismos através dos quais a carga de OMVs molda diretamente o programa das células hospedeiras.

REFERENCES

1. Marshall, B.J. and Warren, J.R. (1984) Unidentified curved bacilli in the stomach of patients with gastritis and peptic ulceration. Lancet. 1(8390): p. 1311-5.
2. Linz, B., Balloux, F., Moodley, Y., Manica, A., Liu, H., Roumagnac, P., Falush, D., Stamer, C., Prugnolle, F., van der Merwe, S.W., Yamaoka, Y., Graham, D.Y., Perez-Trallero, E., Wadstrom, T., Suerbaum, S., and Achtman, M. (2007) An African origin for the intimate association between humans and Helicobacter pylori. Nature. 445(7130): p. 915-918.
3. Moodley, Y., Linz, B., Bond, R.P., Nieuwoudt, M., Soodyall, H., Schlebusch, C.M., Bernhoft, S., Hale, J., Suerbaum, S., Mugisha, L., van der Merwe, S.W., and Achtman, M. (2012) Age of the association between Helicobacter pylori and man. PLoS Pathog. 8(5): p. e1002693.
4. Falush, D., Wirth, T., Linz, B., Pritchard, J.K., Stephens, M., Kidd, M., Blaser, M.J., Graham, D.Y., Vacher, S., Perez-Perez, G.I., Yamaoka, Y., Megraud, F., Otto, K., Reichard, U., Katzowitsch, E., Wang, X., Achtman, M., and Suerbaum, S. (2003) Traces of human migrations in Helicobacter pylori populations. Science. 299(5612): p. 1582-5.
5. Moodley, Y., Brunelli, A., Ghirotto, S., Klyubin, A., Maady, A.S., Tyne, W., Munoz-Ramirez, Z.Y., Zhou, Z., Manica, A., Linz, B., and Achtman, M. (2021) Helicobacter pylori's historical journey through Siberia and the Americas. Proc Natl Acad Sci U S A. 118(25).
6. Hooi, J.K.Y., Lai, W.Y., Ng, W.K., Suen, M.M.Y., Underwood, F.E., Tanyingoh, D., Malfertheiner, P., Graham, D.Y., Wong, V.W.S., Wu, J.C.Y., Chan, F.K.L., Sung, J.J.Y., Kaplan, G.G., and Ng, S.C. (2017) Global Prevalence of Helicobacter pylori Infection: Systematic Review and Meta-Analysis. Gastroenterology. 153(2): p. 420-429.
7. Bastos, J., Peleteiro, B., Barros, R., Alves, L., Severo, M., de Fatima Pina, M., Pinto, H., Carvalho, S., Marinho, A., Guimaraes, J.T., Azevedo, A., La Vecchia, C., Barros, H., and Lunet, N. (2013) Sociodemographic determinants of prevalence and incidence of Helicobacter pylori infection in Portuguese adults. Helicobacter. 18(6): p. 413-22.
8. Malaty, H.M. (2007) Epidemiology of Helicobacter pylori infection. Best Pract Res Clin Gastroenterol. 21(2): p. 205-14.
9. Burucoa, C. and Axon, A. (2017) Epidemiology of Helicobacter pylori infection. Helicobacter. 22 Suppl 1.
10. Kivi, M., Johansson, A.L., Reilly, M., and Tindberg, Y. (2005) Helicobacter pylori status in family members as risk factors for infection in children. Epidemiol Infect. 133(4): p. 645-52.
11. Weyermann, M., Rothenbacher, D., and Brenner, H. (2009) Acquisition of Helicobacter pylori infection in early childhood: independent contributions of infected mothers, fathers, and siblings. Am J Gastroenterol. 104(1): p. 182-9.
12. Luzza, F., Mancuso, M., Imeneo, M., Contaldo, A., Giancotti, L., Pensabene, L., Doldo, P., Liberto, M.C., Strisciuglio, P., Foca, A., Guandalini, S., and Pallone, F. (2000) Evidence favouring the gastro-oral route in the transmission of Helicobacter pylori infection in children. Eur J Gastroenterol Hepatol. 12(6): p. 623-7.
13. Chow, T.K., Lambert, J.R., Wahlqvist, M.L., and Hsu-Hage, B.H. (1995) Helicobacter pylori in Melbourne Chinese immigrants: evidence for oral-oral transmission via chopsticks. J Gastroenterol Hepatol. 10(5): p. 562-9.
14. Kelly, S.M., Pitcher, M.C., Farmery, S.M., and Gibson, G.R. (1994) Isolation of Helicobacter pylori from feces of patients with dyspepsia in the United Kingdom. Gastroenterology. 107(6): p. 1671-4.
15. Klein, P.D., Graham, D.Y., Gaillour, A., Opekun, A.R., and Smith, E.O. (1991) Water source as risk factor for Helicobacter pylori infection in Peruvian children. Gastrointestinal Physiology Working Group. Lancet. 337(8756): p. 1503-6.
16. Hopkins, R.J., Vial, P.A., Ferreccio, C., Ovalle, J., Prado, P., Sotomayor, V., Russell, R.G., Wasserman, S.S., and Morris, J.G., Jr. (1993) Seroprevalence of Helicobacter pylori in Chile: vegetables may serve as one route of transmission. J Infect Dis. 168(1): p. 222-6.
17. Kusters, J.G., van Vliet, A.H., and Kuipers, E.J. (2006) Pathogenesis of Helicobacter pylori infection. Clin Microbiol Rev. 19(3): p. 449-90.

18. Ierardi, E., Losurdo, G., Mileti, A., Paolillo, R., Giorgio, F., Principi, M., and Di Leo, A. (2020) The Puzzle of Coccoid Forms of Helicobacter pylori: Beyond Basic Science. Antibiotics (Basel). 9(6).
19. Schreiber, S., Konradt, M., Groll, C., Scheid, P., Hanauer, G., Werling, H.O., Josenhans, C., and Suerbaum, S. (2004) The spatial orientation of Helicobacter pylori in the gastric mucus. Proc Natl Acad Sci U S A. 101(14): p. 5024-9.
20. Necchi, V., Candusso, M.E., Tava, F., Luinetti, O., Ventura, U., Fiocca, R., Ricci, V., and Solcia, E. (2007) Intracellular, intercellular, and stromal invasion of gastric mucosa, preneoplastic lesions, and cancer by Helicobacter pylori. Gastroenterology. 132(3): p. 1009-23.
21. Hamlet, A., Thoreson, A.C., Nilsson, O., Svennerholm, A.M., and Olbe, L. (1999) Duodenal Helicobacter pylori infection differs in cagA genotype between asymptomatic subjects and patients with duodenal ulcers. Gastroenterology. 116(2): p. 259-68.
22. Keilberg, D. and Ottemann, K.M. (2016) How Helicobacter pylori senses, targets and interacts with the gastric epithelium. Environ Microbiol. 18(3): p. 791-806.
23. Eaton, K.A., Brooks, C.L., Morgan, D.R., and Krakowka, S. (1991) Essential role of urease in pathogenesis of gastritis induced by Helicobacter pylori in gnotobiotic piglets. Infect Immun. 59(7): p. 2470-5.
24. Montecucco, C. and Rappuoli, R. (2001) Living dangerously: how Helicobacter pylori survives in the human stomach. Nat Rev Mol Cell Biol. 2(6): p. 457-66.
25. Backert, S., Clyne, M., and Tegtmeyer, N. (2011) Molecular mechanisms of gastric epithelial cell adhesion and injection of CagA by Helicobacter pylori. Cell Commun Signal. 9: p. 28.
26. Ilver, D., Arnqvist, A., Ogren, J., Frick, I.M., Kersulyte, D., Incecik, E.T., Berg, D.E., Covacci, A., Engstrand, L., and Boren, T. (1998) Helicobacter pylori adhesin binding fucosylated histo-blood group antigens revealed by retagging. Science. 279(5349): p. 373-7.
27. Aspholm-Hurtig, M., Dailide, G., Lahmann, M., Kalia, A., Ilver, D., Roche, N., Vikstrom, S., Sjostrom, R., Linden, S., Backstrom, A., Lundberg, C., Arnqvist, A., Mahdavi, J., Nilsson, U.J., Velapatino, B., Gilman, R.H., Gerhard, M., Alarcon, T., Lopez-Brea, M., Nakazawa, T., Fox, J.G., Correa, P., Dominguez-Bello, M.G., Perez-Perez, G.I., Blaser, M.J., Normark, S., Carlstedt, I., Oscarson, S., Teneberg, S., Berg, D.E., and Boren, T. (2004) Functional adaptation of BabA, the H. pylori ABO blood group antigen binding adhesin. Science. 305(5683): p. 519-22.
28. Ishijima, N., Suzuki, M., Ashida, H., Ichikawa, Y., Kanegae, Y., Saito, I., Boren, T., Haas, R., Sasakawa, C., and Mimuro, H. (2011) BabA-mediated adherence is a potentiator of the Helicobacter pylori type IV secretion system activity. J Biol Chem. 286(28): p. 25256-64.
29. Gerhard, M., Lehn, N., Neumayer, N., Boren, T., Rad, R., Schepp, W., Miehlke, S., Classen, M., and Prinz, C. (1999) Clinical relevance of the Helicobacter pylori gene for blood-group antigen-binding adhesin. Proc Natl Acad Sci U S A. 96(22): p. 12778-83.
30. Mahdavi, J., Sonden, B., Hurtig, M., Olfat, F.O., Forsberg, L., Roche, N., Angstrom, J., Larsson, T., Teneberg, S., Karlsson, K.A., Altraja, S., Wadstrom, T., Kersulyte, D., Berg, D.E., Dubois, A., Petersson, C., Magnusson, K.E., Norberg, T., Lindh, F., Lundskog, B.B., Arnqvist, A., Hammarstrom, L., and Boren, T. (2002) Helicobacter pylori SabA adhesin in persistent infection and chronic inflammation. Science. 297(5581): p. 573-8.
31. Smith, M.F., Jr., Mitchell, A., Li, G., Ding, S., Fitzmaurice, A.M., Ryan, K., Crowe, S., and Goldberg, J.B. (2003) Toll-like receptor (TLR) 2 and TLR5, but not TLR4, are required for Helicobacter pylori-induced NF-kappa B activation and chemokine expression by epithelial cells. J Biol Chem. 278(35): p. 32552-60.
32. Viala, J., Chaput, C., Boneca, I.G., Cardona, A., Girardin, S.E., Moran, A.P., Athman, R., Memet, S., Huerre, M.R., Coyle, A.J., DiStefano, P.S., Sansonetti, P.J., Labigne, A., Bertin, J., Philpott, D.J., and Ferrero, R.L. (2004) Nod1 responds to peptidoglycan delivered by the Helicobacter pylori cag pathogenicity island. Nat Immunol. 5(11): p. 1166-74.
33. Atherton, J.C. and Blaser, M.J. (2009) Coadaptation of Helicobacter pylori and humans: ancient history, modern implications. J Clin Invest. 119(9): p. 2475-87.

34. Backhed, F., Rokbi, B., Torstensson, E., Zhao, Y., Nilsson, C., Seguin, D., Normark, S., Buchan, A.M., and Richter-Dahlfors, A. (2003) Gastric mucosal recognition of Helicobacter pylori is independent of Toll-like receptor 4. J Infect Dis. 187(5): p. 829-36.
35. Cook, K.W., Letley, D.P., Ingram, R.J., Staples, E., Skjoldmose, H., Atherton, J.C., and Robinson, K. (2014) CCL20/CCR6-mediated migration of regulatory T cells to the Helicobacter pylori-infected human gastric mucosa. Gut. 63(10): p. 1550-9.
36. Tegtmeyer, N. and Backert, S., *Molecular Pathogenesis and Signal Transduction by Helicobacter pylori*. 2017: Springer International Publishing.
37. Muotiala, A., Helander, I.M., Pyhala, L., Kosunen, T.U., and Moran, A.P. (1992) Low biological activity of Helicobacter pylori lipopolysaccharide. Infect Immun. 60(4): p. 1714-6.
38. Ramarao, N., Gray-Owen, S.D., and Meyer, T.F. (2000) Helicobacter pylori induces but survives the extracellular release of oxygen radicals from professional phagocytes using its catalase activity. Mol Microbiol. 38(1): p. 103-13.
39. Gobert, A.P., McGee, D.J., Akhtar, M., Mendz, G.L., Newton, J.C., Cheng, Y., Mobley, H.L., and Wilson, K.T. (2001) Helicobacter pylori arginase inhibits nitric oxide production by eukaryotic cells: a strategy for bacterial survival. Proc Natl Acad Sci U S A. 98(24): p. 13844-9.
40. Amedei, A., Bergman, M.P., Appelmelk, B.J., Azzurri, A., Benagiano, M., Tamburini, C., van der Zee, R., Telford, J.L., Vandenbroucke-Grauls, C.M., D'Elios, M.M., and Del Prete, G. (2003) Molecular mimicry between Helicobacter pylori antigens and H+, K+ --adenosine triphosphatase in human gastric autoimmunity. J Exp Med. 198(8): p. 1147-56.
41. D'Elios, M.M., Manghetti, M., De Carli, M., Costa, F., Baldari, C.T., Burroni, D., Telford, J.L., Romagnani, S., and Del Prete, G. (1997) T helper 1 effector cells specific for Helicobacter pylori in the gastric antrum of patients with peptic ulcer disease. J Immunol. 158(2): p. 962-7.
42. Shi, Y., Liu, X.F., Zhuang, Y., Zhang, J.Y., Liu, T., Yin, Z., Wu, C., Mao, X.H., Jia, K.R., Wang, F.J., Guo, H., Flavell, R.A., Zhao, Z., Liu, K.Y., Xiao, B., Guo, Y., Zhang, W.J., Zhou, W.Y., Guo, G., and Zou, Q.M. (2010) Helicobacter pylori-induced Th17 responses modulate Th1 cell responses, benefit bacterial growth, and contribute to pathology in mice. J Immunol. 184(9): p. 5121-9.
43. Serelli-Lee, V., Ling, K.L., Ho, C., Yeong, L.H., Lim, G.K., Ho, B., and Wong, S.B. (2012) Persistent Helicobacter pylori specific Th17 responses in patients with past H. pylori infection are associated with elevated gastric mucosal IL-1beta. PLoS One. 7(6): p. e39199.
44. Enarsson, K., Lundgren, A., Kindlund, B., Hermansson, M., Roncador, G., Banham, A.H., Lundin, B.S., and Quiding-Jarbrink, M. (2006) Function and recruitment of mucosal regulatory T cells in human chronic Helicobacter pylori infection and gastric adenocarcinoma. Clin Immunol. 121(3): p. 358-68.
45. Ford, A.C., Gurusamy, K.S., Delaney, B., Forman, D., and Moayyedi, P. (2016) Eradication therapy for peptic ulcer disease in Helicobacter pylori-positive people. Cochrane Database Syst Rev. 4: p. CD003840.
46. Kuipers, E.J., Thijs, J.C., and Festen, H.P. (1995) The prevalence of Helicobacter pylori in peptic ulcer disease. Aliment Pharmacol Ther. 9 Suppl 2: p. 59-69.
47. Rauws, E.A. and Tytgat, G.N. (1990) Cure of duodenal ulcer associated with eradication of Helicobacter pylori. Lancet. 335(8700): p. 1233-5.
48. Kim, J. and Wang, T.C. (2021) Helicobacter pylori and Gastric Cancer. Gastrointest Endosc Clin N Am. 31(3): p. 451-465.
49. Reports, I.H.p.W.G.J.I.W.G. (2014) Helicobacter pylori eradication as a strategy for preventing gastric cancer. 8.
50. Rawla, P. and Barsouk, A. (2019) Epidemiology of gastric cancer: global trends, risk factors and prevention. Prz Gastroenterol. 14(1): p. 26-38.

51. (1994) Schistosomes, liver flukes and Helicobacter pylori. IARC Working Group on the Evaluation of Carcinogenic Risks to Humans. Lyon, 7-14 June 1994. IARC Monogr Eval Carcinog Risks Hum. 61: p. 1-241.
52. Figueiredo, C., Camargo, M.C., Leite, M., Fuentes-Panana, E.M., Rabkin, C.S., and Machado, J.C. (2017) Pathogenesis of Gastric Cancer: Genetics and Molecular Classification. Curr Top Microbiol Immunol. 400: p. 277-304.
53. Correa, P. (1988) A human model of gastric carcinogenesis. Cancer Res. 48(13): p. 3554-60.
54. Correa, P. (1992) Human gastric carcinogenesis: a multistep and multifactorial process--First American Cancer Society Award Lecture on Cancer Epidemiology and Prevention. Cancer Res. 52(24): p. 6735-40.
55. Atherton, J.C. (2006) The pathogenesis of Helicobacter pylori-induced gastro-duodenal diseases. Annu Rev Pathol. 1: p. 63-96.
56. Ford, A.C., Forman, D., Hunt, R., Yuan, Y., and Moayyedi, P. (2015) Helicobacter pylori eradication for the prevention of gastric neoplasia. Cochrane Database Syst Rev. (7): p. CD005583.
57. Sagaert, X., Van Cutsem, E., De Hertogh, G., Geboes, K., and Tousseyn, T. (2010) Gastric MALT lymphoma: a model of chronic inflammation-induced tumor development. Nat Rev Gastroenterol Hepatol. 7(6): p. 336-46.
58. Zullo, A., Hassan, C., Andriani, A., Cristofari, F., De Francesco, V., Ierardi, E., Tomao, S., Morini, S., and Vaira, D. (2009) Eradication therapy for Helicobacter pylori in patients with gastric MALT lymphoma: a pooled data analysis. Am J Gastroenterol. 104(8): p. 1932-7; quiz 1938.
59. Malfertheiner, P., Megraud, F., O'Morain, C.A., Gisbert, J.P., Kuipers, E.J., Axon, A.T., Bazzoli, F., Gasbarrini, A., Atherton, J., Graham, D.Y., Hunt, R., Moayyedi, P., Rokkas, T., Rugge, M., Selgrad, M., Suerbaum, S., Sugano, K., and El-Omar, E.M. (2017) Management of Helicobacter pylori infection-the Maastricht V/Florence Consensus Report. Gut. 66(1): p. 6-30.
60. Queiroz, D.M., Harris, P.R., Sanderson, I.R., Windle, H.J., Walker, M.M., Rocha, A.M., Rocha, G.A., Carvalho, S.D., Bittencourt, P.F., de Castro, L.P., Villagran, A., Serrano, C., Kelleher, D., and Crabtree, J.E. (2013) Iron status and Helicobacter pylori infection in symptomatic children: an international multi-centered study. PLoS One. 8(7): p. e68833.
61. Neunert, C., Lim, W., Crowther, M., Cohen, A., Solberg, L., Jr., Crowther, M.A., and American Society of, H. (2011) The American Society of Hematology 2011 evidence-based practice guideline for immune thrombocytopenia. Blood. 117(16): p. 4190-207.
62. Huang, B., Chen, Y., Xie, Q., Lin, G., Wu, Y., Feng, Y., Li, J., Zhuo, Y., and Zhang, P. (2011) CagA-positive Helicobacter pylori strains enhanced coronary atherosclerosis by increasing serum OxLDL and HsCRP in patients with coronary heart disease. Dig Dis Sci. 56(1): p. 109-14.
63. Bu, X.L., Wang, X., Xiang, Y., Shen, L.L., Wang, Q.H., Liu, Y.H., Jiao, S.S., Wang, Y.R., Cao, H.Y., Yi, X., Liu, C.H., Deng, B., Yao, X.Q., Xu, Z.Q., Zhou, H.D., and Wang, Y.J. (2015) The association between infectious burden and Parkinson's disease: A case-control study. Parkinsonism Relat Disord. 21(8): p. 877-81.
64. Bu, X.L., Yao, X.Q., Jiao, S.S., Zeng, F., Liu, Y.H., Xiang, Y., Liang, C.R., Wang, Q.H., Wang, X., Cao, H.Y., Yi, X., Deng, B., Liu, C.H., Xu, J., Zhang, L.L., Gao, C.Y., Xu, Z.Q., Zhang, M., Wang, L., Tan, X.L., Xu, X., Zhou, H.D., and Wang, Y.J. (2015) A study on the association between infectious burden and Alzheimer's disease. Eur J Neurol. 22(12): p. 1519-25.
65. Blaser, M.J., Chen, Y., and Reibman, J. (2008) Does Helicobacter pylori protect against asthma and allergy? Gut. 57(5): p. 561-7.
66. Chen, Y. and Blaser, M.J. (2008) Helicobacter pylori colonization is inversely associated with childhood asthma. J Infect Dis. 198(4): p. 553-60.

67. Castano-Rodriguez, N., Kaakoush, N.O., Lee, W.S., and Mitchell, H.M. (2017) Dual role of Helicobacter and Campylobacter species in IBD: a systematic review and meta-analysis. Gut. 66(2): p. 235-249.
68. Kyburz, A. and Muller, A. (2017) Helicobacter pylori and Extragastric Diseases. Curr Top Microbiol Immunol. 400: p. 325-347.
69. Graham, D.Y. (2015) Helicobacter pylori update: gastric cancer, reliable therapy, and possible benefits. Gastroenterology. 148(4): p. 719-31 e3.
70. Figueiredo, C., Machado, J.C., Pharoah, P., Seruca, R., Sousa, S., Carvalho, R., Capelinha, A.F., Quint, W., Caldas, C., van Doorn, L.J., Carneiro, F., and Sobrinho-Simoes, M. (2002) Helicobacter pylori and interleukin 1 genotyping: an opportunity to identify high-risk individuals for gastric carcinoma. J Natl Cancer Inst. 94(22): p. 1680-7.
71. Ohnishi, N., Yuasa, H., Tanaka, S., Sawa, H., Miura, M., Matsui, A., Higashi, H., Musashi, M., Iwabuchi, K., Suzuki, M., Yamada, G., Azuma, T., and Hatakeyama, M. (2008) Transgenic expression of Helicobacter pylori CagA induces gastrointestinal and hematopoietic neoplasms in mouse. Proc Natl Acad Sci U S A. 105(3): p. 1003-8.
72. Censini, S., Lange, C., Xiang, Z., Crabtree, J.E., Ghiara, P., Borodovsky, M., Rappuoli, R., and Covacci, A. (1996) cag, a pathogenicity island of Helicobacter pylori, encodes type I-specific and disease-associated virulence factors. Proc Natl Acad Sci U S A. 93(25): p. 14648-53.
73. Fischer, W., Puls, J., Buhrdorf, R., Gebert, B., Odenbreit, S., and Haas, R. (2001) Systematic mutagenesis of the Helicobacter pylori cag pathogenicity island: essential genes for CagA translocation in host cells and induction of interleukin-8. Mol Microbiol. 42(5): p. 1337-48.
74. Kwok, T., Zabler, D., Urman, S., Rohde, M., Hartig, R., Wessler, S., Misselwitz, R., Berger, J., Sewald, N., Konig, W., and Backert, S. (2007) Helicobacter exploits integrin for type IV secretion and kinase activation. Nature. 449(7164): p. 862-6.
75. Backert, S., Tegtmeyer, N., and Selbach, M. (2010) The versatility of Helicobacter pylori CagA effector protein functions: The master key hypothesis. Helicobacter. 15(3): p. 163-76.
76. Selbach, M., Moese, S., Hauck, C.R., Meyer, T.F., and Backert, S. (2002) Src is the kinase of the Helicobacter pylori CagA protein in vitro and in vivo. J Biol Chem. 277(9): p. 6775-8.
77. Tammer, I., Brandt, S., Hartig, R., Konig, W., and Backert, S. (2007) Activation of Abl by Helicobacter pylori: a novel kinase for CagA and crucial mediator of host cell scattering. Gastroenterology. 132(4): p. 1309-19.
78. Hatakeyama, M. (2011) Anthropological and clinical implications for the structural diversity of the Helicobacter pylori CagA oncoprotein. Cancer Sci. 102(1): p. 36-43.
79. Segal, E.D., Cha, J., Lo, J., Falkow, S., and Tompkins, L.S. (1999) Altered states: involvement of phosphorylated CagA in the induction of host cellular growth changes by Helicobacter pylori. Proc Natl Acad Sci U S A. 96(25): p. 14559-64.
80. Ferreira, R.M., Machado, J.C., and Figueiredo, C. (2014) Clinical relevance of Helicobacter pylori vacA and cagA genotypes in gastric carcinoma. Best Pract Res Clin Gastroenterol. 28(6): p. 1003-15.
81. Blaser, M.J., Perez-Perez, G.I., Kleanthous, H., Cover, T.L., Peek, R.M., Chyou, P.H., Stemmermann, G.N., and Nomura, A. (1995) Infection with Helicobacter pylori strains possessing cagA is associated with an increased risk of developing adenocarcinoma of the stomach. Cancer Res. 55(10): p. 2111-5.
82. Nogueira, C., Figueiredo, C., Carneiro, F., Gomes, A.T., Barreira, R., Figueira, P., Salgado, C., Belo, L., Peixoto, A., Bravo, J.C., Bravo, L.E., Realpe, J.L., Plaisier, A.P., Quint, W.G., Ruiz, B., Correa, P., and van Doorn, L.J. (2001) Helicobacter pylori genotypes may determine gastric histopathology. Am J Pathol. 158(2): p. 647-54.
83. van Doorn, L.J., Figueiredo, C., Sanna, R., Plaisier, A., Schneeberger, P., de Boer, W., and Quint, W. (1998) Clinical relevance of the cagA, vacA, and iceA status of Helicobacter pylori. Gastroenterology. 115(1): p. 58-66.
84. Figueiredo, C., Van Doorn, L.J., Nogueira, C., Soares, J.M., Pinho, C., Figueira, P., Quint, W.G., and Carneiro, F. (2001) Helicobacter pylori genotypes are associated with clinical outcome

in Portuguese patients and show a high prevalence of infections with multiple strains. Scand J Gastroenterol. 36(2): p. 128-35.

85. Ferreira, R.M., Machado, J.C., Leite, M., Carneiro, F., and Figueiredo, C. (2012) The number of Helicobacter pylori CagA EPIYA C tyrosine phosphorylation motifs influences the pattern of gastritis and the development of gastric carcinoma. Histopathology. 60(6): p. 992-8.
86. Leunk, R.D., Johnson, P.T., David, B.C., Kraft, W.G., and Morgan, D.R. (1988) Cytotoxic activity in broth-culture filtrates of Campylobacter pylori. J Med Microbiol. 26(2): p. 93-9.
87. Szabo, I., Brutsche, S., Tombola, F., Moschioni, M., Satin, B., Telford, J.L., Rappuoli, R., Montecucco, C., Papini, E., and Zoratti, M. (1999) Formation of anion-selective channels in the cell plasma membrane by the toxin VacA of Helicobacter pylori is required for its biological activity. EMBO J. 18(20): p. 5517-27.
88. Cover, T.L., Puryear, W., Perez-Perez, G.I., and Blaser, M.J. (1991) Effect of urease on HeLa cell vacuolation induced by Helicobacter pylori cytotoxin. Infect Immun. 59(4): p. 1264-70.
89. Galmiche, A., Rassow, J., Doye, A., Cagnol, S., Chambard, J.C., Contamin, S., de Thillot, V., Just, I., Ricci, V., Solcia, E., Van Obberghen, E., and Boquet, P. (2000) The N-terminal 34 kDa fragment of Helicobacter pylori vacuolating cytotoxin targets mitochondria and induces cytochrome c release. EMBO J. 19(23): p. 6361-70.
90. Torres, V.J., VanCompernolle, S.E., Sundrud, M.S., Unutmaz, D., and Cover, T.L. (2007) Helicobacter pylori vacuolating cytotoxin inhibits activation-induced proliferation of human T and B lymphocyte subsets. J Immunol. 179(8): p. 5433-40.
91. Ilver, D., Barone, S., Mercati, D., Lupetti, P., and Telford, J.L. (2004) Helicobacter pylori toxin VacA is transferred to host cells via a novel contact-dependent mechanism. Cell Microbiol. 6(2): p. 167-74.
92. Atherton, J.C., Cao, P., Peek, R.M., Jr., Tummuru, M.K., Blaser, M.J., and Cover, T.L. (1995) Mosaicism in vacuolating cytotoxin alleles of Helicobacter pylori. Association of specific vacA types with cytotoxin production and peptic ulceration. J Biol Chem. 270(30): p. 17771-7.
93. Atherton, J.C., Peek, R.M., Jr., Tham, K.T., Cover, T.L., and Blaser, M.J. (1997) Clinical and pathological importance of heterogeneity in vacA, the vacuolating cytotoxin gene of Helicobacter pylori. Gastroenterology. 112(1): p. 92-9.
94. Rhead, J.L., Letley, D.P., Mohammadi, M., Hussein, N., Mohagheghi, M.A., Eshagh Hosseini, M., and Atherton, J.C. (2007) A new Helicobacter pylori vacuolating cytotoxin determinant, the intermediate region, is associated with gastric cancer. Gastroenterology. 133(3): p. 926-36.
95. Ferreira, R.M., Machado, J.C., Letley, D., Atherton, J.C., Pardo, M.L., Gonzalez, C.A., Carneiro, F., and Figueiredo, C. (2012) A novel method for genotyping the Helicobacter pylori vacA intermediate region directly in gastric biopsy specimens. J Clin Microbiol. 50(12): p. 3983-9.
96. Lower, M., Weydig, C., Metzler, D., Reuter, A., Starzinski-Powitz, A., Wessler, S., and Schneider, G. (2008) Prediction of extracellular proteases of the human pathogen Helicobacter pylori reveals proteolytic activity of the Hp1018/19 protein HtrA. PLoS One. 3(10): p. e3510.
97. Hoy, B., Lower, M., Weydig, C., Carra, G., Tegtmeyer, N., Geppert, T., Schroder, P., Sewald, N., Backert, S., Schneider, G., and Wessler, S. (2010) Helicobacter pylori HtrA is a new secreted virulence factor that cleaves E-cadherin to disrupt intercellular adhesion. EMBO Rep. 11(10): p. 798-804.
98. Schmidt, T.P., Perna, A.M., Fugmann, T., Bohm, M., Jan, H., Haller, S., Gotz, C., Tegtmeyer, N., Hoy, B., Rau, T.T., Neri, D., Backert, S., Schneider, G., and Wessler, S. (2016) Identification of E-cadherin signature motifs functioning as cleavage sites for Helicobacter pylori HtrA. Sci Rep. 6: p. 23264.
99. Tegtmeyer, N., Wessler, S., Necchi, V., Rohde, M., Harrer, A., Rau, T.T., Asche, C.I., Boehm, M., Loessner, H., Figueiredo, C., Naumann, M., Palmisano, R., Solcia, E., Ricci, V., and

Backert, S. (2017) Helicobacter pylori Employs a Unique Basolateral Type IV Secretion Mechanism for CagA Delivery. Cell Host Microbe. 22(4): p. 552-560 e5.

100. Tegtmeyer, N., Moodley, Y., Yamaoka, Y., Pernitzsch, S.R., Schmidt, V., Traverso, F.R., Schmidt, T.P., Rad, R., Yeoh, K.G., Bow, H., Torres, J., Gerhard, M., Schneider, G., Wessler, S., and Backert, S. (2016) Characterisation of worldwide Helicobacter pylori strains reveals genetic conservation and essentiality of serine protease HtrA. Mol Microbiol. 99(5): p. 925-44.
101. Hoy, B., Brandstetter, H., and Wessler, S. (2013) The stability and activity of recombinant Helicobacter pylori HtrA under stress conditions. J Basic Microbiol. 53(5): p. 402-9.
102. Smith, T.G., Lim, J.M., Weinberg, M.V., Wells, L., and Hoover, T.R. (2007) Direct analysis of the extracellular proteome from two strains of Helicobacter pylori. Proteomics. 7(13): p. 2240-5.
103. Salama, N.R., Shepherd, B., and Falkow, S. (2004) Global transposon mutagenesis and essential gene analysis of Helicobacter pylori. J Bacteriol. 186(23): p. 7926-35.
104. Marques, M.S., Costa, A.C., Osorio, H., Pinto, M.L., Relvas, S., Dinis-Ribeiro, M., Carneiro, F., Leite, M., and Figueiredo, C. (2021) Helicobacter pylori PqqE is a new virulence factor that cleaves junctional adhesion molecule A and disrupts gastric epithelial integrity. Gut Microbes. 13(1): p. 1-21.
105. Cho, J., Prashar, A., Jones, N.L., and Moss, S.F. (2021) Helicobacter pylori Infection. Gastroenterol Clin North Am. 50(2): p. 261-282.
106. Gisbert, J.P. and McNicholl, A.G. (2017) Optimization strategies aimed to increase the efficacy of H. pylori eradication therapies. Helicobacter. 22(4).
107. Thung, I., Aramin, H., Vavinskaya, V., Gupta, S., Park, J.Y., Crowe, S.E., and Valasek, M.A. (2016) Review article: the global emergence of Helicobacter pylori antibiotic resistance. Aliment Pharmacol Ther. 43(4): p. 514-33.
108. Yuan, Y., Ford, A.C., Khan, K.J., Gisbert, J.P., Forman, D., Leontiadis, G.I., Tse, F., Calvet, X., Fallone, C., Fischbach, L., Oderda, G., Bazzoli, F., and Moayyedi, P. (2013) Optimum duration of regimens for Helicobacter pylori eradication. Cochrane Database Syst Rev. (12): p. CD008337.
109. Lu, B. and Li, M. (2014) Helicobacter pylori eradication for preventing gastric cancer. World J Gastroenterol. 20(19): p. 5660-5.
110. Deatherage, B.L. and Cookson, B.T. (2012) Membrane vesicle release in bacteria, eukaryotes, and archaea: a conserved yet underappreciated aspect of microbial life. Infect Immun. 80(6): p. 1948-57.
111. Bishop, D.G. and Work, E. (1965) An extracellular glycolipid produced by Escherichia coli grown under lysine-limiting conditions. Biochem J. 96(2): p. 567-76.
112. Cao, Y. and Lin, H. (2021) Characterization and function of membrane vesicles in Gram-positive bacteria. Appl Microbiol Biotechnol. 105(5): p. 1795-1801.
113. Toyofuku, M., Nomura, N., and Eberl, L. (2019) Types and origins of bacterial membrane vesicles. Nat Rev Microbiol. 17(1): p. 13-24.
114. Furuyama, N. and Sircili, M.P. (2021) Outer Membrane Vesicles (OMVs) Produced by Gram-Negative Bacteria: Structure, Functions, Biogenesis, and Vaccine Application. Biomed Res Int. 2021: p. 1490732.
115. Schwechheimer, C. and Kuehn, M.J. (2015) Outer-membrane vesicles from Gram-negative bacteria: biogenesis and functions. Nat Rev Microbiol. 13(10): p. 605-19.
116. Kulp, A. and Kuehn, M.J. (2010) Biological functions and biogenesis of secreted bacterial outer membrane vesicles. Annu Rev Microbiol. 64: p. 163-84.
117. Keenan, J.I., Allardyce, R.A., and Bagshaw, P.F. (1997) Dual silver staining to characterise Helicobacter spp. outer membrane components. J Immunol Methods. 209(1): p. 17-24.
118. Zavan, L., Bitto, N.J., Johnston, E.L., Greening, D.W., and Kaparakis-Liaskos, M. (2019) Helicobacter pylori Growth Stage Determines the Size, Protein Composition, and

Preferential Cargo Packaging of Outer Membrane Vesicles. Proteomics. 19(1-2): p. e1800209.

119. Olofsson, A., Vallstrom, A., Petzold, K., Tegtmeyer, N., Schleucher, J., Carlsson, S., Haas, R., Backert, S., Wai, S.N., Grobner, G., and Arnqvist, A. (2010) Biochemical and functional characterization of Helicobacter pylori vesicles. Mol Microbiol. 77(6): p. 1539-55.
120. Keenan, J.I., Davis, K.A., Beaugie, C.R., McGovern, J.J., and Moran, A.P. (2008) Alterations in Helicobacter pylori outer membrane and outer membrane vesicle-associated lipopolysaccharides under iron-limiting growth conditions. Innate Immun. 14(5): p. 279-90.
121. Kaparakis, M., Turnbull, L., Carneiro, L., Firth, S., Coleman, H.A., Parkington, H.C., Le Bourhis, L., Karrar, A., Viala, J., Mak, J., Hutton, M.L., Davies, J.K., Crack, P.J., Hertzog, P.J., Philpott, D.J., Girardin, S.E., Whitchurch, C.B., and Ferrero, R.L. (2010) Bacterial membrane vesicles deliver peptidoglycan to NOD1 in epithelial cells. Cell Microbiol. 12(3): p. 372-85.
122. Grande, R., Di Marcantonio, M.C., Robuffo, I., Pompilio, A., Celia, C., Di Marzio, L., Paolino, D., Codagnone, M., Muraro, R., Stoodley, P., Hall-Stoodley, L., and Mincione, G. (2015) Helicobacter pylori ATCC 43629/NCTC 11639 Outer Membrane Vesicles (OMVs) from Biofilm and Planktonic Phase Associated with Extracellular DNA (eDNA). Front Microbiol. 6: p. 1369.
123. Zhang, H., Zhang, Y., Song, Z., Li, R., Ruan, H., Liu, Q., and Huang, X. (2020) sncRNAs packaged by Helicobacter pylori outer membrane vesicles attenuate IL-8 secretion in human cells. Int J Med Microbiol. 310(1): p. 151356.
124. Mullaney, E., Brown, P.A., Smith, S.M., Botting, C.H., Yamaoka, Y.Y., Terres, A.M., Kelleher, D.P., and Windle, H.J. (2009) Proteomic and functional characterization of the outer membrane vesicles from the gastric pathogen Helicobacter pylori. Proteomics Clin Appl. 3(7): p. 785-96.
125. Keenan, J., Day, T., Neal, S., Cook, B., Perez-Perez, G., Allardyce, R., and Bagshaw, P. (2000) A role for the bacterial outer membrane in the pathogenesis of Helicobacter pylori infection. FEMS Microbiol Lett. 182(2): p. 259-64.
126. Turner, L., Bitto, N.J., Steer, D.L., Lo, C., D'Costa, K., Ramm, G., Shambrook, M., Hill, A.F., Ferrero, R.L., and Kaparakis-Liaskos, M. (2018) Helicobacter pylori Outer Membrane Vesicle Size Determines Their Mechanisms of Host Cell Entry and Protein Content. Front Immunol. 9: p. 1466.
127. Lima, S., Matinha-Cardoso, J., Tamagnini, P., and Oliveira, P. (2020) Extracellular Vesicles: An Overlooked Secretion System in Cyanobacteria. Life (Basel). 10(8).
128. Sonntag, I., Schwarz, H., Hirota, Y., and Henning, U. (1978) Cell envelope and shape of Escherichia coli: multiple mutants missing the outer membrane lipoprotein and other major outer membrane proteins. J Bacteriol. 136(1): p. 280-5.
129. Deatherage, B.L., Lara, J.C., Bergsbaken, T., Rassoulian Barrett, S.L., Lara, S., and Cookson, B.T. (2009) Biogenesis of bacterial membrane vesicles. Mol Microbiol. 72(6): p. 1395-407.
130. Moon, D.C., Choi, C.H., Lee, J.H., Choi, C.W., Kim, H.Y., Park, J.S., Kim, S.I., and Lee, J.C. (2012) Acinetobacter baumannii outer membrane protein A modulates the biogenesis of outer membrane vesicles. J Microbiol. 50(1): p. 155-60.
131. Schwechheimer, C., Rodriguez, D.L., and Kuehn, M.J. (2015) NlpI-mediated modulation of outer membrane vesicle production through peptidoglycan dynamics in Escherichia coli. Microbiologyopen. 4(3): p. 375-89.
132. Takaki, K., Tahara, Y.O., Nakamichi, N., Hasegawa, Y., Shintani, M., Ohkuma, M., Miyata, M., Futamata, H., and Tashiro, Y. (2020) Multilamellar and Multivesicular Outer Membrane Vesicles Produced by a Buttiauxella agrestis tolB Mutant. Appl Environ Microbiol. 86(20).
133. Turner, L., Praszkier, J., Hutton, M.L., Steer, D., Ramm, G., Kaparakis-Liaskos, M., and Ferrero, R.L. (2015) Increased Outer Membrane Vesicle Formation in a Helicobacter pylori tolB Mutant. Helicobacter. 20(4): p. 269-83.
134. Mashburn, L.M. and Whiteley, M. (2005) Membrane vesicles traffic signals and facilitate group activities in a prokaryote. Nature. 437(7057): p. 422-5.

135. Mashburn-Warren, L., Howe, J., Garidel, P., Richter, W., Steiniger, F., Roessle, M., Brandenburg, K., and Whiteley, M. (2008) Interaction of quorum signals with outer membrane lipids: insights into prokaryotic membrane vesicle formation. Mol Microbiol. 69(2): p. 491-502.
136. Tashiro, Y., Ichikawa, S., Nakajima-Kambe, T., Uchiyama, H., and Nomura, N. (2010) Pseudomonas quinolone signal affects membrane vesicle production in not only gram-negative but also gram-positive bacteria. Microbes Environ. 25(2): p. 120-5.
137. Schwechheimer, C., Kulp, A., and Kuehn, M.J. (2014) Modulation of bacterial outer membrane vesicle production by envelope structure and content. BMC Microbiol. 14: p. 324.
138. Kaparakis-Liaskos, M. and Kufer, T.A., *Bacterial Membrane Vesicles: Biogenesis, Functions and Applications*. 2020: Springer, Cham.
139. Katsui, N., Tsuchido, T., Hiramatsu, R., Fujikawa, S., Takano, M., and Shibasaki, I. (1982) Heat-induced blebbing and vesiculation of the outer membrane of Escherichia coli. J Bacteriol. 151(3): p. 1523-31.
140. Prados-Rosales, R., Weinrick, B.C., Pique, D.G., Jacobs, W.R., Jr., Casadevall, A., and Rodriguez, G.M. (2014) Role for Mycobacterium tuberculosis membrane vesicles in iron acquisition. J Bacteriol. 196(6): p. 1250-6.
141. Willen, R., Carlen, B., Wang, X., Papadogiannakis, N., Odselius, R., and Wadstrom, T. (2000) Morphologic conversion of Helicobacter pylori from spiral to coccoid form. Scanning (SEM) and transmission electron microscopy (TEM) suggest viability. Ups J Med Sci. 105(1): p. 31-40.
142. Keenan, J.I. and Allardyce, R.A. (2000) Iron influences the expression of Helicobacter pylori outer membrane vesicle-associated virulence factors. Eur J Gastroenterol Hepatol. 12(12): p. 1267-73.
143. Caruana, J.C. and Walper, S.A. (2020) Bacterial Membrane Vesicles as Mediators of Microbe - Microbe and Microbe - Host Community Interactions. Front Microbiol. 11: p. 432.
144. Anand, D. and Chaudhuri, A. (2016) Bacterial outer membrane vesicles: New insights and applications. Molecular Membrane Biology. 33(6-8): p. 125-137.
145. O'Donoghue, E.J. and Krachler, A.M. (2016) Mechanisms of outer membrane vesicle entry into host cells. Cell Microbiol. 18(11): p. 1508-1517.
146. Bomberger, J.M., Maceachran, D.P., Coutermarsh, B.A., Ye, S., O'Toole, G.A., and Stanton, B.A. (2009) Long-distance delivery of bacterial virulence factors by Pseudomonas aeruginosa outer membrane vesicles. PLoS Pathog. 5(4): p. e1000382.
147. Furuta, N., Tsuda, K., Omori, H., Yoshimori, T., Yoshimura, F., and Amano, A. (2009) Porphyromonas gingivalis outer membrane vesicles enter human epithelial cells via an endocytic pathway and are sorted to lysosomal compartments. Infect Immun. 77(10): p. 4187-96.
148. Parker, H., Chitcholtan, K., Hampton, M.B., and Keenan, J.I. (2010) Uptake of Helicobacter pylori outer membrane vesicles by gastric epithelial cells. Infect Immun. 78(12): p. 5054-61.
149. Pollak, C.N., Delpino, M.V., Fossati, C.A., and Baldi, P.C. (2012) Outer membrane vesicles from Brucella abortus promote bacterial internalization by human monocytes and modulate their innate immune response. PLoS One. 7(11): p. e50214.
150. Bielaszewska, M., Ruter, C., Kunsmann, L., Greune, L., Bauwens, A., Zhang, W., Kuczius, T., Kim, K.S., Mellmann, A., Schmidt, M.A., and Karch, H. (2013) Enterohemorrhagic Escherichia coli hemolysin employs outer membrane vesicles to target mitochondria and cause endothelial and epithelial apoptosis. PLoS Pathog. 9(12): p. e1003797.
151. Bauman, S.J. and Kuehn, M.J. (2009) Pseudomonas aeruginosa vesicles associate with and are internalized by human lung epithelial cells. BMC Microbiol. 9: p. 26.
152. Kim, Y.R., Kim, B.U., Kim, S.Y., Kim, C.M., Na, H.S., Koh, J.T., Choy, H.E., Rhee, J.H., and Lee, S.E. (2010) Outer membrane vesicles of Vibrio vulnificus deliver cytolysin-hemolysin VvhA

into epithelial cells to induce cytotoxicity. Biochem Biophys Res Commun. 399(4): p. 607-12.
153. Rompikuntal, P.K., Thay, B., Khan, M.K., Alanko, J., Penttinen, A.M., Asikainen, S., Wai, S.N., and Oscarsson, J. (2012) Perinuclear localization of internalized outer membrane vesicles carrying active cytolethal distending toxin from Aggregatibacter actinomycetemcomitans. Infect Immun. 80(1): p. 31-42.
154. Jager, J., Keese, S., Roessle, M., Steinert, M., and Schromm, A.B. (2015) Fusion of Legionella pneumophila outer membrane vesicles with eukaryotic membrane systems is a mechanism to deliver pathogen factors to host cell membranes. Cell Microbiol. 17(5): p. 607-20.
155. Olofsson, A., Nygard Skalman, L., Obi, I., Lundmark, R., and Arnqvist, A. (2014) Uptake of Helicobacter pylori vesicles is facilitated by clathrin-dependent and clathrin-independent endocytic pathways. mBio. 5(3): p. e00979-14.
156. Mozaheb, N. and Mingeot-Leclercq, M.P. (2020) Membrane Vesicle Production as a Bacterial Defense Against Stress. Front Microbiol. 11: p. 600221.
157. van de Waterbeemd, B., Zomer, G., van den Ijssel, J., van Keulen, L., Eppink, M.H., van der Ley, P., and van der Pol, L.A. (2013) Cysteine depletion causes oxidative stress and triggers outer membrane vesicle release by Neisseria meningitidis; implications for vaccine development. PLoS One. 8(1): p. e54314.
158. Gerritzen, M.J.H., Martens, D.E., Uittenbogaard, J.P., Wijffels, R.H., and Stork, M. (2019) Sulfate depletion triggers overproduction of phospholipids and the release of outer membrane vesicles by Neisseria meningitidis. Sci Rep. 9(1): p. 4716.
159. Biller, S.J., Schubotz, F., Roggensack, S.E., Thompson, A.W., Summons, R.E., and Chisholm, S.W. (2014) Bacterial vesicles in marine ecosystems. Science. 343(6167): p. 183-6.
160. Klieve, A.V., Yokoyama, M.T., Forster, R.J., Ouwerkerk, D., Bain, P.A., and Mawhinney, E.L. (2005) Naturally occurring DNA transfer system associated with membrane vesicles in cellulolytic Ruminococcus spp. of ruminal origin. Appl Environ Microbiol. 71(8): p. 4248-53.
161. Rumbo, C., Fernandez-Moreira, E., Merino, M., Poza, M., Mendez, J.A., Soares, N.C., Mosquera, A., Chaves, F., and Bou, G. (2011) Horizontal transfer of the OXA-24 carbapenemase gene via outer membrane vesicles: a new mechanism of dissemination of carbapenem resistance genes in Acinetobacter baumannii. Antimicrob Agents Chemother. 55(7): p. 3084-90.
162. Koeppen, K., Hampton, T.H., Jarek, M., Scharfe, M., Gerber, S.A., Mielcarz, D.W., Demers, E.G., Dolben, E.L., Hammond, J.H., Hogan, D.A., and Stanton, B.A. (2016) A Novel Mechanism of Host-Pathogen Interaction through sRNA in Bacterial Outer Membrane Vesicles. PLoS Pathog. 12(6): p. e1005672.
163. Bitto, N.J., Chapman, R., Pidot, S., Costin, A., Lo, C., Choi, J., D'Cruze, T., Reynolds, E.C., Dashper, S.G., Turnbull, L., Whitchurch, C.B., Stinear, T.P., Stacey, K.J., and Ferrero, R.L. (2017) Bacterial membrane vesicles transport their DNA cargo into host cells. Sci Rep. 7(1): p. 7072.
164. Grenier, D., Bertrand, J., and Mayrand, D. (1995) Porphyromonas gingivalis outer membrane vesicles promote bacterial resistance to chlorhexidine. Oral Microbiol Immunol. 10(5): p. 319-20.
165. Manning, A.J. and Kuehn, M.J. (2011) Contribution of bacterial outer membrane vesicles to innate bacterial defense. BMC Microbiol. 11: p. 258.
166. Stephens, D.S., Edwards, K.M., Morris, F., and McGee, Z.A. (1982) Pili and outer membrane appendages on Neisseria meningitidis in the cerebrospinal fluid of an infant. J Infect Dis. 146(4): p. 568.
167. Fiocca, R., Necchi, V., Sommi, P., Ricci, V., Telford, J., Cover, T.L., and Solcia, E. (1999) Release of Helicobacter pylori vacuolating cytotoxin by both a specific secretion pathway and budding of outer membrane vesicles. Uptake of released toxin and vesicles by gastric epithelium. J Pathol. 188(2): p. 220-6.

168. Vidakovics, M.L., Jendholm, J., Morgelin, M., Mansson, A., Larsson, C., Cardell, L.O., and Riesbeck, K. (2010) B cell activation by outer membrane vesicles--a novel virulence mechanism. PLoS Pathog. 6(1): p. e1000724.
169. Ismail, S., Hampton, M.B., and Keenan, J.I. (2003) Helicobacter pylori outer membrane vesicles modulate proliferation and interleukin-8 production by gastric epithelial cells. Infect Immun. 71(10): p. 5670-5.
170. Winter, J., Letley, D., Rhead, J., Atherton, J., and Robinson, K. (2014) Helicobacter pylori membrane vesicles stimulate innate pro- and anti-inflammatory responses and induce apoptosis in Jurkat T cells. Infect Immun. 82(4): p. 1372-81.
171. Choi, H.I., Choi, J.P., Seo, J., Kim, B.J., Rho, M., Han, J.K., and Kim, J.G. (2017) Helicobacter pylori-derived extracellular vesicles increased in the gastric juices of gastric adenocarcinoma patients and induced inflammation mainly via specific targeting of gastric epithelial cells. Exp Mol Med. 49(5): p. e330.
172. Choi, M.S., Ze, E.Y., Park, J.Y., Shin, T.S., and Kim, J.G. (2020) Helicobacter pylori-derived outer membrane vesicles stimulate interleukin 8 secretion through nuclear factor kappa B activation. Korean J Intern Med.
173. Keenan, J., Oliaro, J., Domigan, N., Potter, H., Aitken, G., Allardyce, R., and Roake, J. (2000) Immune response to an 18-kilodalton outer membrane antigen identifies lipoprotein 20 as a Helicobacter pylori vaccine candidate. Infect Immun. 68(6): p. 3337-43.
174. Ayala, G., Torres, L., Espinosa, M., Fierros-Zarate, G., Maldonado, V., and Melendez-Zajgla, J. (2006) External membrane vesicles from Helicobacter pylori induce apoptosis in gastric epithelial cells. FEMS Microbiol Lett. 260(2): p. 178-85.
175. Lekmeechai, S., Su, Y.C., Brant, M., Alvarado-Kristensson, M., Vallstrom, A., Obi, I., Arnqvist, A., and Riesbeck, K. (2018) Helicobacter pylori Outer Membrane Vesicles Protect the Pathogen From Reactive Oxygen Species of the Respiratory Burst. Front Microbiol. 9: p. 1837.
176. Uddin, M.J., Dawan, J., Jeon, G., Yu, T., He, X., and Ahn, J. (2020) The Role of Bacterial Membrane Vesicles in the Dissemination of Antibiotic Resistance and as Promising Carriers for Therapeutic Agent Delivery. Microorganisms. 8(5).
177. Schild, S., Nelson, E.J., and Camilli, A. (2008) Immunization with Vibrio cholerae outer membrane vesicles induces protective immunity in mice. Infect Immun. 76(10): p. 4554-63.
178. Kim, O.Y., Hong, B.S., Park, K.S., Yoon, Y.J., Choi, S.J., Lee, W.H., Roh, T.Y., Lotvall, J., Kim, Y.K., and Gho, Y.S. (2013) Immunization with Escherichia coli outer membrane vesicles protects bacteria-induced lethality via Th1 and Th17 cell responses. J Immunol. 190(8): p. 4092-102.
179. Camacho, A.I., de Souza, J., Sanchez-Gomez, S., Pardo-Ros, M., Irache, J.M., and Gamazo, C. (2011) Mucosal immunization with Shigella flexneri outer membrane vesicles induced protection in mice. Vaccine. 29(46): p. 8222-9.
180. Nokleby, H., Aavitsland, P., O'Hallahan, J., Feiring, B., Tilman, S., and Oster, P. (2007) Safety review: two outer membrane vesicle (OMV) vaccines against systemic Neisseria meningitidis serogroup B disease. Vaccine. 25(16): p. 3080-4.
181. Petousis-Harris, H. (2018) Impact of meningococcal group B OMV vaccines, beyond their brief. Hum Vaccin Immunother. 14(5): p. 1058-1063.
182. Kim, S.H., Kim, K.S., Lee, S.R., Kim, E., Kim, M.S., Lee, E.Y., Gho, Y.S., Kim, J.W., Bishop, R.E., and Chang, K.T. (2009) Structural modifications of outer membrane vesicles to refine them as vaccine delivery vehicles. Biochim Biophys Acta. 1788(10): p. 2150-9.
183. Lee, S.R., Kim, S.H., Jeong, K.J., Kim, K.S., Kim, Y.H., Kim, S.J., Kim, E., Kim, J.W., and Chang, K.T. (2009) Multi-immunogenic outer membrane vesicles derived from an MsbB-deficient Salmonella enterica serovar typhimurium mutant. J Microbiol Biotechnol. 19(10): p. 1271-9.

184. Fantappie, L., de Santis, M., Chiarot, E., Carboni, F., Bensi, G., Jousson, O., Margarit, I., and Grandi, G. (2014) Antibody-mediated immunity induced by engineered Escherichia coli OMVs carrying heterologous antigens in their lumen. J Extracell Vesicles. 3.
185. Kadurugamuwa, J.L. and Beveridge, T.J. (1998) Delivery of the non-membrane-permeative antibiotic gentamicin into mammalian cells by using Shigella flexneri membrane vesicles. Antimicrob Agents Chemother. 42(6): p. 1476-83.
186. Kuerban, K., Gao, X., Zhang, H., Liu, J., Dong, M., Wu, L., Ye, R., Feng, M., and Ye, L. (2020) Doxorubicin-loaded bacterial outer-membrane vesicles exert enhanced anti-tumor efficacy in non-small-cell lung cancer. Acta Pharm Sin B. 10(8): p. 1534-1548.
187. Sutton, P. and Boag, J.M. (2019) Status of vaccine research and development for Helicobacter pylori. Vaccine. 37(50): p. 7295-7299.
188. Liu, Q., Li, X., Zhang, Y., Song, Z., Li, R., Ruan, H., and Huang, X. (2019) Orally-administered outer-membrane vesicles from Helicobacter pylori reduce H. pylori infection via Th2-biased immune responses in mice. Pathog Dis. 77(5).
189. Song, Z., Li, B., Zhang, Y., Li, R., Ruan, H., Wu, J., and Liu, Q. (2020) Outer Membrane Vesicles of Helicobacter pylori 7.13 as Adjuvants Promote Protective Efficacy Against Helicobacter pylori Infection. Front Microbiol. 11: p. 1340.
190. Bitto, N.J. and Kaparakis-Liaskos, M. (2017) The Therapeutic Benefit of Bacterial Membrane Vesicles. Int J Mol Sci. 18(6).
191. Costa, A.M., Leite, M., Seruca, R., and Figueiredo, C. (2013) Adherens junctions as targets of microorganisms: a focus on Helicobacter pylori. FEBS Lett. 587(3): p. 259-65.
192. Ruch, T.R. and Engel, J.N. (2017) Targeting the Mucosal Barrier: How Pathogens Modulate the Cellular Polarity Network. Cold Spring Harb Perspect Biol. 9(6).
193. Totland, M.Z., Rasmussen, N.L., Knudsen, L.M., and Leithe, E. (2020) Regulation of gap junction intercellular communication by connexin ubiquitination: physiological and pathophysiological implications. Cell Mol Life Sci. 77(4): p. 573-591.
194. Sluysmans, S., Vasileva, E., Spadaro, D., Shah, J., Rouaud, F., and Citi, S. (2017) The role of apical cell-cell junctions and associated cytoskeleton in mechanotransduction. Biol Cell. 109(4): p. 139-161.
195. Matter, K. and Balda, M.S. (2003) Functional analysis of tight junctions. Methods. 30(3): p. 228-34.
196. Zihni, C., Mills, C., Matter, K., and Balda, M.S. (2016) Tight junctions: from simple barriers to multifunctional molecular gates. Nat Rev Mol Cell Biol. 17(9): p. 564-80.
197. Balda, M.S. and Matter, K. (2008) Tight junctions at a glance. J Cell Sci. 121(Pt 22): p. 3677-82.
198. Zihni, C., Balda, M.S., and Matter, K. (2014) Signalling at tight junctions during epithelial differentiation and microbial pathogenesis. J Cell Sci. 127(Pt 16): p. 3401-13.
199. Balda, M.S. and Matter, K. (2016) Tight junctions as regulators of tissue remodelling. Curr Opin Cell Biol. 42: p. 94-101.
200. Furuse, M., Hirase, T., Itoh, M., Nagafuchi, A., Yonemura, S., Tsukita, S., and Tsukita, S. (1993) Occludin: a novel integral membrane protein localizing at tight junctions. J Cell Biol. 123(6 Pt 2): p. 1777-88.
201. Saitou, M., Furuse, M., Sasaki, H., Schulzke, J.D., Fromm, M., Takano, H., Noda, T., and Tsukita, S. (2000) Complex phenotype of mice lacking occludin, a component of tight junction strands. Mol Biol Cell. 11(12): p. 4131-42.
202. Krause, G., Protze, J., and Piontek, J. (2015) Assembly and function of claudins: Structure-function relationships based on homology models and crystal structures. Semin Cell Dev Biol. 42: p. 3-12.
203. Gunzel, D. and Fromm, M. (2012) Claudins and other tight junction proteins. Compr Physiol. 2(3): p. 1819-52.
204. Garrido-Urbani, S., Bradfield, P.F., and Imhof, B.A. (2014) Tight junction dynamics: the role of junctional adhesion molecules (JAMs). Cell Tissue Res. 355(3): p. 701-15.

205. Mandicourt, G., Iden, S., Ebnet, K., Aurrand-Lions, M., and Imhof, B.A. (2007) JAM-C regulates tight junctions and integrin-mediated cell adhesion and migration. J Biol Chem. 282(3): p. 1830-7.
206. Laukoetter, M.G., Nava, P., Lee, W.Y., Severson, E.A., Capaldo, C.T., Babbin, B.A., Williams, I.R., Koval, M., Peatman, E., Campbell, J.A., Dermody, T.S., Nusrat, A., and Parkos, C.A. (2007) JAM-A regulates permeability and inflammation in the intestine in vivo. J Exp Med. 204(13): p. 3067-76.
207. Ebnet, K. (2008) Organization of multiprotein complexes at cell-cell junctions. Histochem Cell Biol. 130(1): p. 1-20.
208. Katsuno, T., Umeda, K., Matsui, T., Hata, M., Tamura, A., Itoh, M., Takeuchi, K., Fujimori, T., Nabeshima, Y., Noda, T., Tsukita, S., and Tsukita, S. (2008) Deficiency of zonula occludens-1 causes embryonic lethal phenotype associated with defected yolk sac angiogenesis and apoptosis of embryonic cells. Mol Biol Cell. 19(6): p. 2465-75.
209. Xu, J., Kausalya, P.J., Phua, D.C., Ali, S.M., Hossain, Z., and Hunziker, W. (2008) Early embryonic lethality of mice lacking ZO-2, but Not ZO-3, reveals critical and nonredundant roles for individual zonula occludens proteins in mammalian development. Mol Cell Biol. 28(5): p. 1669-78.
210. Niessen, C.M. (2007) Tight junctions/adherens junctions: basic structure and function. J Invest Dermatol. 127(11): p. 2525-32.
211. Angulo-Urarte, A., van der Wal, T., and Huveneers, S. (2020) Cell-cell junctions as sensors and transducers of mechanical forces. Biochim Biophys Acta Biomembr. 1862(9): p. 183316.
212. Martinez-Rico, C., Pincet, F., Perez, E., Thiery, J.P., Shimizu, K., Takai, Y., and Dufour, S. (2005) Separation force measurements reveal different types of modulation of E-cadherin-based adhesion by nectin-1 and -3. J Biol Chem. 280(6): p. 4753-60.
213. Gunther, J. and Seyfert, H.M. (2018) The first line of defence: insights into mechanisms and relevance of phagocytosis in epithelial cells. Semin Immunopathol. 40(6): p. 555-565.
214. Guttman, J.A. and Finlay, B.B. (2009) Tight junctions as targets of infectious agents. Biochim Biophys Acta. 1788(4): p. 832-41.
215. van Amsterdam, K. and van der Ende, A. (2004) Nutrients released by gastric epithelial cells enhance Helicobacter pylori growth. Helicobacter. 9(6): p. 614-21.
216. Tan, S., Tompkins, L.S., and Amieva, M.R. (2009) Helicobacter pylori usurps cell polarity to turn the cell surface into a replicative niche. PLoS Pathog. 5(5): p. e1000407.
217. Lytton, S.D., Fischer, W., Nagel, W., Haas, R., and Beck, F.X. (2005) Production of ammonium by Helicobacter pylori mediates occludin processing and disruption of tight junctions in Caco-2 cells. Microbiology (Reading). 151(Pt 10): p. 3267-3276.
218. Wroblewski, L.E., Shen, L., Ogden, S., Romero-Gallo, J., Lapierre, L.A., Israel, D.A., Turner, J.R., and Peek, R.M., Jr. (2009) Helicobacter pylori dysregulation of gastric epithelial tight junctions by urease-mediated myosin II activation. Gastroenterology. 136(1): p. 236-46.
219. Papini, E., Satin, B., Norais, N., de Bernard, M., Telford, J.L., Rappuoli, R., and Montecucco, C. (1998) Selective increase of the permeability of polarized epithelial cell monolayers by Helicobacter pylori vacuolating toxin. J Clin Invest. 102(4): p. 813-20.
220. Pelicic, V., Reyrat, J.M., Sartori, L., Pagliaccia, C., Rappuoli, R., Telford, J.L., Montecucco, C., and Papini, E. (1999) Helicobacter pylori VacA cytotoxin associated with the bacteria increases epithelial permeability independently of its vacuolating activity. Microbiology (Reading). 145 (Pt 8): p. 2043-2050.
221. Fedwick, J.P., Lapointe, T.K., Meddings, J.B., Sherman, P.M., and Buret, A.G. (2005) Helicobacter pylori activates myosin light-chain kinase to disrupt claudin-4 and claudin-5 and increase epithelial permeability. Infect Immun. 73(12): p. 7844-52.
222. Fiorentino, M., Ding, H., Blanchard, T.G., Czinn, S.J., Sztein, M.B., and Fasano, A. (2013) Helicobacter pylori-induced disruption of monolayer permeability and proinflammatory cytokine secretion in polarized human gastric epithelial cells. Infect Immun. 81(3): p. 876-83.

223. Amieva, M.R., Vogelmann, R., Covacci, A., Tompkins, L.S., Nelson, W.J., and Falkow, S. (2003) Disruption of the epithelial apical-junctional complex by Helicobacter pylori CagA. Science. 300(5624): p. 1430-4.
224. Krueger, S., Hundertmark, T., Kuester, D., Kalinski, T., Peitz, U., and Roessner, A. (2007) Helicobacter pylori alters the distribution of ZO-1 and p120ctn in primary human gastric epithelial cells. Pathol Res Pract. 203(6): p. 433-44.
225. Bagnoli, F., Buti, L., Tompkins, L., Covacci, A., and Amieva, M.R. (2005) Helicobacter pylori CagA induces a transition from polarized to invasive phenotypes in MDCK cells. Proc Natl Acad Sci U S A. 102(45): p. 16339-44.
226. Saadat, I., Higashi, H., Obuse, C., Umeda, M., Murata-Kamiya, N., Saito, Y., Lu, H., Ohnishi, N., Azuma, T., Suzuki, A., Ohno, S., and Hatakeyama, M. (2007) Helicobacter pylori CagA targets PAR1/MARK kinase to disrupt epithelial cell polarity. Nature. 447(7142): p. 330-3.
227. Murata-Kamiya, N., Kurashima, Y., Teishikata, Y., Yamahashi, Y., Saito, Y., Higashi, H., Aburatani, H., Akiyama, T., Peek, R.M., Jr., Azuma, T., and Hatakeyama, M. (2007) Helicobacter pylori CagA interacts with E-cadherin and deregulates the beta-catenin signal that promotes intestinal transdifferentiation in gastric epithelial cells. Oncogene. 26(32): p. 4617-26.
228. Oliveira, M.J., Costa, A.M., Costa, A.C., Ferreira, R.M., Sampaio, P., Machado, J.C., Seruca, R., Mareel, M., and Figueiredo, C. (2009) CagA associates with c-Met, E-cadherin, and p120-catenin in a multiproteic complex that suppresses Helicobacter pylori-induced cell-invasive phenotype. J Infect Dis. 200(5): p. 745-55.
229. Weydig, C., Starzinski-Powitz, A., Carra, G., Lower, J., and Wessler, S. (2007) CagA-independent disruption of adherence junction complexes involves E-cadherin shedding and implies multiple steps in Helicobacter pylori pathogenicity. Exp Cell Res. 313(16): p. 3459-71.
230. Schirrmeister, W., Gnad, T., Wex, T., Higashiyama, S., Wolke, C., Naumann, M., and Lendeckel, U. (2009) Ectodomain shedding of E-cadherin and c-Met is induced by Helicobacter pylori infection. Exp Cell Res. 315(20): p. 3500-8.
231. O'Connor, P.M., Lapointe, T.K., Jackson, S., Beck, P.L., Jones, N.L., and Buret, A.G. (2011) Helicobacter pylori activates calpain via toll-like receptor 2 to disrupt adherens junctions in human gastric epithelial cells. Infect Immun. 79(10): p. 3887-94.
232. Marques, M.S., Melo, J., Cavadas, B., Mendes, N., Pereira, L., Carneiro, F., Figueiredo, C., and Leite, M. (2018) Afadin Downregulation by Helicobacter pylori Induces Epithelial to Mesenchymal Transition in Gastric Cells. Front Microbiol. 9: p. 2712.
233. Hughes, C.S., Moggridge, S., Muller, T., Sorensen, P.H., Morin, G.B., and Krijgsveld, J. (2019) Single-pot, solid-phase-enhanced sample preparation for proteomics experiments. Nat Protoc. 14(1): p. 68-85.
234. Perez-Riverol, Y., Csordas, A., Bai, J., Bernal-Llinares, M., Hewapathirana, S., Kundu, D.J., Inuganti, A., Griss, J., Mayer, G., Eisenacher, M., Perez, E., Uszkoreit, J., Pfeuffer, J., Sachsenberg, T., Yilmaz, S., Tiwary, S., Cox, J., Audain, E., Walzer, M., Jarnuczak, A.F., Ternent, T., Brazma, A., and Vizcaino, J.A. (2019) The PRIDE database and related tools and resources in 2019: improving support for quantification data. Nucleic Acids Res. 47(D1): p. D442-D450.
235. van Doorn, L.J., Figueiredo, C., Rossau, R., Jannes, G., van Asbroek, M., Sousa, J.C., Carneiro, F., and Quint, W.G. (1998) Typing of Helicobacter pylori vacA gene and detection of cagA gene by PCR and reverse hybridization. J Clin Microbiol. 36(5): p. 1271-6.
236. Li, W., Turner, A., Aggarwal, P., Matter, A., Storvick, E., Arnett, D.K., and Broeckel, U. (2015) Comprehensive evaluation of AmpliSeq transcriptome, a novel targeted whole transcriptome RNA sequencing methodology for global gene expression analysis. BMC Genomics. 16: p. 1069.

237. Volpicelli, L.A., Lah, J.J., and Levey, A.I. (2001) Rab5-dependent trafficking of the m4 muscarinic acetylcholine receptor to the plasma membrane, early endosomes, and multivesicular bodies. J Biol Chem. 276(50): p. 47590-8.
238. Klimentova, J. and Stulik, J. (2015) Methods of isolation and purification of outer membrane vesicles from gram-negative bacteria. Microbiol Res. 170: p. 1-9.
239. Kim, G.H., Choi, C.W., Park, E.C., Lee, S.Y., and Kim, S.I. (2014) Isolation and proteomic characterization of bacterial extracellular membrane vesicles. Curr Protein Pept Sci. 15(7): p. 719-31.
240. Testerman, T.L., McGee, D.J., and Mobley, H.L. (2001) Helicobacter pylori growth and urease detection in the chemically defined medium Ham's F-12 nutrient mixture. J Clin Microbiol. 39(11): p. 3842-50.
241. Testerman, T.L., Conn, P.B., Mobley, H.L., and McGee, D.J. (2006) Nutritional requirements and antibiotic resistance patterns of Helicobacter species in chemically defined media. J Clin Microbiol. 44(5): p. 1650-8.
242. Mytilinaios, I., Salih, M., Schofield, H.K., and Lambert, R.J. (2012) Growth curve prediction from optical density data. Int J Food Microbiol. 154(3): p. 169-76.
243. Kusters, J.G., Gerrits, M.M., Van Strijp, J.A., and Vandenbroucke-Grauls, C.M. (1997) Coccoid forms of Helicobacter pylori are the morphologic manifestation of cell death. Infect Immun. 65(9): p. 3672-9.
244. Azevedo, N.F., Almeida, C., Cerqueira, L., Dias, S., Keevil, C.W., and Vieira, M.J. (2007) Coccoid form of Helicobacter pylori as a morphological manifestation of cell adaptation to the environment. Appl Environ Microbiol. 73(10): p. 3423-7.
245. Chutkan, H., Macdonald, I., Manning, A., and Kuehn, M.J. (2013) Quantitative and qualitative preparations of bacterial outer membrane vesicles. Methods Mol Biol. 966: p. 259-72.
246. Liao, S., Klein, M.I., Heim, K.P., Fan, Y., Bitoun, J.P., Ahn, S.J., Burne, R.A., Koo, H., Brady, L.J., and Wen, Z.T. (2014) Streptococcus mutans extracellular DNA is upregulated during growth in biofilms, actively released via membrane vesicles, and influenced by components of the protein secretion machinery. J Bacteriol. 196(13): p. 2355-66.
247. Perez-Cruz, C., Delgado, L., Lopez-Iglesias, C., and Mercade, E. (2015) Outer-inner membrane vesicles naturally secreted by gram-negative pathogenic bacteria. PLoS One. 10(1): p. e0116896.
248. Raudvere, U., Kolberg, L., Kuzmin, I., Arak, T., Adler, P., Peterson, H., and Vilo, J. (2019) g:Profiler: a web server for functional enrichment analysis and conversions of gene lists (2019 update). Nucleic Acids Res. 47(W1): p. W191-w198.
249. Nagy, T.A., Wroblewski, L.E., Wang, D., Piazuelo, M.B., Delgado, A., Romero-Gallo, J., Noto, J., Israel, D.A., Ogden, S.R., Correa, P., Cover, T.L., and Peek, R.M., Jr. (2011) beta-Catenin and p120 mediate PPARdelta-dependent proliferation induced by Helicobacter pylori in human and rodent epithelia. Gastroenterology. 141(2): p. 553-64.
250. De Luca, A., Baldi, A., Russo, P., Todisco, A., Altucci, L., Giardullo, N., Pasquale, L., Iaquinto, S., D'Onofrio, V., Parodi, M.C., Paggi, M.G., and Iaquinto, G. (2003) Coexpression of Helicobacter pylori's proteins CagA and HspB induces cell proliferation in AGS gastric epithelial cells, independently from the bacterial infection. Cancer Res. 63(19): p. 6350-6.
251. Shirin, H., Sordillo, E.M., Oh, S.H., Yamamoto, H., Delohery, T., Weinstein, I.B., and Moss, S.F. (1999) Helicobacter pylori inhibits the G1 to S transition in AGS gastric epithelial cells. Cancer Res. 59(10): p. 2277-81.
252. Ahmed, A., Smoot, D., Littleton, G., Tackey, R., Walters, C.S., Kashanchi, F., Allen, C.R., and Ashktorab, H. (2000) Helicobacter pylori inhibits gastric cell cycle progression. Microbes Infect. 2(10): p. 1159-69.
253. Kim, K.M., Lee, S.G., Kim, J.M., Kim, D.S., Song, J.Y., Kang, H.L., Lee, W.K., Cho, M.J., Rhee, K.H., Youn, H.S., and Baik, S.C. (2010) Helicobacter pylori gamma-glutamyltranspeptidase induces cell cycle arrest at the G1-S phase transition. J Microbiol. 48(3): p. 372-7.

254. Kim, J.J., Tao, H., Carloni, E., Leung, W.K., Graham, D.Y., and Sepulveda, A.R. (2002) Helicobacter pylori impairs DNA mismatch repair in gastric epithelial cells. Gastroenterology. 123(2): p. 542-53.
255. Koeppel, M., Garcia-Alcalde, F., Glowinski, F., Schlaermann, P., and Meyer, T.F. (2015) Helicobacter pylori Infection Causes Characteristic DNA Damage Patterns in Human Cells. Cell Rep. 11(11): p. 1703-13.
256. Park, D.I., Park, S.H., Kim, S.H., Kim, J.W., Cho, Y.K., Kim, H.J., Sohn, C.I., Jeon, W.K., Kim, B.I., Cho, E.Y., Kim, E.J., Chae, S.W., Sohn, J.H., Sung, I.K., Sepulveda, A.R., and Kim, J.J. (2005) Effect of Helicobacter pylori infection on the expression of DNA mismatch repair protein. Helicobacter. 10(3): p. 179-84.
257. Yao, Y., Tao, H., Park, D.I., Sepulveda, J.L., and Sepulveda, A.R. (2006) Demonstration and characterization of mutations induced by Helicobacter pylori organisms in gastric epithelial cells. Helicobacter. 11(4): p. 272-86.
258. Branzei, D. and Foiani, M. (2008) Regulation of DNA repair throughout the cell cycle. Nat Rev Mol Cell Biol. 9(4): p. 297-308.
259. Esashi, F., Christ, N., Gannon, J., Liu, Y., Hunt, T., Jasin, M., and West, S.C. (2005) CDK-dependent phosphorylation of BRCA2 as a regulatory mechanism for recombinational repair. Nature. 434(7033): p. 598-604.
260. Tsolakos, N., Lie, K., Bolstad, K., Maslen, S., Kristiansen, P.A., Hoiby, E.A., Wallington, A., Vipond, C., Skehel, M., Tang, C.M., Feavers, I.M., Wedege, E., and Wheeler, J.X. (2010) Characterization of meningococcal serogroup B outer membrane vesicle vaccines from strain 44/76 after growth in different media. Vaccine. 28(18): p. 3211-8.
261. Adams, B.L., Bates, T.C., and Oliver, J.D. (2003) Survival of Helicobacter pylori in a natural freshwater environment. Appl Environ Microbiol. 69(12): p. 7462-6.
262. Hutton, M.L., Kaparakis-Liaskos, M., Turner, L., Cardona, A., Kwok, T., and Ferrero, R.L. (2010) Helicobacter pylori exploits cholesterol-rich microdomains for induction of NF-kappaB-dependent responses and peptidoglycan delivery in epithelial cells. Infect Immun. 78(11): p. 4523-31.
263. Jimenez-Soto, L.F., Rohrer, S., Jain, U., Ertl, C., Sewald, X., and Haas, R. (2012) Effects of cholesterol on Helicobacter pylori growth and virulence properties in vitro. Helicobacter. 17(2): p. 133-9.
264. van der Pol, L., Stork, M., and van der Ley, P. (2015) Outer membrane vesicles as platform vaccine technology. Biotechnol J. 10(11): p. 1689-706.
265. Marshall, B.J., Barrett, L.J., Prakash, C., McCallum, R.W., and Guerrant, R.L. (1990) Urea protects Helicobacter (Campylobacter) pylori from the bactericidal effect of acid. Gastroenterology. 99(3): p. 697-702.
266. Teymournejad, O., Mobarez, A.M., Hassan, Z.M., and Talebi Bezmin Abadi, A. (2017) Binding of the Helicobacter pylori OipA causes apoptosis of host cells via modulation of Bax/Bcl-2 levels. Sci Rep. 7(1): p. 8036.
267. Tseng, Y.S., Wu, D.C., Chang, C.Y., Kuo, C.H., Yang, Y.C., Jan, C.M., Su, Y.C., Kuo, F.C., and Chang, L.L. (2009) Amoxicillin resistance with beta-lactamase production in Helicobacter pylori. Eur J Clin Invest. 39(9): p. 807-12.
268. Shibayama, K., Kamachi, K., Nagata, N., Yagi, T., Nada, T., Doi, Y., Shibata, N., Yokoyama, K., Yamane, K., Kato, H., Iinuma, Y., and Arakawa, Y. (2003) A novel apoptosis-inducing protein from Helicobacter pylori. Mol Microbiol. 47(2): p. 443-51.
269. Ricci, V., Sommi, P., Fiocca, R., Romano, M., Solcia, E., and Ventura, U. (1997) Helicobacter pylori vacuolating toxin accumulates within the endosomal-vacuolar compartment of cultured gastric cells and potentiates the vacuolating activity of ammonia. J Pathol. 183(4): p. 453-9.
270. de Bernard, M. and D'Elios, M.M. (2010) The immune modulating activity of the Helicobacter pylori HP-NAP: Friend or foe? Toxicon. 56(7): p. 1186-92.

271. Yamaoka, Y., Kikuchi, S., el-Zimaity, H.M., Gutierrez, O., Osato, M.S., and Graham, D.Y. (2002) Importance of Helicobacter pylori oipA in clinical presentation, gastric inflammation, and mucosal interleukin 8 production. Gastroenterology. 123(2): p. 414-24.
272. Schoep, T.D., Fulurija, A., Good, F., Lu, W., Himbeck, R.P., Schwan, C., Choi, S.S., Berg, D.E., Mittl, P.R., Benghezal, M., and Marshall, B.J. (2010) Surface properties of Helicobacter pylori urease complex are essential for persistence. PLoS One. 5(11): p. e15042.
273. Odenbreit, S., Wieland, B., and Haas, R. (1996) Cloning and genetic characterization of Helicobacter pylori catalase and construction of a catalase-deficient mutant strain. J Bacteriol. 178(23): p. 6960-7.
274. Pesci, E.C. and Pickett, C.L. (1994) Genetic organization and enzymatic activity of a superoxide dismutase from the microaerophilic human pathogen, Helicobacter pylori. Gene. 143(1): p. 111-6.
275. Kuhns, L.G., Wang, G., and Maier, R.J. (2015) Comparative Roles of the Two Helicobacter pylori Thioredoxins in Preventing Macromolecule Damage. Infect Immun. 83(7): p. 2935-43.
276. Ge, R. and Sun, X. (2012) Iron trafficking system in Helicobacter pylori. Biometals. 25(2): p. 247-58.
277. Gonzalez-Lopez, M.A. and Olivares-Trejo, J.J. (2009) The gene frpB2 of Helicobacter pylori encodes an hemoglobin-binding protein involved in iron acquisition. Biometals. 22(6): p. 889-94.
278. Sjostrom, A.E., Sandblad, L., Uhlin, B.E., and Wai, S.N. (2015) Membrane vesicle-mediated release of bacterial RNA. Sci Rep. 5: p. 15329.
279. Kolling, G.L. and Matthews, K.R. (1999) Export of virulence genes and Shiga toxin by membrane vesicles of Escherichia coli O157:H7. Appl Environ Microbiol. 65(5): p. 1843-8.
280. Chatterjee, S., Mondal, A., Mitra, S., and Basu, S. (2017) Acinetobacter baumannii transfers the blaNDM-1 gene via outer membrane vesicles. J Antimicrob Chemother. 72(8): p. 2201-2207.
281. Yaron, S., Kolling, G.L., Simon, L., and Matthews, K.R. (2000) Vesicle-mediated transfer of virulence genes from Escherichia coli O157:H7 to other enteric bacteria. Appl Environ Microbiol. 66(10): p. 4414-20.
282. Riley, D.R., Sieber, K.B., Robinson, K.M., White, J.R., Ganesan, A., Nourbakhsh, S., and Dunning Hotopp, J.C. (2013) Bacteria-human somatic cell lateral gene transfer is enriched in cancer samples. PLoS Comput Biol. 9(6): p. e1003107.
283. Cavadas, B., Camacho, R., Ferreira, J.C., Ferreira, R.M., Figueiredo, C., Brazma, A., Fonseca, N.A., and Pereira, L. (2020) Gastric Microbiome Diversities in Gastric Cancer Patients from Europe and Asia Mimic the Human Population Structure and Are Partly Driven by Microbiome Quantitative Trait Loci. Microorganisms. 8(8).
284. Lecrivain, A.L. and Beckmann, B.M. (2020) Bacterial RNA in extracellular vesicles: A new regulator of host-pathogen interactions? Biochim Biophys Acta Gene Regul Mech. 1863(7): p. 194519.
285. Tsatsaronis, J.A., Franch-Arroyo, S., Resch, U., and Charpentier, E. (2018) Extracellular Vesicle RNA: A Universal Mediator of Microbial Communication? Trends Microbiol. 26(5): p. 401-410.
286. Ghosal, A., Upadhyaya, B.B., Fritz, J.V., Heintz-Buschart, A., Desai, M.S., Yusuf, D., Huang, D., Baumuratov, A., Wang, K., Galas, D., and Wilmes, P. (2015) The extracellular RNA complement of Escherichia coli. Microbiologyopen. 4(2): p. 252-266.
287. Blenkiron, C., Simonov, D., Muthukaruppan, A., Tsai, P., Dauros, P., Green, S., Hong, J., Print, C.G., Swift, S., and Phillips, A.R. (2016) Uropathogenic Escherichia coli Releases Extracellular Vesicles That Are Associated with RNA. PLoS One. 11(8): p. e0160440.
288. Choi, J.W., Kim, S.C., Hong, S.H., and Lee, H.J. (2017) Secretable Small RNAs via Outer Membrane Vesicles in Periodontal Pathogens. J Dent Res. 96(4): p. 458-466.

289. Malabirade, A., Habier, J., Heintz-Buschart, A., May, P., Godet, J., Halder, R., Etheridge, A., Galas, D., Wilmes, P., and Fritz, J.V. (2018) The RNA Complement of Outer Membrane Vesicles From Salmonella enterica Serovar Typhimurium Under Distinct Culture Conditions. Front Microbiol. 9: p. 2015.
290. Han, E.C., Choi, S.Y., Lee, Y., Park, J.W., Hong, S.H., and Lee, H.J. (2019) Extracellular RNAs in periodontopathogenic outer membrane vesicles promote TNF-alpha production in human macrophages and cross the blood-brain barrier in mice. FASEB J. 33(12): p. 13412-13422.
291. Dauros-Singorenko, P., Hong, J., Swift, S., Phillips, A., and Blenkiron, C. (2020) Effect of the Extracellular Vesicle RNA Cargo From Uropathogenic Escherichia coli on Bladder Cells. Front Mol Biosci. 7: p. 580913.
292. Turnbull, L., Toyofuku, M., Hynen, A.L., Kurosawa, M., Pessi, G., Petty, N.K., Osvath, S.R., Carcamo-Oyarce, G., Gloag, E.S., Shimoni, R., Omasits, U., Ito, S., Yap, X., Monahan, L.G., Cavaliere, R., Ahrens, C.H., Charles, I.G., Nomura, N., Eberl, L., and Whitchurch, C.B. (2016) Explosive cell lysis as a mechanism for the biogenesis of bacterial membrane vesicles and biofilms. Nat Commun. 7: p. 11220.
293. Kadurugamuwa, J.L. and Beveridge, T.J. (1995) Virulence factors are released from Pseudomonas aeruginosa in association with membrane vesicles during normal growth and exposure to gentamicin: a novel mechanism of enzyme secretion. J Bacteriol. 177(14): p. 3998-4008.
294. Caglar, H.O. and Biray Avci, C. (2020) Alterations of cell cycle genes in cancer: unmasking the role of cancer stem cells. Mol Biol Rep. 47(4): p. 3065-3076.
295. Shirin, H., Weinstein, I.B., and Moss, S.F. (2001) Effects of H. pylori infection of gastric epithelial cells on cell cycle control. Front Biosci. 6: p. E104-18.
296. Moss, S.F., Sordillo, E.M., Abdalla, A.M., Makarov, V., Hanzely, Z., Perez-Perez, G.I., Blaser, M.J., and Holt, P.R. (2001) Increased gastric epithelial cell apoptosis associated with colonization with cagA + Helicobacter pylori strains. Cancer Res. 61(4): p. 1406-11.
297. Machado, A.M., Figueiredo, C., Touati, E., Máximo, V., Sousa, S., Michel, V., Carneiro, F., Nielsen, F.C., Seruca, R., and Rasmussen, L.J. (2009) Helicobacter pylori infection induces genetic instability of nuclear and mitochondrial DNA in gastric cells. Clin Cancer Res. 15(9): p. 2995-3002.
298. Futagami, S., Hiratsuka, T., Shindo, T., Horie, A., Hamamoto, T., Suzuki, K., Kusunoki, M., Miyake, K., Gudis, K., Crowe, S.E., Tsukui, T., and Sakamoto, C. (2008) Expression of apurinic/apyrimidinic endonuclease-1 (APE-1) in H. pylori-associated gastritis, gastric adenoma, and gastric cancer. Helicobacter. 13(3): p. 209-18.
299. Bielaszewska, M., Rüter, C., Bauwens, A., Greune, L., Jarosch, K.A., Steil, D., Zhang, W., He, X., Lloubes, R., Fruth, A., Kim, K.S., Schmidt, M.A., Dobrindt, U., Mellmann, A., and Karch, H. (2017) Host cell interactions of outer membrane vesicle-associated virulence factors of enterohemorrhagic Escherichia coli O157: Intracellular delivery, trafficking and mechanisms of cell injury. PLoS Pathog. 13(2): p. e1006159.
300. Turkina, M.V., Olofsson, A., Magnusson, K.E., Arnqvist, A., and Vikstrom, E. (2015) Helicobacter pylori vesicles carrying CagA localize in the vicinity of cell-cell contacts and induce histone H1 binding to ATP in epithelial cells. FEMS Microbiol Lett. 362(11).
301. Wroblewski, L.E., Piazuelo, M.B., Chaturvedi, R., Schumacher, M., Aihara, E., Feng, R., Noto, J.M., Delgado, A., Israel, D.A., Zavros, Y., Montrose, M.H., Shroyer, N., Correa, P., Wilson, K.T., and Peek, R.M., Jr. (2015) Helicobacter pylori targets cancer-associated apical-junctional constituents in gastroids and gastric epithelial cells. Gut. 64(5): p. 720-30.
302. Harrer, A., Boehm, M., Backert, S., and Tegtmeyer, N. (2017) Overexpression of serine protease HtrA enhances disruption of adherens junctions, paracellular transmigration and type IV secretion of CagA by Helicobacter pylori. Gut Pathog. 9: p. 40.
303. Vetrano, S., Rescigno, M., Cera, M.R., Correale, C., Rumio, C., Doni, A., Fantini, M., Sturm, A., Borroni, E., Repici, A., Locati, M., Malesci, A., Dejana, E., and Danese, S. (2008) Unique

role of junctional adhesion molecule-a in maintaining mucosal homeostasis in inflammatory bowel disease. Gastroenterology. 135(1): p. 173-84.
304. Mandell, K.J., Babbin, B.A., Nusrat, A., and Parkos, C.A. (2005) Junctional adhesion molecule 1 regulates epithelial cell morphology through effects on beta1 integrins and Rap1 activity. J Biol Chem. 280(12): p. 11665-74.
305. Steinbacher, T., Kummer, D., and Ebnet, K. (2018) Junctional adhesion molecule-A: functional diversity through molecular promiscuity. Cell Mol Life Sci. 75(8): p. 1393-1409.

APPENDIX

PAPER

frontiers in Microbiology

METHODS
published: 02 June 2021
doi: 10.3389/fmicb.2021.654193

Isolation Method and Characterization of Outer Membranes Vesicles of *Helicobacter pylori* Grown in a Chemically Defined Medium

Joana Melo[1,2,3], Vanessa Pinto[1,2], Tânia Fernandes[1,2], Ana R. Malheiro[1], Hugo Osório[1,2,4], Ceu Figueiredo[1,2,4†] and Marina Leite[1,2,4*†]*

[1] i3S – Instituto de Investigação e Inovação em Saúde, Universidade do Porto, Porto, Portugal, [2] Ipatimup – Instituto de Patologia e Imunologia Molecular da Universidade do Porto, Porto, Portugal, [3] ICBAS – Instituto de Ciências Biomédicas Abel Salazar, Universidade do Porto, Porto, Portugal, [4] Departamento de Patologia, Faculdade de Medicina da Universidade do Porto, Porto, Portugal

OPEN ACCESS

Edited by:
Christine Josenhans, Ludwig Maximilian University of Munich, Germany

Reviewed by:
Mario M. D'Elios, University of Florence, Italy
Stefan Schild, University of Graz, Austria

***Correspondence:**
Marina Leite
mleite@ipatimup.pt
Ceu Figueiredo
cfigueiredo@ipatimup.pt

† These authors have contributed equally to this work

Specialty section:
This article was submitted to Infectious Diseases, a section of the journal Frontiers in Microbiology

Received: 15 January 2021
Accepted: 27 April 2021
Published: 02 June 2021

Citation:
Melo J, Pinto V, Fernandes T, Malheiro AR, Osório H, Figueiredo C and Leite M (2021) Isolation Method and Characterization of Outer Membranes Vesicles of Helicobacter pylori Grown in a Chemically Defined Medium. Front. Microbiol. 12:654193. doi: 10.3389/fmicb.2021.654193

Outer membrane vesicles (OMVs) are small vesicles constitutively shed by all Gram-negative bacterium, which have been proposed to play a role in *Helicobacter pylori* persistence and pathogenesis. The methods currently available for the isolation of *H. pylori* OMVs are diverse and time-consuming, raising the need for a protocol standardization, which was the main aim of this study. Here, we showed that the chemically defined F12 medium, supplemented with cholesterol, nutritionally supports bacterial growth and maintains *H. pylori* viability for at least 72 h. Additionally, we developed an abridged protocol for isolation of OMVs from these bacterial cultures, which comprises a low-speed centrifugation, supernatant filtration through a 0.45 μm pore, and two ultracentrifugations for OMVs' recovery and washing. Using this approach, a good yield of highly pure *bona fide* OMVs was recovered from cultures of different *H. pylori* strains and in different periods of bacterial growth, as assessed by nanoparticle tracking analysis, transmission electron microscopy (TEM), and proteomic analyses, confirming the reliability of the protocol. Analysis of the proteome of OMVs isolated from *H. pylori* F12-cholesterol cultures at different time points of bacterial growth revealed differentially expressed proteins, including the vacuolating cytotoxin VacA. In conclusion, this work proposes a time- and cost-efficient protocol for the isolation of *H. pylori* OMVs from a chemically defined culture medium that is suitable for implementation in research and in the biopharmaceutical field.

Keywords: *Helicobacter pylori*, bacterial outer membrane vesicles, defined growth medium, OMVs isolation method, proteomics

INTRODUCTION

Helicobacter pylori infects about half of the human population and remains the most common chronic infection in the world (Hooi et al., 2017). This Gram-negative bacterium is acquired in childhood, and unless treated, it establishes a life-long infection of the host gastric mucosa. Persistent *H. pylori* infection is associated with various clinical outcomes, such as peptic ulcer

disease and gastric cancer, both adenocarcinoma and mucosa-associated lymphoid tissue (MALT) lymphoma (Atherton, 2006; Cover and Blaser, 2009).

H. pylori-mediated diseases, as well as bacterial colonization, survival, and persistence in the gastric mucosa depend upon the concerted action of multiple virulence factors and mechanisms (Blaser and Atherton, 2004). The secretion of outer membrane vesicles (OMVs) emerged as an additional means to facilitate such processes in *H. pylori* infection. It has been shown that *H. pylori* OMVs are internalized and deliver their cargo into epithelial cells, resulting in cellular alterations, such as vacuolization, elongation, modulation of proliferation, and a pro-inflammatory immune response (Chatterjee and Das, 1967; Devoe and Gilchrist, 1973; Hoekstra et al., 1976; Fiocca et al., 1999; Heczko et al., 2000; Ismail et al., 2003; Chitcholtan et al., 2008; Parker et al., 2010). The full contribution of OMVs to bacteria-host and bacteria-bacteria interactions is yet to be disclosed, considering that their effects may extend to locations distant from the locally circumscribed bacterial niche (Kulp and Kuehn, 2010).

Outer membrane vesicles are a type of membrane vesicles (MVs) secreted by virtually all Gram-negative bacteria. They have a spherical structure ranging from 20 to 500 nm in size, formed through the blebbing of the bacterial outer membrane (OM), enclosing periplasmic and cytoplasmic proteins, genetic material, and lipids (Kulp and Kuehn, 2010). Although there are other types of MVs secreted by different organisms, OMVs are the only type of MVs secreted by *H. pylori* described so far (Deatherage and Cookson, 2012). Even though OMVs are naturally secreted, vesiculation is strongly influenced by the bacterial growth stage and various environmental and stress conditions (Katsui et al., 1982; Thompson et al., 1985; Willen et al., 2000; Olofsson et al., 2010). *H. pylori* vesiculation, in particular, was shown to increase as bacterial growth progresses from the logarithmic to the stationary phase, and to associate with the morphological transition into the coccoid shape (Willen et al., 2000; Olofsson et al., 2010).

The current methods described for the isolation of *H. pylori*-derived OMVs are diverse and time-consuming. They include several ultracentrifugation and/or density gradient centrifugation steps to purify and recover OMVs, after an initial low-speed centrifugation and culture medium filtration intended to remove the bacteria (Kim et al., 2014; Klimentova and Stulik, 2015). Besides being laborious, the existing methods rely on complex and chemically undefined media for bacterial growth, such as Brucella Broth (BB) or Brain Heart Infusion (BHI), owing to the widely held notion that *H. pylori* is a fastidious organism and requires such enriched media to grow (Keenan et al., 2000; Mullaney et al., 2009; Kaparakis et al., 2010; Zavan et al., 2019). Nonetheless, Testerman et al. have demonstrated that *H. pylori* has few nutritional requirements and can grow in the chemically defined Ham's-F12 (F12) liquid medium. Furthermore, they have shown that supplementation of F12 with cholesterol, bovine serum albumin, or fetal bovine serum, can further enhance *H. pylori* growth (Testerman et al., 2001, 2006).

Here, we developed a simpler and faster method to isolate OMVs from *H. pylori*, based on a chemically defined medium for bacterial growth. This enables the standardization of the isolation method, which is pivotal for downstream applications. Accordingly, we used the F12 liquid medium supplemented with cholesterol for bacterial growth, and carried out the isolation of OMVs with one low-speed centrifugation and a 0.45 μm-filtration to remove bacteria while allowing the recovery of all size-range OMVs, one ultracentrifugation step for vesicle purification, and a last ultracentrifugation as a final wash. Following this approach, a high yield of pure and *bona fide* spherical *H. pylori* OMVs were recovered.

MATERIALS AND METHODS

Helicobacter pylori Strains and Growth Conditions in TSA Plates

Helicobacter pylori strains 26695 (ATCC® 700392, *cagA*$^+$, *vacA* s1/m1), 60190 (ATCC® 49503, *cagA*$^+$, *vacA* s1/m1) and Tx30a (ATCC® 51932; *cagA*$^-$, *vacA* s2/m2) were routinely cultured in Trypticase™ Soy Agar (TSA) supplemented with 5% Sheep Blood (Becton, Dickinson and Company, Franklin Lakes, NJ, United States) and incubated in a sealed jar with a microaerophilic atmosphere (GENBox microaer; bioMérieux S.A., Marcy l'Etoile, France) at 37°C for 48 h. Bacteria were sub-cultured for a maximum of 12 passages.

Helicobacter pylori Growth in Liquid Cultures

Helicobacter pylori previously grown in TSA plates for 48 h was collected with 1 mL of either sterile Ham's F12 with L-glutamine medium (#L0135-500; Biowest, Nuaillé, France) supplemented with 1× cholesterol (Gibco®, Thermo Fisher Scientific, Waltham, MA, United States) (hereafter designated as F12-cholesterol), or BBL™ Brucella broth (BB; #211088; BD Biosciences, San Jose, CA, United States) supplemented with 5% fetal bovine serum (FBS; HyClone™, GE Healthcare Life Sciences, United States) (abbreviated as BB-FBS). The optical density at 600 nm (OD_{600}) was measured using a spectrophotometer (Genesys20; Thermo Fisher Scientific), in polystyrene cuvettes (Thermo Fisher Scientific). The culture medium of the corresponding bacterial culture was used as the blank solution to calibrate the spectrophotometer to 100% absorbance.

The initial OD_{600} of the bacterial suspension was adjusted to 0.02 ($\sim 6 \times 10^6$ colony forming units – CFUs/mL) in 200 mL of F12-cholesterol or BB-FBS. Bacteria were grown in a 500 mL Schott flask, placed in a sealed jar, under microaerophilic conditions, at 37°C, and with a constant rotation of 100 rpm (SI600 Large Shaking Incubator; Stuart, Staffordshire, United Kingdom) for the defined periods of time, 24, 48, 64, or 72 h. Bacterial growth was monitored at the referred time points by measuring the OD_{600} of the liquid bacterial cultures.

Bacterial Viability

The viability of *H. pylori* grown in liquid media was assessed by two methods: CFUs counting and flow cytometry using the LIVE/DEAD BacLight Bacterial Viability Kit (Thermo Fisher Scientific), according to the manufacturers' instructions.

For the CFUs counting, at the referred time points, 100 μL of bacterial suspension was collected, serially diluted by 10-fold in BB, and 10 μL of each dilution was plated on TSA plates, in quadruplicates. Plates were incubated in a sealed jar with a microaerophilic atmosphere, at 37°C for 48 h. At this time, colonies were counted and the number of CFUs/mL was calculated (CFUs/mL = number of colonies ÷ inoculum × dilution factor × 1,000 μL).

For the LIVE/DEAD assay, a bacterial suspension of 2×10^6 cells was filtered through a 10 μm CellTrics® filter (Sysmex Partec, Göerlitz, Germany) to remove aggregates. Bacteria were then stained with 0.5 nM SYTO9, a cell-permeant green fluorescent nucleic acid stain that labels both live and dead cells, and with 2 μg/mL propidium iodide, a nucleic acid red-fluorescent dye that labels non-viable cells with damaged membranes, for 15 min at room temperature (RT) and in the dark. Data acquisition was immediately performed on a FACSCanto II cytometer (BD Biosciences), and analyzed using the FlowJo™ version 10 software (BD Biosciences). $SYTO9^+$ stained bacterial cells were defined as $SYTO9^+PI^-$ (live) or $SYTO9^+PI^+$ (dead) and results are shown as the frequency of gated cells. SYTO9 and PI single stainings and unstained samples were used as controls.

Isolation of OMVs From Bacterial Liquid Cultures

Isolation of *H. pylori*-derived OMVs was performed from the supernatant of the liquid bacterial cultures. At the specified time points of bacterial growth, 200 mL of bacterial cultures were subjected to low-speed centrifugation at 15,000 × *g*, for 15 min at 4°C, in a JA25-50 rotor (Avanti J-25; Beckman Coulter, Fullerton, CA, United States), to pellet bacteria. The bacteria-free supernatant was filtered through a 0.45 μm cellulose acetate bottle-top filter unit (Corning, NY, United States), and then OMVs were pelleted by ultracentrifugation at 200,000 × *g*, for 90 min at 4°C, in a 70Ti rotor (Optima XE-100; Beckman Coulter). OMVs from the different centrifuge tubes were pooled and washed once in 20 mL sterile 0.9% NaCl solution (saline) (Braun; Kronberg im Taunus, Germany) (200,000 × *g*, 90 min, 4°C), resuspended in 100 μL saline and frozen at −80°C until use.

Transmission Electron Microscopy

The morphology and purity of *H. pylori* cultures grown in F12-cholesterol and of *H. pylori*-derived OMVs were confirmed by transmission electron microscopy (TEM). The presence of protein aggregates in the liquid media was also evaluated by TEM. For negative staining, 7 μL of sample (bacterial suspensions, OMVs or liquid medium) was mounted in Formvar/carbon film-coated mesh nickel grids (Electron Microscopy Sciences, Hatfield, PA, United States), and after the excess liquid was removed, 2 μL of aqueous 1% uranyl acetated solution (#22400; Electron Microscopy Sciences) were added onto the grids. For the ultrastructure analysis, OMVs samples were fixed in a solution of 2% glutaraldehyde (#16316; Electron Microscopy sciences) with 2.5% formaldehyde (#15713; Electron Microscopy sciences) in 0.1 M sodium cacodylate buffer (pH 7.4) for 1 h, at RT, and post fixed in 1% osmium tetroxide (#19190; Electron Microscopy Sciences) diluted in 0.1 M sodium cacodylate buffer. After ultracentrifugation (200,000 × *g*, 90 min, 4°C), the pellet was resuspended in Histogel™ (HG-4000-012, Thermo Fisher Scientific) and then stained with aqueous 1% uranyl acetate solution overnight, dehydrated and embedded in Embed-812 resin (#14120; Electron Microscopy sciences). Ultra-thin sections (50 nm thickness) were cut on a RMC Ultramicrotome (PowerTome, United States) using Diatome diamond knifes (DDK, Wilmington, DE, United States), mounted on mesh nickel grids (Electron Microscopy Sciences), and stained with uranyl acetate substitute (#11000; Electron Microscopy Sciences) and lead citrate (#11300; Electron Microscopy Sciences) for 5 min each. Negative staining samples and thin sections were examined under a JEOL JEM 1400 transmission electron microscope (JEOL, Tokyo, Japan) and images were digitally recorded using a CCD digital camera Orius 1100W (Tokyo, Japan).

Scanning Electron Microscopy

For scanning electron microscopy (SEM) analysis, 5 mL of bacterial suspension from F12-cholesterol cultures were pre-fixed in 2.5% glutaraldehyde solution, diluted in 0.2 M sodium phosphate buffer (0.2 M $Na_2HPO_4 \cdot 2H_2O$ and 0.2 M $NaH_2PO_4 \cdot H_2O$ in H_2O; PB; pH 7.3), for 24 h at RT. After two washes in PB, samples were post-fixed in 2% osmium tetroxide for 48 h at RT, rinsed in distilled water, and dehydrated in graded ethanol solutions of 50, 70, 80, and 95%, with two final 100% ethanol changes, for 10 min in each dilution. Samples were chemically dried in Hexamethyldisilazane (HMDS) (Sigma-Aldrich Co., St. Louis, MO, United States) by a first incubation in 50% HMDS diluted in absolute ethanol for 24 h, followed by a 15 min incubation in 100% HMDS. Samples were left to air-dry in a fume hood at RT. Dried samples were mounted on an aluminum stub with double-sided adhesive carbon tape and sputter-coated with a thin film of Au/Pd, to improve the electrically conducting properties of the sample surface. Image acquisition was performed using a High resolution (Schottky) Environmental Scanning Electron Microscope with X-Ray Microanalysis and Electron Backscattered Diffraction analysis (FEI Quanta 400 FEG ESEM/EDAX Genesis X4M; Thermo Fisher Scientific).

Nanoparticle Tracking Analysis of OMVs

The quantification and sizing of the OMVs were determined using a NS300 particle−size tracker with the Nanosight NTA 3.0 software (Malvern, Worcestershire, United Kingdom). Samples were diluted (1:40,000) in saline to achieve a concentration of 10^7–10^9 particles/mL for the analysis. Under controlled fluid flow, three measurements (videos of 30 s each) of each sample were acquired as technical replicates and results were averaged. Reads were performed using the camera level adjusted to a value between 14 and 16, and a detection threshold fixed at five. The sample chamber was flushed with sterile PBS between samples, to avoid cross-contamination.

Protein Quantification of OMVs

A total of 10^{11} OMVs were diluted in 4× Laemmli buffer (Bio-Rad Laboratories Inc.) with β-mercaptoethanol (Sigma-Aldrich), denaturated at 95°C for 5 min and loaded onto 7.5% sodium dodecyl sulfate–polyacrylamide gels (SDS-PAGE). After electrophoresis, gels were stained with 25 mL of BlueSafe (NZYTech, Lisbon, Portugal), for 1 h at RT with gentle rotation, washed with distilled water for 10 min three times, and visualized in a GS-800 Calibrated Densitometer (Bio-Rad Laboratories Inc.). Bands were quantified by densitometry using the Quantity One® 1-D version 4.6.8 software (Bio-Rad Laboratories Inc.). Bovine serum albumin (#05482, Sigma-Aldrich Co.) was used as a protein standard to draw a calibration curve, following the same procedure as OMVs samples. The protein concentration of the OMVs samples was determined by the interpolation from the standard curve. This protocol was optimized by Steeve Lima and Paulo Oliveira at i3S (unpublished).

Proteomics Analysis

A pellet of 5×10^{11} *H. pylori* 26695 OMVs isolated from liquid bacterial cultures at 48, 64, and 72 h of growth was lysed in cold lysis buffer (1% NP-40, 1% Triton X-100 diluted in PBS, pH7.4) containing 1× Bacterial Protease Arrest™ (GBiosciences, St. Louis, MO, United States) and 6 mg/mL lysozyme (PanReac AppliChem S. L. U., Barcelona, Spain), for 1 h on ice. Upon centrifugation (21,000 × *g* for 15 min at 4°C), the cleared lysate was recovered and solubilized in a solution of 100 mM Tris pH 8.5, 1% sodium deoxycholate, 10 mM tris(2-carboxyethyl)phosphine (TCEP), 40 mM chloroacetamide and 1× complete™ protease inhibitor cocktail (Roche Applied Science, Mannheim, Germany), for 10 min, at 95°C, with a constant rotation of 1,000 rpm (Thermomixer, Eppendorf, Hamburg, Germany). Samples were processed for proteomics following the solid-phase-enhanced sample-preparation (SP3) protocol as described in Hughes et al. (2019). Briefly, enzymatic digestion was achieved by adding 2 μg Trypsin/LysC to each sample and incubated overnight at 37°C with constant rotation (1,000 rpm). Protein identification and quantitation was performed by nanoLC-MS/MS using an Ultimate 3000 liquid chromatography system coupled to a Q-Exactive Hybrid Quadrupole-Orbitrap mass spectrometer (Thermo Fisher Scientific). Samples were loaded onto a trapping cartridge (Acclaim PepMap C18 100Å, 5 mm × 300 μm i.d., 160454, Thermo Fisher Scientific) in a mobile phase of 2% acetonitrile (ACN), 0.1% formic acid (FA) at 10 μL/min. After 3 min loading, the trap column was switched in-line to a 50 cm by 75 μm inner diameter EASY-Spray column (ES803, PepMap RSLC, C18, 2 μm, Thermo Fisher Scientific), at 300 nL/min. Separation was generated by gradient mixing A (0.1% FA) and B (80% ACN, 0.1% FA) as follows: 5 min (2.5% B to 10% B), 120 min (10% B to 30% B), 20 min (30% B to 50% B), 5 min (50% B to 99% B), and 10 min (hold 99% B). Subsequently, the column was equilibrated with 2.5% B for 17 min. Data acquisition was controlled by Xcalibur 4.0 and Tune 2.9 software (Thermo Fisher Scientific). The mass spectrometer was operated in data-dependent (dd) positive acquisition mode alternating between a full scan (m/z 380–1,580) and subsequent HCD MS/MS of the 10 most intense peaks from full scan (normalized collision energy of 27%). ESI spray voltage was 1.9 kV. Global settings: use lock masses best (m/z 445.12003), lock mass injection Full MS, chrom. peak width (FWHM) 15s. Full scan settings: 70k resolution (m/z 200), AGC target 3×10^6, maximum injection time 120 ms. dd settings: minimum AGC target 8×10^3, intensity threshold 7.3×10^4, charge exclusion: unassigned, 1, 8, > 8, peptide match preferred, exclude isotopes on, dynamic exclusion 45 s. MS2 settings: microscans 1, resolution 35k (m/z 200), AGC target 2×10^5, maximum injection time 110 ms, isolation window 2.0 m/z, isolation offset 0.0 m/z, spectrum data type profile. Three biological replicates were used for each time point and the LC-MS acquisition of each sample was performed in triplicate.

Database Searching, Protein Identification, and Classification

Raw data was processed using the Proteome Discoverer 2.5.0.400 software (Thermo Fisher Scientific) and searched against the UniProt[1] database for the *H. pylori* 26695 Proteome 2021_01 release, 1552 entries, and a common contaminant database from MaxQuant (version 1.6.2.6, Max Planck Institute of Biochemistry, Munich, Germany). The Sequest HT and the MS Amanda 2.0 search engines, together with the Inferys PSM rescoring node, were used to identify tryptic peptides. The ion mass tolerance was 10 ppm for precursor ions and 0.02 Da for fragment ions. Maximum allowed missing cleavage sites was set to 2. Cysteine carbamidomethylation was defined as constant modification. Methionine oxidation, asparagine and glutamine deamidation, peptide N-terminus glutamine to pyro-glutamine, and protein N-terminus acetylation, methionine loss, and methionine loss plus acetylation, were defined as variable modifications. Peptide confidence was set to high. The processing node Percolator was enabled with the following settings: maximum delta Cn 0.05; decoy database search target false discovery rate 1%, validation based on q-value. Protein label free quantitation was performed with the Minora feature detector node at the processing step. Precursor ions quantification was performed at the processing step with the following parameters: unique plus razor peptides were used for quantification, precursor abundance based on intensity and normalization based on total peptide amount. Common contaminants were excluded from data analysis. The ANOVA hypothesis test (individual proteins) for *p*-value calculation was performed for the three bacterial growth periods. Differentially expressed proteins were identified using the following parameters: fold change ratios ± 2.00 and $p < 0.05$. The total abundance of the predicted groups was calculated by the sum of the abundance of proteins classified for each group Prediction of proteins cellular localization and molecular function was obtained from the gene ontology (GO) UniProt database (see text foot note 1). The mass spectrometry proteomics data have been deposited to the ProteomeXchange Consortium via the PRIDE (Perez-Riverol et al., 2019) partner repository with the dataset identifier PXD025393 and 10.6019/PXD025393.

[1] www.uniprot.org

Statistical Analysis

Data were analyzed using the GraphPad Prism version 8.4.3 software (San Diego, CA, United States). The one-, two-way and Brown-Forsythe ANOVA, with the *post hoc* Tukey's, Dunnett's or Sidak's tests for paired comparisons, were applied for comparisons between three independent groups. Statistically significance was set at p-values ≤ 0.05 ($^{*}p \leq 0.05$, $^{**}p \leq 0.01$, $^{***}p \leq 0.001$, $^{****}p \leq 0.0001$).

RESULTS

Helicobacter pylori Growth and Viability in F12 Liquid Medium Supplemented With Cholesterol

Considering the goal to isolate OMVs from *H. pylori* cultures grown in a chemically defined medium, we started by characterizing the bacterial growth and viability in the Ham's F-12 liquid medium supplemented with cholesterol, previously reported to support *H. pylori* growth (Testerman et al., 2001).

The bacterial growth of *H. pylori* 26695 was monitored by measuring the optical density at 600 nm (OD_{600}) of the bacterial liquid cultures at 24, 48, 64, and 72 h, starting with an inoculum density of 0.02 per mL at OD_{600} ($\sim 6 \times 10^6$ CFUs/mL) in 200 mL of F12-cholesterol medium (**Figure 1A**). The growth curve was predicted using the Gompertz model (Mytilinaios et al., 2012) fitted to our data. *H. pylori* presented an exponential growth during the first 32 h of culture, after which it reached a stationary phase that lasted nearly until the endpoint of 72 h. The experimental OD_{600} values at 24 h, 48 h, 64 h, and 72 h were, respectively, 0.127 ± 0.004, 0.147 ± 0.003, 0.148 ± 0.004, and 0.139 ± 0.003, decreasing 6.1% from 64 h to 72 h, although not statistically significant ($p = 0.3528$; one-way ANOVA with *post hoc* Tukey's test), indicating that bacterial growth might become limited by nutrient availability. The growth kinetics of *H. pylori* 26695 in the chemically defined F12-cholesterol medium and in the complex BB medium supplemented with 5% FBS was compared, under the same experimental conditions (**Supplementary Figure 1A**). The growth curve was similar for both media, although bacteria grew faster in BB-FBS, with bacterial cultures reaching higher densities (OD_{600} at 24 h: 0.160 ± 0.010; 48 h: 0.199 ± 0.004; 64 h: 0.206 ± 0.011; and 72 h: 0.209 ± 0.005).

To assess the viability of *H. pylori* 26695 strain in F12-cholesterol, we determined the number of CFUs and performed the LIVE/DEAD BacLight Bacterial Viability assay using flow cytometry. The number of CFUs increased until 48 h of bacterial growth (24 h: $9.46 \pm 0.96 \times 10^7$ CFUs/mL; 48 h: $1.12 \pm 0.06 \times 10^8$ CFUs/mL), and decreased slightly at 64 h, although not statistically significant (64 h: $9.11 \pm 0.71 \times 10^7$ CFUs/mL; 48 h *vs.* 64 h: $p = 0.2080$), and until 72 h ($6.38 \pm 0.66 \times 10^7$ CFUs/mL, 48 h *vs.* 72 h: $p = 0.0082$; 64 h *vs.* 72 h: $p = 0.0571$) (**Figure 1B**). For comparative purposes, we also evaluated the number of CFUs in BB-FBS bacterial cultures (**Supplementary Figure 1B**). The number of CFUs was similar at 24 h of growth in both media (24 h: $8.47 \pm 0.38 \times 10^7$ CFUs/mL; $p = 0.8217$), and significantly lower in BB-FBS at 48 h ($6.88 \pm 0.44 \times 10^7$ CFUs/mL; $p < 0.0001$), 64 h ($4.58 \pm 0.71 \times 10^7$ CFUs/mL; $p < 0.0001$), and 72 h ($3.00 \pm 0.70 \times 10^7$ CFUs/mL; $p = 0.0030$). These results show that F12-cholesterol medium sustains the growth and a higher number of viable *H. pylori*, although at a slower rate than BB-FBS medium. The viability of *H. pylori* 26695 grown in F12-cholesterol was also evaluated by another method, the LIVE/DEAD BacLight assay. This assay relies on the simultaneous staining with two fluorescent nucleic acids dyes to distinguish between live and dead bacteria: SYTO9 (green) that enters in all bacterial cells, staining both live and dead cells, and PI (red) that enters in cells with a disrupted membrane, labeling only dead bacteria. Using SYTO9 to define the bacterial cell population, the percentage of live ($SYTO9^+PI^-$) and dead ($SYTO9^+PI^+$) bacteria was then calculated for each sample. No statistically significant differences in the percentage of live (48 h: $93.3 \pm 1.8\%$; 64 h: $92.8 \pm 1.6\%$; 72 h: $91.0 \pm 1.7\%$) and dead (48 h: $6.7 \pm 1.8\%$; 64 h: $7.1 \pm 1.6\%$; 72 h: $8.7 \pm 1.7\%$) bacteria were found between the experimental time points (**Figure 1B** and **Supplementary Figure 2** for gating strategy). This shows that bacteria remained viable until 72 h, despite the above-mentioned decrease in the number of CFUs.

Knowing that *H. pylori* morphology changes from a bacillary to a coccoid structure in response to nutrient deprivation and other adverse environmental conditions (Kusters et al., 1997; Azevedo et al., 2007), which could explain the differences between CFUs counts and LIVE/DEAD assay results, we evaluated the morphological alterations during the bacterial growth in F12-cholesterol. Bacillary, U-shaped, and coccoid bacteria were manually counted from negative stain TEM micrographs taken from 48, 64, and 72 h bacterial liquid cultures (**Figure 1C**). No statistically significant differences were found regarding the frequency of each morphological shape between samples collected at 48 and 64 h, and between 64 and 72 h samples (**Figure 1D**). However, a significant decrease in the number of bacillary ($p = 0.003$) and an increase in the number of coccoid *H. pylori* ($p = 0.012$) were observed in samples collected at 72 h when compared to those obtained at 48 h. This observation suggests that coccoid forms are viable but non-culturable (Ierardi et al., 2020), as there was no alteration in the frequency of viable bacteria, assessed by the LIVE/DEAD assay, at this time point. As an ancillary analysis, we checked the morphology of *H. pylori* grown in F12-cholesterol by SEM (**Supplementary Figure 3**), which confirmed that the bacillary shape was predominant at all time points, with the U-shape and coccoid bacteria becoming noticeable in the 72 h cultures.

Altogether, these results show that the F12-cholesterol medium is capable of nutritionally support *H. pylori* growth, preserving its typical bacillary morphology and viability.

Quantification and Morphological Characterization of OMVs Secreted by *Helicobacter pylori* Grown in F12-Cholesterol Medium

After ensuring that the F12-cholesterol medium supports both growth and viability of *H. pylori* 26695 under our experimental

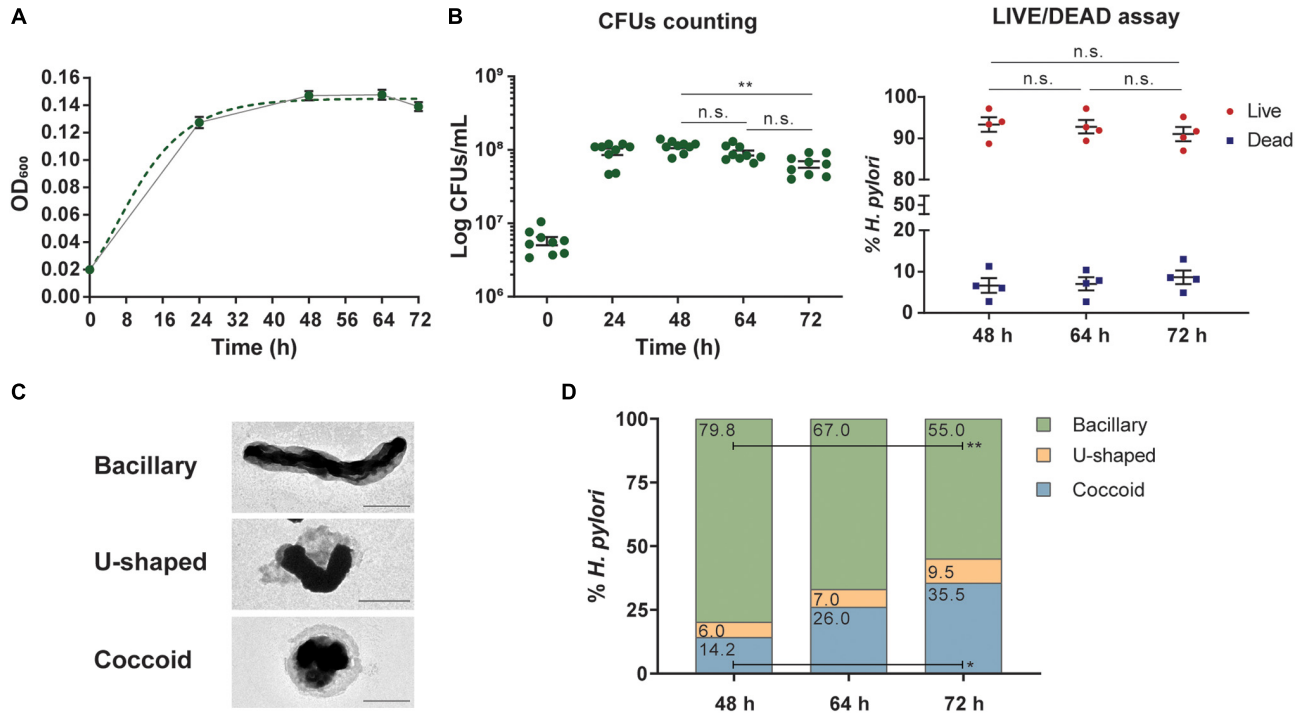

FIGURE 1 | Kinetics, viability, and morphology of *Helicobacter pylori* growth in liquid F-12-cholesterol. **(A)** Growth curve of *Helicobacter pylori* 26695 grown in F12 liquid medium supplemented with 1× cholesterol (continuous line), modeled using the Gompertz growth equation model (dotted line), calculated with GraphPad Prism, and based on the optical density measurements of the bacterial suspension at 600 nm (OD_{600}) from 24, 48, 64, and 72 h cultures. Data are shown as mean ± SEM of 16 biological replicates. **(B)** Bacterial viability evaluated by colony-forming units (CFUs) counting (left graph) and the LIVE/DEAD BacLight Bacterial Viability assay (right graph). The number of CFUs was determined at the referred time points, represented as CFUs/mL. Each dot represents a biological replicate ($n = 9$) and data are shown as mean ± SEM. Statistical significance was evaluated using the one-way ANOVA with *post hoc* Tukey's test, comparing all datasets with each other; only comparisons between 48, 64, and 72 h were illustrated for the sake of simplicity; $^{**}p \leq 0.01$, n.s. – not significant. LIVE/DEAD BacLight Bacterial Viability assay at 48, 64, and 72 h of growth, by flow cytometry. After sample staining with SYTO9 and PI dies and acquisition on a FACSCanto II cytometer, live and dead bacteria were gated and defined as $SYTO9^{+}PI^{-}$ and $SYTO9^{+}PI^{+}$, respectively. Each dot represents a biological replicate ($n = 4$) and data are shown as mean ± SEM of the frequency of gated $SYTO9^{+}PI^{-}$ and $SYTO9^{+}PI^{+}$ bacteria. Statistical significance was evaluated using the two-way ANOVA with *post hoc* Tukey's test; n.s. – not significant. **(C)** Representative negative stain TEM micrographs of bacillary, U-shaped, and coccoid forms of *H. pylori* from a 64 h liquid culture. Scale bars: 1 μm; 80,000× (bacillary and coccoid) and 8,000× (U-shaped) original magnifications. **(D)** Quantification of bacillary, U-shaped, and coccoid forms of *H. pylori* present in F12-cholesterol liquid cultures at 48, 64, and 72 h from negative stained TEM micrographs, using manual counting. The frequency of each bacterial form was calculated considering the total number of bacteria (741, 1,215, and 1,061) counted in micrographs taken from samples of each time point, 48 h ($n = 5$), 64 h ($n = 5$), and 72 h ($n = 2$), respectively. The mean frequency of each form is displayed inside the respective bar. Statistical significance was evaluated using the two-way ANOVA with *post hoc* Tukey's test, comparing all datasets with each other; statistical significance was only observed between 72 and 48 h for bacillary and coccoid forms; $^{*}p \leq 0.05$ and $^{**}p \leq 0.01$.

settings, we optimized the OMVs' isolation protocol to be fast and simple, while reliable. This protocol comprises one low-speed centrifugation followed by a 0.45 μm-filtration to deplete both bacterial cells and debris, one ultracentrifugation to recover OMVs, and a final ultracentrifugation to wash the OMVs fraction (**Figure 2**). The overall duration of the protocol is of approximately 4 h, distributed in 60 min of hands-on and 195 min of hands-off time. This protocol is substantially shorter than those published, which report the hands-off time between 335 min to 1,170 min (Mullaney et al., 2009; Olofsson et al., 2010).

The OMVs recovered following this protocol exhibited a spherical shape with a central depression and a heterogeneous size, as visualized by negative staining followed by TEM (**Figure 3A**), matching the OMVs' prototypical morphology and size distribution (Chutkan et al., 2013). Moreover, ultrastructural analysis enabled validation of the vesicles as OMVs, since they are delimited by a single lipid bilayer (**Figure 3B**). TEM analysis revealed the absence of bacterial debris, flagella, and proteins, showing that OMVs preparations were highly pure. The comparative analysis of the negative staining images of OMVs isolated from *H. pylori* 26695 grown in F12-cholesterol and in complex BB-FBS medium, and between the respective culture media alone, highlighted the importance of using the synthetic medium for the recovery of highly pure OMVs. F12-cholesterol medium and OMVs isolated from F12-cholesterol bacterial cultures had a clear background, without protein aggregates (**Figure 3A** and **Supplementary Figure 4A**), distinctly from BB-FBS medium and the respective OMVs samples, in which the presence of proteins was detected (**Supplementary Figures 4B,C**).

We next characterized the size distribution and number of OMVs recovered from the 48, 64, and 72 h *H. pylori* cultures by

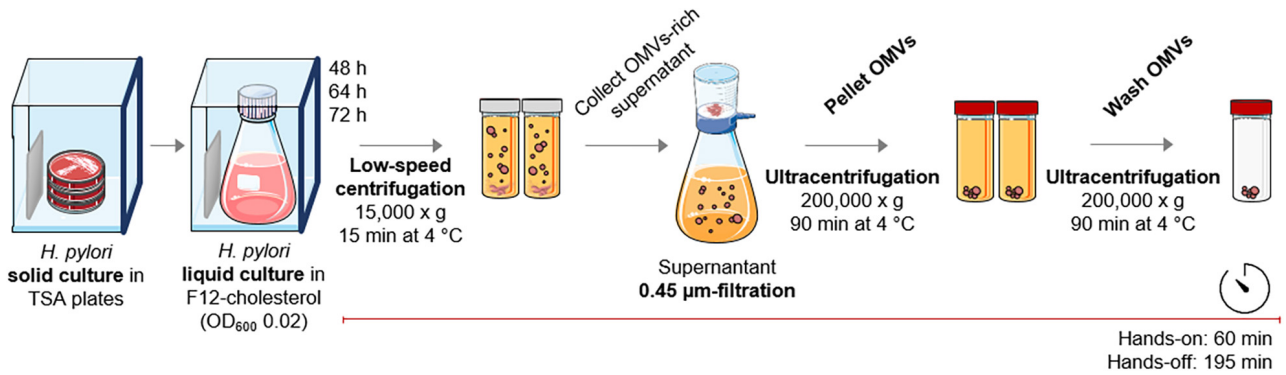

FIGURE 2 | Outline of the OMVs isolation method from *Helicobacter pylori* cultures in F12-cholesterol medium. After the establishment of the liquid bacterial culture, the protocol for OMVs isolation includes one low-speed centrifugation, a 0.45 μm-filtration of the bacteria-free supernatant, and two ultracentrifugations for the recovery and wash of OMVs, comprising 60 min of hands-on period and 195 min of hands-off period (see details in Materials and Methods section). This figure used elements from Servier Medical Art (www.servier.fr/servier-medical-art).

NTA (**Figure 3C**). More than 99% of all OMVs presented a size range between 20 and 200 nm, regardless of the culture time, and 0.66% of vesicles were detected above the 200 nm. The presence of OMVs higher than 450 nm was negligible, which matched the exclusion filter pore-size and demonstrated the absence of vesicle aggregates. From the NTA data, we also identified that the mode sizes of OMVs isolated from the 48, 64, and 72 h liquid cultures were, respectively, 84.3 ± 1.7, 79.8 ± 6.4, and 83.3 ± 5.0 nm. Despite the fact that OMVs isolated from 48 h bacterial cultures were more heterogeneous in size than OMVs from 64 and 72 h cultures, presenting a distinctive population of smaller OMVs with a diameter ranging from 15 to 60 nm, the size distribution of OMVs from the three time points presented no statistically significant differences between them.

Concerning the yield of OMVs, an average of $1.68 \pm 0.24 \times 10^{10}$, $3.37 \pm 0.31 \times 10^{10}$, and $3.59 \pm 0.91 \times 10^{10}$ OMVs per mL of liquid culture was recovered from the 48, 64, and 72 h bacterial cultures, respectively (**Figure 3D**). The 64 h bacterial cultures produced a significantly higher number of OMVs/mL when compared to the 48 h cultures ($p = 0.014$), but not significantly different from the 72 h cultures. Although we cannot exclude some loss of OMVs during the isolation procedure, we assume that the number of secreted vesicles is likely near the recovered ones, given that no vesicles were detected in the supernatant collected after the first ultracentrifugation, both in F12-cholesterol and in BB-FBS, when analyzed by TEM (**Supplementary Figures 4D,E**). As so, the shorter number of steps and the recovery of a high yield of vesicles emphasize the efficacy of our protocol, even when different culture media are used.

To ascertain the applicability of this protocol to *H. pylori* strains other than 26695, we selected two additional *H. pylori* reference strains, 60190 and Tx30a. These strains were grown in F12-cholesterol medium, under the same conditions as strain 26695, and their OMVs were isolated and characterized by TEM and NTA, in the 64 h bacterial cultures. OMVs recovered from *H. pylori* 60190 and TX30a were highly pure and with the same size heterogeneity as 26695-OMVs (**Figures 3E,F**). The number of OMVs recovered per mL of bacterial culture was similar between the three strains at 64 h of bacterial growth (26695: $3.37 \pm 6.27 \times 10^9$; 60190: $3.09 \pm 1.29 \times 10^{10}$; Tx30a: $2.45 \pm 1.01 \times 10^{10}$ OMVs/mL) (**Figure 3G**).

In summary, these results show that OMVs recovered from *H. pylori* grown in F12-cholesterol cultures are *bona fide*, presenting the same morphology and ultrastructure as those isolated from complex media (Chutkan et al., 2013; Turner et al., 2018). Furthermore, our abridged protocol provided a good yield and a highly pure population of OMVs from various *H. pylori* strains and in different phases of bacterial growth.

Proteomic Content and Proteomic Analysis of OMVs Isolated From *Helicobacter pylori* 26695 Grown in F12-Cholesterol Culture Medium

The next aim was to characterize and compare the protein cargo of OMVs secreted by *H. pylori* grown in F12-cholesterol at different time points of bacterial growth. The total protein amount from OMVs was assessed by SDS-PAGE and gel staining with BlueSafe, using lysates from 10^{11} OMVs (**Figure 4**). OMVs isolated from 48, 64 and 72 h bacterial cultures presented an identical protein profile (**Figure 4A**) and similar total protein amounts (48 h: 3.55 ± 1.16; 64 h: 4.02 ± 0.95; 72 h: 4.25 ± 1.42 μg of protein per 10^{11} OMVs) (**Figure 4B**).

Next, we applied nanoscale liquid chromatography coupled to tandem mass spectrometry (nanoLC-MS/MS) to 5×10^{11} OMVs of each time point of bacterial growth, and analyzed the differential expression of proteins between each of them. A total of 267, 268 and 269 proteins from *H. pylori* 26695 were identified on 48, 64, and 72 h-OMVs, respectively (**Supplementary Table 1**). Of these, 233, 231, and 232 proteins with a false discovery rate of 1% were further classified according to their predicted cellular localization, biological process and molecular function, using the GO UniProt database resource and manual curation (**Supplementary Table 2**). All proteins identified in 64 h-OMVs (231) were common to 48 and 72 h samples.

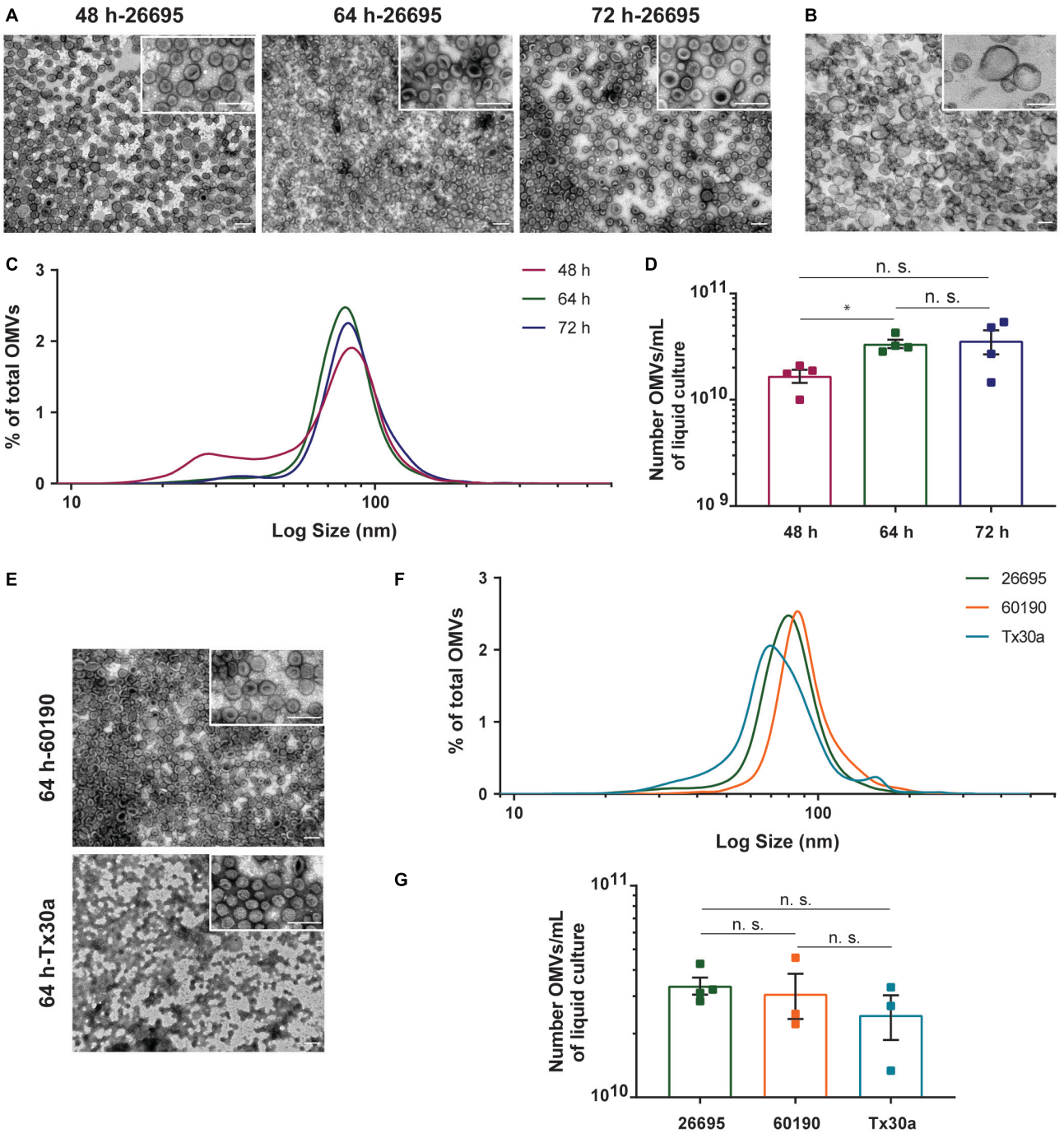

FIGURE 3 | Morphological characterization, size distribution, and yield of OMVs secreted by *Helicobacter pylori* grown in F12-cholesterol medium. **(A)** Negative staining of OMVs isolated from *H. pylori* 26695 F12-cholesterol liquid cultures at 48, 64, and 72 h of growth, and **(B)** ultrastructure section of OMVs from 64 h *H. pylori* cultures. Scale bars: 200 nm; 50,000×, 100,000× [insets in panel **(A)**] and 200,000× [inset in panel **(B)**] original magnifications. **(C)** Size distribution, represented as percentage of the total number of isolated OMVs; data are shown as mean ± SEM of four biological replicates and statistical significance was evaluated using the one-way ANOVA with *post hoc* Tukey's test; n.s. – not significant. **(D)** Number of recovered OMVs per mL of bacterial culture, determined using Nanoparticle Tracking Analysis (NTA) at 48, 64, and 72 h periods of bacterial growth; data are shown as mean ± SEM of four biological replicates and statistical significance was evaluated using the one-way ANOVA with *post hoc* Tukey's test; $^*p \leq 0.05$, n.s. – not significant. **(E)** Representative negative stain TEM micrographs of *H. pylori* 60190 and Tx30a-OMVs generated from 64 h F12-cholesterol bacterial cultures. Scale bars: 200 nm; 50,000× and 100,000× (insets) original magnification. **(F)** Size distribution, represented as percentage of the total number of isolated OMVs at 64 h of liquid culture, and **(G)** number of recovered OMVs per mL of bacterial culture determined by NTA; data are shown as mean ± SEM of 4 (for 26695) or 3 (for 60190 and Tx30a) biological replicates and statistical significance was evaluated using the Brown-Forsythe and Welch ANOVA with *post hoc* Dunnett's test; n.s. – not significant.

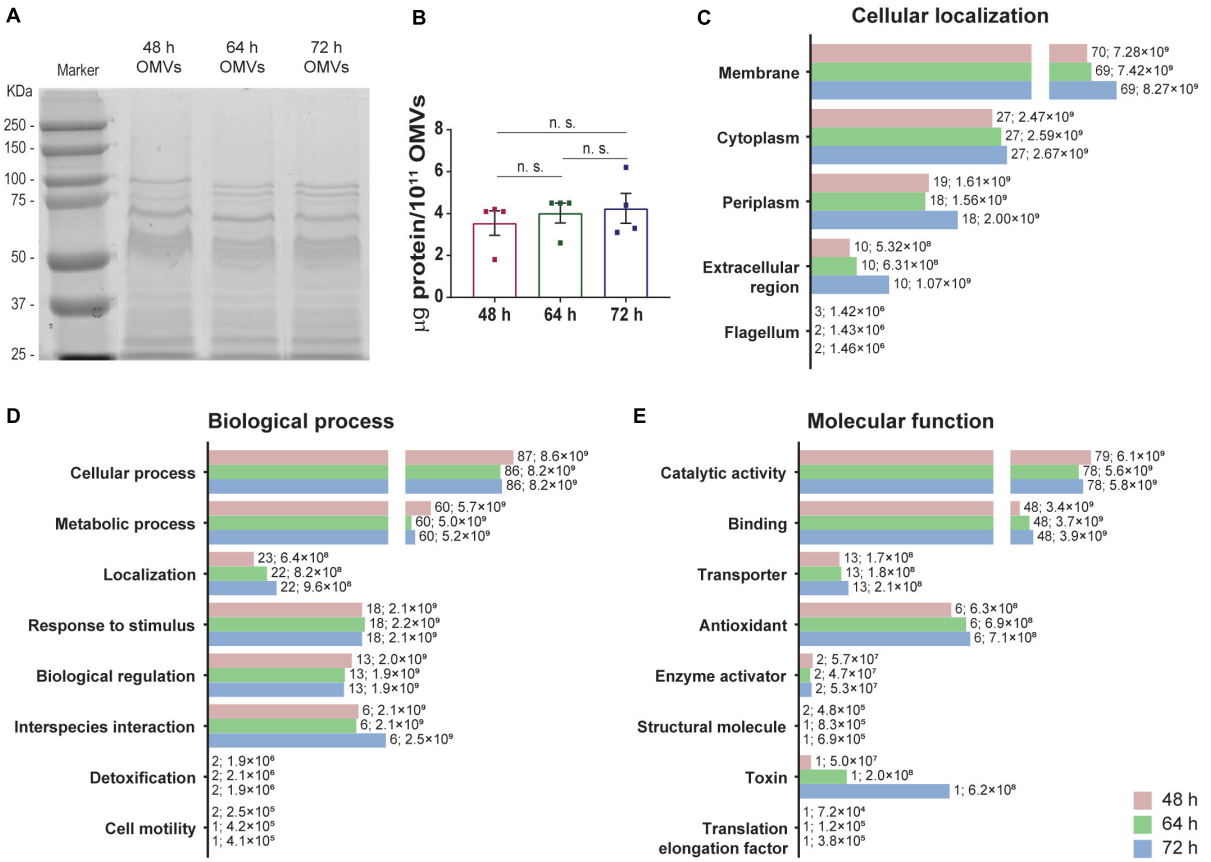

FIGURE 4 | Protein profile and proteomic analysis of OMVs secreted by *Helicobacter pylori* grown in F12-cholesterol medium. **(A)** Protein profile of 10^{11} OMVs isolated from 48, 64, and 72 h-*H. pylori* 26695 bacterial cultures, after staining a SDS-PAGE with BlueSafe, and corresponding **(B)** protein quantification. Data are shown as mean ± SEM of four biological replicates and statistical significance was evaluated using the one-way ANOVA with *post hoc* Tukey's test; n.s. – not significant. Proteomic analysis of 48, 64, and 72 h-OMVs isolated from *H. pylori* 26695 F12-cholesterol liquid cultures by nanoLC-MS/MS and prediction of the **(C)** cellular localization, **(D)** biological process, and **(E)** molecular function of the identified proteins using the gene ontology UniProt database. Data are shown as the abundance of proteins in each group; for each bar, the number of proteins and respective abundance is indicated.

Pyruvate ferredoxin oxidoreductase was identified only in 48 and 72 h samples, whereas flagellar P-ring protein was detected exclusively in 48 h-OMVs.

In terms of cellular localization (**Figure 4C**), the most diverse and abundant group of proteins identified in OMVs from all time points analyzed was predicted to be associated with the bacterial membrane, and within this group outer membrane proteins (OMPs) were the most frequent (48 h: $n = 50$, abundance = $5.67 \pm 0.41 \times 10^9$; 64 h: $n = 49$, abundance = $5.73 \pm 1.25 \times 10^9$; 72 h: $n = 49$, abundance = $6.52 \pm 0.74 \times 10^9$). Periplasmic, cytoplasmic and extracellular region-associated proteins were also detected. In addition, 3 flagellar proteins were identified in 48 h samples, while only 2 were detected in 64 and 72 h-OMVs. Considering that OMVs originate from the blebbing of the OM, a high abundance of membrane-associated proteins was expected, and is in agreement with previous proteomic data from *H. pylori* 26695 OMVs (Zavan et al., 2019).

Concerning the biological process analysis, proteins were distributed into eight groups (**Figure 4D**). Proteins involved in cellular processes constituted the most numerous and abundant group, followed by proteins involved in metabolic processes, localization proteins, response to stimulus, biological regulation, and interspecies interaction proteins. Detoxification and cell motility proteins were the less abundant.

Regarding the molecular functions (**Figure 4E**), the majority of the classified proteins was predicted to have catalytic, binding and/or transporter activities, followed by proteins with antioxidant and structural molecular activities, enzyme activators, a toxin, and a translation elongation factor. Besides the above-mentioned molecular functions, several of the identified proteins are also involved in processes related with *H. pylori* colonization, survival, and pathogenesis. In particular, urease α/β neutralizes the acidic environment of the gastric mucosa (Marshall et al., 1990), which together with outer membrane proteins (BabA and OipA), contributes to *H. pylori* colonization (Ishijima et al., 2011; Teymournejad et al., 2017); β-lactamase (HcpA, HcpC, HcpD, and HcpE) provides resistance to amoxicillin (Tseng et al., 2009); HtrA disrupts the epithelial cell-cell junctions, enabling transmigration of *H. pylori* across

the gastric epithelium (Tegtmeyer et al., 2017); VacA and GGT induce, vacuolization and apoptosis (Ricci et al., 1997; Shibayama et al., 2003); HP-NAP, OipA, and urease β act as immune modulators by inducing pro-inflammatory responses (Yamaoka et al., 2002; de Bernard and D'Elios, 2010; Schoep et al., 2010); catalase, superoxide dismutase and thioredoxin protect *H. pylori* from the oxidative stress (Pesci and Pickett, 1994; Odenbreit et al., 1996; Kuhns et al., 2015); HP-NAP and bacterial non-heme ferritin are iron storage proteins, a key element for bacterial survival (Ge and Sun, 2012). The presence of these virulence factors in *H. pylori* OMVs isolated from F12-cholesterol and from other complex liquid cultures (Mullaney et al., 2009; Olofsson et al., 2010; Zavan et al., 2019) denotes that some proteins may be preferably loaded onto OMVs, independently of the culture media or bacterial strain, and highlights the importance of OMVs for the success of *H. pylori* infection. Seventy of the 233 identified proteins were uncharacterized and approximately half of them did not have a predicted cellular localization or molecular function.

Although OMVs isolated from 48, 64, and 72 h-bacterial cultures had a similar protein diversity, some of the proteins were differentially expressed (**Supplementary Table 3** for the comparison between 48 and 64 h; **Supplementary Table 4** for the comparison between 48 and 72 h; **Supplementary Table 5** for the comparison between 64 and 72 h). In particular, the virulence factor VacA was found to be significantly more abundant in 64 and 72 h-OMVs, differently from the data of Zavan et al. (2019) that shows an enrichment of this protein in 16 h-OMVs in comparison to vesicles isolated from 48 h and 72 h bacterial cultures. Additionally, the thioredoxin reductase, which protects *H. pylori* from the oxidative stress (Kuhns et al., 2015), and 2 proteins involved in iron acquisition and transport across the membrane, which is an essential micronutrient for bacterial survival, FrpB (Gonzalez-Lopez and Olivares-Trejo, 2009) and FecA, presented a significantly higher expression in 64 and 72 h-OMVs, in comparison to 48 h samples.

Overall, our proteomic analysis confirms the reliability of the protocol, by showing that the cargo of OMVs contain proteins from the membrane, periplasmic, and cytoplasmic bacterial compartments, and supports the selective sorting of protein cargo into OMVs, as only a fraction of the total bacterial proteins is represented in the cargo of OMVs.

DISCUSSION

Outer membrane vesicles have emerged as an important delivery system of bacterial components with an impact on bacteria-bacteria and bacteria-host interactions. In addition, OMVs are increasingly used for diverse therapeutic applications, namely vaccine development, taking advantage of their flexibility to genetic manipulation and nanosized structure for dissemination throughout the body, besides their easy production at large-scale and reduced costs (Bitto and Kaparakis-Liaskos, 2017).

The prevailing methods for the isolation of *H. pylori* OMVs are time-consuming and diverse, hampering the standardization of a suitable protocol for OMVs isolation, which is essential for downstream research and biomedical applications, namely the assessment of the functional roles of OMVs *in vitro* and *in vivo*, and large-scale production. The current published protocols have various disadvantages. First, they rely on the use of complex undefined media that contain yeast and animal tissue extracts, thus affecting the purity, content, and variability of OMVs between samples (Olofsson et al., 2010; Tsolakos et al., 2010). Second, they have a lengthy duration due to the multiple centrifugation steps, which might compromise the final yield of OMVs (Chutkan et al., 2013). Finally, the high variability of procedures and diversity of protocols weakens the comparison between studies, as the recovered fractions of OMVs can be different.

To overcome these drawbacks, we developed an isolation method of *H. pylori* OMVs trimming non-essential steps after selecting F12 supplemented with cholesterol, a chemically defined medium, as the bacterial culture medium for *H. pylori* growth. The final layout of this method included one low-speed centrifugation followed by supernatant 0.45 μm-filtration to remove bacteria and debris from the culture medium and to collect all range of OMVs sizes, and finally two ultracentrifugations for the recovery and washing of the OMVs.

Our results showed that the F12-cholesterol medium was effective in sustaining bacterial growth, while achieving higher viability than the complex BB-FBS medium. Like previously described for other bacterial culture media (Kusters et al., 1997; Adams et al., 2003; Olofsson et al., 2010), we observed a morphological change of *H. pylori* from the bacillary to the coccoid forms throughout bacterial growth. The significant decrease in the number of CFUs at 72 h was not mirrored by the loss of bacterial viability using the LIVE/DEAD assay, likely due to the fact that coccoid forms are viable but non-culturable bacteria, with minimal metabolic activity, and preserved membrane and genetic material integrities (Adams et al., 2003; Ierardi et al., 2020).

Associated with the bacterial growth was the increased number of secreted OMVs, in accordance with descriptions of OMVs isolated from complex liquid cultures (Olofsson et al., 2010; Zavan et al., 2019). Over 99% of OMVs measured between 20 and 200 nm, with mode of nearly 80 nm, which is distinct from the enrichment in 100 to 200 nm sized OMVs isolated from *H. pylori* grown in BHI supplemented with 0.2% β-cyclodextrin (Zavan et al., 2019). This difference might be related with the distinct medium used, as well as with the effect of β-cyclodextrin, which chelates cholesterol that is essential for *H. pylori* growth (Hutton et al., 2010; Jimenez-Soto et al., 2012), highlighting how bacterial growth conditions impact on the properties of OMVs. Our findings also demonstrated the reproducibility of this protocol, as OMVs isolated from different *H. pylori* strains presented a similar size heterogeneity and were equally pure.

OMVs isolated from F12-cholesterol medium using our shorter protocol were highly pure, free from protein aggregates, flagella, and other bacterial contaminants, while requiring significantly less hands-on/hands-off time. Of relevance was also the high yield of OMVs, with around 10^{10} OMVs per mL of bacterial culture. Moreover, the proteomic analysis of our OMVs confirmed that their cargo

contained proteins from several bacterial compartments (e.g., membrane, periplasm, and cytoplasm) and with diverse biological functions, in particular known bacterial virulence factors, already described for different *H. pylori* strains (Jarzab et al., 2020), reinforcing their reliability. Besides the common proteins identified between our and other OMVs' proteomes (Mullaney et al., 2009; Olofsson et al., 2010; Zavan et al., 2019), there were also unique proteins ascribed to each one. Such differences in OMVs protein cargo might be related to the underlying growth conditions (bacterial strain, culture media, and initial bacterial density), which influence bacterial growth and the vesiculation process, in addition to technical issues (isolation method and proteomic analysis).

Considering the therapeutic potential of bacterial OMVs, it is of uttermost importance that the harvest of OMVs occurs from a chemically defined bacterial culture without animal-derived components that hinder the purification process and ultimately interfere with the host immune response (van der Pol et al., 2015). Our method overcomes this issue and, by having increased time-efficiency in comparison to previous protocols, is a suitable approach for application in the biomedical field. Still, the yield and purity of *H. pylori* OMVs on a large-scale implementation of the protocol, and its application for the isolation of OMVs from other bacteria species, needs further evaluation. Currently, OMVs have been licensed for human use as adjuvant (Nokleby et al., 2007) or vaccine against the serogroup B *Neisseria meningitides*, namely the Bexsero® (Novartis) and VA-MENGOC-BC® (Finlay Institute, Cuba) vaccines (Petousis-Harris, 2018), and other OMVs-based vaccines against infectious diseases are already in preclinical studies (Zhang et al., 2019). In the case of *H. pylori*, the development of an effective prophylactic or therapeutic vaccine, predominantly composed of purified or recombinant components of *H. pylori* antigens with an adjuvant, has proven challenging and not yet a reality (Sutton and Boag, 2019). Promising data showed that intragastric immunization with OMVs from *H. pylori* 7.13, resulted in the development of a specific systemic immune response in mice, and in the significant reduction of bacterial load after challenging with *H. pylori* SS1 (Liu et al., 2019; Song et al., 2020).

In conclusion, we described an abridged protocol for isolation of OMVs resorting to a synthetic chemically defined liquid medium for bacterial growth ensuing a high yield of pure and *bona fide H. pylori* OMVs, in a time- and cost-efficient manner, suitable for research, biomedical, and biopharmaceutical downstream applications.

DATA AVAILABILITY STATEMENT

The mass spectrometry proteomic data presented in the study is deposited in the ProteomeXchange Consortium via the PRIDE partner repository with the dataset identifier PXD025393 and doi: 10.6019/PXD025393.

AUTHOR CONTRIBUTIONS

JM and ML conceptualized the study. JM, VP, TF, AM, and HO acquired the data. JM, VP, TF, AM, HO, CF, and ML performed the data analysis and interpretation. JM drafted the manuscript. All authors revised the manuscript for important intellectual content. CF acquired the funding.

FUNDING

This article is a result of the project NORTE-01-0145-FEDER-000029, supported by Norte Portugal Regional Program (NORTE 2020), under the PORTUGAL 2020 Partnership Agreement, through the European Regional Development Fund (ERDF). The i3S HEMS Scientific Platform is member of the national infrastructure PPBI – Portuguese Platform of Bioimaging (PPBI-POCI-01-0145-FEDER-022122). The i3S Proteomics Scientific Platform is funded by the Portuguese Mass Spectrometry Network, integrated in the National Roadmap of Research Infrastructures of Strategic Relevance (ROTEIRO/0028/2013; LISBOA-01-0145-FEDER-022125). JM and ML had fellowships from FCT – Fundação para a Ciência e a Tecnologia (SFRH/BD/116965/2016 and SFRH/BDP/110065/2015). ML has a FCT RJEC Id 3762 contract.

ACKNOWLEDGMENTS

The authors acknowledge the help of Bruno Cavadas for assistance in proteomic analysis, Cecília Durães for NTA acquisition, Rui Fernandes and Francisco Figueiredo for the contribution on the ultrastructural analysis of OMVs, Daniela Silva (CEMUP – Centro de Materiais da Universidade do Porto) for SEM acquisition, and Steeve Lima and Paulo Oliveira for sharing their optimized protocol of OMVs protein quantification and for the helpful discussions. The authors also thank the i3S HEMS and Proteomics Scientific Platforms.

SUPPLEMENTARY MATERIAL

The Supplementary Material for this article can be found online at: https://www.frontiersin.org/articles/10.3389/fmicb.2021.654193/full#supplementary-material

REFERENCES

Adams, B. L., Bates, T. C., and Oliver, J. D. (2003). Survival of *Helicobacter pylori* in a natural freshwater environment. *Appl. Environ. Microbiol.* 69, 7462–7466. doi: 10.1128/aem.69.12.7462-7466.2003

Atherton, J. C. (2006). The pathogenesis of *Helicobacter pylori*-induced gastro-duodenal diseases. *Annu. Rev. Pathol.* 1, 63–96. doi: 10.1146/annurev.pathol.1.110304.100125

Azevedo, N. F., Almeida, C., Cerqueira, L., Dias, S., Keevil, C. W., and Vieira, M. J. (2007). Coccoid form of *Helicobacter pylori* as a morphological manifestation

of cell adaptation to the environment. *Appl. Environ. Microbiol.* 73, 3423–3427. doi: 10.1128/AEM.00047-07

Bitto, N. J., and Kaparakis-Liaskos, M. (2017). The therapeutic benefit of bacterial membrane vesicles. *Int. J. Mol. Sci.* 18:1287. doi: 10.3390/ijms18061287

Blaser, M. J., and Atherton, J. C. (2004). *Helicobacter pylori* persistence: biology and disease. *J. Clin. Invest.* 113, 321–333. doi: 10.1172/JCI20925

Chatterjee, S. N., and Das, J. (1967). Electron microscopic observations on the excretion of cell-wall material by *Vibrio cholerae*. *J. Gen. Microbiol.* 49, 1–11. doi: 10.1099/00221287-49-1-1

Chitcholtan, K., Hampton, M. B., and Keenan, J. I. (2008). Outer membrane vesicles enhance the carcinogenic potential of *Helicobacter pylori*. *Carcinogenesis* 29, 2400–2405. doi: 10.1093/carcin/bgn218

Chutkan, H., Macdonald, I., Manning, A., and Kuehn, M. J. (2013). Quantitative and qualitative preparations of bacterial outer membrane vesicles. *Methods Mol. Biol.* 966, 259–272. doi: 10.1007/978-1-62703-245-2_16

Cover, T. L., and Blaser, M. J. (2009). *Helicobacter pylori* in health and disease. *Gastroenterology* 136, 1863–1873. doi: 10.1053/j.gastro.2009.01.073

de Bernard, M., and D'Elios, M. M. (2010). The immune modulating activity of the *Helicobacter pylori* HP-NAP: friend or foe? *Toxicon* 56, 1186–1192. doi: 10.1016/j.toxicon.2009.09.020

Deatherage, B. L., and Cookson, B. T. (2012). Membrane vesicle release in bacteria, eukaryotes, and archaea: a conserved yet underappreciated aspect of microbial life. *Infect Immun.* 80, 1948–1957. doi: 10.1128/IAI.06014-11

Devoe, I. W., and Gilchrist, J. E. (1973). Release of endotoxin in the form of cell wall blebs during in vitro growth of *Neisseria meningitidis*. *J. Exp. Med.* 138, 1156–1167. doi: 10.1084/jem.138.5.1156

Fiocca, R., Necchi, V., Sommi, P., Ricci, V., Telford, J., Cover, T. L., et al. (1999). Release of *Helicobacter pylori* vacuolating cytotoxin by both a specific secretion pathway and budding of outer membrane vesicles. Uptake of released toxin and vesicles by gastric epithelium. *J. Pathol.* 188, 220–226.

Ge, R., and Sun, X. (2012). Iron trafficking system in *Helicobacter pylori*. *Biometals* 25, 247–258. doi: 10.1007/s10534-011-9512-8

Gonzalez-Lopez, M. A., and Olivares-Trejo, J. J. (2009). The gene frpB2 of *Helicobacter pylori* encodes an hemoglobin-binding protein involved in iron acquisition. *Biometals* 22, 889–894. doi: 10.1007/s10534-009-9240-5

Heczko, U., Smith, V. C., Mark Meloche, R., Buchan, A. M., and Finlay, B. B. (2000). Characteristics of *Helicobacter pylori* attachment to human primary antral epithelial cells. *Microb. Infect* 2, 1669–1676. doi: 10.1016/s1286-4579(00)01322-8

Hoekstra, D., van der Laan, J. W., de Leij, L., and Witholt, B. (1976). Release of outer membrane fragments from normally growing *Escherichia coli*. *Biochim. Biophys. Acta* 455, 889–899. doi: 10.1016/0005-2736(76)90058-4

Hooi, J. K. Y., Lai, W. Y., Ng, W. K., Suen, M. M. Y., Underwood, F. E., Tanyingoh, D., et al. (2017). Global prevalence of *Helicobacter pylori* infection: systematic review and meta-analysis. *Gastroenterology* 153, 420–429. doi: 10.1053/j.gastro.2017.04.022

Hughes, C. S., Moggridge, S., Muller, T., Sorensen, P. H., Morin, G. B., and Krijgsveld, J. (2019). Single-pot, solid-phase-enhanced sample preparation for proteomics experiments. *Nat. Protoc.* 14, 68–85. doi: 10.1038/s41596-018-0082-x

Hutton, M. L., Kaparakis-Liaskos, M., Turner, L., Cardona, A., Kwok, T., and Ferrero, R. L. (2010). *Helicobacter pylori* exploits cholesterol-rich microdomains for induction of NF-kappaB-dependent responses and peptidoglycan delivery in epithelial cells. *Infect Immun.* 78, 4523–4531. doi: 10.1128/IAI.00439-10

Ierardi, E., Losurdo, G., Mileti, A., Paolillo, R., Giorgio, F., Principi, M., et al. (2020). The puzzle of coccoid forms of *Helicobacter pylori*: beyond basic science. *Antibiotics* 9:293. doi: 10.3390/antibiotics9060293

Ishijima, N., Suzuki, M., Ashida, H., Ichikawa, Y., Kanegae, Y., Saito, I., et al. (2011). BabA-mediated adherence is a potentiator of the *Helicobacter pylori* type IV secretion system activity. *J. Biol. Chem.* 286, 25256–25264. doi: 10.1074/jbc.M111.233601

Ismail, S., Hampton, M. B., and Keenan, J. I. (2003). *Helicobacter pylori* outer membrane vesicles modulate proliferation and interleukin-8 production by gastric epithelial cells. *Infect Immun.* 71, 5670–5675. doi: 10.1128/iai.71.10.5670-5675.2003

Jarzab, M., Posselt, G., Meisner-Kober, N., and Wessler, S. (2020). *Helicobacter pylori*-derived outer membrane vesicles (OMVs): role in bacterial pathogenesis? *Microorganisms* 8:1328. doi: 10.3390/microorganisms8091328

Jimenez-Soto, L. F., Rohrer, S., Jain, U., Ertl, C., Sewald, X., and Haas, R. (2012). Effects of cholesterol on *Helicobacter pylori* growth and virulence properties in vitro. *Helicobacter* 17, 133–139. doi: 10.1111/j.1523-5378.2011.00926.x

Kaparakis, M., Turnbull, L., Carneiro, L., Firth, S., Coleman, H. A., Parkington, H. C., et al. (2010). Bacterial membrane vesicles deliver peptidoglycan to NOD1 in epithelial cells. *Cell Microbiol.* 12, 372–385. doi: 10.1111/j.1462-5822.2009.01404.x

Katsui, N., Tsuchido, T., Hiramatsu, R., Fujikawa, S., Takano, M., and Shibasaki, I. (1982). Heat-induced blebbing and vesiculation of the outer membrane of *Escherichia coli*. *J. Bacteriol.* 151, 1523–1531. doi: 10.1128/JB.151.3.1523-1531.1982

Keenan, J., Day, T., Neal, S., Cook, B., Perez-Perez, G., Allardyce, R., et al. (2000). A role for the bacterial outer membrane in the pathogenesis of *Helicobacter pylori* infection. *FEMS Microbiol. Lett.* 182, 259–264. doi: 10.1111/j.1574-6968.2000.tb08905.x

Kim, G. H., Choi, C. W., Park, E. C., Lee, S. Y., and Kim, S. I. (2014). Isolation and proteomic characterization of bacterial extracellular membrane vesicles. *Curr. Protein Pept. Sci.* 15, 719–731. doi: 10.2174/1573403x10666140505163121

Klimentova, J., and Stulik, J. (2015). Methods of isolation and purification of outer membrane vesicles from gram-negative bacteria. *Microbiol. Res.* 170, 1–9. doi: 10.1016/j.micres.2014.09.006

Kuhns, L. G., Wang, G., and Maier, R. J. (2015). Comparative roles of the two *Helicobacter pylori* thioredoxins in preventing macromolecule damage. *Infect Immun.* 83, 2935–2943. doi: 10.1128/IAI.00232-15

Kulp, A., and Kuehn, M. J. (2010). Biological functions and biogenesis of secreted bacterial outer membrane vesicles. *Annu. Rev. Microbiol.* 64, 163–184. doi: 10.1146/annurev.micro.091208.073413

Kusters, J. G., Gerrits, M. M., Van Strijp, J. A., and Vandenbroucke-Grauls, C. M. (1997). Coccoid forms of *Helicobacter pylori* are the morphologic manifestation of cell death. *Infect Immun.* 65, 3672–3679. doi: 10.1128/IAI.65.9.3672-3679.1997

Liu, Q., Li, X., Zhang, Y., Song, Z., Li, R., Ruan, H., et al. (2019). Orally-administered outer-membrane vesicles from *Helicobacter pylori* reduce *H. pylori* infection via Th2-biased immune responses in mice. *Pathog. Dis.* 77:ftz050. doi: 10.1093/femspd/ftz050

Marshall, B. J., Barrett, L. J., Prakash, C., McCallum, R. W., and Guerrant, R. L. (1990). Urea protects *Helicobacter* (Campylobacter) pylori from the bactericidal effect of acid. *Gastroenterology* 99, 697–702. doi: 10.1016/0016-5085(90)90957-3

Mullaney, E., Brown, P. A., Smith, S. M., Botting, C. H., Yamaoka, Y. Y., Terres, A. M., et al. (2009). Proteomic and functional characterization of the outer membrane vesicles from the gastric pathogen *Helicobacter pylori*. *Proteom. Clin. Appl.* 3, 785–796. doi: 10.1002/prca.200800192

Mytilinaios, I., Salih, M., Schofield, H. K., and Lambert, R. J. (2012). Growth curve prediction from optical density data. *Int. J. Food Microbiol.* 154, 169–176. doi: 10.1016/j.ijfoodmicro.2011.12.035

Nokleby, H., Aavitsland, P., O'Hallahan, J., Feiring, B., Tilman, S., and Oster, P. (2007). Safety review: two outer membrane vesicle (OMV) vaccines against systemic *Neisseria meningitidis* serogroup B disease. *Vaccine* 25, 3080–3084. doi: 10.1016/j.vaccine.2007.01.022

Odenbreit, S., Wieland, B., and Haas, R. (1996). Cloning and genetic characterization of *Helicobacter pylori* catalase and construction of a catalase-deficient mutant strain. *J. Bacteriol.* 178, 6960–6967. doi: 10.1128/jb.178.23.6960-6967.1996

Olofsson, A., Vallstrom, A., Petzold, K., Tegtmeyer, N., Schleucher, J., Carlsson, S., et al. (2010). Biochemical and functional characterization of *Helicobacter pylori* vesicles. *Mol. Microbiol.* 77, 1539–1555. doi: 10.1111/j.1365-2958.2010.07307.x

Parker, H., Chitcholtan, K., Hampton, M. B., and Keenan, J. I. (2010). Uptake of *Helicobacter pylori* outer membrane vesicles by gastric epithelial cells. *Infect Immun.* 78, 5054–5061. doi: 10.1128/IAI.00299-10

Perez-Riverol, Y., Csordas, A., Bai, J., Bernal-Llinares, M., Hewapathirana, S., Kundu, D. J., et al. (2019). The PRIDE database and related tools and resources in 2019: improving support for quantification data. *Nucleic Acids Res.* 47, D442–D450. doi: 10.1093/nar/gky1106

Pesci, E. C., and Pickett, C. L. (1994). Genetic organization and enzymatic activity of a superoxide dismutase from the microaerophilic human pathogen, *Helicobacter pylori*. *Gene* 143, 111–116. doi: 10.1016/0378-1119(94)90614-9

Petousis-Harris, H. (2018). Impact of meningococcal group B OMV vaccines, beyond their brief. *Hum. Vaccin. Immunother.* 14, 1058–1063. doi: 10.1080/21645515.2017.1381810

Ricci, V., Sommi, P., Fiocca, R., Romano, M., Solcia, E., and Ventura, U. (1997). *Helicobacter pylori* vacuolating toxin accumulates within the endosomal-vacuolar compartment of cultured gastric cells and potentiates the vacuolating activity of ammonia. *J. Pathol.* 183, 453–459. doi: 10.1002/(SICI)1096-9896(199712)183:4<453:AID-PATH950<3.0.CO;2-2

Schoep, T. D., Fulurija, A., Good, F., Lu, W., Himbeck, R. P., Schwan, C., et al. (2010). Surface properties of *Helicobacter pylori* urease complex are essential for persistence. *PLoS One* 5:e15042. doi: 10.1371/journal.pone.0015042

Shibayama, K., Kamachi, K., Nagata, N., Yagi, T., Nada, T., Doi, Y., et al. (2003). A novel apoptosis-inducing protein from *Helicobacter pylori*. *Mol. Microbiol.* 47, 443–451. doi: 10.1046/j.1365-2958.2003.03305.x

Song, Z., Li, B., Zhang, Y., Li, R., Ruan, H., Wu, J., et al. (2020). Outer membrane vesicles of *Helicobacter pylori* 7.13 as adjuvants promote protective efficacy against *Helicobacter pylori* infection. *Front. Microbiol.* 11:1340. doi: 10.3389/fmicb.2020.01340

Sutton, P., and Boag, J. M. (2019). Status of vaccine research and development for *Helicobacter pylori*. *Vaccine* 37, 7295–7299. doi: 10.1016/j.vaccine.2018.01.001

Tegtmeyer, N., Wessler, S., Necchi, V., Rohde, M., Harrer, A., Rau, T. T., et al. (2017). *Helicobacter pylori* employs a unique basolateral Type IV secretion mechanism for CagA delivery. *Cell Host Microb.* 22, 552–560.e555. doi: 10.1016/j.chom.2017.09.005

Testerman, T. L., Conn, P. B., Mobley, H. L., and McGee, D. J. (2006). Nutritional requirements and antibiotic resistance patterns of *Helicobacter* species in chemically defined media. *J. Clin. Microbiol.* 44, 1650–1658. doi: 10.1128/JCM.44.5.1650-1658.2006

Testerman, T. L., McGee, D. J., and Mobley, H. L. (2001). *Helicobacter pylori* growth and urease detection in the chemically defined medium Ham's F-12 nutrient mixture. *J. Clin. Microbiol.* 39, 3842–3850. doi: 10.1128/JCM.39.11.3842-3850.2001

Teymournejad, O., Mobarez, A. M., Hassan, Z. M., and Talebi Bezmin Abadi, A. (2017). Binding of the *Helicobacter pylori* OipA causes apoptosis of host cells via modulation of Bax/Bcl-2 levels. *Sci. Rep.* 7:8036. doi: 10.1038/s41598-017-08176-7

Thompson, S. S., Naidu, Y. M., and Pestka, J. J. (1985). Ultrastructural localization of an extracellular protease in *Pseudomonas* fragi by using the peroxidase-antiperoxidase reaction. *Appl. Environ. Microbiol.* 50, 1038–1042. doi: 10.1128/AEM.50.4.1038-1042.1985

Tseng, Y. S., Wu, D. C., Chang, C. Y., Kuo, C. H., Yang, Y. C., Jan, C. M., et al. (2009). Amoxicillin resistance with beta-lactamase production in *Helicobacter pylori*. *Eur. J. Clin. Invest.* 39, 807–812. doi: 10.1111/j.1365-2362.2009.02166.x

Tsolakos, N., Lie, K., Bolstad, K., Maslen, S., Kristiansen, P. A., Hoiby, E. A., et al. (2010). Characterization of meningococcal serogroup B outer membrane vesicle vaccines from strain 44/76 after growth in different media. *Vaccine* 28, 3211–3218. doi: 10.1016/j.vaccine.2010.02.023

Turner, L., Bitto, N. J., Steer, D. L., Lo, C., D'Costa, K., Ramm, G., et al. (2018). *Helicobacter pylori* outer membrane vesicle size determines their mechanisms of host cell entry and protein content. *Front. Immunol.* 9:1466. doi: 10.3389/fimmu.2018.01466

van der Pol, L., Stork, M., and van der Ley, P. (2015). Outer membrane vesicles as platform vaccine technology. *Biotechnol. J.* 10, 1689–1706. doi: 10.1002/biot.201400395

Willen, R., Carlen, B., Wang, X., Papadogiannakis, N., Odselius, R., and Wadstrom, T. (2000). Morphologic conversion of *Helicobacter pylori* from spiral to coccoid form. Scanning (SEM) and transmission electron microscopy (TEM) suggest viability. *Ups. J. Med. Sci.* 105, 31–40. doi: 10.1517/03009734000000045

Yamaoka, Y., Kikuchi, S., El-Zimaity, H. M., Gutierrez, O., Osato, M. S., and Graham, D. Y. (2002). Importance of *Helicobacter pylori* oipA in clinical presentation, gastric inflammation, and mucosal interleukin 8 production. *Gastroenterology* 123, 414–424. doi: 10.1053/gast.2002.34781

Zavan, L., Bitto, N. J., Johnston, E. L., Greening, D. W., and Kaparakis-Liaskos, M. (2019). *Helicobacter pylori* growth stage determines the size, protein composition, and preferential cargo packaging of outer membrane vesicles. *Proteomics* 19:e1800209. doi: 10.1002/pmic.201800209

Zhang, Y., Fang, Z., Li, R., Huang, X., and Liu, Q. (2019). Design of outer membrane vesicles as cancer vaccines: a new toolkit for cancer therapy. *Cancers* 11:1314. doi: 10.3390/cancers11091314

Conflict of Interest: The authors declare that the research was conducted in the absence of any commercial or financial relationships that could be construed as a potential conflict of interest.

SUPPLEMENTARY TABLES

Supplementary Table 1. Classification of proteins with high FDR according to their predicted cellular localization, biological process and molecular function, using the GO (GO) UniProt database resource and manual curation

Accession number	Protein names	GO-cellular component; *Manual curation	GO-biological process	GO-molecular function	Abundance 48h	Abundance SD 48h	Abundance 64h	Abundance SD 64h	Abundance 72h	Abundance SD 72h
P0A0R3	Heat shock protein 10	cytoplasm	chaperone cofactor-dependent protein refolding	ATP binding; chaperone binding; identical protein binding; metal ion binding; unfolded protein binding	6,15E+05	1,56E+05	1,49E+06	6,55E+05	1,25E+06	4,30E+05
O24930	2',3'-cyclic-nucleotide 2'-phosphodiesterase (CpdB)	outer membrane-bounded periplasmic space	nucleotide catabolic process	hydrolase activity, acting on ester bonds; metal ion binding; nucleotide binding	6,13E+07	7,95E+05	5,69E+07	1,35E+07	5,80E+07	1,44E+06
P56027	30S ribosomal protein S20	cytosol; small ribosomal subunit	translation	small ribosomal subunit rRNA binding; structural constituent of ribosome	4,78E+05	1,28E+05	8,31E+05	3,49E+05	6,85E+05	2,35E+05
Q48255	3-dehydroquinate dehydratase		aromatic amino acid family biosynthetic process; cellular amino acid biosynthetic process; chorismate biosynthetic process	3-dehydroquinate dehydratase activity	1,52E+06	1,57E+05	2,90E+06	1,73E+05	2,23E+06	1,02E+06
O25698	3-methyl-2-oxobutanoate hydroxymethyltransferase	cytoplasm	pantothenate biosynthetic process	3-methyl-2-oxobutanoate hydroxymethyltransferase activity; magnesium ion binding	9,61E+05	1,33E+05	1,55E+06	8,61E+05	1,30E+06	7,02E+05
O25657	4-hydroxy-tetrahydrodipicolinate synthase	cytoplasm	diaminopimelate biosynthetic process; lysine biosynthetic process via diaminopimelate	4-hydroxy-tetrahydrodipicolinate synthase activity	2,15E+05	0,00E+00	5,11E+05	0,00E+00	4,74E+05	1,16E+05
P42383	Heat shock protein 60	GroEL-GroES complex	chaperone cofactor-dependent protein refolding; protein folding; protein refolding; response to heat	ATP binding; unfolded protein binding	3,26E+08	7,61E+07	5,36E+08	3,41E+08	4,79E+08	1,69E+08
O25399	Thiolase		fatty acid beta-oxidation	acetyl-CoA C-acetyltransferase activity; acetyl-CoA C-acyltransferase activity	1,24E+06	1,56E+05	1,79E+06	7,96E+04	1,44E+06	4,42E+05
P56418	Aconitate hydratase B	cytosol	propionate catabolic process, 2-methylcitrate cycle; tricarboxylic acid cycle	2-methylisocitrate dehydratase activity; 4 iron, 4 sulfur cluster binding; aconitate hydratase activity; citrate dehydratase activity; metal ion binding; mRNA 3'-UTR binding; mRNA binding	9,31E+05	2,87E+04	1,07E+06	2,64E+05	1,74E+06	4,99E+05
O25075	Alginate lyase domain-containing protein	periplasmic space		lyase activity	1,02E+07	2,97E+05	1,24E+07	1,77E+06	1,34E+07	1,64E+06
O25067	Aliphatic amidase		nitrogen compound metabolic process	amidase activity; hydrolase activity, acting on carbon-nitrogen (but not peptide) bonds, in linear amides; indoleacetamide hydrolase activity	5,07E+06	3,89E+05	7,06E+06	2,06E+05	4,33E+06	1,81E+06
P21762	Alkyl hydroperoxide reductase C	cytosol	cell redox homeostasis	alkylhydroperoxide reductase activity; thioredoxin peroxidase activity	2,48E+06	4,32E+06	6,01E+06	3,71E+06	1,10E+07	1,85E+06
O25594	Amino acid ABC transporter, periplasmic binding protein (YckK)				1,29E+07	6,41E+05	1,13E+07	4,32E+05	1,21E+07	5,19E+05
P56149	Aspartase	cytosol	aspartate metabolic process; tricarboxylic acid cycle	aspartate ammonia-lyase activity	1,68E+06	1,20E+06	8,22E+06	3,98E+06	8,17E+06	2,66E+06
O25052	ATP-dependent nuclease (AddB)				9,47E+07	4,44E+06	6,38E+07	1,42E+07	5,95E+07	3,74E+06
O25253	ATP-dependent protease subunit HslV	HslUV protease complex; proteasome core complex	proteolysis involved in cellular protein catabolic process	metal ion binding; threonine-type endopeptidase activity	8,50E+05	1,40E+05	1,47E+06	8,33E+05	1,63E+06	5,79E+05

P52093	Bacterial non-heme ferritin	cytoplasm; cytosol	intracellular sequestering of iron ion; iron ion transport	ferric iron binding; ferrous iron binding; ferroxidase activity; iron ion binding	3,24E+08	4,67E+07	4,75E+08	3,24E+08	5,82E+08	9,51E+07
O25345	Beta-lactamase	extracellular region	response to antibiotic	beta-lactamase activity	3,20E+07	4,73E+04	2,53E+07	3,90E+05	2,64E+07	2,12E+04
O25256	Beta-lactamase		response to antibiotic	beta-lactamase activity	1,64E+06	1,44E+05	1,49E+06	1,31E+05	1,95E+06	1,34E+05
O25742	Beta-lactamase		response to antibiotic	beta-lactamase activity; enzyme activator activity	1,53E+06	1,42E+06	1,24E+06	8,05E+06	6,36E+05	3,48E+06
O25001	Beta-lactamase HcpA	extracellular region	response to antibiotic	beta-lactamase activity; enzyme activator activity [GO:0008047]	5,58E+07	3,35E+06	4,60E+07	4,32E+06	5,21E+07	1,20E+06
O25135	Biotin carboxyl carrier protein of acetyl-CoA carboxylase	acetyl-CoA carboxylase complex	fatty acid biosynthetic process	acetyl-CoA carboxylase activity	3,61E+04	9,43E+04	5,06E+04	2,26E+04	1,06E+05	5,62E+04
O25163	Biotin sulfoxide reductase (BisC)	outer membrane-bounded periplasmic space	anaerobic respiration	4 iron, 4 sulfur cluster binding; electron transfer activity; molybdenum ion binding; molybdopterin cofactor binding	4,35E+06	3,16E+05	6,34E+06	2,77E+06	7,20E+06	3,13E+06
O25257	Cag pathogenicity island protein 1 (Cagζ)	integral component of membrane			1,46E+05	5,36E+04	1,86E+05	1,46E+05	3,99E+05	1,88E+04
O25270	Cag pathogenicity island protein 16 (CagM)	*outer membrane			5,54E+05	1,30E+04	4,71E+05	1,45E+04	4,54E+05	1,27E+04
O25271	Cag pathogenicity island protein 17 (CagN)	*periplasmic space; membrane			2,47E+06	7,66E+04	1,90E+06	4,91E+04	1,80E+06	1,44E+05
O25277	Cag pathogenicity island protein 24 (CagD)	*periplasmic space; membrane; cell surface			1,35E+08	3,76E+06	1,18E+08	1,53E+07	1,31E+08	2,56E+06
O25258	Cag pathogenicity island protein 3 (Cagδ)	*outer membrane			1,86E+07	4,20E+05	1,37E+07	2,96E+06	1,82E+07	1,63E+06
P97245	CAG pathogenicity island protein 12 (CagT)	outer membrane; plasma membrane	protein secretion		2,81E+07	2,29E+06	2,93E+07	7,54E+05	3,10E+07	1,97E+06
Q48252	CAG pathogenicity island protein 23 (CagE)	*membrane		ATP binding	4,64E+06	5,15E+05	9,85E+06	1,52E+06	1,36E+07	4,38E+06
O25798	Carbonic anhydrase			carbonate dehydratase activity; zinc ion binding	5,07E+07	5,58E+06	3,80E+07	8,64E+06	3,69E+07	3,57E+06
P77872	Catalase	cytoplasm	hydrogen peroxide catabolic process; response to hydrogen peroxide	catalase activity; heme binding; metal ion binding	4,64E+08	3,99E+07	5,13E+08	5,07E+07	4,94E+08	2,13E+07
O25229	Catalase-related peroxidase	cytoplasm	hydrogen peroxide catabolic process; response to hydrogen peroxide	catalase activity; heme binding; metal ion binding	1,15E+08	7,35E+06	1,20E+08	7,17E+06	1,54E+08	1,76E+07
O25886	Cation efflux system protein (CzcA)	cell envelope; outer membrane-bounded periplasmic space	cellular copper ion homeostasis; copper ion export; detoxification of copper ion; plasma membrane copper ion transport; response to silver ion; transmembrane transport	transition metal ion binding; transmembrane transporter activity	1,25E+06	4,15E+04	9,18E+05	9,22E+04	9,52E+05	1,41E+05
O24958	Cbb3-type cytochrome c oxidase subunit CcoP	integral component of membrane; plasma membrane; respirasome	ion transport; oxidative phosphorylation	electron transfer activity; heme binding; metal ion binding	2,38E+06	4,08E+05	5,54E+06	3,34E+06	6,17E+06	2,19E+06
Q48248	CDP-diacylglycerol pyrophosphatase	integral component of membrane; plasma membrane	CDP-diacylglycerol catabolic process; phospholipid biosynthetic process	CDP-diacylglycerol diphosphatase activity	2,01E+07	5,99E+05	2,13E+07	2,69E+05	2,30E+07	2,36E+06
O25089	Chemotaxis regulatory protein ChePep	cytoplasm			6,40E+04	9,50E+03	6,47E+04	3,61E+04	1,35E+05	3,10E+04
P56062	Citrate synthase	cytoplasm	tricarboxylic acid cycle	citrate (Si)-synthase activity	1,24E+07	6,92E+05	1,93E+07	1,00E+07	1,31E+07	4,45E+06
O25873	Conserved hypothetical secreted protein		positive regulation by symbiont of host apoptotic process		1,00E+09	5,14E+07	7,88E+08	2,43E+07	7,00E+08	1,36E+07
O25872	Conserved hypothetical secreted protein	cell outer membrane			1,66E+08	2,38E+06	1,32E+08	1,41E+07	1,23E+08	3,80E+06
O25038	Conserved hypothetical secreted protein				3,14E+06	3,00E+05	2,36E+06	2,70E+05	2,85E+06	2,68E+05

O25997	Cytochrome c551 peroxidase	periplasmic space		cytochrome-c peroxidase activity; electron transfer activity; heme binding; metal ion binding	4,35E+07	3,28E+06	4,77E+07	9,51E+06	4,39E+07	6,35E+06
O25825	Cytochrome c-553 (Cytochrome c553)	periplasmic space		electron transfer activity; heme binding; iron ion binding	3,89E+08	2,34E+07	3,16E+08	2,91E+07	3,45E+08	1,87E+07
O25294	Cytosol aminopeptidase	cytoplasm		manganese ion binding; metalloaminopeptidase activity	4,35E+07	2,51E+06	8,37E+07	4,60E+07	6,74E+07	3,47E+07
O25069	Dipeptide ABC transporter, periplasmic dipeptide-binding protein (DppA)	ATP-binding cassette (ABC) transporter complex; outer membrane-bounded periplasmic space	peptide transport	peptide transmembrane transporter activity	3,96E+06	4,70E+05	4,21E+06	1,21E+06	4,77E+06	6,60E+05
P43313	HP-NAP	cytoplasm	cellular iron ion homeostasis; pathogenesis	ferric iron binding; oxidoreductase activity, oxidizing metal ions	1,70E+08	2,34E+07	2,10E+08	1,13E+08	1,57E+08	7,30E+07
O25017	DsbG_N domain-containing protein				7,76E+08	5,15E+07	5,79E+08	1,17E+08	6,37E+08	3,79E+07
O25672	DUF2147 domain-containing protein				7,42E+05	5,84E+04	6,48E+05	1,13E+05	6,18E+05	9,01E+04
P56003	Elongation factor Tu (EF-Tu)	cytoplasm	translational elongation	GTPase activity; GTP binding; translation elongation factor activity	7,17E+04	5,39E+04	1,24E+05	9,12E+04	3,81E+05	9,01E+04
O26091	Endolytic peptidoglycan transglycosylase RlpA	plasma membrane	cell wall organization; peptidoglycan metabolic process	lyase activity; lytic endotransglycosylase activity; peptidoglycan binding	1,58E+07	1,39E+06	1,57E+07	2,53E+06	1,49E+07	1,58E+06
P48285	Enolase	cell surface; extracellular region; phosphopyruvate hydratase complex	glycolytic process; regulation of vacuole fusion, non-autophagic	magnesium ion binding; phosphopyruvate hydratase activity	3,93E+05	6,42E+04	9,85E+05	2,03E+05	7,81E+05	1,09E+05
O25312	Ferredoxin oxidoreductase, beta subunit			catalytic activity; thiamine pyrophosphate binding	1,91E+05	1,13E+04	7,37E+05	3,99E+05	6,32E+05	2,09E+05
O26012	Flagella basal body P-ring formation protein FlgA	periplasmic space; *bacterial-type flagellum assembly	bacterial-type flagellum assembly		1,17E+06	1,80E+05	1,00E+06	5,66E+04	1,05E+06	5,25E+03
P50610	Flagellar hook protein FlgE	bacterial-type flagellum basal body; bacterial-type flagellum hook	bacterial-type flagellum-dependent swarming motility; bacterial-type flagellum organization		2,45E+05	3,42E+04	4,24E+05	9,66E+04	4,07E+05	1,97E+05
O25028	Flagellar P-ring protein	bacterial-type flagellum basal body, distal rod, P ring; outer membrane-bounded periplasmic space	bacterial-type flagellum-dependent cell motility	structural molecule activity						
O26011	Flavin prenyltransferase UbiX			carboxy-lyase activity; flavin prenyltransferase activity	7,65E+04	1,65E+04	1,53E+05	9,18E+03	1,32E+05	3,17E+04
O25776	Flavodoxin			FMN binding	6,70E+04	1,98E+04	8,23E+04	5,80E+04	1,40E+05	4,48E+04
O25836	Formamidase		nitrogen compound metabolic process	formamidase activity; hydrolase activity, acting on carbon-nitrogen (but not peptide) bonds, in linear amides	1,11E+05	3,82E+04	2,92E+05	1,50E+05	2,76E+05	7,07E+04
P56109	Fructose-bisphosphate aldolase		fructose 1,6-bisphosphate metabolic process; glycolytic process	fructose-bisphosphate aldolase activity; zinc ion binding	1,02E+05	3,38E+04	1,39E+05	9,62E+03	1,75E+05	1,88E+04
O25883	Fumarate hydratase class II	tricarboxylic acid cycle enzyme complex [GO:0045239]	fumarate metabolic process; malate metabolic process; tricarboxylic acid cycle	fumarate hydratase activity	3,66E+05	2,87E+05	8,71E+05	4,06E+05	1,53E+06	3,73E+05
O25743	Gamma-glutamyltranspeptidase (Ggt)		glutathione catabolic process; negative regulation of cell cycle G1/S phase transition; negative regulation of T cell proliferation; positive regulation of interleukin-8 production	glutathione hydrolase activity; hypoglycin A gamma-glutamyl transpeptidase activity; leukotriene C4 gamma-glutamyl transferase activity	3,13E+08	3,36E+07	2,61E+08	4,58E+07	2,63E+08	9,56E+06

P56110	Glucose-6-phosphate 1-dehydrogenase		glucose metabolic process; pentose-phosphate shunt	glucose-6-phosphate dehydrogenase activity; NADP binding	3,44E+06	3,24E+05	2,80E+06	2,74E+05	3,00E+06	3,57E+05
O25786	Glutamine ABC transporter, periplasmic glutamine-binding protein (GlnH)				5,53E+06	2,38E+05	5,76E+06	6,04E+05	6,32E+06	8,63E+05
P94845	Glutamine synthetase	cytoplasm; membrane	glutamine biosynthetic process; nitrogen utilization	ATP binding; glutamate-ammonia ligase activity; metal ion binding	2,46E+07	3,33E+06	3,21E+07	1,59E+07	3,62E+07	1,31E+07
P56114	Glutamyl-tRNA(Gln) amidotransferase subunit A	glutamyl-tRNA(Gln) amidotransferase complex	translation	ATP binding; glutaminyl-tRNA synthase (glutamine-hydrolyzing) activity; hydrolase activity	6,58E+07	6,45E+06	5,77E+07	6,03E+06	5,60E+07	9,39E+06
O25321	Hemolysin secretion protein (HylB)	membrane	signal transduction		2,06E+05	1,01E+05	3,55E+05	1,88E+05	6,45E+05	6,61E+04
P56429	Homoserine dehydrogenase		isoleucine biosynthetic process; methionine biosynthetic process; threonine biosynthetic process	homoserine dehydrogenase activity; NADP binding	4,09E+05	5,48E+04	4,09E+05	5,45E+04	2,62E+05	3,98E+04
O25402	Hydantoin utilization protein A (HyuA)	cytosol	glutathione metabolic process	5-oxoprolinase (ATP-hydrolyzing) activity	1,74E+07	1,72E+06	8,48E+05	1,47E+06	1,19E+06	1,90E+06
O26082	Iron(III) ABC transporter, periplasmic iron-binding protein (CeuE)				3,09E+08	2,71E+06	2,56E+08	8,01E+06	2,90E+08	2,08E+06
O26083	Iron(III) ABC transporter, periplasmic iron-binding protein (CeuE)				7,74E+07	1,13E+07	6,47E+07	5,64E+07	7,26E+07	1,19E+07
O25395	Iron(III) dicitrate transport protein (FecA)	cell outer membrane	iron ion transport	ferric iron transmembrane transporter activity	3,87E+06	3,06E+04	4,14E+06	1,34E+05	8,47E+06	4,09E+05
O25950	Iron(III) dicitrate transport protein (FecA)	cell outer membrane	iron ion transport	ferric iron transmembrane transporter activity	4,31E+05	5,50E+05	8,93E+05	4,81E+06	1,07E+06	4,90E+06
O26042	Iron-regulated outer membrane protein (FrpB)	intrinsic component of cell outer membrane	siderophore transmembrane transport	siderophore uptake transmembrane transporter activity	9,21E+07	6,49E+06	9,77E+07	6,76E+07	1,27E+08	4,84E+07
O25573	Iron-regulated outer membrane protein (FrpB)	intrinsic component of cell outer membrane	siderophore transmembrane transport	siderophore uptake transmembrane transporter activity	3,91E+05	7,84E+04	1,75E+06	4,33E+05	2,20E+06	6,87E+05
P56063	Isocitrate dehydrogenase [NADP]		glyoxylate cycle; tricarboxylic acid cycle	isocitrate dehydrogenase (NADP+) activity; magnesium ion binding; NAD binding	1,37E+05	2,22E+04	2,80E+05	1,41E+05	3,60E+05	9,03E+04
O25097	Ketol-acid reductoisomerase (NADP+)	cytosol	isoleucine biosynthetic process; valine biosynthetic process	ketol-acid reductoisomerase activity; magnesium ion binding; NADP binding	3,64E+05	7,59E+04	8,70E+05	1,41E+05	3,74E+05	1,37E+05
O26022	Lipase-like protein	efflux pump complex		efflux transmembrane transporter activity; porin activity	5,82E+06	3,92E+05	7,76E+06	2,82E+06	5,42E+06	1,73E+06
O26084	Lipoprotein	membrane			1,16E+08	5,47E+06	9,31E+07	1,85E+07	1,09E+08	6,91E+06
P0A0V0	LPP20 lipoprotein	cell outer membrane			1,24E+09	1,70E+07	1,32E+09	1,10E+08	1,36E+09	1,06E+08
O25090	Membrane bound endonuclease (Nuc)		piRNA metabolic process	endonuclease activity	1,99E+07	3,42E+05	2,36E+07	2,44E+06	2,01E+07	3,23E+06
O25327	Membrane fusion protein (MtrC)	efflux pump complex		efflux transmembrane transporter activity	2,61E+07	1,18E+06	2,54E+07	2,61E+06	1,89E+07	6,45E+06
O25219	Molybdenum ABC transporter, periplasmic molybdate-binding protein (ModA)	outer membrane-bounded periplasmic space	molybdate ion transport	metal ion binding; molybdate ion binding	4,25E+06	2,59E+05	5,26E+06	1,91E+05	5,14E+06	5,56E+05
O25464	N-acetylmuramoyl-L-alanine amidase	outer membrane-bounded periplasmic space	peptidoglycan catabolic process	N-acetylmuramoyl-L-alanine amidase activity	1,94E+05	3,64E+04	2,29E+05	9,32E+04	3,01E+05	4,72E+04
P55990	NADP-specific glutamate dehydrogenase	cytoplasm; cytosol	glutamate biosynthetic process	glutamate dehydrogenase (NADP+) activity	2,51E+06	1,35E+05	3,06E+06	1,41E+06	3,60E+06	1,25E+06
O25166	Neuraminyllactose-binding hemagglutinin	cell outer membrane			4,32E+07	5,18E+06	4,00E+07	3,50E+06	4,58E+07	9,79E+05

O25234	Neuraminyllactose-binding hemagglutinin	cell outer membrane			1,04E+07	1,77E+06	9,27E+06	2,01E+06	1,08E+07	1,15E+06
P55969	Neuraminyllactose-binding hemagglutinin	cell outer membrane			3,31E+08	2,49E+07	2,59E+08	1,43E+07	2,67E+08	1,38E+07
O25623	Nickel-cobalt-cadmium resistance protein (NccB)	cell envelope	transmembrane transport	transmembrane transporter activity	3,23E+06	3,85E+04	2,46E+06	3,70E+05	2,49E+06	3,06E+05
O25403	N-methylhydantoinase	cytosol	glutathione metabolic process	5-oxoprolinase (ATP-hydrolyzing) activity	1,77E+07	3,08E+06	1,23E+06	1,89E+06	1,52E+06	1,75E+06
O25465	NMO domain-containing protein			nitronate monooxygenase activity	2,14E+04	0,00E+00	8,88E+04	5,72E+03	1,41E+05	2,20E+04
O25216	Oligoendopeptidase F (PepF)		peptide metabolic process; proteolysis	metal ion binding; metalloendopeptidase activity	1,21E+05	6,14E+04	4,29E+05	9,83E+03	3,55E+05	1,07E+05
O26088	OstA-like_N domain-containing protein	cell outer membrane; outer membrane-bounded periplasmic space	lipopolysaccharide transport	glycolipid transfer activity; lipopolysaccharide binding	2,54E+06	6,67E+05	2,57E+06	1,25E+06	2,34E+06	2,01E+05
O25091	Outer membrane protein (Omp10)	*cell outer membrane			1,60E+06	2,34E+05	1,22E+06	5,06E+05	1,45E+06	3,71E+05
O25218	Outer membrane protein (Omp11)	*cell outer membrane			8,16E+07	1,83E+07	2,27E+08	3,59E+07	2,54E+08	4,73E+07
O25355	Outer membrane protein (Omp13)	*cell outer membrane			7,24E+07	5,19E+06	9,77E+07	2,26E+07	1,10E+08	3,34E+07
O25382	Outer membrane protein (Omp14)	*cell outer membrane			4,17E+07	7,18E+06	4,75E+07	1,28E+07	4,57E+07	2,56E+06
O25410	Outer membrane protein (Omp15)	*cell outer membrane			1,73E+07	1,67E+06	3,34E+07	3,97E+06	4,03E+07	1,63E+07
O24870	Outer membrane protein (Omp2)	*cell outer membrane			1,69E+08	8,90E+06	1,69E+08	3,89E+07	2,05E+08	3,29E+07
O25570	Outer membrane protein (Omp20)	*cell outer membrane			3,85E+08	4,70E+07	3,83E+08	8,69E+07	4,01E+08	5,35E+07
O25571	Outer membrane protein (Omp21)	*cell outer membrane			2,14E+08	2,62E+07	2,56E+08	6,24E+07	2,46E+08	3,35E+07
O25580	Outer membrane protein (Omp22)	*cell outer membrane			9,44E+06	1,24E+06	1,22E+07	1,95E+06	1,44E+07	9,80E+05
O25735	Outer membrane protein (Omp23)	*cell outer membrane			2,06E+06	2,95E+05	3,25E+06	5,05E+05	3,95E+06	6,04E+05
O25771	Outer membrane protein (Omp25)	*cell outer membrane			1,12E+07	1,21E+06	9,76E+06	1,61E+06	9,97E+06	9,48E+05
O25772	Outer membrane protein (Omp26)	*cell outer membrane			1,79E+06	1,85E+05	1,90E+06	7,82E+05	1,77E+06	5,31E+05
O25791	Outer membrane protein (Omp27)	*cell outer membrane			1,28E+09	9,37E+07	1,28E+09	3,58E+08	1,35E+09	1,22E+08
O25840	Outer membrane protein (Omp28)	*cell outer membrane			3,46E+07	2,43E+06	3,39E+07	8,88E+06	4,03E+07	4,38E+06
O34523	Outer membrane protein (Omp29; Omp5)	*cell outer membrane			7,08E+07	7,27E+06	6,70E+07	1,90E+07	8,11E+07	5,25E+06
O25945	Outer membrane protein (Omp30)	*cell outer membrane			1,33E+08	5,32E+06	1,17E+08	1,05E+07	1,31E+08	5,77E+06
O26005	Outer membrane protein (Omp31)	*cell outer membrane			5,48E+07	1,10E+07	5,65E+07	1,30E+07	6,63E+07	1,19E+07
O26031	Outer membrane protein (Omp32)	*cell outer membrane			8,27E+07	1,12E+07	9,44E+07	1,27E+07	9,63E+07	1,30E+07
O24941	Outer membrane protein (Omp4)	*cell outer membrane			3,08E+07	6,85E+06	3,30E+07	1,07E+07	4,26E+07	3,99E+06
O25015	Outer membrane protein (Omp6)	*cell outer membrane			1,61E+08	1,35E+07	1,48E+08	3,33E+07	1,59E+08	5,74E+06
O25034	Outer membrane protein (Omp7)	*cell outer membrane			2,13E+07	2,85E+06	1,99E+07	6,77E+06	2,14E+07	3,36E+06

O25036	Outer membrane protein (Omp8)	*cell outer membrane			2,69E+07	3,67E+06	2,56E+07	9,92E+06	2,76E+07	7,46E+06
O25086	Outer membrane protein (Omp9)	*cell outer membrane			3,31E+08	2,75E+07	2,76E+08	7,40E+07	3,03E+08	2,37E+07
O25369	Outer membrane protein assembly factor BamA	cell outer membrane; integral component of membrane	Gram-negative-bacterium-type cell outer membrane assembly; protein insertion into membrane		6,03E+06	5,62E+05	8,72E+06	5,89E+06	1,27E+07	4,14E+06
O25930	Outer membrane protein assembly factor BamD	Bam protein complex	Gram-negative-bacterium-type cell outer membrane assembly; protein insertion into membrane		1,87E+07	9,74E+05	1,69E+07	4,27E+06	1,84E+07	2,12E+06
O25510	Outer membrane protein P1 (OmpP1)	*cell outer membrane		long-chain fatty acid transporting porin activity	1,54E+07	1,29E+06	1,48E+07	4,41E+06	1,87E+07	3,56E+06
O25474	Outer-membrane lipoprotein carrier protein	outer membrane-bounded periplasmic space	lipoprotein localization to outer membrane; lipoprotein transport		7,18E+06	1,24E+06	6,77E+06	4,50E+05	6,70E+06	1,86E+05
O25011	Peptide methionine sulfoxide reductase MsrA/MsrB	cytoplasm	cellular protein modification process; protein repair; response to oxidative stress	peptide-methionine (R)-S-oxide reductase activity; peptide-methionine (S)-S-oxide reductase activity	8,02E+08	6,19E+07	6,05E+08	1,35E+08	5,94E+08	7,16E+07
O25750	Peptidoglycan associated lipoprotein (Omp18)	integral component of membrane			6,31E+07	7,89E+05	5,91E+07	4,54E+06	6,33E+07	4,54E+06
O25080	Peptidoglycan deacetylase		cell wall organization; xylan catabolic process	acetylxylan esterase activity; hydrolase activity, acting on carbon-nitrogen (but not peptide) bonds; metal ion binding	1,65E+06	9,87E+04	2,27E+06	2,16E+05	1,48E+06	5,52E+05
O25663	Periplasmic serine endoprotease DegP-like	periplasmic space		serine-type endopeptidase activity	6,85E+08	3,76E+07	5,74E+08	7,72E+07	5,52E+08	5,37E+07
O25249	Plasminogen-binding protein PgbA	cell surface			5,10E+07	1,87E+06	4,18E+07	1,16E+07	4,04E+07	5,15E+06
O25534	Plasminogen-binding protein PgbB	cell surface			3,63E+07	1,37E+06	4,15E+07	9,93E+06	4,47E+07	3,89E+06
O25045	Probable dihydroorotase-like protein (Aspartate carbamoyltransferase 42 kDa non-catalytic chain)		pyrimidine nucleotide biosynthetic process	hydrolase activity, acting on carbon-nitrogen (but not peptide) bonds	6,02E+04	2,32E+04	1,59E+05	6,26E+04	1,40E+05	3,00E+04
O25424	Probable L-asparaginase	cytoplasm	asparagine metabolic process	asparaginase activity	5,93E+07	5,41E+06	6,69E+07	1,32E+07	5,81E+07	8,91E+06
O25371	Processing protease (YmxG)			metal ion binding; peptidase activity	1,18E+08	6,40E+06	1,03E+08	1,76E+07	1,03E+08	7,46E+06
O25905	Protease	outer membrane-bounded periplasmic space	signal transduction	endopeptidase activity; serine-type peptidase activity	1,23E+08	1,63E+07	1,09E+08	2,89E+07	1,21E+08	7,25E+06
O25656	Protease (PqqE)			metal ion binding; peptidase activity	2,21E+08	8,10E+06	1,60E+08	1,72E+07	1,56E+08	7,12E+06
O87326	Protein trl (tRNA-associated locus protein)				1,35E+07	2,36E+06	1,54E+07	8,87E+05	1,65E+07	1,02E+06
P56463	Purine nucleoside phosphorylase DeoD-type (PNP)		purine nucleoside metabolic process	purine-nucleoside phosphorylase activity	4,47E+04	4,44E+03	5,54E+05	7,82E+04	7,37E+05	1,08E+05
O25728	Putative beta-lactamase HcpC	extracellular region	response to antibiotic	beta-lactamase activity	1,30E+08	4,58E+06	1,10E+08	7,36E+06	1,04E+08	3,50E+06
O24968	Putative beta-lactamase HcpD	extracellular region	response to antibiotic	beta-lactamase activity	3,97E+07	5,02E+06	5,00E+07	1,07E+07	5,23E+07	8,88E+06
O25021	Putative beta-lactamase HcpE	extracellular region	response to antibiotic	beta-lactamase activity	4,17E+05	4,12E+04	4,47E+05	8,37E+04	3,92E+05	4,65E+04
P56112	Putative peptidyl-prolyl cis-trans isomerase HP_0175			peptidyl-prolyl cis-trans isomerase activity	7,39E+08	2,39E+07	5,05E+08	8,22E+07	4,99E+08	3,16E+07
O25739	Pyruvate ferredoxin oxidoreductase, beta subunit			catalytic activity; thiamine pyrophosphate binding	5,65E+05	3,17E+05	7,15E+05	3,45E+05	1,17E+06	4,80E+05

O25737	Pyruvate ferredoxin oxidoreductase, delta subunit			4 iron, 4 sulfur cluster binding; metal ion binding; oxidoreductase activity, acting on the aldehyde or oxo group of donors, iron-sulfur protein as acceptor	3,70E+04	5,20E+04	6,66E+04	2,81E+04	1,26E+05	2,07E+04
O25736	Pyruvate ferredoxin oxidoreductase, gamma subunit			oxidoreductase activity, acting on the aldehyde or oxo group of donors, iron-sulfur protein as acceptor	4,38E+04	0,00E+00			5,26E+04	3,11E+03
O25349	Quinone-reactive Ni/Fe hydrogenase, large subunit (HydB)			ferredoxin hydrogenase activity; nickel cation binding	5,25E+05	2,83E+05	1,35E+06	3,35E+05	1,96E+06	3,81E+05
O25348	Quinone-reactive Ni/Fe hydrogenase, small subunit (HydA)	[Ni-Fe] hydrogenase complex; ferredoxin hydrogenase complex; membrane	anaerobic respiration	3 iron, 4 sulfur cluster binding; 4 iron, 4 sulfur cluster binding; electron transfer activity; ferredoxin hydrogenase activity; metal ion binding	8,89E+04	1,98E+04	8,58E+04	1,63E+04	1,16E+05	1,75E+04
O25972	Ribosomal RNA small subunit methyltransferase A	cytoplasm	rRNA methylation	16S rRNA (adenine(1518)-N(6)/adenine(1519)-N(6))-dimethyltransferase activity; RNA binding; rRNA (adenine-N6,N6-)-dimethyltransferase activity	2,35E+07	5,29E+06	4,70E+07	5,99E+06	4,41E+07	1,08E+07
O25998	Secreted protein involved in flagellar motility				1,91E+07	1,16E+06	1,79E+07	3,17E+06	1,94E+07	2,03E+06
P56089	Serine hydroxymethyltransferase	cytosol	folic acid metabolic process; glycine biosynthetic process from serine; L-serine catabolic process; one-carbon metabolic process; tetrahydrofolate interconversion; tetrahydrofolate metabolic process	amino acid binding; cobalt ion binding; glycine hydroxymethyltransferase activity; pyridoxal phosphate binding; serine binding; zinc ion binding	2,99E+05	4,41E+04	5,45E+05	2,39E+04	5,34E+05	1,06E+05
O25362	Soluble lytic murein transglycosylase (Slt)				1,84E+07	1,11E+06	2,13E+07	2,36E+06	2,10E+07	1,66E+06
O25146	SPOR domain-containing protein			peptidoglycan binding	2,05E+07	1,48E+06	1,50E+07	4,01E+06	1,45E+07	1,24E+06
P43312	Superoxide dismutase [Fe]		cellular response to iron ion	metal ion binding; superoxide dismutase activity	6,43E+05	1,67E+05	9,26E+05	5,38E+05	1,27E+06	2,90E+05
O25373	SurA_N domain-containing protein				3,50E+07	1,56E+06	3,21E+07	9,76E+06	3,36E+07	4,63E+06
O25140	Thiol:disulfide interchange protein (DsbC)				5,53E+07	1,25E+06	4,40E+07	6,37E+06	4,24E+07	1,05E+06
P66928	Thioredoxin (Trx)		cell redox homeostasis; glycerol ether metabolic process	protein disulfide oxidoreductase activity	1,87E+06	2,19E+05	2,46E+06	7,18E+05	2,69E+06	8,95E+04
P56431	Thioredoxin reductase (TRXR)	cytoplasm	removal of superoxide radicals	thioredoxin-disulfide reductase activity	6,06E+05	9,53E+04	1,16E+06	3,99E+04	9,79E+05	2,49E+05
O25751	Tol-Pal system protein TolB	periplasmic space	cell cycle; cell division; protein import		8,08E+07	4,11E+06	9,96E+07	8,52E+06	8,82E+07	1,79E+07
O25331	Toxin-like outer membrane protein	*cell outer membrane	pathogenesis		5,57E+05	9,21E+04	5,79E+05	3,03E+05	9,66E+05	2,42E+05
O25511	UDP-N-acetylglucosamine 4,6-dehydratase			lyase activity; nucleotide binding	1,31E+05	2,61E+04	2,29E+05	3,33E+04	1,95E+05	6,64E+04
O25436	Uncharacterized aminotransferase HP_0736			transaminase activity	1,49E+05	3,05E+04	3,25E+05	6,94E+04	2,33E+05	6,61E+04
O25442	Uncharacterized protein				9,89E+08	1,71E+06	9,08E+08	3,97E+06	1,00E+09	3,93E+06
O24923	Uncharacterized protein				7,13E+08	7,14E+06	7,18E+08	2,96E+07	6,85E+08	1,22E+07

O25715	Uncharacterized protein				6,28E+08	2,46E+06	4,88E+08	1,24E+07	4,85E+08	1,18E+07
O26014	Uncharacterized protein	integral component of membrane	cell division		5,65E+08	1,13E+04	5,87E+08	1,26E+04	5,54E+08	2,28E+04
O24983	Uncharacterized protein	integral component of membrane	toxin biosynthetic process		4,10E+08	2,09E+05	3,59E+08	3,26E+05	3,88E+08	1,55E+05
O25999	Uncharacterized protein				2,63E+08	1,13E+06	2,41E+08	1,62E+06	2,59E+08	1,30E+06
O25230	Uncharacterized protein				2,35E+08	1,64E+06	2,34E+08	1,56E+07	2,62E+08	1,65E+07
O26071	Uncharacterized protein	outer membrane	Gram-negative-bacterium-type cell outer membrane assembly		2,25E+08	8,46E+04	2,05E+08	3,89E+04	2,22E+08	2,76E+04
O25507	Uncharacterized protein	integral component of membrane			1,89E+08	4,64E+05	1,73E+08	5,10E+05	1,77E+08	1,76E+05
O25281	Uncharacterized protein				1,48E+08	7,34E+05	1,15E+08	1,50E+06	1,10E+08	1,52E+06
O25231	Uncharacterized protein				1,21E+08	3,11E+04	1,56E+08	2,25E+05	1,34E+08	6,05E+04
O25717	Uncharacterized protein				1,03E+08	7,14E+04	9,31E+07	5,56E+04	1,02E+08	1,57E+04
O25413	Uncharacterized protein				7,87E+07	1,14E+06	8,33E+07	1,51E+05	8,22E+07	6,66E+05
O25697	Uncharacterized protein				5,19E+07	6,13E+05	5,61E+07	6,68E+05	4,96E+07	6,92E+05
O25470	Uncharacterized protein				4,02E+07	1,96E+06	3,85E+07	3,27E+06	4,40E+07	8,21E+05
O26052	Uncharacterized protein				3,42E+07	9,01E+06	4,08E+07	1,70E+06	4,17E+07	2,58E+06
O25421	Uncharacterized protein				2,73E+07	4,36E+06	3,16E+07	1,01E+07	3,36E+07	1,69E+07
O25585	Uncharacterized protein				2,26E+07	2,62E+03	1,92E+07	1,01E+04	2,43E+07	2,53E+04
O26055	Uncharacterized protein				1,94E+07	1,42E+06	2,63E+07	1,23E+06	5,11E+07	2,62E+06
O25648	Uncharacterized protein				1,80E+07	2,16E+06	1,75E+07	1,41E+07	1,78E+07	4,59E+06
O25414	Uncharacterized protein				1,72E+07	2,83E+07	1,18E+07	4,51E+07	2,87E+07	1,09E+07
O25995	Uncharacterized protein				1,70E+07	6,85E+06	1,22E+07	1,97E+07	1,22E+07	2,24E+07
O25508	Uncharacterized protein				1,57E+07	8,04E+05	1,45E+07	2,84E+06	1,36E+07	1,48E+06
O25477	Uncharacterized protein				1,56E+07	2,30E+05	2,02E+07	1,84E+06	2,61E+07	1,50E+06
O25994	Uncharacterized protein				1,46E+07	1,84E+05	1,87E+07	5,15E+05	1,70E+07	6,13E+05
O26003	Uncharacterized protein				1,41E+07	3,16E+04	8,77E+06	1,15E+05	8,12E+06	1,24E+05
O25287	Uncharacterized protein				1,26E+07	6,28E+04	1,30E+07	4,50E+05	1,33E+07	4,11E+05
O24996	Uncharacterized protein				1,21E+07	1,49E+05	1,41E+07	3,69E+05	1,64E+07	1,61E+05
O25426	Uncharacterized protein	integral component of membrane			1,18E+07	9,48E+05	9,62E+06	3,43E+06	7,85E+06	5,70E+06
O25469	Uncharacterized protein				1,15E+07	7,63E+05	1,24E+07	3,22E+05	1,22E+07	1,11E+05
O25885	Uncharacterized protein			efflux transmembrane transporter activity	1,15E+07	2,17E+04	1,11E+07	8,97E+04	1,13E+07	4,22E+04
O25625	Uncharacterized protein				9,79E+06	1,31E+06	9,33E+06	1,49E+06	9,63E+06	3,13E+06
O25749	Uncharacterized protein				8,18E+06	6,08E+05	1,24E+07	1,29E+06	1,35E+07	2,03E+06
O25891	Uncharacterized protein				6,85E+06	8,45E+04	5,71E+06	9,19E+04	6,15E+06	4,72E+04
O25495	Uncharacterized protein				6,71E+06	1,84E+04	1,66E+05	8,70E+03	2,52E+05	9,94E+03
O25607	Uncharacterized protein				6,62E+06	6,74E+06	1,23E+07	2,59E+06	1,08E+07	5,41E+06
O25423	Uncharacterized protein				6,47E+06	1,67E+07	5,28E+06	1,78E+07	5,30E+06	3,89E+07
O25967	Uncharacterized protein				6,03E+06	1,14E+05	8,50E+06	1,49E+04	1,09E+07	1,39E+05
O25164	Uncharacterized protein				5,03E+06	1,72E+07	4,06E+06	1,47E+07	5,36E+06	2,08E+07
O25504	Uncharacterized protein				4,83E+06	4,22E+04	1,01E+07	3,98E+04	1,01E+07	1,93E+04
O25572	Uncharacterized protein				4,45E+06	1,87E+05	5,98E+06	1,05E+06	5,91E+06	9,34E+05
O24914	Uncharacterized protein				4,38E+06	2,90E+05	3,23E+06	1,01E+07	3,89E+06	6,47E+06
O25586	Uncharacterized protein				4,17E+06	1,68E+05	4,98E+06	4,30E+05	4,62E+06	1,32E+06
O25509	Uncharacterized protein				2,60E+06	9,02E+05	1,94E+06	1,57E+06	2,34E+06	1,35E+06
O24863	Uncharacterized protein				2,43E+06	4,14E+05	2,06E+06	8,54E+05	2,87E+06	6,07E+05
O25344	Uncharacterized protein				1,98E+06	1,38E+05	2,56E+06	5,33E+05	5,41E+06	1,03E+05
O25326	Uncharacterized protein	efflux pump complex [GO:1990281]		efflux transmembrane transporter activity; porin activity	1,69E+06	2,07E+06	1,51E+06	2,74E+07	1,60E+06	9,36E+06
O25667	Uncharacterized protein				1,58E+06	2,82E+04	1,48E+06	1,62E+05	1,30E+06	1,60E+05
O25137	Uncharacterized protein				1,46E+06	2,22E+05	2,01E+06	1,44E+05	1,29E+06	7,27E+04
O25713	Uncharacterized protein				9,96E+05	6,41E+04	7,16E+05	9,31E+04	1,60E+06	1,15E+05
O24995	Uncharacterized protein				8,10E+05	2,44E+05	1,38E+06	9,68E+05	1,66E+06	5,12E+05
O24944	Uncharacterized protein				7,89E+05	2,50E+07	1,19E+06	7,60E+07	2,48E+06	3,15E+07
O25787	Uncharacterized protein				6,86E+05	1,88E+07	1,01E+06	4,90E+06	9,39E+05	1,72E+07
O25696	Uncharacterized protein				6,64E+05	7,41E+05	5,96E+05	1,23E+06	4,79E+05	7,49E+05

O25472	Uncharacterized protein				5,67E+05	3,59E+06	4,29E+05	2,40E+06	5,03E+05	2,36E+06
O25993	Uncharacterized protein				4,83E+05	9,22E+06	7,38E+05	2,78E+07	9,64E+05	3,49E+07
O25329	Uncharacterized protein				3,64E+05	7,62E+03	4,41E+05	5,95E+03	5,15E+05	1,50E+04
O25318	Uncharacterized protein				2,58E+05	9,12E+06	2,50E+05	1,84E+07	2,84E+05	1,13E+07
O24938	Uncharacterized protein				1,94E+05	1,08E+06	3,00E+05	2,05E+05	5,18E+05	6,36E+05
O25354	Uncharacterized protein	integral component of membrane			1,90E+05	2,66E+05	2,10E+05	8,13E+05	5,96E+05	3,85E+05
O25695	Uncharacterized protein				1,84E+05	1,70E+06	1,24E+05	1,33E+06	1,73E+05	1,29E+06
O24943	Uncharacterized protein				1,23E+05	1,79E+07	1,27E+05	5,54E+07	9,74E+04	1,91E+07
O25404	Uncharacterized protein				8,40E+04	9,48E+05	1,01E+05	3,90E+05	7,14E+04	4,59E+05
O25401	Uncharacterized protein				7,37E+04	7,38E+05	2,29E+05	1,72E+06	2,11E+05	1,22E+06
O25992	Uncharacterized protein				5,52E+04	1,09E+06	1,02E+05	1,06E+06	3,36E+05	1,77E+06
O24909	Uncharacterized protein				2,27E+04	1,28E+06	2,60E+04	5,13E+06	7,11E+04	3,01E+06
O25353	Uncharacterized protein				6,64E+03	1,98E+04	2,51E+04	9,22E+04	4,62E+04	5,76E+04
P64653	Uncharacterized protein HP_0122				1,05E+08	1,57E+05	1,20E+08	1,05E+05	1,23E+08	1,41E+05
P64655	Uncharacterized protein HP_0135				2,17E+07	2,09E+06	2,04E+07	1,19E+06	2,87E+07	7,72E+05
P56117	Uncharacterized protein HP_0190	integral component of membrane; plasma membrane	cardiolipin biosynthetic process	transferase activity	6,15E+05	7,12E+04	5,39E+05	3,03E+05	6,43E+05	2,09E+05
O24989	UPF0114 protein HP_0189	integral component of membrane; plasma membrane			1,61E+07	2,51E+06	1,53E+07	2,37E+06	1,82E+07	2,84E+06
O25018	UPF0323 lipoprotein HP_0232	plasma membrane			8,69E+07	4,78E+06	6,29E+07	1,09E+07	5,55E+07	7,26E+06
P14916	Urease subunit alpha	urease complex	pathogenesis; urea catabolic process	nickel cation binding; urease activity	4,74E+08	9,04E+07	4,76E+08	2,66E+08	5,56E+08	1,92E+08
P69996	Urease subunit beta	cytoplasm	pathogenesis; urea catabolic process	nickel cation binding; urease activity	3,89E+08	6,51E+07	3,91E+08	2,31E+08	4,35E+08	1,59E+08
O25325	Uroporphyrinogen decarboxylase	cytosol	heme biosynthetic process; protoporphyrinogen IX biosynthetic process from glutamate	uroporphyrinogen decarboxylase activity	1,08E+05	9,71E+03	5,46E+05	1,66E+05	6,67E+05	1,73E+04
P55981	Vacuolating cytotoxin autotransporter (VacA)	cell outer membrane; cell surface; extracellular region; integral component of membrane; periplasmic space	pathogenesis	toxin activity	5,01E+07	2,43E+07	1,98E+08	1,46E+08	6,20E+08	1,03E+08
O25076	YceI domain-containing protein				3,51E+08	1,48E+07	2,98E+08	2,54E+07	2,77E+08	1,18E+07
O25884	YtkA domain-containing protein				2,74E+05	5,98E+06	2,03E+05	5,90E+06	1,20E+06	

Supplementary Table 2. Differentially expressed genes (adjusted $p < 0.05$) in MKN74 cells challenged with *H. pylori* OMVs when compared to the control cells. The Table displays fold changes and adjusted *p* values of the differentially expressed genes. Genes with log2-FC > 1 are upregulated and log2-FC < 1 are downregulated.

Gene ID	log_2-FC	*p*adj	Gene ID	log_2-FC	*p*adj	Gene ID	log_2-FC	*p*adj
GPR97	6.85466	1.31E-06	**RSAD2**	2.58899	4.95E-04	**ISG20**	2.04947	5.16E-14
KLHDC7B	6.57186	1.01E-18	**TACC2**	2.57838	2.28E-13	**ZEB1**	2.04553	4.50E-02
GPR1	5.78300	2.19E-06	**ASIC3**	2.55539	1.93E-07	**NCF2**	2.03906	7.14E-03
C3orf20	5.03105	5.25E-04	**RNASE7**	2.53901	2.18E-03	**SNAI2**	2.03400	3.18E-02
LOC338651	4.80507	3.62E-03	**KIAA0226L**	2.53272	7.47E-05	**KLF6**	2.03388	3.58E-06
BEST1	4.76293	3.00E-06	**RENBP**	2.53158	2.69E-07	**SLC22A15**	2.03087	4.03E-17
SAA2	4.62836	4.41E-03	**LINC00341**	2.52965	1.43E-17	**LOC100506844**	2.01580	6.91E-06
SLC9A3	4.42779	2.29E-02	**PDE2A**	2.51870	9.10E-07	**VEGFA**	2.00189	8.39E-30
CCDC3	4.31810	2.17E-02	**LOC100128054**	2.49796	2.08E-02	**KCND1**	1.99862	2.95E-06
INHBE	4.26159	1.38E-14	**RASL10B**	2.48610	9.11E-03	**CHAC1**	1.99055	6.75E-11
C19orf38	4.23411	8.24E-04	**TMIE**	2.47763	4.59E-04	**TACC1**	1.98446	1.91E-04
SH2D4B	4.18460	1.02E-02	**KCNJ5**	2.46744	1.95E-02	**SLAMF7**	1.98257	4.19E-02
PRPH	4.13026	4.24E-17	**CSTA**	2.46201	3.60E-03	**ZNF385C**	1.97650	9.48E-06
DMGDH	4.02264	3.16E-04	**CERS3**	2.45728	6.09E-03	**DISP2**	1.97625	2.70E-04
CNN1	3.99898	4.44E-03	**NCR3LG1**	2.42761	2.18E-04	**PSG3**	1.97485	3.28E-02
GALNT9	3.98684	1.94E-02	**METTL20**	2.42154	3.70E-02	**LYPD5**	1.96911	1.54E-02
PRSS3	3.92567	4.70E-02	**ULBP1**	2.39797	1.50E-27	**CLDN1**	1.96492	9.69E-12
FAM167A	3.92259	2.14E-10	**FAM86B1**	2.38754	1.68E-05	**CDKN2B**	1.96059	2.87E-24
RTN1	3.86745	1.81E-02	**SAA1**	2.37914	1.24E-02	**TMEM198**	1.95170	1.63E-06
UBL4B	3.83733	2.40E-02	**ATF3**	2.36954	2.44E-26	**LCP1**	1.94891	1.75E-02
BHLHE41	3.75026	5.13E-07	**NOS3**	2.35261	1.55E-05	**CD8A**	1.94583	2.55E-02
NPHS1	3.70327	5.38E-08	**DUSP6**	2.34909	1.11E-25	**ATP8A2**	1.93733	1.70E-04
ALOX12B	3.68583	9.20E-07	**SLC1A4**	2.33933	1.05E-16	**CREBRF**	1.93728	6.91E-11
IL6	3.68392	4.49E-06	**ARHGAP9**	2.32625	4.66E-02	**TP53INP2**	1.93495	1.84E-07
S1PR1	3.55393	2.46E-08	**SOCS2**	2.32201	8.22E-07	**SLC27A5**	1.93419	4.83E-09
PKD1L2	3.52603	2.39E-09	**KIF5A**	2.29876	1.65E-02	**AKNA**	1.92577	9.00E-10
IL1A	3.52068	1.68E-09	**LAMP3**	2.28680	1.49E-14	**CCDC176**	1.91707	3.22E-05
LURAP1L	3.48741	5.14E-42	**KRT16**	2.28665	3.03E-06	**TLCD2**	1.91479	3.06E-12
FAM129A	3.45062	6.68E-35	**MAB21L3**	2.28628	2.23E-03	**ALDH2**	1.90390	4.61E-02
INHBA	3.40254	2.95E-03	**SYNE3**	2.27584	1.23E-16	**LOC400680**	1.89679	5.90E-03
ROBO4	3.30825	3.75E-05	**PCK2**	2.27217	4.28E-16	**SLC6A3**	1.89259	2.30E-02
GATM	3.30191	6.02E-03	**POU4F3**	2.26159	2.94E-02	**HOXB9**	1.88987	3.04E-20
A1BG	3.29425	2.42E-02	**LAMB3**	2.26122	1.26E-18	**MAP1LC3B2**	1.88732	4.43E-44
FBXO39	3.29228	3.58E-02	**SH2D5**	2.25533	2.16E-08	**AHRR**	1.88605	3.83E-06
SPRR2D	3.29028	5.48E-06	**LCN2**	2.24907	6.83E-04	**CDKN1A**	1.88114	1.33E-44
KLF15	3.25547	2.73E-02	**CLIP4**	2.24852	1.79E-12	**PKD1L1**	1.87977	3.88E-02
PLA2G4C	3.25238	8.91E-10	**FAM186B**	2.22901	1.16E-04	**SNX24**	1.87890	1.50E-27
CUZD1	3.24326	1.18E-19	**ALOXE3**	2.22031	8.77E-06	**KGFLP1**	1.86367	1.25E-12
NLRP1	3.21000	9.12E-05	**TGM1**	2.20039	1.78E-13	**ZHX2**	1.85847	6.00E-13
PTAFR	3.13593	3.56E-02	**WARS**	2.19984	7.30E-51	**SLC4A5**	1.85189	2.38E-06
PSG2	3.11925	1.98E-02	**LOC100506178**	2.18921	1.19E-06	**DDR2**	1.84278	1.71E-04
DUSP1	3.08543	8.71E-69	**DNHD1**	2.18774	1.03E-02	**SIRT4**	1.84026	2.94E-03
FAM86B2	3.06179	4.29E-03	**NUPR1**	2.18182	6.21E-16	**FAM189A2**	1.83758	1.46E-04
IFIT2	2.97111	8.80E-13	**ELFN1**	2.16998	4.27E-02	**GLI1**	1.83236	3.27E-02
ADAMTS9	2.95631	3.77E-05	**HMX3**	2.15875	6.18E-03	**TMPRSS6**	1.83206	3.36E-02
PPP1R15A	2.91331	4.45E-75	**LOC100505633**	2.14981	3.39E-03	**TRIB3**	1.82598	5.24E-24
SLFN5	2.88687	5.44E-33	**FAM24B**	2.14424	2.21E-17	**GATA6**	1.81457	6.35E-07
TYMP	2.88004	9.51E-20	**SLC6A9**	2.14354	1.05E-10	**CXCL3**	1.80980	4.98E-02
NAGPA-AS1	2.87522	3.14E-02	**GBP1**	2.14011	7.64E-05	**PSD**	1.80609	3.07E-02
LOC100130705	2.87508	1.74E-02	**TMC8**	2.13201	1.53E-02	**SHISA4**	1.80568	2.09E-07
ALOX5AP	2.86078	2.18E-03	**LOC284889**	2.12858	5.12E-04	**RSPH1**	1.80443	1.21E-02
FAM70B	2.85669	2.13E-03	**C15orf48**	2.12532	4.80E-11	**NFKBIZ**	1.80171	1.98E-11
SCN3B	2.85627	4.15E-02	**FLJ46906**	2.11326	8.23E-17	**HBEGF**	1.79909	2.06E-16
MIR181A2HG	2.82532	1.26E-04	**NUAK2**	2.11236	4.27E-07	**FAM86EP**	1.79472	1.27E-07
HDAC9	2.82358	4.10E-17	**GOLT1A**	2.11210	2.04E-12	**WNK4**	1.79071	1.29E-06
RPLP0P2	2.79515	3.48E-04	**AHNAK2**	2.10167	1.80E-10	**CTAGE1**	1.78388	1.45E-02
NEURL3	2.78241	6.59E-09	**RAB3IL1**	2.10040	7.58E-23	**IRAK2**	1.77725	7.48E-06
GADD45A	2.70865	6.30E-12	**TNFAIP2**	2.09672	3.91E-03	**HOTAIRM1**	1.77394	2.38E-05
S100P	2.67225	1.54E-13	**ASNS**	2.06449	6.44E-39	**CCDC113**	1.77363	1.50E-07
FYN	2.63987	2.86E-41	**TSC22D3**	2.06433	3.44E-02	**RNF157-AS1**	1.77238	7.76E-03
ANKRD1	2.63923	2.63E-10	**ADTRP**	2.05489	6.71E-07	**ATP2C2**	1.76733	1.70E-04
IER2	2.62070	3.93E-02	**UPP1**	2.05479	1.01E-05	**SESN2**	1.76681	1.07E-10
GDF15	2.61650	6.13E-38	**ZNF502**	2.05197	1.79E-04	**VGF**	1.76666	1.23E-02
HRK	2.59107	1.09E-22	**TIGD6**	2.05045	5.67E-04	**RRAGD**	1.76593	8.29E-12

FAM86HP	1.75326	7.13E-06	**FRY**	1.54506	4.17E-02	**NFE2L2**	1.35280	2.04E-27
EPG5	1.75212	2.54E-22	**MAPK8IP2**	1.53427	2.39E-16	**SPATA17**	1.35081	8.99E-03
XBP1	1.74112	1.13E-22	**ICAM1**	1.52949	5.23E-07	**MAGEA2**	1.35022	2.56E-02
DDIT3	1.73676	2.00E-08	**ATG9B**	1.52471	1.98E-04	**LOC100506385**	1.34892	4.83E-02
LAMB2P1	1.72647	1.20E-02	**TAP1**	1.51876	1.32E-13	**SLC3A2**	1.34797	3.26E-56
CPEB1	1.72361	4.73E-06	**CLGN**	1.51212	1.29E-02	**TSEN15**	1.34645	3.59E-18
CRHR1-IT1	1.72346	2.89E-03	**LONRF3**	1.50870	3.73E-03	**LOC399744**	1.34510	1.81E-04
RBCK1	1.72280	1.88E-14	**HSBP1L1**	1.50389	1.33E-21	**CHD5**	1.34368	1.68E-02
SPIRE1	1.72211	7.67E-38	**MXD1**	1.50363	2.07E-19	**FTH1**	1.34363	3.06E-21
TPRA1	1.71939	2.08E-27	**GFPT1**	1.50336	1.07E-31	**SLC16A8**	1.34330	3.97E-02
SLC17A7	1.71706	8.16E-04	**PTP4A3**	1.50188	7.91E-03	**IRS2**	1.34295	3.71E-15
TMEM40	1.71558	1.18E-20	**RNF32**	1.49620	5.63E-03	**COA6**	1.34212	8.45E-07
RPS10P7	1.70704	2.78E-07	**TG**	1.48981	3.09E-02	**LRRC73**	1.34149	1.61E-02
SQSTM1	1.70486	3.86E-13	**BTC**	1.48658	8.36E-03	**SARS**	1.34077	1.67E-30
IDNK	1.70210	3.01E-03	**RASIP1**	1.48396	2.75E-06	**HS1BP3**	1.33650	7.04E-16
BBC3	1.69897	5.46E-12	**RNF216P1**	1.48308	2.92E-15	**ENO3**	1.32844	1.32E-06
SLC6A13	1.68862	1.56E-02	**PQLC2**	1.47994	5.30E-19	**PGPEP1**	1.32793	4.26E-08
SOCS2-AS1	1.68370	2.45E-02	**SAT2**	1.47810	1.40E-12	**TNFRSF10B**	1.32555	1.46E-14
LOC100506804	1.67954	2.28E-02	**AAK1**	1.47410	1.10E-17	**BHLHE40**	1.32297	4.44E-27
IFIT1	1.67396	8.76E-03	**ETV5**	1.46814	1.41E-06	**LOC646329**	1.32296	7.02E-04
LETM2	1.66755	1.51E-04	**TUBB2B**	1.46525	1.04E-11	**MOAP1**	1.31925	3.83E-09
HSD17B3	1.66511	3.01E-03	**PRKAB2**	1.46495	1.39E-11	**PTPRH**	1.31829	1.83E-02
SLPI	1.66294	2.01E-06	**ATP6V0E2-AS1**	1.46430	2.60E-03	**CPEB3**	1.31613	8.78E-11
OXLD1	1.65469	2.02E-15	**DGCR10**	1.46373	4.19E-06	**ZNF221**	1.31029	3.00E-02
GSTO2	1.65088	2.37E-03	**FAM161B**	1.46165	7.71E-07	**GOLGA7B**	1.31027	3.70E-02
DLK2	1.64926	3.75E-06	**LOC100129534**	1.45843	1.77E-07	**KLF7**	1.31006	1.51E-05
TRPV6	1.64296	1.01E-04	**TFEB**	1.45534	2.11E-17	**TRIM58**	1.30915	2.11E-02
VIMP	1.63585	3.17E-11	**RELB**	1.45107	3.57E-09	**DGCR9**	1.30913	1.14E-05
FADS3	1.63190	2.00E-13	**CYSTM1**	1.44796	4.20E-26	**MAP1LC3A**	1.30892	2.46E-08
CTH	1.63173	1.61E-04	**PTCH2**	1.44501	2.93E-04	**CLDN15**	1.30739	4.52E-08
LOC554206	1.62945	4.74E-04	**MIR100HG**	1.44415	1.75E-02	**C14orf159**	1.30686	4.07E-02
ERN1	1.62367	2.53E-13	**CCL22**	1.44233	1.32E-02	**ODF3B**	1.30672	3.34E-03
LOC100289187	1.62237	4.77E-02	**DOK7**	1.44202	1.97E-05	**TUBE1**	1.30387	2.15E-09
STX11	1.61903	8.64E-06	**LOC100507206**	1.44182	1.37E-02	**CTNS**	1.30323	5.56E-12
EPAS1	1.61638	1.47E-11	**PARD3B**	1.43672	1.57E-02	**WDR45**	1.30290	5.70E-07
LHFP	1.61482	2.53E-04	**GPR56**	1.43606	1.89E-11	**DET1**	1.30201	1.20E-03
MAFF	1.61379	3.78E-02	**SYBU**	1.43505	3.92E-10	**BLOC1S3**	1.30111	5.83E-07
KRT17	1.61082	7.63E-10	**PHYHIPL**	1.43099	2.77E-03	**LRRC37B**	1.29900	1.06E-08
LOC100507501	1.60453	7.01E-03	**FAM22D**	1.42830	5.91E-03	**ASS1**	1.29884	1.77E-03
GGACT	1.60314	1.69E-02	**PRSS22**	1.42752	7.85E-27	**CENPT**	1.29865	1.68E-02
MYO15B	1.60304	2.16E-04	**SBDSP1**	1.42644	3.67E-10	**LOC643650**	1.29864	1.22E-02
IGDCC4	1.60256	1.81E-09	**RAB17**	1.42499	8.20E-15	**ZCWPW1**	1.29837	1.01E-05
ZNF674	1.59903	9.07E-14	**ZNF772**	1.42430	9.14E-05	**LOC100128822**	1.29802	2.46E-04
TNFAIP3	1.59438	1.49E-02	**CDPF1**	1.41557	1.31E-09	**SLC43A1**	1.29750	6.61E-04
AOC3	1.59415	2.70E-08	**CHRM4**	1.41461	4.86E-03	**LMLN**	1.29516	3.00E-14
DAPP1	1.59266	2.69E-17	**NBR2**	1.41151	7.88E-13	**PYCR1**	1.28843	2.74E-11
LOC100133091	1.58656	4.61E-03	**OSCP1**	1.41002	1.68E-05	**SH3TC1**	1.28683	3.58E-05
SGPP2	1.58373	1.39E-11	**LINC00471**	1.40879	1.37E-02	**RIOK3**	1.28547	5.43E-17
KCNH8	1.58273	1.37E-02	**IFIT3**	1.40823	4.18E-03	**SLC8A2**	1.28378	4.76E-03
LINC00622	1.58250	7.16E-09	**CARD16**	1.40794	2.75E-02	**AMOTL2**	1.28226	2.58E-25
TNFSF4	1.58086	3.71E-02	**RAET1L**	1.40486	8.44E-06	**IFIT5**	1.28223	4.37E-03
TNFRSF9	1.57930	2.97E-04	**TOB2P1**	1.39823	2.81E-03	**ZNF572**	1.28019	6.66E-04
CBX4	1.57836	3.14E-12	**HERPUD1**	1.39714	4.48E-21	**CCDC121**	1.27950	2.75E-06
PLCH2	1.57764	1.35E-03	**CATSPER2**	1.39705	3.07E-03	**ANK2**	1.27884	6.44E-08
CCDC148	1.57714	2.08E-03	**ACAD11**	1.39683	3.92E-10	**MTHFR**	1.27760	2.47E-13
C14orf79	1.57693	1.85E-07	**ABL2**	1.39418	2.01E-11	**ANKRD33B**	1.27744	1.07E-05
CD72	1.57550	1.60E-02	**COX19**	1.39391	9.81E-20	**ACTA2**	1.27740	3.80E-04
GLT25D2	1.57457	4.11E-02	**YPEL5**	1.38952	3.64E-15	**MFSD6L**	1.27638	4.04E-05
PSMB9	1.57284	2.53E-07	**FLJ20021**	1.38917	8.10E-06	**LRRC27**	1.27594	3.55E-02
STC2	1.57282	1.14E-10	**LOC100289495**	1.38848	1.66E-03	**MICAL2**	1.27448	2.03E-07
LBX2-AS1	1.56918	4.14E-15	**RPL23AP7**	1.38662	2.64E-05	**MORN4**	1.27429	2.60E-10
DDIT4	1.56897	7.62E-04	**FAM206A**	1.38571	3.73E-13	**ZNF84**	1.27202	1.58E-08
MAPK8	1.56707	2.42E-02	**NOXA1**	1.38499	1.38E-03	**MIR22HG**	1.27018	9.29E-03
CCDC157	1.56393	4.15E-09	**MAPK8IP1**	1.38445	2.56E-02	**TOM1**	1.26793	3.55E-11
SCARF1	1.56360	1.93E-02	**WBSCR27**	1.38407	7.33E-03	**MX2**	1.26754	2.34E-02
RND3	1.56158	2.01E-30	**C17orf97**	1.38186	6.08E-05	**BCDIN3D**	1.26712	1.89E-08
LOC100130357	1.56031	2.41E-03	**PTK6**	1.37462	1.31E-04	**AGPAT4**	1.26669	2.97E-03
GTPBP2	1.56020	1.29E-19	**KLF11**	1.37019	3.96E-11	**MGC39372**	1.26572	2.39E-03
C6orf48	1.55653	1.14E-19	**TGFB1I1**	1.36277	1.33E-03	**ZBED3**	1.26555	1.24E-07
LOC645638	1.55532	1.33E-05	**NEURL2**	1.35871	1.61E-04	**SLC15A3**	1.26437	2.35E-03
ZNF263	1.55256	7.30E-09	**UFM1**	1.35786	3.68E-05	**SNHG15**	1.26430	2.26E-05
ABCA3	1.55168	1.20E-07	**MORN3**	1.35686	3.54E-03	**ARG2**	1.26210	1.64E-02
TMEM140	1.54776	2.64E-02	**RAB30**	1.35452	6.06E-05	**ELOVL7**	1.26174	2.11E-09
KIAA1211	1.54535	9.32E-09	**IRF1**	1.35309	7.32E-13	**FAM131A**	1.26142	8.54E-08

FAHD2CP	1.26006	5.95E-03	**AXL**	1.14482	2.02E-09	**NDUFA4L2**	1.06679	3.45E-03
IQCG	1.25996	1.27E-04	**ELL2**	1.14375	2.87E-07	**MIF4GD**	1.06629	2.04E-04
RRNAD1	1.25833	2.61E-04	**FBLIM1**	1.14196	1.41E-11	**TTC21A**	1.06520	1.07E-02
ABLIM2	1.25630	1.12E-02	**PLAC8L1**	1.14165	3.86E-02	**MED18**	1.06296	3.82E-12
KLF4	1.24908	3.14E-11	**HSPA13**	1.14147	1.41E-08	**TSNARE1**	1.06246	2.07E-14
ODF2L	1.24737	4.35E-07	**HHLA3**	1.14074	5.04E-03	**ZFAND3**	1.06099	7.16E-16
TRNP1	1.24623	6.82E-05	**SLC7A1**	1.14042	5.80E-17	**LITAF**	1.06029	3.52E-12
SRP19	1.24543	4.19E-04	**SNHG1**	1.13944	3.87E-06	**ZNF134**	1.05862	1.04E-05
LOC653712	1.24507	2.69E-03	**LOC100131096**	1.13938	1.27E-04	**RNMT**	1.05765	7.49E-08
MICALCL	1.24500	3.70E-06	**KIF17**	1.13748	2.41E-06	**HSPBAP1**	1.05665	2.15E-10
ZC2HC1A	1.24489	8.33E-03	**PABPC1L**	1.13733	2.30E-18	**SDSL**	1.05546	2.26E-08
LAMC2	1.24483	6.16E-07	**GOLGA8B**	1.13342	4.59E-08	**C11orf54**	1.05466	1.21E-08
DHX58	1.24421	2.36E-05	**GCC1**	1.13271	3.83E-23	**ANGPT1**	1.05339	4.33E-07
CEBPD	1.24094	1.51E-07	**LOC100129858**	1.13168	6.35E-03	**IFI35**	1.05276	1.82E-02
ABCA12	1.23985	2.07E-06	**GEM**	1.12986	7.63E-03	**UBXN11**	1.05265	3.31E-04
KLF10	1.23874	1.76E-02	**PIM3**	1.12905	1.34E-13	**SMCR7**	1.04920	3.62E-08
BTG1	1.23818	4.61E-16	**YBEY**	1.12612	7.44E-06	**POLR3C**	1.04618	2.23E-14
GAS7	1.23769	1.64E-02	**MTO1**	1.12396	9.17E-16	**DGAT2**	1.04457	3.06E-06
STOML1	1.23575	2.10E-07	**TRAPPC2P1**	1.12227	4.06E-05	**PARP9**	1.04431	1.58E-02
STAT5A	1.23511	3.00E-04	**WDR5B**	1.12126	1.45E-12	**ZNF26**	1.04367	3.44E-05
NFKB2	1.23478	4.22E-09	**TTC18**	1.12047	2.54E-03	**PDGFB**	1.04348	2.02E-10
LOC100131067	1.23441	4.93E-02	**RIT1**	1.11999	2.58E-16	**CSF2RA**	1.04316	1.06E-11
GADD45B	1.23337	3.08E-15	**GOT1**	1.11964	1.06E-09	**PLEKHG1**	1.04297	1.31E-05
SNHG8	1.22958	5.60E-10	**TMEM186**	1.11892	2.02E-04	**TRIML2**	1.04294	9.44E-04
EPHA1-AS1	1.22952	2.75E-03	**CFB**	1.11769	2.76E-02	**KLF12**	1.04284	1.60E-08
SLC16A5	1.22865	5.29E-06	**COL1A1**	1.11514	4.67E-12	**THAP9-AS1**	1.04244	7.16E-06
NCOA7	1.22777	4.02E-14	**KCTD15**	1.11421	2.11E-08	**CASZ1**	1.04225	1.16E-06
LOC728730	1.22662	3.32E-02	**ABCC3**	1.11221	1.20E-02	**AREG**	1.03811	2.97E-03
FLT3LG	1.22548	6.48E-04	**PPP2R5B**	1.11112	3.17E-08	**ZNF226**	1.03760	8.88E-08
MARCH4	1.22526	2.05E-02	**ST7L**	1.10971	1.86E-02	**MOSPD2**	1.03642	2.55E-11
ZNF699	1.22365	6.73E-06	**SAT1**	1.10868	9.19E-15	**SLC16A11**	1.03580	1.21E-02
MILR1	1.22187	3.18E-02	**DTX3L**	1.10831	1.99E-07	**ZSCAN21**	1.03541	1.96E-09
PSORS1C1	1.22040	6.78E-04	**C7orf13**	1.10827	3.13E-04	**C11orf74**	1.03534	4.50E-03
PMAIP1	1.21970	3.44E-10	**ALKBH2**	1.10582	3.62E-06	**GPHA2**	1.03526	1.36E-02
SFTA1P	1.21548	9.44E-03	**FAHD2B**	1.10571	9.14E-04	**PVR**	1.03429	1.97E-17
FMNL1	1.21537	1.54E-02	**PBLD**	1.10518	1.83E-04	**LOC652276**	1.03408	7.31E-04
KIFC3	1.21345	2.69E-14	**ROPN1L**	1.10462	1.29E-02	**WDR78**	1.03306	2.90E-03
FLJ42627	1.20921	4.30E-09	**LOC170425**	1.10336	1.33E-02	**ZNF397**	1.03187	3.74E-03
RRAS	1.20915	8.53E-05	**GLI4**	1.10309	8.06E-08	**PRDX1**	1.03165	1.28E-08
SERPINE1	1.20738	3.26E-04	**CYP4V2**	1.10216	1.02E-02	**STYXL1**	1.03088	1.17E-06
TAF12	1.20734	5.22E-07	**ZNF566**	1.10157	1.81E-06	**AARS**	1.03010	2.09E-10
SLFNL1-AS1	1.20717	7.48E-04	**ZNF517**	1.10072	5.38E-08	**ELF3**	1.02926	5.62E-13
CCND2	1.20019	1.83E-03	**POLL**	1.09878	1.41E-10	**KIAA1908**	1.02829	2.05E-02
HMGCL	1.19950	2.18E-09	**ENDOV**	1.09846	3.91E-05	**ZNF420**	1.02817	1.56E-05
C21orf67	1.19802	2.05E-03	**NEU1**	1.09797	1.54E-12	**GBP3**	1.02699	6.87E-08
LRIF1	1.19791	8.86E-12	**RAB9A**	1.09677	1.41E-08	**IL1RAP**	1.02652	1.55E-04
LAMTOR3	1.19697	7.16E-17	**TMEM128**	1.09624	3.92E-03	**TES**	1.02578	8.47E-20
FBXO36	1.19321	4.13E-11	**GPR124**	1.09555	9.67E-03	**SLC20A1**	1.02537	2.50E-07
IRF7	1.18871	1.11E-06	**RSPH10B**	1.09356	1.20E-02	**KRT80**	1.02406	1.02E-06
CCDC112	1.18556	4.13E-04	**SLC25A14**	1.09212	5.55E-03	**SERTAD4-AS1**	1.02375	7.12E-04
CLDN9	1.18330	9.03E-05	**PIM1**	1.09079	3.12E-16	**DUSP14**	1.02325	1.18E-06
BET1	1.18217	9.23E-18	**KLHL24**	1.09068	2.35E-05	**IQCB1**	1.02077	3.50E-08
THBS3	1.18167	1.04E-02	**SMCR8**	1.08976	5.79E-18	**DUSP8**	1.02052	2.97E-06
PSPH	1.17960	3.37E-29	**OPTN**	1.08811	7.76E-05	**ITPKA**	1.01978	1.21E-03
AP5Z1	1.17918	1.75E-13	**TRIM15**	1.08725	2.44E-04	**NKX6-1**	1.01949	1.92E-02
PEX12	1.17895	1.20E-07	**RAPH1**	1.08586	1.24E-07	**ZFP36**	1.01841	1.83E-08
PCDHB19P	1.17884	1.41E-02	**H1F0**	1.08568	7.70E-08	**GRB10**	1.01819	2.79E-06
ATP10A	1.17859	6.44E-06	**DUSP10**	1.08473	8.15E-09	**NEAT1**	1.01442	1.91E-09
RBKS	1.17739	8.08E-03	**STPG1**	1.08314	9.95E-16	**LOC253039**	1.01431	4.09E-06
ARL8B	1.17556	3.31E-25	**TTLL3**	1.08170	1.83E-03	**FAM21A**	1.01405	1.91E-06
LOC100506190	1.17045	8.31E-07	**C4A**	1.07902	6.86E-03	**RP9**	1.01309	4.68E-07
RNF41	1.16914	5.00E-09	**BTN2A2**	1.07876	6.44E-06	**EDF1**	1.01237	6.99E-20
ADAMTSL5	1.16888	3.04E-08	**FAM111A**	1.07868	7.76E-10	**CCDC9**	1.01237	1.31E-12
LOC729678	1.16708	1.05E-02	**HIVEP1**	1.07662	2.77E-07	**STX1A**	1.01179	2.29E-02
TRIM56	1.16204	7.59E-08	**NABP1**	1.07478	1.97E-08	**METTL23**	1.01094	1.78E-06
MOSPD1	1.16090	2.83E-06	**CIDECP**	1.07444	1.59E-04	**EXD3**	1.01048	3.83E-02
NFE2L1	1.15901	2.62E-10	**MARS**	1.07399	1.22E-18	**MYEOV**	1.00885	1.80E-17
AOC2	1.15446	8.64E-04	**WDR25**	1.07186	1.38E-02	**GARS**	1.00875	3.65E-12
MX1	1.15331	7.84E-04	**PRKCE**	1.07064	9.13E-10	**ZNF460**	1.00864	1.89E-05
ZNF597	1.15163	9.31E-04	**CSF1**	1.07034	1.80E-03	**WIPI1**	1.00787	1.95E-02
ZDHHC11	1.14894	5.36E-04	**RRAGC**	1.07032	7.18E-07	**NTN4**	1.00782	6.60E-04
KIAA1984-AS1	1.14749	9.09E-07	**ZNF598**	1.07018	8.82E-14	**ZNF181**	1.00751	1.10E-06
ERVV-2	1.14563	1.33E-04	**L1CAM**	1.06885	1.51E-03	**FLJ42969**	1.00662	2.86E-02
BACE1	1.14561	4.26E-05	**PGLS**	1.06793	2.50E-04	**LOC388152**	1.00655	9.42E-05

LINC00152	1.00614	2.06E-03	**COX7B**	-1.05489	1.31E-21	**PXMP4**	-1.12715	4.94E-11
MTHFD2	1.00613	1.34E-06	**LOC100506599**	-1.05777	3.32E-03	**VSIG10L**	-1.12876	3.54E-03
CSF1R	1.00491	4.62E-02	**MEX3A**	-1.05919	1.82E-04	**OAZ2**	-1.12914	3.20E-04
C19orf21	1.00348	2.93E-08	**SMARCA1**	-1.05975	1.31E-04	**ARHGAP29**	-1.12953	3.63E-07
SNHG5	1.00272	2.00E-09	**HMMR**	-1.06018	1.20E-04	**DOCK8**	-1.12969	8.44E-10
CYB5D1	1.00265	7.76E-03	**EHMT2**	-1.06136	7.89E-15	**HIST1H2BO**	-1.13042	8.26E-03
ATP6V0A1	1.00194	2.58E-11	**FANCA**	-1.06187	1.80E-05	**ZNF175**	-1.13043	2.27E-04
N4BP2L2	1.00169	5.70E-04	**TMEM201**	-1.06188	9.61E-13	**LPAR1**	-1.13054	1.71E-03
TIMM9	1.00111	2.67E-11	**HPRT1**	-1.06189	1.38E-06	**HADH**	-1.13084	3.68E-14
IL6ST	1.00101	4.59E-05	**CDT1**	-1.06257	2.04E-08	**FBN3**	-1.13235	2.92E-03
LOC100128531	-1.00208	2.30E-02	**TROAP**	-1.06380	1.41E-10	**CSRP2**	-1.13421	3.85E-03
CHAF1B	-1.00217	1.83E-11	**PIR**	-1.06381	1.14E-08	**SLC2A1**	-1.13438	4.56E-05
DLGAP5	-1.00284	2.64E-12	**CRYZ**	-1.06433	5.65E-08	**HN1**	-1.13452	1.44E-10
KRT19	-1.00366	3.25E-11	**FAM122B**	-1.06487	3.95E-11	**MIR205HG**	-1.13594	4.55E-02
SKA3	-1.00373	4.77E-07	**RASSF2**	-1.06668	1.17E-05	**IGFL2**	-1.13729	3.75E-03
TMEM164	-1.00535	1.38E-04	**PFN2**	-1.06847	1.92E-07	**RGS19**	-1.13769	5.48E-03
MYCBP	-1.00539	1.04E-06	**FAM171A2**	-1.06923	2.26E-03	**HIST1H2AK**	-1.13937	1.60E-07
ACTRT3	-1.00578	8.35E-03	**SLC44A3**	-1.06949	1.35E-07	**COL17A1**	-1.14157	1.24E-04
MUC16	-1.00626	2.85E-02	**CDH24**	-1.06953	6.29E-06	**USPL1**	-1.14290	4.24E-10
UBASH3B	-1.00788	1.63E-11	**SORD**	-1.07028	1.17E-06	**SNORA55**	-1.14302	1.77E-07
CD320	-1.00946	4.86E-05	**PCDHB2**	-1.07448	1.25E-08	**IL17RE**	-1.14345	4.67E-06
CD81	-1.01014	3.81E-14	**PARPBP**	-1.07630	4.95E-07	**HIST1H2BJ**	-1.14377	3.75E-02
PPAP2B	-1.01057	2.97E-10	**IDI1**	-1.07918	5.79E-06	**USP13**	-1.14451	7.50E-11
SHPK	-1.01289	3.70E-08	**USP5**	-1.07919	1.75E-11	**PLK4**	-1.14490	2.27E-10
ADCK3	-1.01332	4.95E-05	**HCAR1**	-1.08081	3.39E-07	**FANCI**	-1.14613	5.27E-06
SPTBN2	-1.01339	4.63E-07	**FANCD2**	-1.08104	5.17E-06	**LOC642846**	-1.14615	1.72E-07
PLA2G4A	-1.01546	1.49E-03	**LAMB1**	-1.08344	8.80E-14	**C16orf59**	-1.14652	4.53E-05
ACOT11	-1.01602	1.72E-04	**CD46**	-1.08478	2.24E-02	**POLR3K**	-1.14705	6.09E-14
QSOX1	-1.01701	3.44E-10	**TRIM62**	-1.08522	3.84E-06	**PLCG1**	-1.14806	1.92E-14
PGAM1	-1.01766	2.61E-12	**RBM14**	-1.08604	1.16E-04	**CDCA7**	-1.14807	8.05E-08
C19orf57	-1.01830	2.79E-03	**TMTC4**	-1.08648	4.54E-06	**KREMEN2**	-1.14928	7.01E-04
NAAA	-1.01927	1.80E-07	**MPND**	-1.08713	2.54E-02	**PACSIN1**	-1.14932	4.26E-02
GLB1L2	-1.02026	2.64E-05	**PGM1**	-1.08783	1.14E-11	**CC2D2A**	-1.14967	8.41E-03
PSMA1	-1.02059	7.17E-18	**PDK1**	-1.08882	2.33E-09	**DCTPP1**	-1.14971	2.97E-16
HIST1H2AL	-1.02084	1.44E-02	**ARHGDIB**	-1.08894	1.19E-17	**NYNRIN**	-1.14991	1.50E-04
SCARB1	-1.02097	7.50E-06	**FGFR4**	-1.08911	2.72E-04	**TMEM48**	-1.15012	2.39E-09
SHCBP1	-1.02136	3.89E-06	**GABRA3**	-1.08982	2.11E-04	**GPRC5C**	-1.15059	8.85E-04
LGR4	-1.02230	2.42E-09	**TSC22D2**	-1.09033	4.61E-03	**ATP7B**	-1.15267	4.20E-02
CDC25A	-1.02257	3.91E-04	**MAD2L1**	-1.09106	1.92E-09	**E2F8**	-1.15292	2.63E-12
IGSF8	-1.02476	2.60E-04	**KANSL1-AS1**	-1.09160	9.18E-03	**ESCO2**	-1.15329	1.34E-05
FAM83D	-1.02491	1.19E-09	**CLCN2**	-1.09246	5.54E-08	**EFNA3**	-1.15343	2.35E-03
SMC4	-1.02495	7.19E-09	**MNX1**	-1.09802	1.54E-02	**ZYG11A**	-1.15747	3.61E-06
RIMS3	-1.02778	4.63E-03	**CDC20**	-1.09853	2.28E-08	**GDF11**	-1.16287	1.17E-05
ZAK	-1.02830	1.54E-07	**KIAA1549L**	-1.09857	2.52E-02	**ASF1B**	-1.16292	2.07E-09
EML3	-1.02872	6.26E-12	**HCFC1R1**	-1.09863	1.43E-04	**FAH**	-1.16341	2.84E-05
FLJ23867	-1.03019	1.09E-04	**SPC24**	-1.09988	3.90E-11	**MCM6**	-1.16405	8.26E-14
CCNA2	-1.03145	1.60E-05	**RNF182**	-1.10021	2.68E-02	**WDR76**	-1.16500	2.11E-16
CEBPA	-1.03197	8.21E-04	**FAM40B**	-1.10035	2.30E-03	**WDHD1**	-1.16538	1.05E-08
SHISA2	-1.03293	4.93E-02	**NTHL1**	-1.10073	1.27E-03	**SLC40A1**	-1.16634	4.99E-03
PDCL	-1.03306	2.48E-13	**AURKA**	-1.10117	6.06E-09	**EXO1**	-1.16687	8.49E-05
CUEDC2	-1.03314	3.73E-03	**PSMD3**	-1.10147	1.94E-20	**MAN1A1**	-1.16724	1.62E-02
C1QL1	-1.03385	2.92E-02	**E2F7**	-1.10167	6.98E-04	**FASN**	-1.16940	1.04E-17
MSH2	-1.03446	1.97E-17	**PARP1**	-1.10191	1.15E-08	**KIAA0101**	-1.17015	1.32E-07
IDH2	-1.03521	2.56E-04	**SARS2**	-1.10261	3.25E-07	**RAB27B**	-1.17375	9.99E-04
GPR137C	-1.03625	5.54E-03	**FUT8-AS1**	-1.10349	7.93E-04	**KIAA1462**	-1.17605	1.50E-08
GGCT	-1.03699	1.44E-13	**NR2F1**	-1.10447	9.05E-04	**SPR**	-1.17714	1.14E-12
TTF2	-1.03705	8.06E-07	**DLX2**	-1.10544	7.77E-08	**RNF141**	-1.17920	1.09E-15
ARHGEF26	-1.03772	8.73E-06	**SLC35G1**	-1.10555	7.87E-04	**MXD3**	-1.17934	1.61E-05
BUB1B	-1.03798	1.50E-11	**HIST2H2BE**	-1.10795	4.35E-07	**SLC30A3**	-1.18062	4.91E-02
BLM	-1.03851	1.08E-07	**SIRPA**	-1.10860	8.96E-07	**AK4**	-1.18168	1.02E-10
KDM1A	-1.03986	5.88E-13	**LHX4**	-1.10880	2.66E-04	**CHAF1A**	-1.18177	2.07E-17
TRIP13	-1.04103	4.93E-06	**CCNB1**	-1.11037	1.17E-17	**PAICS**	-1.18255	1.11E-08
SMARCB1	-1.04108	1.65E-08	**ABCA2**	-1.11077	6.41E-04	**GATA2**	-1.18261	1.09E-08
CCT4	-1.04259	2.21E-12	**UPK1B**	-1.11240	2.11E-04	**HELLS**	-1.18487	2.69E-14
PFKL	-1.04340	1.47E-10	**HIST1H3I**	-1.11284	2.10E-04	**IFRD1**	-1.18582	1.80E-02
POLR3G	-1.04387	2.66E-03	**TRIM16L**	-1.11305	3.67E-07	**CTSL2**	-1.19058	2.05E-10
SLC45A3	-1.04523	2.71E-06	**UFD1L**	-1.11385	7.86E-08	**POLE**	-1.19068	4.43E-21
TTK	-1.04524	2.39E-10	**TIPIN**	-1.11432	7.77E-10	**POU5F1**	-1.19212	1.36E-03
CENPV	-1.04651	1.27E-05	**FBXO33**	-1.11454	5.52E-10	**SNORA69**	-1.19244	2.94E-03
GALM	-1.04720	5.66E-04	**PCNA**	-1.11611	1.17E-08	**SPTLC3**	-1.19487	3.08E-02
PPP5C	-1.04751	9.25E-11	**TTC32**	-1.11822	5.32E-05	**TUSC3**	-1.19745	5.36E-03
SAPCD2	-1.05131	1.05E-09	**GYLTL1B**	-1.11875	4.30E-07	**PSCA**	-1.19884	1.69E-02
UBAC1	-1.05145	2.34E-11	**GOT2**	-1.11980	8.96E-07	**ABCC5**	-1.20103	5.27E-06
BAHCC1	-1.05167	4.32E-04	**HIST1H3J**	-1.12005	2.41E-04	**TUBA1B**	-1.20127	6.39E-11
MSH6	-1.05393	1.56E-28	**L3HYPDH**	-1.12486	2.50E-02	**CEP78**	-1.20170	2.04E-09
NMB	-1.05412	4.72E-03	**DLX3**	-1.12516	2.90E-03	**ZNF792**	-1.20225	7.55E-04
NCAPG2	-1.05448	1.17E-11	**DMBX1**	-1.12591	1.84E-02	**CTSC**	-1.20309	2.10E-07
CDK2AP1	-1.05471	1.10E-18	**AMPD2**	-1.12702	2.76E-08	**ISYNA1**	-1.20635	8.00E-10

LOC440288	-1.20796	1.25E-03	**ARID5B**	-1.31429	3.93E-06	**GPD1L**	-1.44499	2.13E-07
FAM105A	-1.20830	3.84E-03	**SUSD3**	-1.31581	7.50E-04	**PRICKLE2**	-1.44660	2.49E-04
OR2J3	-1.20978	3.84E-02	**OIP5**	-1.31700	3.28E-20	**NAALADL2**	-1.44751	1.24E-04
HIST1H2BL	-1.21028	5.37E-03	**SHROOM2**	-1.32022	4.34E-02	**SEMA6B**	-1.45425	1.69E-02
TMEM158	-1.21037	3.84E-03	**TSPAN13**	-1.32057	4.50E-12	**LOC730102**	-1.45697	3.73E-02
TRMT2B	-1.21147	8.43E-04	**ZIC2**	-1.32089	2.10E-05	**RFC3**	-1.46061	2.49E-14
SYT8	-1.21361	1.09E-02	**CYP24A1**	-1.32111	4.29E-08	**MEOX1**	-1.46134	5.11E-04
SPAG5	-1.21665	4.46E-09	**HIST1H2AG**	-1.32120	6.90E-04	**DEPDC7**	-1.46321	1.05E-03
PRAME	-1.21697	2.97E-06	**ZNRF3**	-1.32193	3.68E-12	**MYBL2**	-1.46501	1.31E-17
KLK6	-1.21720	1.26E-02	**EPS8**	-1.32255	1.48E-06	**SH3TC2**	-1.47363	1.77E-07
LINC00085	-1.21802	1.64E-06	**HIST2H3D**	-1.32290	1.44E-06	**PCDHA4**	-1.47945	9.65E-04
PIDD	-1.21805	2.41E-08	**FUT4**	-1.32732	5.30E-08	**FAM117B**	-1.48302	1.15E-08
HSP90AB1	-1.21825	4.15E-13	**FERMT1**	-1.32793	3.76E-12	**CAPN5**	-1.48513	1.57E-04
PIF1	-1.21962	2.00E-05	**MCM4**	-1.32858	2.39E-41	**EIF5**	-1.48638	7.78E-36
ADD3	-1.22231	2.95E-07	**HSPB1**	-1.33219	8.46E-10	**HPSE**	-1.48859	1.60E-03
HIST1H2BH	-1.22241	8.22E-07	**CEP128**	-1.33399	9.80E-11	**RPS26**	-1.49968	1.12E-07
CLSPN	-1.22437	3.98E-17	**KIF20A**	-1.33465	1.59E-11	**MTRNR2L2**	-1.50014	3.73E-02
B4GALT6	-1.22569	1.10E-13	**TNS4**	-1.33468	3.84E-02	**CAB39L**	-1.50224	8.78E-08
EEPD1	-1.22643	1.77E-04	**RFC5**	-1.33584	2.85E-08	**SECTM1**	-1.50444	3.34E-09
HIST1H4D	-1.22805	2.27E-09	**TNNT3**	-1.34148	5.20E-03	**HSPA2**	-1.50943	4.95E-07
TCF7	-1.22922	3.76E-02	**ITGB8**	-1.34432	8.95E-05	**HSPH1**	-1.51023	1.50E-27
PFKFB3	-1.22961	2.15E-04	**BMP7**	-1.34449	3.08E-16	**FABP5**	-1.51054	4.93E-09
PANX2	-1.23451	1.91E-03	**XRCC6BP1**	-1.34469	8.30E-07	**BZRAP1-AS1**	-1.51617	2.27E-02
MMP9	-1.23630	1.04E-02	**GPI**	-1.34615	2.20E-18	**HIST1H3C**	-1.51676	1.56E-07
RNU12	-1.23904	2.15E-04	**GPER**	-1.34674	3.30E-07	**FREM2**	-1.51976	2.24E-02
PVRL1	-1.23951	5.71E-08	**BCL11A**	-1.34779	5.25E-06	**PLOD1**	-1.52552	3.88E-16
SLC25A1	-1.24203	4.50E-12	**FGFR3**	-1.35197	6.10E-03	**GAMT**	-1.52556	3.31E-04
RTEL1	-1.24232	1.56E-06	**HSPA1B**	-1.35242	1.73E-08	**SLC7A2**	-1.52664	1.85E-05
GHRLOS	-1.24237	5.22E-04	**PHLPP1**	-1.35350	8.87E-08	**LRP4**	-1.52714	3.13E-04
DOK4	-1.24335	1.18E-06	**TNFAIP8**	-1.35552	1.57E-11	**ITIH5**	-1.53509	3.56E-03
SCN1B	-1.24347	1.22E-03	**FAM102B**	-1.35708	4.16E-11	**HOXB5**	-1.53972	1.10E-06
SMARCA2	-1.24380	2.06E-06	**FOS**	-1.35921	1.48E-05	**B4GALNT1**	-1.54017	2.26E-12
GMNN	-1.24418	2.03E-10	**GALNT12**	-1.36287	2.91E-03	**ROM1**	-1.54351	3.17E-02
DHFR	-1.24488	8.65E-08	**HIST1H4B**	-1.36537	4.38E-09	**STRA13**	-1.54411	9.94E-25
RECQL4	-1.24504	2.63E-18	**KIF4B**	-1.36696	1.03E-02	**ARRB1**	-1.54828	3.72E-13
TMEM143	-1.24748	4.20E-04	**HOXB6**	-1.36865	4.62E-04	**FBXO41**	-1.55435	1.18E-04
PBK	-1.24756	1.43E-08	**ZNF618**	-1.36998	3.23E-06	**CDC45**	-1.55543	3.25E-09
LPCAT1	-1.24785	7.12E-21	**HIST1H4L**	-1.37117	1.05E-08	**PTCH1**	-1.55724	1.86E-09
KREMEN1	-1.24808	1.22E-06	**RFX7**	-1.37168	1.41E-25	**SOX4**	-1.55810	7.18E-12
TK1	-1.24957	3.09E-14	**GATSL2**	-1.37658	1.77E-06	**UHRF1**	-1.55840	2.02E-38
TMEM98	-1.24991	5.64E-04	**ADAM11**	-1.37672	3.44E-06	**COL9A3**	-1.56509	8.41E-07
RAD54B	-1.25273	2.69E-25	**SPC25**	-1.37716	8.83E-07	**FHOD1**	-1.56743	4.29E-14
DUSP13	-1.25384	2.01E-02	**COX7A2**	-1.38014	7.77E-04	**CDX2**	-1.57090	4.49E-13
GARNL3	-1.25411	1.09E-04	**P2RY2**	-1.38074	1.98E-04	**SLC6A6**	-1.57319	3.67E-12
GPRC5B	-1.25579	1.52E-07	**MYO7A**	-1.38328	7.68E-04	**VWA1**	-1.57414	2.94E-14
KIAA1524	-1.25837	1.44E-05	**ZBTB7C**	-1.38811	7.23E-06	**RBPMS2**	-1.57463	6.02E-03
SLC29A4	-1.26560	1.44E-06	**FLJ30403**	-1.39171	4.61E-02	**MSRB1**	-1.58463	3.15E-13
METTL7A	-1.26797	4.85E-03	**S100A2**	-1.39356	1.12E-02	**STMN3**	-1.58511	1.17E-09
ASIC1	-1.27177	4.17E-05	**TONSL**	-1.39395	5.39E-20	**JAKMIP3**	-1.58699	2.75E-07
NCAPH	-1.27258	2.53E-24	**FAM65A**	-1.39486	4.34E-02	**POLE2**	-1.59534	1.00E-10
TMEM97	-1.27299	1.03E-10	**IL22RA1**	-1.39572	1.46E-02	**UNG**	-1.59609	7.74E-16
ATAD5	-1.27315	3.51E-26	**SLC19A1**	-1.40109	4.64E-08	**ALPP**	-1.60288	2.22E-02
SNCG	-1.27371	3.61E-05	**RPS6KA5**	-1.40478	8.52E-06	**IGFBP2**	-1.60340	2.06E-02
DHCR24	-1.27569	1.05E-08	**E2F1**	-1.40524	4.44E-09	**NMU**	-1.60525	1.32E-02
RTKN2	-1.27830	8.78E-10	**CNIH2**	-1.40654	2.14E-13	**NOTUM**	-1.60567	1.27E-07
SLC9A3R1	-1.27870	6.11E-18	**ACTL10**	-1.40868	1.65E-07	**C5orf30**	-1.60818	2.81E-05
TMEM171	-1.27922	4.28E-02	**PRDX6**	-1.41247	3.56E-13	**TICRR**	-1.61226	3.55E-22
HSPB11	-1.27967	9.65E-12	**NOTCH3**	-1.41320	9.21E-11	**GLA**	-1.61449	1.34E-29
SFXN5	-1.28064	1.32E-10	**PCDHB8**	-1.41574	2.61E-02	**EFNA4**	-1.61663	3.18E-05
PRSS23	-1.28067	6.36E-12	**COL27A1**	-1.41644	1.30E-03	**HIST1H1D**	-1.61804	2.71E-04
LEPREL2	-1.28573	5.23E-07	**SLC29A1**	-1.41664	1.34E-06	**FAM69B**	-1.62119	2.01E-03
SLC2A1-AS1	-1.28615	9.59E-07	**LDHA**	-1.41692	5.30E-38	**KCNAB2**	-1.62223	1.10E-03
TERT	-1.29217	3.05E-03	**FRMD4B**	-1.41977	7.33E-09	**CHRD**	-1.62341	4.19E-02
MEIS2	-1.29242	1.21E-11	**B3GNT1**	-1.42042	4.47E-05	**FAM69A**	-1.62699	1.23E-04
HIST1H3G	-1.29414	1.27E-03	**SERPINB5**	-1.42672	2.67E-11	**SERPINF1**	-1.62711	3.64E-02
PTDSS1	-1.29950	2.00E-09	**DPP4**	-1.42730	5.07E-06	**RRM1**	-1.62839	1.77E-18
PMEL	-1.29982	2.43E-02	**SHC3**	-1.42925	4.27E-05	**MCM5**	-1.62919	5.20E-25
RRM2	-1.30105	1.16E-09	**SFTA2**	-1.42931	3.31E-02	**ZBED2**	-1.62940	1.01E-02
EPHB3	-1.30125	5.24E-09	**PALM3**	-1.42994	1.06E-02	**SRSF2**	-1.63130	7.44E-12
B4GALNT4	-1.30434	8.61E-06	**TEAD2**	-1.43013	4.80E-04	**CHRNA5**	-1.63324	7.37E-14
BRI3BP	-1.30719	1.00E-11	**BID**	-1.43057	6.24E-10	**NCAPD3**	-1.63341	9.95E-33
LMNB1	-1.30820	9.86E-14	**TSHZ1**	-1.43126	1.75E-02	**FKBP4**	-1.63607	6.41E-21
ZWINT	-1.30846	2.55E-15	**DUSP9**	-1.43144	3.61E-03	**SPAG4**	-1.63856	1.68E-04
KHK	-1.30875	2.46E-04	**TYMS**	-1.43311	1.33E-12	**BCL2L15**	-1.63891	2.19E-02
RARRES2	-1.30943	6.30E-06	**EMP2**	-1.43934	2.01E-09	**ALYREF**	-1.63922	4.68E-30
ERCC6L	-1.31124	8.29E-12	**DTL**	-1.44030	1.31E-23	**ZNF385A**	-1.64013	6.61E-13
POLD1	-1.31209	1.54E-09	**HIST1H4A**	-1.44148	4.34E-07	**PGF**	-1.64920	2.13E-02
FLJ13224	-1.31226	3.96E-02	**FAM111B**	-1.44289	3.08E-18	**HSPA4L**	-1.65140	1.66E-15

PLA2G4F	-1.65887	2.02E-04	**KRT6A**	-2.03952	8.77E-03	**SPP1**	-3.03114	2.44E-07
HIST1H4I	-1.66125	1.27E-04	**PRR15L**	-2.04390	1.10E-06	**IGFBP3**	-3.03715	6.13E-06
TBX3	-1.66265	3.62E-14	**CCL2**	-2.04515	6.57E-03	**ID3**	-3.06269	3.64E-05
PLA2G16	-1.66390	1.06E-03	**PARM1**	-2.05175	7.21E-03	**LFNG**	-3.08769	8.86E-13
C2orf54	-1.66423	9.06E-06	**IGFL4**	-2.05186	2.59E-19	**KRT5**	-3.09675	2.98E-03
MCM10	-1.66811	1.55E-14	**PTTG2**	-2.05233	2.18E-02	**MANSC4**	-3.13164	4.27E-03
HPGD	-1.67353	3.05E-03	**TMOD1**	-2.06356	2.40E-03	**FAM115C**	-3.13855	3.55E-30
BCL11B	-1.67594	9.09E-03	**HRCT1**	-2.07412	2.14E-04	**CHST4**	-3.15494	1.18E-04
HIST1H3H	-1.67993	6.72E-04	**GINS2**	-2.07761	1.32E-23	**ID1**	-3.17398	4.14E-09
HSPE1	-1.68029	3.51E-17	**KRTAP2-3**	-2.07786	6.04E-03	**SIGLEC14**	-3.26662	1.26E-02
HIST1H1B	-1.68509	2.09E-04	**CYP3A5**	-2.07807	2.06E-03	**SLC30A10**	-3.33706	2.27E-02
LTBP1	-1.68687	3.60E-06	**WWC3**	-2.08042	3.54E-06	**ZNF488**	-3.39367	4.84E-27
OMP	-1.68932	2.13E-03	**SERPINB2**	-2.08403	2.61E-02	**FAM213A**	-3.76053	1.05E-05
BRIP1	-1.68997	5.05E-17	**EDAR**	-2.08758	3.49E-05	**GPX2**	-3.78871	7.67E-05
CRABP2	-1.69252	3.11E-05	**PCSK2**	-2.09717	2.04E-04	**STC1**	-3.79224	9.93E-03
E2F2	-1.69351	5.85E-10	**RHOBTB1**	-2.10004	8.94E-12	**LHX1**	-3.87073	5.54E-05
SP5	-1.70026	3.50E-07	**TNS1**	-2.10404	9.32E-07	**SIGLEC5**	-3.92273	3.06E-07
KCNK5	-1.70127	3.30E-06	**AQP3**	-2.10428	5.32E-04	**MAP2K6**	-3.94073	1.47E-12
C20orf151	-1.70286	6.95E-06	**MARCKSL1**	-2.11595	8.49E-08	**EGLN3**	-3.98337	2.57E-17
PSMD1	-1.70773	1.24E-41	**BCAS1**	-2.13002	1.56E-03	**PPFIA4**	-4.59477	5.48E-18
MSX1	-1.71057	1.43E-05	**PARD6G**	-2.16476	2.64E-02	**CA9**	-4.87876	3.97E-06
SYTL4	-1.72212	6.74E-07	**C1orf186**	-2.16906	2.00E-03			
LSM3	-1.73041	3.48E-31	**HSPA8**	-2.17945	6.09E-23			
IQGAP2	-1.73143	1.87E-07	**MRVI1**	-2.18234	2.99E-02			
MPP1	-1.73740	1.82E-08	**HNMT**	-2.19130	2.13E-03			
SEMA3F	-1.73746	1.06E-09	**CLEC1A**	-2.19473	1.57E-02			
FAM156A	-1.74171	5.34E-03	**PDE4D**	-2.19756	1.99E-05			
FAM222A	-1.74595	2.22E-05	**NDRG2**	-2.20414	1.17E-17			
DDX60L	-1.74886	4.98E-02	**DNAJC22**	-2.20506	8.80E-03			
MALL	-1.75103	6.75E-09	**CRISPLD2**	-2.21717	3.52E-25			
SESTD1	-1.75214	4.13E-04	**TUBA4A**	-2.22576	3.96E-19			
SP8	-1.77637	9.66E-06	**ABCG1**	-2.23989	4.64E-02			
ALDOC	-1.77729	4.39E-19	**ISM2**	-2.24891	7.36E-05			
RAB40B	-1.78259	6.62E-06	**VTCN1**	-2.25003	1.34E-04			
DSCC1	-1.78504	1.29E-17	**CBR3**	-2.26184	5.98E-06			
RAD54L	-1.79835	1.59E-13	**MARC1**	-2.26396	1.71E-04			
IL17RB	-1.80013	2.32E-08	**C2CD4A**	-2.26504	1.71E-13			
MATN2	-1.80214	6.66E-10	**RGCC**	-2.27984	5.99E-03			
HMCN1	-1.80359	1.80E-02	**SMTNL2**	-2.28157	5.99E-07			
MID1	-1.80765	9.06E-08	**SMAD6**	-2.28212	1.12E-12			
ALDH3B2	-1.80898	2.41E-02	**HIST1H3A**	-2.28956	2.26E-08			
ZNF703	-1.83152	6.99E-20	**C7orf61**	-2.29424	5.54E-03			
MICALL2	-1.83399	1.79E-16	**CCNE2**	-2.30873	3.65E-20			
CCNE1	-1.83567	2.14E-08	**AKR1C3**	-2.30874	1.13E-09			
EPN3	-1.84584	1.62E-09	**RAB3A**	-2.31158	1.45E-12			
RNF157	-1.85532	4.58E-02	**RAPGEF5**	-2.35149	7.22E-09			
RASSF9	-1.85860	2.62E-02	**GABRP**	-2.36006	6.99E-03			
PFKFB4	-1.86330	2.64E-22	**PKP1**	-2.37856	2.77E-02			
FOXO4	-1.87122	9.52E-07	**LRP8**	-2.38367	5.14E-42			
LRRC45	-1.87530	4.94E-11	**TMC1**	-2.39836	2.06E-02			
ORC1	-1.88167	2.28E-27	**EDNRB**	-2.41789	3.50E-04			
GADD45G	-1.91310	4.77E-07	**ANK1**	-2.43614	3.62E-14			
SYT16	-1.91333	1.20E-02	**KRT13**	-2.43914	1.82E-03			
SNRNP25	-1.91633	7.00E-16	**AXIN2**	-2.45372	3.16E-16			
CDKN2C	-1.91770	4.95E-18	**TM4SF1**	-2.45655	2.42E-03			
PRRT4	-1.91886	4.21E-02	**LOC100506810**	-2.46360	7.50E-04			
SLC5A3	-1.92037	2.01E-13	**GCNT3**	-2.47321	2.81E-02			
ARRDC3	-1.93860	8.99E-14	**NES**	-2.48172	1.95E-13			
CSF2RB	-1.94520	4.88E-04	**CST1**	-2.50028	2.14E-02			
WNT11	-1.94897	1.68E-05	**KRTAP3-1**	-2.50333	6.31E-03			
HSP90AA1	-1.94993	2.81E-47	**BTBD11**	-2.51901	3.22E-02			
NRGN	-1.95190	1.12E-03	**RIMKLA**	-2.52478	1.55E-03			
ATP6V1B1	-1.95736	3.01E-04	**CD52**	-2.60828	7.23E-03			
MYCN	-1.95788	8.12E-07	**TNNI2**	-2.64214	1.93E-03			
PRSS35	-1.96714	4.34E-02	**AKNAD1**	-2.66545	2.28E-05			
STAB1	-1.99334	1.96E-03	**STOX2**	-2.67744	6.21E-05			
CTAGE6P	-1.99945	8.12E-03	**ABCA4**	-2.68780	2.22E-06			
ZSCAN4	-1.99970	1.43E-02	**FGFBP3**	-2.71165	2.92E-04			
ACPP	-2.00217	2.78E-07	**MIR210HG**	-2.75880	1.70E-02			
LIG1	-2.00393	1.37E-06	**SIGLEC6**	-2.77409	2.87E-03			
DPYSL4	-2.01155	2.91E-07	**APCDD1**	-2.84018	8.16E-12			
ADAM22	-2.01382	2.29E-02	**VANGL2**	-2.86530	5.64E-03			
LOC401164	-2.01789	2.83E-02	**APLN**	-2.87056	5.25E-04			
ANKRD37	-2.01913	1.04E-11	**NEU2**	-2.87100	1.33E-02			
NKD1	-2.03173	4.56E-17	**SGK2**	-2.87354	8.32E-16			
ID2	-2.03296	5.55E-18	**SLC16A10**	-2.88894	1.37E-10			
KRT15	-2.03533	4.75E-10	**TNFRSF19**	-2.98246	5.34E-16			
MMP20	-2.03703	2.25E-02	**LOC154761**	-3.02073	1.01E-21			

Supplementary Table 3. Differentially expressed genes (adjusted $p < 0.05$) in MKN74 cells challenged with *H. pylori* when compared to the control cells. The Table displays fold changes and adjusted *p* values of the differentially expressed genes. Genes with log2-FC > 1 are upregulated and log2-FC < 1 are downregulated.

Gene ID	log_2-FC	*p*adj	Gene ID	log_2-FC	*p*adj	Gene ID	log_2-FC	*p*adj
DOPEY1	11.33100	9.81E-20	**CENPVP2**	5.11780	9.58E-03	**PLAG1**	4.68719	1.37E-03
GPR97	7.92582	1.63E-08	**OR4K17**	5.11713	3.36E-02	**PPBPP2**	4.68107	2.57E-02
C3orf20	7.60139	3.37E-08	**OR51B6**	5.11538	2.82E-03	**OR8B8**	4.65556	7.45E-03
NFATC4	7.22768	3.82E-07	**OR52A5**	5.11346	3.75E-04	**SLC15A1**	4.65222	3.86E-02
C19orf38	7.02499	4.72E-09	**OR2T12**	5.10107	9.16E-03	**POU3F4**	4.64887	2.87E-02
INHBA	6.99453	6.99E-09	**PWRN2**	5.08836	3.99E-03	**OR1B1**	4.64535	2.43E-02
UGT1A8	6.76508	4.52E-05	**KRTAP13-2**	5.08059	4.71E-03	**CALB1**	4.63580	9.33E-18
LCE1B	6.72240	1.35E-04	**OCEL1**	5.08057	1.15E-05	**PRODH2**	4.63004	3.71E-02
CLDN17	6.52199	6.30E-04	**OR6N1**	5.06785	1.96E-03	**FAM92A1P2**	4.62593	1.28E-02
SLC9A3	6.51184	7.59E-04	**MC4R**	5.06540	4.30E-02	**SLC17A3**	4.61667	2.47E-02
UBASH3A	6.46526	5.06E-06	**PKD1L2**	5.05396	1.23E-16	**UGT1A9**	4.60363	1.40E-02
TMEM95	6.21930	3.04E-04	**WBP11P1**	5.05358	2.81E-02	**OR1S1**	4.60075	2.70E-04
CYSLTR2	6.18973	1.97E-04	**IL6ST**	5.05091	2.95E-93	**PDCD1LG2**	4.59958	6.64E-03
OR51G2	6.15349	2.69E-03	**AKR1CL1**	5.04861	3.70E-02	**HBB**	4.59639	1.11E-02
OR2M7	6.04921	4.03E-04	**MT1JP**	5.04423	5.29E-05	**KRTAP25-1**	4.59404	3.74E-05
IGFBP3	6.03970	1.50E-17	**DEFB103A**	5.04241	1.07E-06	**OR4A5**	4.58550	5.86E-03
OR4S1	6.02918	9.91E-04	**CD1C**	5.03717	2.77E-02	**ROBO4**	4.58439	5.26E-08
OR5H14	5.93367	4.39E-04	**IGDCC3**	5.03335	4.63E-03	**TFDP3**	4.58063	3.43E-02
OR4D6	5.93312	1.81E-03	**IL1A**	5.00518	6.80E-16	**ADAM30**	4.57981	4.78E-02
SLAMF7	5.86937	1.40E-11	**KRTAP1-1**	5.00453	3.00E-02	**OR10J3**	4.57632	7.30E-03
MT1H	5.86637	2.25E-03	**KRTAP6-3**	5.00267	3.68E-03	**IL6**	4.57316	1.72E-07
RNASE7	5.82441	6.25E-12	**PSG1**	4.99328	5.22E-04	**HSPA7**	4.55770	4.54E-02
OR51L1	5.80903	4.79E-04	**HIGD1B**	4.98695	2.32E-02	**MT2A**	4.55213	1.65E-09
OR9G4	5.73914	1.42E-02	**OR8K1**	4.97505	4.45E-04	**IL2RG**	4.54831	1.51E-14
WFIKKN1	5.73905	1.24E-03	**PSG11**	4.97452	5.37E-03	**OR6C6**	4.53640	3.44E-02
KRTAP9-3	5.69842	8.65E-04	**OR13C8**	4.96628	9.42E-03	**SNRPD2P2**	4.53475	1.07E-02
GLUD2	5.69318	2.55E-03	**OR4D11**	4.96009	4.03E-02	**MT1E**	4.51992	5.64E-04
OR7G3	5.69050	8.18E-03	**KLHL14**	4.95938	5.14E-03	**DUOXA1**	4.51730	3.27E-02
SH2D4B	5.65797	4.08E-04	**KRTAP13-4**	4.95428	2.66E-02	**OR14C36**	4.50698	3.41E-04
C14orf162	5.65591	2.83E-03	**MPV17L**	4.95014	1.01E-02	**OR4K14**	4.47922	2.71E-04
UBL4B	5.65515	6.03E-04	**OR2M3**	4.93112	1.55E-03	**OR6Q1**	4.47795	4.08E-02
MTRNR2L5	5.59844	5.06E-04	**NAP1L2**	4.92236	4.55E-02	**RNF148**	4.47648	1.08E-03
TAS2R1	5.58502	1.55E-03	**ACTRT1**	4.91799	8.56E-03	**OR5F1**	4.46777	7.06E-03
LOC338651	5.58327	9.05E-04	**FRMD7**	4.91318	4.88E-02	**OR5H6**	4.44449	3.24E-02
OR4D1	5.57837	6.13E-03	**IFNA14**	4.89878	8.91E-03	**OR4D10**	4.43030	9.94E-03
EIF3IP1	5.53590	1.29E-02	**OR10R2**	4.89170	4.26E-04	**ELFN1**	4.42978	8.98E-06
TEX101	5.52538	2.39E-03	**MT1G**	4.88836	9.17E-09	**OR8B4**	4.42650	8.78E-04
OR4C13	5.51439	8.96E-04	**C6orf141**	4.88053	4.08E-03	**MYH8**	4.42494	1.98E-02
KRTAP9-2	5.46316	4.19E-03	**MAP6**	4.87746	4.82E-04	**CCDC172**	4.42408	2.76E-02
MT1X	5.44445	7.33E-07	**LCE1F**	4.87402	6.83E-03	**OR52L1**	4.42055	1.86E-02
OR9K2	5.43499	8.75E-04	**OR6K2**	4.87392	1.78E-03	**FCGR2B**	4.41895	2.33E-02
TNFSF14	5.41031	1.74E-02	**OR4A16**	4.82932	1.69E-03	**TAS2R7**	4.41765	4.34E-03
OR6M1	5.39735	1.04E-03	**MAP3K15**	4.82920	3.75E-05	**KRTAP23-1**	4.41334	3.19E-02
PSG2	5.39303	7.62E-05	**OR7A10**	4.82561	1.17E-02	**HAVCR1P1**	4.40640	3.90E-03
EMR1	5.38666	7.31E-03	**OR5B12**	4.82493	2.37E-04	**SFTA1P**	4.38790	4.00E-22
OR1J2	5.34235	3.11E-03	**KLF7**	4.82250	3.68E-61	**OR10G4**	4.38519	5.91E-03
DACH2	5.33397	1.87E-02	**RPS6**	4.81797	3.73E-210	**OR51M1**	4.38270	7.19E-03
CTAGE10P	5.33297	1.19E-02	**UPP1**	4.80957	1.47E-24	**LINC00482**	4.38161	4.71E-02
CCER1	5.31933	1.87E-02	**OR4D5**	4.80678	1.47E-04	**KRTAP13-1**	4.37456	4.57E-02
OR2T35	5.30500	2.01E-02	**TCP11**	4.80106	1.10E-02	**OR52R1**	4.37224	4.11E-02
CCDC3	5.30025	5.94E-03	**BHLHE41**	4.80027	5.21E-10	**RFPL3**	4.37054	4.21E-04
LINC00520	5.28289	5.67E-03	**VIM**	4.79882	3.13E-03	**OR2AK2**	4.36829	8.05E-03
OR1D5	5.25037	1.58E-02	**NDRG1**	4.79071	1.36E-128	**KRTAP4-9**	4.36324	3.62E-03
C16orf82	5.23893	3.19E-02	**OR1G1**	4.77279	4.59E-02	**HEXA-AS1**	4.35817	4.17E-03
KRTAP26-1	5.23362	1.24E-02	**OR4N2**	4.76680	7.89E-03	**RPLP0P2**	4.35332	1.52E-07
OR5I1	5.22543	4.97E-03	**LOC728392**	4.74186	1.47E-02	**OR2G3**	4.34010	1.31E-02
OR8D1	5.21565	4.27E-02	**LCP1**	4.73754	3.87E-09	**OR52E6**	4.33609	5.03E-03
DNAJB3	5.21496	2.34E-02	**PI3**	4.73631	5.12E-05	**PLA2G4C**	4.33531	3.81E-15
KRTAP2-1	5.18224	1.09E-02	**OR1A2**	4.73486	2.55E-03	**OR8D4**	4.33479	3.73E-02
OR1D4	5.17481	3.69E-03	**OR10AG1**	4.71535	2.77E-02	**CETN1**	4.33467	3.71E-02
IFNA8	5.16690	1.85E-02	**HPYR1**	4.71035	2.98E-05	**BTBD16**	4.32698	2.52E-02
OR10G7	5.15741	5.02E-06	**SNAI2**	4.70687	1.20E-07	**TNFRSF9**	4.32432	6.84E-21
OR51F2	5.15567	2.80E-03	**OR5M9**	4.70447	1.22E-04	**OR11H1**	4.32168	4.12E-02
CFL1P1	5.12242	9.31E-03	**OR6F1**	4.69175	1.13E-02	**OR8G5**	4.30954	5.28E-05

CTSF	4.30824	2.53E-02	**RGAG4**	3.94670	4.66E-02	**OR6C76**	3.63881	3.96E-02
MSX2P1	4.29787	5.48E-03	**OR7C1**	3.94572	1.64E-02	**TANK**	3.63513	8.82E-03
FAM70B	4.29325	3.47E-06	**UBTFL1**	3.94549	2.20E-03	**TRAM1L1**	3.63438	2.78E-03
OR2G6	4.28906	7.21E-03	**OR51G1**	3.93982	6.31E-03	**OR5W2**	3.62030	1.40E-02
PDXDC1	4.28652	1.85E-14	**OR1N1**	3.93394	1.22E-02	**P2RY1**	3.61460	4.45E-02
TMEM240	4.28094	1.41E-06	**KRTAP4-6**	3.92699	2.20E-02	**STC2**	3.61434	1.79E-41
VMO1	4.28069	3.91E-02	**SOX21**	3.92439	2.25E-02	**GOLT1A**	3.60887	5.29E-29
KRTAP13-3	4.27080	4.06E-02	**OR4C6**	3.92180	6.88E-03	**MAS1L**	3.60830	4.05E-02
CAPZA3	4.26439	2.31E-02	**AOC3**	3.92077	2.39E-39	**OR13C9**	3.59203	1.19E-02
HDAC9	4.25862	1.61E-30	**LOC150185**	3.91704	3.66E-02	**DNAH10**	3.59029	4.50E-02
NGFRAP1	4.25177	8.95E-03	**OR2M4**	3.91021	7.57E-03	**FAM167A**	3.58258	8.11E-08
LIMS3L	4.25046	2.33E-02	**LOC401164**	3.90890	1.48E-08	**IFNA22P**	3.57939	1.01E-02
ANXA2P3	4.24969	3.41E-04	**PLA2G4D**	3.90052	2.19E-16	**GPR32**	3.57363	5.50E-03
SAA2	4.24410	1.37E-02	**SCN4B**	3.89631	2.24E-02	**GOLGA8F**	3.56773	2.23E-02
OR6C70	4.23801	9.97E-04	**OR5T2**	3.88587	1.08E-02	**TRIM55**	3.55901	2.17E-08
KRTAP24-1	4.23128	1.61E-02	**KRTAP27-1**	3.88143	3.47E-02	**SLCO1B3**	3.55834	9.14E-41
OR8A1	4.23081	9.69E-03	**OR4K2**	3.87304	8.76E-04	**A1BG**	3.55450	1.91E-02
BEST1	4.22965	7.23E-05	**LOC728819**	3.86823	4.95E-03	**PAR1**	3.55341	2.00E-02
SRL	4.22769	4.02E-02	**OR8H1**	3.86798	2.59E-03	**LCE1A**	3.55089	4.92E-02
MIR490	4.22518	4.46E-04	**OR4A15**	3.85407	1.53E-02	**GABRA1**	3.54669	2.74E-02
ALOXE3	4.21800	8.60E-16	**ITGA5**	3.85025	7.94E-61	**OR52A1**	3.54662	1.12E-02
OR6P1	4.20548	3.47E-02	**LOC729176**	3.84969	3.89E-03	**OR8H3**	3.54339	3.35E-02
ASIC3	4.18285	7.86E-16	**OR10AD1**	3.84755	2.43E-02	**SLC6A3**	3.54260	3.28E-05
GPD1	4.17464	2.38E-04	**REXO1L1**	3.83949	2.88E-04	**OR10G8**	3.53258	2.21E-03
OR6Y1	4.16960	4.50E-02	**ARL14EPL**	3.83847	4.11E-03	**TAAR3**	3.52875	7.61E-03
KRTAP19-4	4.16740	1.14E-02	**REG1P**	3.83443	1.80E-02	**OR9Q2**	3.52757	1.66E-02
MTRNR2L7	4.16052	1.67E-04	**OC90**	3.83292	1.67E-02	**FBXO39**	3.51933	3.15E-02
OR5H15	4.15896	1.33E-03	**RPSAP52**	3.83114	2.66E-02	**CD163L1**	3.51536	2.56E-02
CLEC2B	4.15599	8.97E-05	**KDM4E**	3.83035	2.94E-02	**ZNF699**	3.51392	2.21E-35
OR56B1	4.14343	2.33E-03	**PRR23A**	3.82572	4.14E-02	**MYH4**	3.51180	1.50E-02
ENKUR	4.13724	4.20E-06	**C15orf48**	3.82482	3.21E-27	**OR5AR1**	3.50389	1.77E-03
OR8I2	4.13692	3.42E-03	**PDHA2**	3.81480	5.15E-04	**OR5A2**	3.50064	1.36E-02
LCE4A	4.13057	2.31E-03	**PER4**	3.80960	3.98E-04	**CRHR1-IT1**	3.49522	7.94E-10
KRTAP4-2	4.12735	3.08E-02	**SLC25A51P1**	3.79119	1.40E-02	**GBP5**	3.49483	1.48E-04
YPEL4	4.11433	9.82E-05	**GLDC**	3.79058	2.88E-02	**ADH1A**	3.49468	1.52E-02
OR2T33	4.11155	2.79E-03	**SH2D5**	3.78674	4.16E-18	**KRTAP19-7**	3.49301	3.98E-03
OR5K1	4.10964	3.87E-03	**OR1L1**	3.78241	8.93E-03	**KRT34**	3.49284	5.20E-08
CH25H	4.10717	2.22E-03	**CCRL1**	3.77955	4.40E-03	**DDIT4**	3.48785	2.22E-12
LOC649395	4.10311	2.39E-02	**OR4D9**	3.77576	3.18E-04	**OR5M1**	3.47952	1.98E-02
OR5T3	4.09743	8.87E-04	**ZNF546**	3.76998	6.87E-05	**OR5M10**	3.47149	2.57E-02
TFPI	4.09639	2.91E-07	**BHLHE40**	3.75658	4.31E-167	**OR6K6**	3.46872	9.24E-03
OR10G9	4.09001	2.63E-03	**EGLN3**	3.75606	6.99E-15	**RNF112**	3.46097	4.35E-03
FLJ35282	4.08906	2.89E-02	**OR13C3**	3.75312	4.99E-02	**LOC100507034**	3.45234	8.60E-03
CPAMD8	4.08843	4.84E-06	**KRTAP22-2**	3.75235	3.64E-03	**ATP8A2**	3.44748	1.55E-10
OR10K1	4.08620	2.01E-02	**OR51Q1**	3.74936	1.43E-02	**OR2B6**	3.44736	1.32E-02
KDM3A	4.08238	1.66E-117	**NPY1R**	3.74698	2.28E-02	**OR5AS1**	3.44577	1.10E-02
ELL2	4.08060	8.43E-66	**OR14I1**	3.74632	2.67E-02	**OR4K15**	3.43684	6.64E-03
OR6C4	4.07537	1.37E-02	**OR2K2**	3.74199	2.96E-05	**NR1D1**	3.43656	2.92E-71
KIF5A	4.07348	1.11E-05	**OR7A17**	3.74029	2.10E-02	**OR51T1**	3.43603	1.78E-02
RPL31P11	4.07239	3.32E-02	**TAAR9**	3.74019	8.62E-03	**DACH1**	3.43544	8.68E-03
PDE2A	4.06798	7.31E-14	**GAL3ST1**	3.73363	2.20E-06	**IL6R**	3.43318	2.12E-22
TM6SF2	4.06785	4.91E-02	**TCTE1**	3.73261	2.55E-05	**OR4F21**	3.43128	5.77E-03
DUSP1	4.06386	5.26E-92	**ERO1L**	3.72856	4.44E-105	**LCAT**	3.43092	6.72E-12
OR2T1	4.05376	9.86E-03	**GRIN3B**	3.72791	6.20E-04	**RRAGD**	3.42971	2.84E-34
VNN1	4.05123	1.17E-02	**COL20A1**	3.72451	2.70E-02	**OR6T1**	3.42665	1.03E-02
CREBRF	4.04805	8.35E-36	**TMEM40**	3.71959	1.57E-74	**ATG9B**	3.42379	3.06E-17
OR5B17	4.03880	1.14E-02	**PKD1L1**	3.71927	2.27E-05	**KRTAP3-2**	3.42349	2.23E-02
CSF2	4.03376	1.54E-05	**OR2T27**	3.71721	1.32E-02	**DUOX2**	3.42202	8.91E-03
OR2T4	4.02781	1.79E-02	**LOC644936**	3.71123	1.58E-02	**OR5L2**	3.41854	1.73E-03
OR2L2	4.02054	2.96E-02	**OR4F3**	3.70738	1.54E-03	**ADCY10P1**	3.40948	1.41E-10
ANKRD37	4.01982	1.93E-42	**KRTAP1-5**	3.69592	1.80E-02	**OR10W1**	3.40824	7.71E-03
LAMB3	4.01936	8.93E-45	**PRPS1L1**	3.69274	4.70E-05	**ISG20**	3.40661	2.93E-30
NEURL3	4.01691	3.18E-14	**HOTAIRM1**	3.69245	9.74E-18	**CNN1**	3.40158	2.53E-02
AFF3	4.01286	1.77E-02	**TMPRSS6**	3.69243	1.19E-05	**ZNF292**	3.39957	6.61E-40
RPL10L	4.00720	9.86E-04	**MAPK8**	3.68589	2.20E-08	**CCT8L2**	3.39830	1.01E-02
RASL10B	4.00656	3.13E-05	**OR6C1**	3.67514	5.85E-03	**PRR23B**	3.39340	2.98E-02
OR6C75	4.00255	5.13E-03	**HLA-F-AS1**	3.67504	5.13E-08	**KLHDC7B**	3.38713	9.24E-05
SERPINB2	3.98753	2.78E-05	**OR51A4**	3.67011	1.09E-02	**ERRFI1**	3.37959	2.69E-54
ZP4	3.98568	9.97E-03	**WASH5P**	3.66084	6.77E-12	**CCDC54**	3.36918	3.80E-03
KRTAP2-4	3.97682	2.67E-02	**OR2S2**	3.65846	2.59E-02	**HMOX1**	3.36014	1.28E-47
OR8D2	3.97432	6.05E-03	**OR8U1**	3.65329	2.20E-04	**TP53INP2**	3.35661	3.74E-17
GATA6	3.96118	5.96E-25	**OR5T1**	3.65123	3.92E-02	**OR8H2**	3.35124	6.24E-04
OR6W1P	3.95661	3.68E-02	**SPZ1**	3.64601	2.65E-02	**SCP2D1**	3.35071	3.60E-02
OR8B12	3.95388	9.30E-04	**OR5B2**	3.64326	6.79E-03	**FBXO32**	3.34982	2.61E-42

OR10C1	3.34870	3.71E-02	**OR51A7**	3.07670	5.40E-03	**PLEKHA8P1**	2.80158	5.08E-16
OR56A5	3.34354	1.17E-02	**OR5M8**	3.05788	4.53E-04	**NPR1**	2.79514	4.06E-03
FSCN2	3.34212	5.77E-19	**ABL2**	3.05426	1.12E-40	**CLIP4**	2.79064	4.77E-15
PPP1R15A	3.34100	7.45E-76	**IRAK2**	3.05289	8.69E-13	**OR51A2**	2.78934	3.74E-02
FAM172BP	3.34004	2.58E-02	**OR6K3**	3.04910	3.48E-02	**CENPT**	2.78731	4.54E-07
ACTR3BP2	3.33859	2.81E-02	**OR10A3**	3.04719	1.11E-02	**IL23A**	2.78274	2.07E-09
LACC1	3.33777	4.21E-02	**ATP8B5P**	3.04323	7.18E-05	**REPS2**	2.77824	6.99E-12
OR8J1	3.33513	3.86E-02	**IL18R1**	3.03654	1.82E-05	**OR5D14**	2.77779	3.03E-03
GJC1	3.33485	2.29E-06	**LINC00152**	3.03140	2.49E-19	**STX11**	2.77410	1.70E-12
C2orf61	3.33206	4.90E-05	**VN1R4**	3.02760	3.22E-03	**VCL**	2.77400	7.25E-16
LOC100128023	3.33121	2.87E-02	**CD59**	3.02630	6.05E-03	**GJD4**	2.76786	3.21E-03
PCNAP1	3.32368	3.25E-02	**TNXB**	3.02616	3.47E-05	**OR5H1**	2.76477	4.71E-02
OR5AU1	3.32209	3.08E-03	**LOC219731**	3.02179	7.84E-07	**NKAPL**	2.76203	3.02E-02
C3	3.31756	2.20E-17	**FRMD6**	3.01907	3.90E-18	**HOXB9**	2.74967	6.99E-34
OR4C15	3.31559	2.46E-02	**LOC286367**	3.01716	1.17E-02	**BTG1**	2.74946	1.21E-59
OR12D3	3.31005	1.23E-02	**TAAR1**	3.01655	3.06E-02	**IER2**	2.74356	4.54E-02
NOS3	3.30630	7.29E-09	**LYPD1**	3.01301	1.37E-04	**ECEL1P2**	2.74147	4.79E-02
PPIAL4F	3.30522	3.40E-02	**PPP3R2**	3.01284	2.67E-03	**OR1E2**	2.74027	4.38E-02
IFNA21	3.30148	3.60E-02	**OR4F17**	3.00814	8.25E-03	**G0S2**	2.74013	3.27E-02
CABP1	3.30096	1.49E-02	**OR51I1**	3.00587	4.20E-02	**TMEM25**	2.73460	2.16E-04
TNFAIP3	3.29825	1.59E-06	**ISLR**	3.00483	1.55E-03	**DUSP6**	2.72532	2.01E-27
OR4F4	3.29301	3.23E-02	**OR10V1**	3.00024	2.37E-02	**ARL9**	2.72407	9.20E-03
OR13C5	3.29015	6.04E-03	**PP12613**	2.99957	4.85E-02	**EBI3**	2.72043	9.80E-06
OR13C4	3.28545	4.17E-02	**STAR**	2.99613	2.68E-02	**TMC8**	2.71963	3.34E-03
IFNA5	3.28178	2.59E-02	**MMP9**	2.99281	1.55E-10	**CNTNAP1**	2.71769	3.60E-14
NWD1	3.27766	2.87E-04	**OR1S2**	2.98925	5.03E-03	**CHRM4**	2.71659	1.16E-07
SCN3B	3.26628	2.61E-02	**OR51F1**	2.98792	4.17E-02	**OR11H2**	2.71621	4.90E-06
GCSAML	3.26483	3.29E-02	**OR8J3**	2.97698	2.66E-02	**SPDYA**	2.71584	3.31E-03
PVT1	3.26426	1.50E-23	**IPMK**	2.97661	2.83E-25	**GPRC5A**	2.71309	1.46E-39
OR5R1	3.25743	3.26E-02	**OR4N5**	2.97537	2.63E-02	**OR10S1**	2.71208	2.79E-02
HIF3A	3.25728	2.34E-02	**OR6C68**	2.97363	2.45E-02	**PRDM1**	2.71173	6.30E-15
PFKFB3	3.25687	6.17E-21	**LINC00622**	2.97096	1.22E-23	**IFNA13**	2.70738	3.55E-02
MIR181A2HG	3.25515	2.90E-05	**CYP21A2**	2.96947	1.58E-03	**CPEB1**	2.70654	1.79E-11
BIRC3	3.25096	1.03E-06	**GOLGA8CP**	2.96710	2.92E-02	**SBDSP1**	2.70082	3.45E-28
ADAM21P1	3.24653	2.57E-02	**ATF3**	2.96352	5.46E-32	**ALDOC**	2.69659	7.93E-38
OR2T10	3.23975	2.22E-02	**TRNP1**	2.95737	3.08E-19	**RCSD1**	2.69620	4.59E-02
NAT10	3.23522	1.28E-28	**SERPINB8**	2.95411	2.37E-12	**SLCO1B1**	2.69575	4.18E-07
CTAGE11P	3.23276	1.53E-02	**ARL14**	2.95295	2.92E-03	**SCUBE2**	2.69132	4.49E-02
USP17L6P	3.22672	7.15E-04	**GEM**	2.94285	9.40E-12	**FAM183B**	2.68894	1.72E-02
CTSS	3.22378	3.75E-05	**HSD3B2**	2.93963	2.87E-02	**NPC1**	2.68668	5.73E-35
ZNF300	3.22378	4.79E-03	**OR11H4**	2.93327	3.12E-02	**LRIF1**	2.67405	1.14E-44
OR1L4	3.21285	2.00E-02	**ENO2**	2.93045	1.77E-41	**OR4M2**	2.66979	2.60E-02
PTENP1	3.20688	6.73E-05	**S1PR1**	2.92943	4.56E-05	**SAT1**	2.66599	3.99E-64
OR4C46	3.18655	8.11E-03	**KRTAP5-1**	2.92398	5.76E-03	**FNDC7**	2.66157	3.49E-03
FTH1	3.18638	1.47E-90	**DNHD1**	2.91990	1.20E-03	**LAMC2**	2.65874	1.41E-22
OR5H2	3.18046	3.08E-02	**SLC6A13**	2.91651	4.25E-05	**HRK**	2.65725	6.59E-19
OR5L1	3.17874	4.52E-02	**IGFL1**	2.91481	1.78E-03	**P4HA1**	2.65591	6.17E-38
CPEB2	3.17003	1.95E-22	**LOC100507410**	2.90144	3.48E-02	**COL13A1**	2.65225	7.92E-03
KRTAP19-1	3.16745	2.97E-02	**ALOX12B**	2.89990	5.49E-04	**DPYSL2**	2.64480	3.71E-02
MXD1	3.16448	1.82E-66	**OR5D13**	2.89762	2.59E-02	**IER5**	2.64139	7.79E-36
OR52J3	3.16410	4.18E-02	**TXK**	2.89597	7.84E-28	**RELB**	2.64099	1.49E-22
TMEM61	3.15946	3.87E-02	**MAB21L3**	2.89581	2.27E-04	**ASPHD2**	2.64074	3.53E-05
MYO1A	3.15843	1.34E-03	**MXI1**	2.89470	7.45E-29	**TBC1D2B**	2.63735	1.09E-13
GPR1	3.15691	2.42E-02	**CHIC2**	2.88335	2.93E-37	**C8G**	2.63308	5.86E-03
KCTD11	3.14693	2.72E-28	**BNIP3**	2.88305	2.48E-02	**OR7E37P**	2.63301	7.32E-03
OR52K1	3.14652	4.72E-02	**CR2**	2.88259	3.09E-02	**KCND1**	2.63234	1.50E-08
OR2M1P	3.14323	6.22E-03	**TAAR8**	2.87893	3.94E-02	**TP53AIP1**	2.63158	1.22E-03
PGK2	3.13325	4.13E-02	**ADTRP**	2.87126	1.58E-10	**GADD45B**	2.63026	1.32E-52
AOC2	3.13164	7.10E-18	**FAM86B2**	2.86689	1.47E-02	**LOC100131691**	2.62976	1.58E-02
KCNA3	3.12533	3.52E-02	**SIGLEC10**	2.85654	1.74E-02	**ADHFE1**	2.62848	1.32E-02
EPG5	3.12048	5.66E-55	**DAPP1**	2.85600	1.94E-42	**TIPARP**	2.62798	2.34E-22
FGF14-AS2	3.11431	1.28E-02	**RNMT**	2.85383	7.05E-42	**NAMPT**	2.62495	1.06E-78
OR2M5	3.11430	2.56E-02	**OR4M1**	2.85245	1.30E-02	**NCR3LG1**	2.62437	3.29E-04
PYDC2	3.11151	1.51E-03	**WNK4**	2.84959	7.04E-13	**FAM24B**	2.62433	1.53E-20
OR1J1	3.10978	3.90E-02	**PNMA2**	2.84674	1.22E-02	**RNF157-AS1**	2.62392	1.70E-04
OR9I1	3.10864	2.67E-02	**SLC9A5**	2.84429	1.48E-05	**NFKBIZ**	2.62388	6.06E-19
SLC4A5	3.10614	5.05E-14	**OR52H1**	2.83638	3.69E-03	**HIST1H2AA**	2.62141	4.44E-02
GADD45A	3.10470	2.43E-12	**CXADRP2**	2.83620	9.94E-03	**SHISA4**	2.62092	7.12E-12
OR5M11	3.10203	5.60E-03	**ANP32D**	2.83534	4.63E-02	**GPHA2**	2.61958	5.84E-10
PLAU	3.10153	8.76E-04	**AMN**	2.81982	2.81E-05	**OR2F1**	2.61772	4.91E-02
FYN	3.10142	1.06E-44	**OR52I2**	2.81656	4.22E-02	**CYP26B1**	2.60846	1.66E-04
MAP1LC3B2	3.10066	5.44E-92	**SAA1**	2.81370	6.17E-03	**NEDD4L**	2.60548	2.41E-29
OR6X1	3.08825	1.73E-02	**OR5AK4P**	2.81068	3.40E-02	**FOXN3**	2.60374	4.53E-04
ITGB2	3.07859	8.13E-06	**CSF1R**	2.80781	7.16E-09	**CACNA1H**	2.60317	3.24E-04

OR8K3	2.60010	4.45E-02	**FMNL2**	2.35569	9.09E-50	**MAFF**	2.20597	7.56E-03
PSORS1C1	2.59350	4.70E-12	**LETM2**	2.35456	6.69E-07	**NPHS1**	2.20450	7.24E-03
RIOK3	2.58675	3.20E-53	**LIMCH1**	2.34862	1.09E-19	**ACTG1P4**	2.20404	1.52E-03
DDI1	2.58518	2.82E-02	**RFESD**	2.34448	2.13E-11	**ARC**	2.20402	5.25E-03
ARID3B	2.58255	4.14E-19	**LONRF3**	2.34344	2.21E-05	**FLCN**	2.20182	1.10E-42
ERVV-2	2.57895	7.48E-16	**YEATS2**	2.34280	4.92E-50	**TM4SF19**	2.20149	2.76E-13
LOC100130357	2.57123	1.77E-06	**PTCH2**	2.34003	4.92E-08	**LIPG**	2.19872	1.68E-20
LOC646214	2.57118	1.44E-02	**USP32P1**	2.33978	1.42E-05	**SGPP2**	2.19590	4.31E-17
PRPF3	2.57024	1.17E-21	**KRTAP6-2**	2.33786	3.62E-02	**RPL17**	2.19564	7.26E-07
ZC2HC1A	2.56866	1.09E-07	**PRSS22**	2.33318	1.94E-55	**ADORA2A**	2.19468	6.93E-13
FOSL2	2.56110	8.51E-59	**GVINP1**	2.33014	2.57E-03	**CELSR3**	2.19460	8.95E-13
KLHL24	2.56043	9.00E-21	**LOC100129924**	2.33001	1.46E-05	**ZNF26**	2.18948	5.28E-16
MIR100HG	2.55456	4.15E-05	**KLF4**	2.32685	4.09E-29	**S100P**	2.18759	1.28E-07
PRKCE	2.55064	2.22E-42	**C1orf63**	2.31764	8.03E-18	**SAP30**	2.18735	1.49E-25
CYB5D1	2.54716	3.56E-11	**CRMP1**	2.31439	2.19E-03	**LOC541471**	2.17955	4.21E-15
OR2L1P	2.54609	1.80E-02	**LOC100507250**	2.31422	6.47E-03	**RASA4CP**	2.17931	5.66E-04
TEAD1	2.54596	1.86E-113	**TCP11L2**	2.31098	4.11E-09	**JUN**	2.17733	4.90E-03
ZNF502	2.54542	1.93E-05	**ASAP1**	2.30660	6.42E-39	**FERMT2**	2.17522	8.82E-23
KRTDAP	2.54487	4.29E-02	**LOC387895**	2.30584	4.06E-03	**DLK2**	2.17106	3.21E-08
ACTA2	2.54342	1.93E-11	**RNF24**	2.30576	2.09E-34	**CNTD2**	2.16975	2.25E-02
KIAA1551	2.52198	2.34E-37	**FMNL1**	2.30519	7.82E-06	**TRIML2**	2.16818	1.13E-10
OPTN	2.52120	1.24E-17	**GSTM2P1**	2.30475	4.24E-02	**RALB**	2.16757	4.03E-69
REM2	2.51512	5.29E-05	**ANKRD33B**	2.30251	2.17E-13	**KMO**	2.16582	9.83E-03
DKFZP686I15217	2.51432	8.93E-06	**AOX1**	2.30163	2.67E-02	**ZNF571**	2.16287	1.50E-28
SMIM6	2.51393	9.83E-03	**AQPEP**	2.29757	1.22E-02	**SOCS2-AS1**	2.16173	7.33E-03
PQLC2	2.51125	8.18E-42	**NDUFAF4P1**	2.29645	5.14E-04	**MOSPD1**	2.16127	1.12E-15
TPRA1	2.50834	1.06E-44	**WDR45**	2.29263	3.25E-16	**FUT11**	2.16054	8.18E-15
CDKN1A	2.50380	1.19E-60	**SPRR2D**	2.29138	6.89E-03	**KLF6**	2.15940	1.15E-05
NT5E	2.50310	7.90E-10	**EIF1**	2.29062	9.01E-85	**LDHA**	2.15722	2.63E-67
BNC1	2.50118	8.62E-05	**NUPL1**	2.29043	1.41E-38	**IL8**	2.15672	7.96E-03
GPR75	2.50019	6.79E-08	**AKIRIN2**	2.28655	3.23E-29	**PLCH2**	2.15606	5.10E-05
LINC00460	2.49533	2.13E-02	**COL5A3**	2.28105	2.43E-03	**MICB**	2.14906	1.21E-10
CTGF	2.48982	6.69E-07	**IRS2**	2.28032	4.29E-33	**TNFRSF10B**	2.14666	6.24E-29
AHNAK2	2.48866	1.14E-11	**PGK1**	2.27988	3.21E-127	**LOC338758**	2.14353	8.63E-03
MPZL3	2.48279	1.63E-78	**MRC1**	2.27960	3.46E-03	**C6orf130**	2.14249	1.11E-05
DISC1	2.48249	4.38E-32	**LRRC8C**	2.27601	9.37E-15	**ZNF432**	2.14178	3.55E-56
TMEM236	2.48138	3.53E-06	**ILDR2**	2.27501	3.24E-02	**RRAGC**	2.14164	8.40E-20
PIGA	2.47666	1.28E-39	**WIPI1**	2.27206	2.60E-07	**VEGFA**	2.14088	2.32E-26
NLRP1	2.47627	8.53E-03	**TMEM45A**	2.26974	3.01E-08	**CTNS**	2.14049	2.12E-24
LINC00341	2.47446	1.62E-13	**PLEK2**	2.26928	2.29E-24	**CD274**	2.13976	3.10E-14
RPL23P8	2.47366	1.57E-02	**NPPB**	2.26746	2.71E-02	**CTAGE1**	2.13951	7.36E-03
IKBKG	2.46869	2.53E-07	**SDCBP**	2.26654	1.31E-20	**ELL**	2.13929	2.23E-32
COL7A1	2.46728	8.51E-13	**BBC3**	2.26493	1.65E-16	**SLC22A15**	2.13365	7.57E-15
SNHG5	2.46424	7.62E-42	**CA9**	2.26384	1.60E-04	**SLC17A7**	2.13268	1.50E-04
REXO1L2P	2.45780	9.71E-03	**OR9A4**	2.26258	2.97E-03	**LOC389765**	2.12746	3.64E-03
ALOX5AP	2.45720	1.99E-02	**B2M**	2.26071	1.34E-35	**LOC401074**	2.12513	3.71E-02
IL1RAP	2.45610	2.95E-18	**IL32**	2.25889	6.51E-13	**DUSP10**	2.11829	3.88E-25
MCL1	2.45493	2.68E-22	**DNER**	2.25317	2.53E-05	**IGDCC4**	2.11430	9.05E-13
HBEGF	2.44937	2.24E-23	**IFI16**	2.25249	3.48E-02	**NLRP3**	2.11342	2.99E-04
LYPD5	2.44729	5.49E-03	**IQCG**	2.25131	1.47E-10	**S100A3**	2.11234	3.44E-05
CASS4	2.44406	2.18E-05	**SRP19**	2.25002	1.60E-09	**GLS**	2.10796	1.63E-31
DNAH5	2.43692	1.63E-03	**SORBS3**	2.24876	9.37E-04	**PFKFB2**	2.09597	8.06E-60
SHH	2.43605	9.01E-03	**HERPUD1**	2.24509	1.57E-41	**MTRNR2L4**	2.09439	1.87E-04
MT1F	2.43282	7.59E-04	**KRTAP19-2**	2.24394	4.15E-02	**RASL10A**	2.09256	1.31E-03
FAM186B	2.42304	1.42E-04	**BACH1**	2.24361	8.62E-39	**ZNF83**	2.09034	1.25E-24
TTC36	2.42170	1.55E-05	**THAP9-AS1**	2.24273	4.80E-19	**PDK1**	2.08994	2.72E-28
PPP2R2A	2.41505	1.58E-39	**TRIM36**	2.24136	3.97E-04	**R3HCC1L**	2.08804	3.41E-29
GJA3	2.41248	5.09E-16	**SPNS2**	2.24091	6.69E-17	**ELOVL7**	2.08584	3.00E-19
ARRDC3	2.41076	1.03E-18	**BMF**	2.23894	1.46E-05	**CATSPER2**	2.08383	3.99E-05
KLF11	2.40589	8.40E-26	**LOC392196**	2.23780	3.81E-02	**N4BP3**	2.08329	3.92E-11
DLL4	2.40542	1.08E-02	**RAB8B**	2.23630	3.96E-55	**NAT8B**	2.07711	1.65E-02
UBE2D1	2.40121	4.96E-46	**OR5K2**	2.23578	1.16E-02	**TGFB2**	2.07613	1.28E-03
PREPL	2.39785	1.74E-02	**TGFBR1**	2.23328	2.15E-16	**PARD6B**	2.07296	7.22E-47
TNFRSF10D	2.39562	1.76E-38	**GDA**	2.23271	9.26E-10	**KIFC3**	2.07278	1.35E-31
IFNA1	2.39439	3.32E-03	**OR11H6**	2.23090	3.33E-02	**GOLGA6L1**	2.07176	1.25E-02
C1orf116	2.39435	3.39E-14	**EGLN1**	2.23013	2.83E-43	**ZNF382**	2.06891	4.10E-03
INSIG2	2.38900	3.56E-50	**SLCO1B7**	2.22917	3.97E-20	**KDM4C**	2.06743	2.64E-21
PTGER1	2.38456	3.89E-02	**DGCR9**	2.22488	7.37E-12	**KLF9**	2.06579	8.86E-07
PTPN22	2.38312	4.00E-02	**AGFG1**	2.22052	7.90E-03	**RAB30**	2.06392	2.14E-08
LHX2	2.37964	5.76E-03	**ULBP1**	2.21785	1.64E-18	**STARD9**	2.06364	1.28E-02
SLC28A1	2.37699	1.17E-03	**OR11H12**	2.21750	1.65E-03	**LOC729970**	2.06330	9.44E-09
ADM	2.37532	9.98E-14	**AP1S2**	2.21348	2.82E-22	**CCL19**	2.06227	2.15E-02
CDKN2B	2.36985	9.78E-28	**ARL8B**	2.21338	6.90E-68	**INHBE**	2.06214	2.30E-03
ASNS	2.36568	3.14E-39	**TAF13**	2.21017	2.41E-34	**RASA1**	2.06207	3.50E-17
HSD17B3	2.36500	8.36E-05	**NR4A3**	2.20917	5.11E-08	**MICALCL**	2.06207	1.87E-12
PYY2	2.36417	4.56E-06	**RAET1L**	2.20868	9.38E-11	**CCNG2**	2.06031	1.22E-21
APCDD1L-AS1	2.35993	1.88E-10	**ABTB2**	2.20688	5.70E-23	**LOC400927**	2.05894	2.42E-02
BNIP3L	2.35665	1.24E-22	**TES**	2.20656	1.56E-69	**APCDD1L**	2.05857	2.25E-02

LYST	2.05819	3.19E-27	**GSDMC**	1.91609	1.01E-09	**C7orf41**	1.81089	3.71E-18
OR2A20P	2.05458	3.98E-17	**OR13J1**	1.91516	3.57E-02	**CUZD1**	1.80924	2.18E-05
TG	2.05410	5.45E-03	**NFKB2**	1.91111	2.20E-16	**LOC100506422**	1.80896	4.81E-02
NFKBIE	2.05405	1.11E-09	**ANKRD20A9P**	1.91045	3.84E-12	**ORAI3**	1.80818	4.21E-02
BCL10	2.05174	1.11E-23	**MARK1**	1.90908	5.09E-04	**SASH1**	1.80742	1.60E-15
CTNND1	2.04464	5.12E-07	**ELF3**	1.90863	1.41E-33	**BUD31**	1.80617	5.52E-50
CLDN15	2.04175	8.71E-15	**DNTTIP1**	1.90633	3.56E-28	**TSC22D1**	1.80564	1.81E-11
ANKRA2	2.04143	1.88E-14	**C17orf103**	1.90626	1.77E-08	**IL18BP**	1.80365	3.31E-02
SGMS1	2.04032	7.10E-21	**LOC728537**	1.90436	4.10E-02	**HERC3**	1.80297	1.50E-26
NR4A2	2.03779	2.76E-10	**BLZF1**	1.90400	5.97E-32	**AAK1**	1.80194	3.30E-20
LOC100506136	2.03524	8.65E-03	**LOC284889**	1.90109	7.09E-03	**MICA**	1.80179	4.41E-22
POM121L10P	2.03509	6.18E-04	**HIVEP2**	1.89866	2.31E-12	**AVPI1**	1.80091	1.17E-11
MYBL1	2.03475	5.23E-21	**JHDM1D**	1.89751	1.47E-08	**PTPN2**	1.80050	2.83E-20
EIF1B	2.03138	1.78E-27	**ZDHHC2**	1.89661	7.43E-15	**SELPLG**	1.80021	2.44E-03
SYF2	2.03038	7.99E-25	**HSD3BP4**	1.89651	4.94E-03	**RLF**	1.79781	1.28E-25
PSG3	2.02953	4.83E-02	**ARF4**	1.89483	3.60E-33	**PSORS1C3**	1.79521	3.12E-05
CSTA	2.02837	3.82E-02	**CRTAM**	1.89319	2.72E-02	**C3orf62**	1.79226	2.09E-08
ATP13A3	2.02495	2.48E-46	**PRKACA**	1.89262	5.43E-23	**COL6A2**	1.78780	1.10E-08
WNK1	2.02227	9.35E-15	**PAIP2**	1.89111	4.29E-48	**EIF2S3**	1.78463	1.85E-32
AK4	2.02103	2.90E-24	**DGKI**	1.88913	2.96E-03	**KLHL28**	1.78415	6.20E-17
TRPV3	2.01994	2.52E-13	**PMEPA1**	1.88647	8.85E-12	**MT1M**	1.78208	7.44E-03
DNAH14	2.01838	8.46E-07	**DNAJB9**	1.88581	3.10E-23	**IL21R-AS1**	1.78192	4.05E-02
PLAC8L1	2.01694	4.29E-04	**MARCH9**	1.88265	2.52E-13	**HLA-H**	1.78137	2.60E-02
PHLDB1	2.01482	6.52E-03	**CLK3**	1.88215	4.81E-50	**LOC646762**	1.78038	1.38E-23
MYEOV	2.01238	9.63E-53	**SLC41A2**	1.88205	1.55E-27	**LINC00616**	1.78033	1.31E-02
HSF2BP	2.01227	3.10E-10	**MATN3**	1.88181	2.88E-05	**ZNF461**	1.78032	1.49E-06
MAK	2.00746	8.79E-03	**CYSTM1**	1.88157	1.01E-33	**PTPN12**	1.77995	1.22E-15
DERL2	2.00250	5.93E-46	**JAK1**	1.88136	6.15E-61	**FAM210A**	1.77857	5.31E-19
LACTB	2.00194	9.45E-12	**PTPRH**	1.87874	1.85E-03	**RAB3IL1**	1.77799	6.71E-13
RHEBL1	2.00020	6.29E-03	**RSPH10B**	1.87730	4.76E-05	**PANX1**	1.77783	5.96E-17
SERPINE2	1.99858	3.86E-22	**USP17L5**	1.87414	4.10E-02	**PDCD4**	1.77585	2.76E-13
ODC1	1.99795	1.56E-09	**RAB1A**	1.87193	2.40E-24	**TMEM106A**	1.77581	9.15E-03
ZHX2	1.99632	9.06E-12	**PSD**	1.87188	4.60E-02	**PSMB9**	1.77265	2.43E-07
CCDC82	1.99489	4.98E-25	**IVD**	1.86927	5.12E-07	**CAPN3**	1.77189	1.62E-03
PP7080	1.99106	2.64E-02	**RAB10**	1.86758	9.21E-62	**CTRB2**	1.77073	1.91E-02
TP53BP2	1.99080	1.89E-63	**PER1**	1.86531	2.12E-14	**FRZB**	1.77001	6.81E-03
ANXA5	1.99020	1.05E-13	**MGLL**	1.86413	3.05E-21	**HSPBAP1**	1.76945	9.49E-22
MARCH4	1.98950	4.15E-04	**LRRC58**	1.86379	5.85E-34	**EIF4E3**	1.76907	1.80E-04
KDM4B	1.98741	1.70E-39	**GABARAPL1**	1.86300	1.66E-25	**AVIL**	1.76835	5.85E-08
C5orf51	1.98689	2.29E-35	**C6orf62**	1.86228	2.26E-33	**CCRN4L**	1.76821	5.56E-08
FAM129A	1.98609	1.60E-09	**PLAC8**	1.86065	7.87E-03	**ZFP2**	1.76740	2.83E-02
FP588	1.98185	2.54E-02	**STBD1**	1.86048	6.07E-06	**CFB**	1.76720	1.11E-03
MED10	1.98137	5.59E-21	**ICAM1**	1.85981	4.37E-08	**PRPH**	1.76652	5.01E-03
FAM22D	1.97914	4.38E-04	**SPATA25**	1.85967	1.40E-02	**RSL24D1**	1.76526	5.25E-24
HIVEP3	1.97885	6.52E-12	**LOC100506804**	1.85952	2.39E-02	**TAS1R3**	1.76499	4.73E-06
F3	1.97874	7.09E-14	**KLF10**	1.85877	9.01E-04	**SNX29P2**	1.76468	4.44E-03
NKD2	1.97816	4.55E-08	**GOLGA7**	1.85753	5.72E-20	**SLFN5**	1.76434	5.05E-10
SLC2A3	1.97705	1.65E-20	**NCF2**	1.85720	3.00E-02	**LOC100506844**	1.76329	7.61E-04
ZNF221	1.97688	2.07E-03	**EMR2**	1.85611	3.07E-06	**FBLN7**	1.76150	1.69E-02
KLF3	1.97599	2.36E-33	**SLC8A2**	1.85564	1.71E-04	**FNTA**	1.76047	2.43E-26
SLC26A1	1.97527	3.53E-02	**WSB1**	1.85557	4.55E-25	**TNNT2**	1.76016	9.52E-05
LOC154761	1.97419	7.09E-11	**OXSR1**	1.85459	1.68E-27	**LOC728875**	1.75991	4.61E-13
PODXL	1.97391	4.27E-12	**ZNF385C**	1.85366	3.13E-04	**MAP2K1**	1.75959	4.67E-50
CPLX3	1.97235	1.38E-03	**DOK3**	1.85363	6.54E-07	**RIT1**	1.75892	1.79E-30
N4BP2L1	1.97119	2.30E-02	**SNX24**	1.85212	1.44E-20	**DNMBP**	1.75832	7.36E-21
TUBB2B	1.96917	3.18E-16	**DAAM1**	1.85121	1.30E-47	**KIAA0907**	1.75802	5.64E-13
CPEB4	1.96669	1.48E-40	**ZFAND3**	1.84926	2.03E-36	**CSF1**	1.75687	2.02E-06
ARNTL2	1.96570	1.59E-29	**SMG1**	1.84884	1.94E-27	**SF3B14**	1.75377	1.67E-15
PRKAB2	1.96499	5.58E-16	**ZDHHC11**	1.84730	2.77E-07	**RASGEF1C**	1.75077	5.06E-05
PIK3IP1	1.96307	1.50E-02	**ZNF622**	1.84678	2.91E-13	**RAPGEF4**	1.75003	2.07E-02
UFM1	1.96189	5.42E-08	**FLJ39639**	1.84653	1.59E-02	**CXorf23**	1.74805	1.76E-04
MIR210HG	1.96090	4.84E-02	**CLK1**	1.84586	3.62E-44	**MYL12B**	1.74790	7.58E-32
NPR3	1.96082	3.63E-02	**EIF5A2**	1.84372	6.54E-06	**MIR22HG**	1.74782	1.01E-03
ACRBP	1.96049	2.07E-03	**IL10RB**	1.84065	5.37E-22	**PIM3**	1.74773	1.14E-24
MAST1	1.94936	3.94E-03	**ZNF143**	1.83985	1.45E-28	**RICTOR**	1.74746	5.40E-34
SLC6A8	1.93929	3.78E-10	**ADAMTS9**	1.83852	3.50E-02	**EFHD2**	1.74269	2.30E-20
UBE2B	1.93823	1.88E-47	**ATP6V1D**	1.83460	2.69E-29	**INPP5K**	1.74170	9.42E-23
ACTBL2	1.93803	4.62E-02	**ACR**	1.83093	1.14E-03	**HN1**	1.74112	6.10E-19
SLC37A2	1.93690	4.05E-05	**USP2**	1.83062	5.28E-09	**CBL**	1.74105	2.71E-23
TMEM158	1.93556	2.23E-06	**MSMO1**	1.83024	1.48E-18	**SLC30A1**	1.74054	3.28E-04
ABCA3	1.93513	3.13E-09	**CDK17**	1.82990	9.60E-45	**CCDC93**	1.74019	3.30E-24
SESN2	1.93002	3.80E-10	**SYDE1**	1.82670	8.07E-13	**NEDD9**	1.73999	7.97E-07
SNX16	1.92841	4.69E-30	**RINT1**	1.82441	5.65E-16	**FAM86B1**	1.73903	9.01E-03
ZNF841	1.92538	1.19E-18	**CYP21A1P**	1.82399	3.91E-03	**UBLCP1**	1.73674	1.66E-05
SYNE3	1.92424	1.24E-09	**LOC550112**	1.82256	2.45E-12	**FAM111A**	1.73665	4.34E-19
FOSB	1.92092	8.63E-06	**CCNH**	1.81895	4.56E-18	**USP53**	1.73527	9.34E-12
LOC654342	1.92052	1.34E-02	**C4orf47**	1.81200	3.06E-02	**NCCRP1**	1.73505	2.64E-05
KIAA0226L	1.91799	1.12E-02	**YIPF4**	1.81131	4.07E-04	**WDR66**	1.73376	2.21E-06

FGD4	1.73301	9.45E-14	**CPEB3**	1.64492	7.29E-13	**CDC42EP1**	1.56952	1.06E-15
TUBE1	1.73061	1.10E-12	**NUDT9P1**	1.64430	4.76E-02	**WNT2B**	1.56934	1.85E-06
HCG18	1.73011	1.58E-12	**MET**	1.64400	1.05E-36	**MED18**	1.56930	4.73E-20
PLEKHA3	1.72725	2.44E-27	**LOC220906**	1.64341	1.45E-12	**KIAA1244**	1.56692	4.31E-11
FAM200A	1.72573	2.61E-12	**FAM162A**	1.64322	7.05E-22	**ROPN1L**	1.56643	1.28E-03
AMD1	1.72473	3.61E-24	**IFIH1**	1.64145	2.29E-08	**SMNDC1**	1.56595	2.65E-27
EPB41L4B	1.72257	1.59E-02	**GOLGA7B**	1.64125	1.78E-02	**EGR2**	1.56545	2.43E-02
FGD6	1.72247	5.01E-35	**CSRNP1**	1.64063	3.93E-08	**MMP13**	1.56455	2.75E-02
BZW1	1.72105	6.45E-22	**NME7**	1.64054	6.13E-12	**FADS3**	1.56368	6.60E-10
DENND2C	1.71883	1.03E-05	**NKIRAS1**	1.63992	5.73E-26	**TPT1-AS1**	1.56209	7.15E-10
SLC3A2	1.71774	1.56E-69	**MFNG**	1.63778	1.34E-02	**ZNF263**	1.56069	4.55E-07
EGFR	1.71439	7.99E-37	**NXNL2**	1.63728	1.21E-02	**BTN2A2**	1.56046	4.01E-09
OSBPL2	1.71384	1.09E-17	**ZNF770**	1.63676	2.41E-02	**CAP1**	1.56036	2.67E-23
SEC61G	1.71354	1.17E-21	**NR1D2**	1.63547	2.35E-18	**BTBD10**	1.56014	4.19E-29
PPP4R1L	1.71328	9.18E-12	**TMEM88**	1.63406	2.58E-05	**ARHGAP21**	1.55970	7.94E-18
LOC401127	1.71312	2.28E-02	**ARID4A**	1.63167	7.27E-14	**ZNF674**	1.55907	3.56E-10
KCNQ1OT1	1.71299	1.26E-11	**PGM2**	1.63136	6.92E-12	**TFEB**	1.55856	2.43E-15
NBR2	1.71053	1.73E-14	**LOC650623**	1.62866	1.64E-09	**CASKIN1**	1.55801	2.34E-03
ZBTB25	1.71023	3.77E-14	**ZNF670**	1.62730	4.41E-24	**ISCA1**	1.55759	1.49E-09
EFNB2	1.70976	1.81E-13	**FAM106CP**	1.62616	1.54E-04	**WASF2**	1.55739	4.22E-16
ERN1	1.70831	1.26E-11	**FAM211A**	1.62605	1.31E-02	**CYTH3**	1.55669	3.92E-10
EPAS1	1.70817	2.63E-10	**NRP1**	1.62601	2.10E-06	**KIAA1033**	1.55559	4.06E-10
ERVV-1	1.70670	8.68E-06	**ZFAND2A**	1.62514	5.30E-24	**SERPINE1**	1.55521	2.64E-05
BNIP2	1.70590	3.16E-27	**IRF6**	1.62496	3.50E-20	**C1orf109**	1.55491	9.20E-19
LAMTOR3	1.70293	5.55E-26	**UBR4**	1.62478	1.14E-19	**MKI67IP**	1.55378	2.75E-09
PCF11	1.70292	3.37E-26	**NCK1**	1.62362	5.55E-21	**PIK3CD**	1.55373	3.20E-08
ZNF616	1.70193	2.67E-12	**AMZ2P1**	1.62292	8.81E-04	**DMTF1**	1.55361	8.41E-17
CASP4	1.70106	3.71E-20	**PPFIBP2**	1.62046	6.72E-03	**SLC39A14**	1.55352	4.49E-24
CHMP4C	1.70013	7.25E-26	**FAHD2B**	1.62024	1.03E-05	**AGPAT4**	1.55200	1.16E-03
ITGB1	1.69975	2.32E-28	**AFAP1**	1.62018	1.87E-09	**MYO15B**	1.55029	1.65E-03
MCOLN3	1.69889	2.36E-09	**ATP6V1C1**	1.61956	1.71E-28	**SLC35A1**	1.54955	3.60E-14
HSBP1L1	1.69872	5.14E-21	**CYLD**	1.61829	9.61E-09	**ETV5**	1.54868	6.17E-06
LOC100134368	1.69822	3.23E-02	**RFX2**	1.61681	4.63E-11	**GAS5**	1.54652	1.07E-23
HIVEP1	1.69535	2.32E-13	**C12orf49**	1.61616	1.40E-14	**ZC3H6**	1.54552	3.03E-10
HBP1	1.69418	2.27E-20	**SYNGAP1**	1.61428	9.65E-15	**SERPINB1**	1.54302	5.38E-09
RAB5A	1.69381	5.92E-63	**UGCG**	1.61380	9.01E-11	**CCDC148**	1.54149	9.14E-03
SREK1IP1	1.69241	4.54E-29	**UBE2H**	1.61275	5.19E-17	**FRA10AC1**	1.54088	1.90E-14
GPR126	1.69094	5.42E-22	**LOC400657**	1.60808	1.82E-04	**RNF216P1**	1.53979	9.19E-13
RAB14	1.68986	4.37E-62	**CARS**	1.60600	5.71E-18	**NEK6**	1.53861	9.28E-09
GOLGA6C	1.68979	2.93E-02	**ARL6IP6**	1.60549	8.69E-31	**RBM15**	1.53851	8.93E-14
N4BP2L2	1.68895	7.86E-08	**PI4K2A**	1.60535	5.62E-24	**FAM83B**	1.53425	3.31E-14
FLNB	1.68798	2.04E-29	**MKNK2**	1.60488	1.45E-15	**RPA4**	1.53416	4.89E-02
LY6G5C	1.68602	6.92E-07	**WRNIP1**	1.60345	1.85E-16	**TMEM242**	1.53365	4.30E-17
DGCR10	1.68368	2.36E-06	**HINT3**	1.60314	2.19E-16	**APOL6**	1.53346	1.91E-08
SLC38A2	1.68368	4.89E-17	**SLC1A4**	1.60271	1.07E-06	**ZSCAN12P1**	1.53344	8.93E-14
STX1A	1.68352	3.98E-04	**SBDS**	1.60247	6.00E-27	**TTBK2**	1.53207	5.72E-17
SOCS3	1.68348	2.77E-03	**IFFO2**	1.60211	7.69E-14	**FLJ46906**	1.53181	2.99E-07
CDK6	1.68257	1.27E-19	**LPIN1**	1.60189	6.28E-10	**PRKCI**	1.53068	8.20E-22
CA5BP1	1.68221	2.90E-06	**RAB7A**	1.60175	6.41E-33	**DDIT3**	1.52892	2.96E-05
ACSL4	1.67985	3.93E-11	**ZNF160**	1.60110	2.52E-12	**SLC16A8**	1.52871	3.68E-02
CHD5	1.67593	7.28E-03	**RAB18**	1.60096	1.60E-16	**TIAL1**	1.52780	2.72E-28
ZNF654	1.67519	4.83E-18	**SOD2**	1.60063	2.44E-08	**GFPT2**	1.52741	2.09E-03
HIST1H1T	1.67290	2.01E-03	**BCL3**	1.59749	1.02E-04	**ZFYVE1**	1.52156	5.52E-19
RPF2	1.67177	4.13E-11	**SEC24A**	1.59726	2.41E-07	**LOC100506385**	1.52126	4.64E-02
GDF15	1.67093	1.86E-12	**ITPR2**	1.59726	1.76E-05	**TRIB3**	1.52113	2.43E-13
FOXO3	1.66993	1.98E-42	**HNF4G**	1.59634	4.22E-02	**CCDC85B**	1.52110	1.65E-12
BACH2	1.66857	1.11E-07	**ZFP36L1**	1.59451	1.95E-04	**TAS2R5**	1.52084	4.43E-04
FAM118B	1.66825	4.57E-26	**ULBP2**	1.59406	1.25E-16	**FBXO42**	1.51996	3.47E-19
USP32	1.66410	1.07E-13	**LOC646329**	1.59223	2.33E-04	**ROCK1**	1.51931	3.83E-11
SGK494	1.66111	2.73E-07	**LCOR**	1.59176	9.75E-03	**PLAUR**	1.51929	3.87E-09
TAP1	1.66021	9.22E-13	**MYL12A**	1.59092	5.43E-16	**TAOK1**	1.51929	9.30E-14
GATAD1	1.65933	5.39E-25	**HLA-DRB1**	1.58776	2.78E-03	**POU2F1**	1.51925	9.40E-18
ZNF318	1.65781	3.46E-36	**TYMP**	1.58650	2.21E-05	**MOSPD2**	1.51894	2.42E-18
NFATC1	1.65758	1.72E-03	**APOPT1**	1.58576	5.04E-04	**CECR6**	1.51795	7.94E-03
SLC22A1	1.65615	4.09E-03	**GTPBP2**	1.58573	6.72E-16	**AMOTL2**	1.51794	3.24E-27
GPR160	1.65610	8.19E-10	**PPP1R14C**	1.58374	2.38E-07	**SP4**	1.51671	6.05E-15
SNHG15	1.65466	5.29E-07	**FOSL1**	1.58358	4.09E-03	**SLC22A13**	1.51558	1.67E-03
ATP6V1B2	1.65438	5.97E-32	**CSGALNACT2**	1.58166	7.64E-11	**PAWR**	1.51495	7.82E-15
ARAP2	1.65317	2.88E-20	**PHLDA1**	1.58123	6.05E-09	**PGAM1**	1.51384	1.00E-20
SHB	1.65273	6.83E-18	**FAM189A2**	1.58025	4.80E-03	**JUNB**	1.51353	2.55E-20
DNAJC6	1.65179	6.18E-16	**GNAL**	1.58023	1.99E-02	**BTF3**	1.51158	1.16E-22
ADAMTS16	1.65137	2.23E-08	**ZFHX2**	1.57886	1.34E-04	**CHD2**	1.51130	3.39E-14
DHX40	1.65072	3.55E-34	**YPEL5**	1.57729	2.96E-15	**MICAL2**	1.51114	3.76E-08
FAM206A	1.64982	2.43E-14	**ZSWIM4**	1.57711	3.06E-11	**AP3S1**	1.50999	5.04E-12
ANKRD12	1.64916	4.22E-15	**C14orf28**	1.57522	1.43E-03	**PRSS8**	1.50933	8.49E-09
TNRC6C	1.64869	6.35E-06	**GOT1**	1.57038	1.60E-14	**ZNF283**	1.50774	1.42E-07
PHACTR2	1.64581	5.02E-15	**SEMA4B**	1.56995	5.89E-24	**MAPK8IP3**	1.50734	2.36E-24
CEBPB	1.64539	1.23E-08	**TNIP1**	1.56965	1.62E-24	**BRWD3**	1.50700	6.29E-08

DIS3	1.50590	6.29E-15	**CREBBP**	1.44359	2.81E-18	**KCNK1**	1.39021	6.63E-22
NCEH1	1.50500	2.74E-23	**SMPD1**	1.44283	7.87E-20	**SLC22A14**	1.38972	2.98E-02
DDX11-AS1	1.50443	1.41E-10	**LINC00623**	1.44251	5.68E-08	**ADAM8**	1.38901	2.89E-11
GPN2	1.50432	2.22E-09	**FBXO8**	1.44234	2.40E-15	**SERTAD4-AS1**	1.38837	4.10E-05
UVRAG	1.50393	4.74E-15	**UBE2W**	1.44212	3.76E-24	**TGFBR2**	1.38533	1.26E-06
SSH1	1.50274	1.64E-18	**PPIL4**	1.44211	9.45E-20	**MEF2D**	1.38404	7.09E-15
CREB1	1.50244	5.08E-36	**SP100**	1.44177	9.03E-07	**PLSCR1**	1.38286	7.12E-05
LOC100506710	1.50022	2.53E-29	**ATG12**	1.44159	6.86E-19	**SLC6A9**	1.38273	4.58E-04
CHTOP	1.49972	8.82E-25	**TSNAX**	1.44034	1.59E-20	**OSBP**	1.38238	2.04E-16
PPP2R5B	1.49750	2.58E-11	**USP31**	1.43935	7.94E-12	**KDSR**	1.38223	1.44E-08
VPS37D	1.49704	4.51E-03	**PTRF**	1.43890	1.24E-11	**VPS13C**	1.38182	4.77E-15
RTN4RL2	1.49689	5.55E-04	**TAF2**	1.43652	2.03E-15	**BLOC1S3**	1.38096	3.60E-06
AIM1L	1.49620	1.38E-16	**NFATC2**	1.43613	1.59E-05	**THSD1**	1.37935	4.23E-03
HKDC1	1.49501	3.16E-02	**SBF2-AS1**	1.43445	3.43E-09	**NUDCD1**	1.37850	7.33E-09
TAX1BP1	1.49386	3.47E-13	**IFNAR2**	1.43381	4.94E-18	**IKBIP**	1.37846	2.44E-07
OBSCN	1.49310	1.10E-06	**SLC25A36**	1.43326	3.04E-11	**DUSP8**	1.37804	1.45E-08
TYW5	1.49112	1.01E-05	**C9orf85**	1.43265	3.52E-06	**ABTB1**	1.37771	1.45E-08
YY1AP1	1.49077	9.64E-04	**TBC1D23**	1.43255	7.24E-20	**C2orf76**	1.37762	3.91E-05
ANAPC11	1.49012	1.48E-02	**PIP5K1A**	1.43252	5.19E-11	**RBPJ**	1.37721	2.99E-19
TPT1	1.48726	8.98E-37	**BCOR**	1.43250	1.44E-25	**PFKFB4**	1.37665	4.04E-11
LOC399744	1.48658	3.15E-04	**ARHGEF40**	1.43237	1.62E-03	**ZNF426**	1.37588	1.48E-17
SOX15	1.48657	4.43E-12	**SYTL3**	1.43158	3.63E-06	**PPP1R15B**	1.37509	8.26E-12
CABLES1	1.48621	2.33E-08	**CDC42**	1.43080	2.23E-10	**TMEM80**	1.37475	4.83E-07
NEU1	1.48539	1.46E-17	**YOD1**	1.43017	2.38E-13	**NOP10**	1.37467	1.38E-11
ANGPT1	1.48477	2.48E-10	**TAF12**	1.42982	1.12E-07	**NFKBIB**	1.37342	1.63E-18
ARL13B	1.48452	6.84E-14	**ABCA5**	1.42928	6.42E-08	**TPRN**	1.37305	4.20E-11
SOAT1	1.48423	1.01E-15	**FAM209A**	1.42912	3.00E-02	**NRD1**	1.37212	5.67E-12
UTP23	1.48386	3.58E-19	**C12orf60**	1.42911	5.32E-04	**OXSM**	1.37183	1.67E-15
JMJD1C	1.48315	1.81E-10	**FOXD1**	1.42863	1.16E-15	**UPF3B**	1.37014	4.15E-12
IST1	1.48252	1.94E-42	**LINS**	1.42636	3.41E-05	**RBM7**	1.36979	3.49E-09
TLL2	1.48106	1.10E-02	**RPL22L1**	1.42625	3.01E-09	**ZFYVE28**	1.36838	3.11E-03
RP9	1.48084	3.05E-11	**MR1**	1.42599	7.04E-08	**C14orf119**	1.36809	1.12E-16
APC2	1.48070	2.03E-02	**SOS2**	1.42538	2.78E-18	**B4GALT1**	1.36762	4.45E-25
DLEU1	1.47923	7.67E-10	**CHMP4B**	1.42444	2.52E-28	**FAM91A1**	1.36738	8.00E-41
DUSP14	1.47910	2.03E-10	**MED19**	1.42434	3.77E-20	**LTN1**	1.36566	1.48E-11
AZIN1	1.47751	2.45E-30	**RPL21P44**	1.42373	2.33E-02	**STX2**	1.36551	8.25E-13
PDGFA	1.47697	4.84E-20	**ST3GAL1**	1.42286	4.61E-18	**C16orf72**	1.36487	2.55E-20
CLCN7	1.47645	2.71E-19	**DBNDD2**	1.42199	5.49E-12	**CCDC157**	1.36368	1.73E-05
RRNAD1	1.47616	1.31E-04	**PHLDA2**	1.42174	8.76E-07	**TFB2M**	1.36172	3.42E-06
GLIS2	1.47538	2.15E-06	**SERPINB9**	1.42152	5.26E-07	**RTN4R**	1.36159	1.32E-13
C17orf107	1.47498	3.10E-12	**ACSL3**	1.42152	3.25E-11	**DCAF10**	1.35974	3.05E-21
SLC35E3	1.47442	5.58E-14	**DET1**	1.42030	1.89E-03	**CRKL**	1.35937	5.52E-38
ZNF607	1.47404	1.28E-17	**C7orf60**	1.41856	2.32E-05	**NCOA7**	1.35923	2.70E-13
RAB33B	1.47347	4.01E-08	**SEC24D**	1.41798	4.63E-07	**RSC1A1**	1.35879	1.29E-12
EIF2B2	1.47214	1.41E-19	**SPRED3**	1.41794	2.62E-02	**AS3MT**	1.35876	9.23E-04
SLCO4A1	1.47184	7.04E-14	**STARD4**	1.41693	2.17E-05	**ZNF568**	1.35772	4.82E-02
HSPA13	1.47141	5.95E-11	**ZDHHC7**	1.41662	2.15E-25	**PIM1**	1.35646	2.78E-19
CSRP2	1.47133	2.15E-04	**PPP1CC**	1.41604	3.79E-20	**NFE2L2**	1.35627	2.32E-21
RAD50	1.47127	1.86E-21	**RB1CC1**	1.41541	5.34E-11	**CNEP1R1**	1.35587	2.27E-10
SLU7	1.47002	1.93E-14	**HDAC5**	1.41495	4.92E-17	**BRAF**	1.35557	7.36E-18
EIF4A3	1.46901	6.73E-13	**CLIC4**	1.41450	2.18E-16	**FAM46A**	1.35533	1.55E-09
ANLN	1.46869	1.50E-34	**SLC16A3**	1.41438	4.35E-08	**NCKAP1**	1.35502	3.25E-17
CDKN1C	1.46726	2.35E-05	**MACF1**	1.41434	2.36E-17	**PCDHB19P**	1.35441	1.39E-02
IFNGR1	1.46450	2.02E-25	**AJUBA**	1.41224	7.08E-13	**IRF2BP2**	1.35426	3.06E-13
RUSC2	1.46198	4.54E-35	**RAP1B**	1.41218	1.23E-12	**KGFLP1**	1.35216	2.20E-05
NAGS	1.46198	5.37E-04	**ZNF706**	1.41206	5.19E-17	**RAPGEF6**	1.35202	2.76E-16
FBXL3	1.46183	8.71E-18	**ANO6**	1.41197	3.35E-21	**SEC14L1**	1.35148	7.70E-23
GSTO2	1.46085	2.23E-02	**LOC100289495**	1.41142	5.51E-03	**E2F6**	1.35124	1.84E-13
PPP3CC	1.45863	2.76E-10	**PORCN**	1.41060	9.76E-11	**UBL3**	1.35086	2.69E-32
SLC22A4	1.45813	7.54E-05	**GNAI3**	1.41011	1.38E-23	**HSF2**	1.35020	3.19E-06
TBC1D12	1.45807	5.30E-13	**COX19**	1.40951	7.97E-16	**ZNF669**	1.35009	1.11E-08
ADAM9	1.45622	8.37E-35	**L3MBTL3**	1.40886	1.31E-04	**TMEM38A**	1.35005	1.79E-10
STX3	1.45491	2.36E-13	**FNIP1**	1.40801	3.76E-13	**ITSN2**	1.34812	2.56E-19
ST6GALNAC6	1.45471	2.13E-13	**C2orf72**	1.40571	2.39E-02	**YAF2**	1.34760	8.95E-05
UCHL3	1.45346	1.95E-19	**EFNA3**	1.40365	6.14E-04	**ZNF28**	1.34730	3.49E-11
AMY2B	1.45146	1.21E-02	**COQ10B**	1.40029	1.24E-20	**SLC10A5**	1.34692	1.05E-02
LOC100270746	1.45141	8.46E-03	**CLDN1**	1.40021	2.72E-05	**MTHFR**	1.34677	1.76E-11
NFYB	1.45008	7.92E-22	**SAMD8**	1.39999	1.22E-21	**JDP2**	1.34563	5.53E-07
PPCDC	1.44960	9.27E-09	**PLEKHA5**	1.39926	8.26E-12	**NARF**	1.34560	7.50E-16
AKT3	1.44959	2.82E-12	**SOCS2**	1.39896	1.56E-02	**CGRRF1**	1.34502	1.01E-09
KIAA0922	1.44931	8.39E-07	**FAM131C**	1.39822	2.37E-02	**ZBTB10**	1.34493	2.51E-15
STYK1	1.44919	8.67E-10	**SAFB2**	1.39728	3.77E-09	**GNG12**	1.34491	1.31E-25
FAM18B1	1.44767	4.87E-18	**ARL5B**	1.39689	1.54E-11	**LOC400027**	1.34355	6.65E-06
C10orf118	1.44663	8.57E-13	**FLJ42627**	1.39677	2.03E-09	**TTC1**	1.34247	4.43E-17
RAPGEF2	1.44642	3.13E-05	**ESAM**	1.39493	8.24E-05	**STK24**	1.34214	8.56E-12
ZNF566	1.44601	1.96E-08	**PTRH2**	1.39462	3.11E-03	**LOC100132352**	1.34204	1.20E-04
SERINC1	1.44548	1.46E-24	**ACTR3**	1.39393	1.38E-17	**CDCP1**	1.34183	6.70E-20
AMN1	1.44377	2.07E-06	**RPS13**	1.39294	7.38E-22	**SPATA2L**	1.34079	6.69E-13

PRRG1	1.34047	1.38E-06	**GBP1**	1.29556	4.88E-02	**CAMTA1**	1.24153	1.14E-04
SGMS2	1.33938	1.39E-12	**GRHL1**	1.29548	3.46E-11	**TJP1**	1.24137	4.80E-19
SLC25A45	1.33934	4.53E-03	**IRF1**	1.29522	1.66E-09	**VWCE**	1.24073	1.37E-03
ZBTB11	1.33850	7.54E-13	**SEL1L3**	1.29379	7.82E-19	**ZSWIM6**	1.24017	1.17E-10
VDAC2	1.33698	4.84E-25	**SKAP2**	1.28993	3.56E-11	**MRFAP1L1**	1.24010	7.18E-17
COL17A1	1.33591	4.44E-05	**ZNF778**	1.28893	1.74E-02	**GJB3**	1.23983	4.41E-04
TMCO3	1.33578	2.16E-08	**GSK3B**	1.28885	4.25E-19	**SUMO1P3**	1.23928	9.82E-12
NLGN3	1.33559	1.06E-03	**PCNXL4**	1.28856	6.92E-12	**LRRC1**	1.23828	9.98E-14
RALA	1.33390	1.86E-04	**BAGE2**	1.28843	4.76E-20	**GART**	1.23747	5.82E-15
TUBB2A	1.32959	1.87E-06	**SDHAF2**	1.28692	1.55E-10	**ZNF646**	1.23707	1.04E-08
ZFYVE26	1.32858	3.08E-12	**CNBP**	1.28615	1.48E-18	**PMS2CL**	1.23666	1.21E-12
ZNF140	1.32774	2.55E-17	**CRY1**	1.28609	1.25E-04	**ENO3**	1.23523	1.36E-04
FNBP1	1.32714	7.13E-23	**RAB21**	1.28580	1.08E-05	**CMC1**	1.23501	1.11E-09
CDKL4	1.32700	4.12E-03	**LAMP2**	1.28550	6.74E-11	**SLC7A1**	1.23434	1.51E-15
ZNF14	1.32602	2.47E-11	**METTL6**	1.28504	2.65E-11	**BTBD1**	1.23428	3.49E-20
CCNI	1.32595	1.21E-19	**KATNA1**	1.28438	6.32E-12	**KRAS**	1.23399	1.45E-11
C10orf2	1.32588	7.70E-09	**LOC100128822**	1.28181	1.95E-03	**ZNF439**	1.23350	1.11E-03
AXL	1.32516	7.72E-10	**H1F0**	1.28146	1.35E-08	**KIAA0513**	1.23292	1.86E-12
AKIRIN1	1.32501	1.21E-15	**BRSK1**	1.28113	2.75E-05	**MTMR14**	1.23230	1.10E-19
ZBTB1	1.32380	5.43E-16	**QSOX1**	1.28000	1.43E-12	**LRRC69**	1.23194	3.96E-02
PGRMC2	1.32237	8.23E-16	**DCBLD1**	1.27972	4.82E-06	**EPN2**	1.23152	1.22E-09
CEP170	1.32178	2.54E-07	**MAPK6**	1.27959	7.47E-13	**LINC00174**	1.23085	5.23E-03
SETX	1.32115	1.98E-15	**ZNF880**	1.27894	1.66E-02	**GRB2**	1.23047	2.81E-12
RTN2	1.32059	4.10E-04	**SCG5**	1.27888	1.40E-03	**SPIRE1**	1.23007	9.53E-15
ATP6V0A4	1.32040	1.39E-04	**EAPP**	1.27493	9.86E-23	**CIB1**	1.22910	5.85E-14
NKRF	1.31990	1.59E-02	**STOML1**	1.27457	2.80E-06	**GON4L**	1.22827	4.26E-11
TTLL3	1.31983	7.16E-04	**CWC22**	1.27454	5.42E-11	**RAB11FIP5**	1.22716	1.08E-10
TUBA1A	1.31965	5.53E-06	**C1orf27**	1.27252	4.40E-05	**PNO1**	1.22714	1.84E-05
TMTC2	1.31943	6.53E-04	**SRGAP2**	1.27238	2.51E-11	**GFPT1**	1.22629	1.80E-16
DENND4A	1.31932	1.25E-28	**AHNAK**	1.27187	4.29E-12	**DDI2**	1.22626	3.36E-02
LOC387647	1.31872	2.38E-23	**UAP1**	1.27127	6.29E-12	**JMJD6**	1.22574	5.69E-07
POGZ	1.31846	1.86E-20	**AKAP10**	1.26924	3.69E-10	**LOC170425**	1.22560	1.63E-02
NADK	1.31811	3.47E-02	**LOC643837**	1.26828	2.05E-08	**SIM2**	1.22398	3.28E-07
FAM190B	1.31797	6.86E-11	**EIF4A2**	1.26816	4.47E-24	**ABHD5**	1.22290	4.19E-05
PPP2R3C	1.31789	8.71E-13	**FBXO25**	1.26797	4.02E-13	**MKL1**	1.22146	1.65E-12
SDC4	1.31737	1.66E-11	**SLFNL1-AS1**	1.26784	2.41E-03	**CEP95**	1.22092	6.68E-03
RAB23	1.31732	3.13E-20	**MYO9A**	1.26727	1.48E-18	**CREM**	1.22060	9.43E-05
TMCC3	1.31724	4.36E-04	**CSAG1**	1.26608	4.89E-14	**SNX32**	1.21994	2.46E-02
THAP6	1.31572	6.38E-13	**MFSD12**	1.26572	3.31E-06	**C1orf226**	1.21981	2.50E-07
NOC3L	1.31568	2.79E-07	**ZNF491**	1.26554	3.61E-02	**SNX9**	1.21920	8.41E-13
TAF4B	1.31564	3.39E-04	**GRIK5**	1.26386	6.94E-03	**PPP2R5C**	1.21804	3.56E-03
LOC100133091	1.31333	4.98E-02	**SPRED1**	1.26374	2.18E-14	**RIPK2**	1.21744	8.53E-27
HLA-E	1.31312	2.77E-05	**VPS4B**	1.26282	1.80E-22	**RAB11FIP2**	1.21711	4.27E-12
PLA2G6	1.31307	1.52E-05	**ATAD1**	1.26216	9.60E-13	**SAT2**	1.21679	4.25E-07
CLTC	1.31278	4.05E-15	**DST**	1.26200	9.27E-17	**SLC25A51**	1.21597	6.91E-16
SNAPC1	1.31239	5.53E-11	**ZNF558**	1.25924	1.62E-06	**PUM2**	1.21573	1.82E-28
CEP120	1.31209	1.96E-09	**RAPH1**	1.25798	5.42E-08	**CTDSP2**	1.21547	8.31E-09
P4HA2	1.31191	3.56E-14	**HOMER2**	1.25775	8.57E-08	**POU6F1**	1.21509	3.29E-04
PATL1	1.31087	3.82E-13	**SMG1P1**	1.25705	2.47E-16	**RYBP**	1.21481	3.06E-13
GOLGA8B	1.31059	2.89E-08	**LOC652276**	1.25485	2.29E-04	**DNM2**	1.21408	1.59E-12
VAPB	1.31038	9.33E-30	**PDLIM2**	1.25472	5.20E-04	**SMEK2**	1.21346	1.48E-10
TRPM7	1.31035	1.76E-23	**PAFAH1B1**	1.25436	6.67E-35	**USP43**	1.21332	2.07E-16
LOC150197	1.31031	2.53E-02	**ILK**	1.25339	3.05E-18	**FBXL12**	1.21245	3.72E-21
SPOPL	1.30940	1.32E-18	**CD101**	1.25269	1.50E-04	**PLEKHA8**	1.21240	7.37E-08
MYC	1.30927	2.53E-02	**STAU1**	1.25246	5.44E-18	**IMMP1L**	1.21235	4.41E-05
LOC439990	1.30917	1.28E-13	**LOC100506668**	1.25176	9.44E-12	**RBM18**	1.21216	2.89E-11
TACC2	1.30876	2.15E-03	**SMG6**	1.25161	4.60E-09	**ZNF155**	1.21179	4.61E-03
PITPNB	1.30865	7.08E-12	**ATP6V0A1**	1.25132	1.42E-13	**COMMD3**	1.21090	5.26E-16
PPP3CB	1.30824	1.68E-16	**OSTM1**	1.25118	7.72E-10	**ENOPH1**	1.21082	2.95E-13
ZXDB	1.30712	2.75E-09	**CTIF**	1.25067	1.26E-18	**RBCK1**	1.21000	3.38E-06
PIGH	1.30682	3.25E-22	**KIAA1614**	1.25019	5.97E-03	**WAC**	1.20975	7.67E-11
ALCAM	1.30591	1.28E-19	**FZD6**	1.25013	4.65E-18	**MPP6**	1.20939	1.74E-07
LOC100507217	1.30587	6.34E-13	**MTM1**	1.24969	5.19E-07	**TBX19**	1.20911	1.45E-05
FGF11	1.30587	1.33E-04	**S100A13**	1.24967	3.44E-09	**DAD1**	1.20844	1.10E-13
ZNF44	1.30192	2.05E-05	**GDPD1**	1.24898	2.17E-04	**CELF1**	1.20803	7.26E-09
ZNF136	1.30172	5.56E-08	**SCARNA9**	1.24866	3.18E-11	**NOS1AP**	1.20787	5.36E-05
EXOC1	1.30132	1.47E-11	**ODF2L**	1.24794	1.01E-05	**ATG5**	1.20724	3.59E-18
PIBF1	1.30067	8.90E-08	**GPR115**	1.24786	1.10E-02	**KLHL9**	1.20694	8.39E-14
KIDINS220	1.30055	5.35E-20	**STXBP1**	1.24778	5.38E-05	**TSPAN2**	1.20674	6.03E-05
WHAMM	1.30037	4.71E-09	**KRT80**	1.24721	9.09E-08	**KLHL5**	1.20674	8.19E-21
SEPSECS	1.30036	3.83E-06	**LDLR**	1.24682	7.16E-09	**MTERFD1**	1.20521	3.13E-05
STAT5A	1.29947	8.31E-04	**ZNF121**	1.24659	7.69E-13	**SLC15A3**	1.20464	1.11E-02
SYS1	1.29924	1.74E-14	**MLL5**	1.24567	2.72E-28	**SNW1**	1.20372	1.34E-19
FAM131A	1.29901	2.00E-06	**CHRNB1**	1.24471	1.37E-15	**SCYL2**	1.20284	8.76E-09
DDR2	1.29845	3.20E-02	**ZFP30**	1.24463	4.49E-10	**TMEM41B**	1.20172	7.07E-11
ZNF398	1.29816	4.82E-20	**TRIB1**	1.24440	1.17E-05	**MGA**	1.20099	5.27E-09
SHOC2	1.29799	1.76E-15	**TMED7**	1.24243	3.97E-11	**RFX3**	1.19988	8.06E-07
CNN3	1.29679	8.03E-20	**KRT16**	1.24236	3.64E-02	**ATRX**	1.19865	6.16E-10

IL36RN	1.19848	1.19E-02	**GABARAP**	1.16445	1.88E-06	**SLC25A22**	1.12109	8.87E-08
RBFOX2	1.19748	2.43E-21	**LARS**	1.16318	1.10E-08	**FOXD4**	1.11915	1.54E-02
RPP30	1.19733	4.08E-07	**GGPS1**	1.16259	2.25E-21	**KLF13**	1.11908	4.72E-13
TPRG1L	1.19713	3.05E-12	**TAF9**	1.16234	5.45E-07	**TGFB1**	1.11728	7.58E-14
HS1BP3	1.19696	3.33E-10	**HAS3**	1.16209	4.59E-02	**SNAP23**	1.11693	1.93E-09
MAFK	1.19663	5.28E-10	**ADNP2**	1.16191	4.60E-15	**MAPKAPK2**	1.11576	2.44E-15
RNF6	1.19645	3.51E-13	**SMCR8**	1.16157	6.41E-16	**TAF1B**	1.11559	7.88E-08
RAB3IP	1.19639	2.52E-13	**ABHD12**	1.16124	3.69E-13	**SPTBN5**	1.11543	7.25E-03
UTRN	1.19635	1.98E-11	**CYP1A1**	1.16091	1.68E-02	**MEGF9**	1.11490	9.19E-06
HSCB	1.19608	1.54E-08	**ATG7**	1.16063	7.89E-10	**ACOT9**	1.11367	5.27E-08
L1CAM	1.19554	1.43E-03	**SSR4P1**	1.16047	4.09E-02	**HARBI1**	1.11289	3.84E-09
PKP2	1.19413	2.72E-14	**ZNF107**	1.16033	4.21E-07	**CDC14A**	1.11272	2.36E-06
PHLPP2	1.19376	6.23E-09	**DHX32**	1.15753	5.87E-17	**MED13**	1.11257	7.65E-11
C15orf57	1.19293	1.06E-07	**ZNF224**	1.15592	4.14E-03	**RBM33**	1.11249	1.29E-11
TMEM128	1.19278	6.74E-03	**EDEM1**	1.15547	7.06E-10	**GSPT1**	1.11129	2.11E-18
GSE1	1.19238	8.07E-13	**FAM8A1**	1.15534	8.78E-06	**LMTK2**	1.11055	1.99E-17
ATP6V1H	1.19203	1.00E-09	**LRRC37A4P**	1.15439	2.30E-03	**HOMER1**	1.11006	1.58E-09
CDV3	1.19197	3.82E-07	**VPS37B**	1.15283	3.93E-18	**VAT1**	1.10947	5.52E-17
SAV1	1.19153	2.09E-16	**SLC33A1**	1.15280	2.16E-08	**ABCA12**	1.10900	2.03E-04
TMEM194A	1.19031	1.30E-12	**SQLE**	1.15253	3.80E-13	**TAS2R4**	1.10879	1.28E-02
SPOP	1.18946	1.09E-07	**YTHDC1**	1.15208	3.50E-08	**PANK3**	1.10875	3.02E-07
MSANTD1	1.18937	4.45E-02	**ZNF284**	1.15206	2.48E-03	**NAP1L1**	1.10809	4.47E-24
HSPB6	1.18907	1.10E-03	**CLCN6**	1.15160	7.56E-09	**ZNF529**	1.10808	4.45E-04
FUNDC2	1.18839	2.32E-12	**PIK3C2A**	1.15155	1.11E-13	**FAM160A1**	1.10663	6.18E-13
C20orf111	1.18801	7.16E-17	**MICAL1**	1.15089	1.93E-06	**HGSNAT**	1.10550	1.43E-06
ZNF230	1.18659	2.79E-07	**MC1R**	1.15022	2.67E-03	**METTL23**	1.10541	5.83E-06
PLS3	1.18580	6.19E-15	**BTF3L4**	1.14997	7.97E-18	**SLC38A1**	1.10517	3.33E-08
MIR548I1	1.18570	1.51E-02	**ZNF75A**	1.14953	1.79E-10	**MYNN**	1.10441	4.77E-13
EIF2C4	1.18530	3.34E-08	**USP37**	1.14829	2.39E-17	**LZTFL1**	1.10390	1.21E-10
FAM161B	1.18489	7.75E-04	**LOC388796**	1.14714	2.27E-08	**DDX21**	1.10377	1.50E-04
PCID2	1.18424	7.10E-19	**SLC7A5**	1.14595	1.85E-09	**DUSP4**	1.10366	2.80E-05
PJA2	1.18405	5.70E-09	**TMEM39A**	1.14509	1.13E-11	**GRB7**	1.10328	6.30E-05
BAIAP3	1.18363	2.28E-02	**ADAMTSL5**	1.14496	3.21E-06	**WDR45L**	1.10319	2.17E-10
CAMSAP2	1.18270	1.26E-13	**MAP3K14**	1.14430	4.77E-04	**USP34**	1.10304	2.57E-13
RPL34	1.18057	2.63E-07	**METTL14**	1.14424	1.09E-07	**ATP6V0E1**	1.10276	1.90E-12
CYB561D1	1.18056	3.25E-06	**MIR1307**	1.14351	1.06E-06	**TTC21A**	1.10273	2.16E-02
HN1L	1.18031	9.86E-38	**SLC27A5**	1.14350	5.16E-03	**CYP51A1**	1.10238	2.09E-05
TBCEL	1.18010	7.02E-10	**KIF5B**	1.14341	6.12E-09	**MAP1LC3A**	1.10214	4.26E-05
ZNF354A	1.17907	1.13E-07	**HUWE1**	1.14255	2.67E-11	**DEDD2**	1.10093	3.17E-03
GNB5	1.17825	7.47E-10	**CNNM2**	1.14220	1.07E-04	**SMAP2**	1.10081	5.79E-13
ZSCAN21	1.17803	2.87E-09	**ZNF599**	1.14163	9.86E-05	**ACP1**	1.09994	1.06E-13
DFNA5	1.17782	1.49E-02	**TBKBP1**	1.14123	1.18E-07	**NBPF14**	1.09983	3.55E-09
ANAPC13	1.17609	6.89E-08	**CCNB1IP1**	1.14118	1.77E-07	**SUPT7L**	1.09960	2.29E-12
GOLGA4	1.17604	1.69E-09	**WDR60**	1.14113	9.41E-08	**SLC17A5**	1.09942	1.26E-06
ETV6	1.17598	3.27E-11	**PXDC1**	1.14099	1.39E-14	**LAPTM4A**	1.09935	3.91E-17
SEC23B	1.17523	1.85E-17	**E2F4**	1.13942	4.54E-13	**C15orf40**	1.09750	2.88E-09
ERBB2IP	1.17512	3.42E-24	**ATXN3**	1.13903	4.90E-10	**CCDC7**	1.09745	1.84E-04
TSNARE1	1.17468	3.20E-13	**VILL**	1.13901	1.83E-02	**PPP1R3F**	1.09713	4.19E-02
CLDN12	1.17465	2.34E-12	**PHF20L1**	1.13862	4.21E-09	**MAPKAPK5-AS1**	1.09670	4.43E-06
LOC100527964	1.17392	7.81E-07	**TPM3**	1.13814	3.58E-14	**LOC653712**	1.09638	2.56E-02
MYO10	1.17361	8.79E-10	**RDH5**	1.13806	2.14E-02	**SSR3**	1.09587	1.01E-06
LOC100506054	1.17253	3.54E-04	**EMC7**	1.13792	1.77E-14	**ZFP161**	1.09516	3.45E-07
CD47	1.17252	1.73E-09	**RPL21**	1.13771	3.44E-14	**RASA2**	1.09479	4.86E-09
KDM4D	1.17248	1.06E-03	**GULP1**	1.13692	2.71E-07	**CNOT7**	1.09467	5.79E-11
MNT	1.17209	3.82E-16	**COMMD8**	1.13656	1.94E-08	**LOC100289561**	1.09447	5.33E-05
FAM22A	1.17014	2.49E-02	**GNPNAT1**	1.13635	5.54E-08	**TRIP10**	1.09384	1.45E-22
DMPK	1.17012	2.61E-08	**TRIM15**	1.13497	7.85E-04	**CAPZA2**	1.09374	2.94E-12
KIF17	1.16945	2.87E-05	**ARL8A**	1.13480	7.60E-07	**HNRPDL**	1.09356	5.62E-08
CCDC17	1.16931	8.45E-03	**FKBP11**	1.13431	2.39E-02	**ZNF259**	1.09319	2.17E-08
EAF1	1.16928	1.20E-21	**GPX3**	1.13389	3.26E-02	**DHRS2**	1.09304	5.34E-05
TARS	1.16908	5.44E-12	**ZNF271**	1.13242	1.33E-06	**MAN1A1**	1.09212	3.50E-02
LOC100129534	1.16886	4.80E-04	**SLC2A12**	1.13148	5.48E-03	**SPAG1**	1.09141	1.21E-11
C11orf54	1.16864	2.23E-08	**TOB2P1**	1.13103	4.56E-02	**ST3GAL2**	1.09118	2.34E-02
PPP2R5A	1.16857	1.62E-09	**ALS2**	1.13035	7.51E-12	**SLC26A6**	1.09040	2.90E-06
HSD17B7	1.16856	4.84E-10	**INSIG1**	1.13005	4.54E-06	**UBR5**	1.09004	4.00E-15
TLR3	1.16795	2.35E-05	**SLC1A5**	1.12846	1.35E-09	**FOXO3B**	1.08910	5.94E-05
PHLDB2	1.16793	8.64E-07	**LLPH**	1.12825	4.52E-08	**SNORA53**	1.08896	1.11E-23
ANXA2P2	1.16693	2.01E-06	**SEC22B**	1.12812	5.20E-08	**LRRC37A**	1.08714	1.17E-03
PPM1K	1.16676	2.29E-06	**LOC440354**	1.12608	9.86E-06	**MORF4L2**	1.08660	5.62E-10
H3F3B	1.16660	1.63E-11	**SPRED2**	1.12599	9.32E-16	**TMEM127**	1.08648	9.36E-15
FRYL	1.16621	4.32E-09	**SEPT10**	1.12493	3.46E-22	**AMFR**	1.08578	4.05E-09
CCDC91	1.16602	1.02E-11	**HELZ**	1.12444	4.87E-13	**LOC440944**	1.08535	3.07E-04
TBL1XR1	1.16589	2.35E-15	**RHEB**	1.12439	4.63E-13	**CBLB**	1.08511	1.30E-03
MTFP1	1.16528	4.72E-13	**ZNF527**	1.12385	9.02E-04	**MTMR12**	1.08496	6.66E-08
DNAJC25	1.16483	7.81E-06	**ADAM17**	1.12367	5.50E-16	**ZNF397**	1.08434	8.48E-03
CD55	1.16475	8.51E-03	**ZNF84**	1.12246	1.27E-05	**ZNF425**	1.08422	7.12E-07
FAM214A	1.16468	6.78E-10	**TRAF2**	1.12173	4.67E-05	**DPP9**	1.08405	5.62E-10
EPRS	1.16466	9.29E-15	**C16orf52**	1.12159	1.49E-13	**FNBP4**	1.08403	3.75E-10

SCARNA5	1.08380	2.94E-08	**STYXL1**	1.05021	1.58E-05	**PARP9**	1.01243	3.87E-02
UBN1	1.08336	8.60E-09	**SLC19A2**	1.04982	3.49E-07	**PLEKHM1**	1.01190	4.35E-10
NIPA1	1.08330	8.23E-16	**PPP6R3**	1.04884	5.63E-16	**H1FX**	1.01178	3.32E-07
SCARNA1	1.08329	1.08E-02	**STEAP4**	1.04860	3.21E-02	**BAZ2A**	1.01177	4.55E-07
SZT2	1.08277	7.54E-18	**MFAP1**	1.04805	1.89E-13	**MGAT5B**	1.01165	4.23E-04
ATG2B	1.08251	3.69E-07	**AMMECR1L**	1.04558	7.75E-04	**RCHY1**	1.01147	1.19E-07
RTN4	1.08217	2.82E-18	**CLK4**	1.04556	1.65E-04	**RAB22A**	1.01091	1.43E-18
LOC100506963	1.08179	2.41E-02	**CYP2D6**	1.04522	2.95E-04	**MRGBP**	1.00955	4.85E-11
RNF122	1.08121	5.49E-03	**SLC25A32**	1.04469	6.56E-11	**DNAJB2**	1.00917	1.20E-06
PRRC2C	1.08040	3.52E-14	**SLC35E4**	1.04430	9.35E-03	**RIOK2**	1.00914	1.01E-05
ZNF226	1.08014	1.37E-06	**PLCB4**	1.04371	2.50E-04	**DDB2**	1.00844	1.56E-09
PAK1IP1	1.08004	1.14E-05	**RASIP1**	1.04354	4.80E-03	**UBE2V2**	1.00784	6.73E-15
BCAR3	1.08000	2.11E-06	**ZMYM2**	1.04268	1.61E-08	**C20orf194**	1.00771	8.91E-08
BRWD1	1.07969	1.34E-14	**ITPR3**	1.04250	6.60E-18	**PDE8A**	1.00759	7.32E-10
USP32P2	1.07829	4.48E-03	**TRAPPC6B**	1.04229	4.24E-11	**ZNF350**	1.00729	3.21E-06
GCC2	1.07711	5.03E-08	**HECA**	1.04218	9.01E-08	**PPTC7**	1.00614	2.95E-11
HES1	1.07702	8.18E-04	**MORC3**	1.04176	1.70E-11	**PUS3**	1.00611	4.63E-06
ANKRD9	1.07689	9.61E-05	**RNF169**	1.04008	1.44E-08	**ECE1**	1.00528	3.64E-08
CD83	1.07596	1.06E-02	**PGBD3**	1.04003	5.50E-04	**C2orf49**	1.00446	3.46E-15
SCNM1	1.07553	1.39E-09	**CHAC1**	1.03989	4.16E-03	**ZNF709**	1.00355	2.08E-02
VTI1A	1.07430	8.29E-08	**SQSTM1**	1.03917	1.50E-04	**ZNF507**	1.00322	2.31E-08
GOLGA5	1.07379	1.93E-08	**HPS4**	1.03829	2.02E-14	**KLF12**	1.00222	2.67E-06
TOR1AIP2	1.07379	5.40E-15	**VPS26A**	1.03815	1.31E-08	**MUC1**	1.00128	4.15E-02
PPP3R1	1.07311	3.71E-20	**PRDM16**	1.03798	1.01E-06	**PMM2**	1.00078	5.73E-08
ZNF627	1.07304	1.24E-03	**TMBIM1**	1.03793	5.67E-18	**FRRS1**	1.00062	2.14E-10
MRPS10	1.07296	6.86E-17	**TRAPPC4**	1.03683	2.06E-06	**ZNHIT6**	1.00025	1.30E-06
JAZF1	1.07287	5.46E-04	**NFYA**	1.03680	1.38E-07	**HPS6**	-1.00001	5.50E-07
MYO1E	1.07279	7.36E-08	**MVK**	1.03582	2.72E-06	**SMARCD2**	-1.00102	4.38E-05
VPS8	1.07255	1.01E-10	**LIAS**	1.03561	2.96E-06	**CNPY4**	-1.00110	4.45E-02
FBXO5	1.07108	3.01E-08	**AHR**	1.03449	1.67E-07	**APOBEC3D**	-1.00125	5.12E-04
IWS1	1.07096	1.59E-13	**DNASE1L2**	1.03410	4.77E-02	**LOC100128881**	-1.00175	6.74E-05
MLL	1.06971	6.51E-12	**FOXD2-AS1**	1.03408	3.68E-03	**ZNF827**	-1.00272	1.93E-05
NPPA	1.06964	7.95E-03	**GOLGB1**	1.03252	5.23E-08	**HOXB6**	-1.00283	3.33E-02
SLC38A7	1.06962	1.61E-04	**SNX8**	1.03241	3.56E-12	**DOLPP1**	-1.00324	4.13E-09
NOXA1	1.06848	4.28E-02	**ZNF702P**	1.03190	4.21E-11	**C1QTNF3**	-1.00368	9.57E-03
HABP4	1.06838	9.66E-05	**C4A**	1.03064	2.73E-02	**GPC1**	-1.00582	4.77E-08
C17orf49	1.06793	5.09E-07	**GTPBP10**	1.03037	1.11E-12	**SAP130**	-1.00607	4.65E-11
XRCC4	1.06770	2.94E-05	**USP28**	1.03015	2.10E-07	**LOC100129480**	-1.00664	1.32E-02
ZNF780B	1.06769	4.97E-14	**RARA**	1.02950	2.63E-07	**LOC100129961**	-1.00667	2.42E-02
GIPC1	1.06697	2.63E-10	**NCKIPSD**	1.02926	1.25E-07	**ZNF708**	-1.00715	1.97E-05
ZNF799	1.06697	2.94E-04	**CDC73**	1.02911	7.47E-15	**STK11IP**	-1.00758	1.10E-08
SAFB	1.06643	2.38E-09	**DYRK3**	1.02906	2.05E-02	**SNX21**	-1.00788	2.17E-03
FAM126B	1.06537	2.95E-12	**MPI**	1.02850	5.66E-08	**PABPN1**	-1.00796	1.65E-06
SPEN	1.06514	6.33E-14	**CCDC92**	1.02814	5.42E-08	**COMT**	-1.00814	8.46E-07
IDI1	1.06483	6.90E-05	**ZDHHC8P1**	1.02667	4.50E-02	**NEO1**	-1.00819	3.23E-04
DCAF16	1.06475	5.49E-12	**SEC31A**	1.02549	1.41E-12	**AMACR**	-1.00821	3.32E-03
HCFC2	1.06461	4.40E-06	**TRMT10B**	1.02520	2.26E-03	**GEMIN5**	-1.00826	1.16E-05
KPNA4	1.06435	6.78E-07	**PDE9A**	1.02518	6.27E-03	**NYAP1**	-1.00963	3.24E-02
YBEY	1.06376	2.68E-04	**SCAND2**	1.02486	1.45E-02	**SH2B1**	-1.00971	1.50E-08
KIF3B	1.06363	6.73E-14	**LRRFIP1**	1.02403	9.60E-14	**TIMP2**	-1.01006	7.71E-06
FLJ20021	1.06314	4.61E-03	**KLHL21**	1.02356	2.11E-03	**ATF7IP**	-1.01024	1.79E-06
PPP2CB	1.06085	1.03E-13	**SNX2**	1.02351	1.96E-09	**GHRLOS**	-1.01071	3.12E-02
RPS10P7	1.06046	1.12E-02	**RAB2A**	1.02300	8.76E-15	**AMPD2**	-1.01072	1.41E-05
APLF	1.06019	2.95E-03	**FXR2**	1.02284	3.39E-14	**UXS1**	-1.01135	7.69E-15
FAM63B	1.06017	2.29E-11	**PIK3C3**	1.02274	3.31E-04	**COG8**	-1.01137	5.53E-06
CDK11A	1.05922	7.88E-07	**NUPR1**	1.02178	1.55E-03	**SLC35B2**	-1.01148	1.63E-08
C6orf1	1.05909	1.20E-08	**LSR**	1.02164	4.60E-05	**TMEM201**	-1.01153	7.32E-09
JMY	1.05806	5.14E-06	**CSDE1**	1.02124	1.45E-06	**C20orf112**	-1.01161	6.02E-04
MEF2A	1.05679	4.46E-14	**KIAA1109**	1.02095	3.55E-05	**DNM1L**	-1.01174	2.55E-20
CNST	1.05617	1.06E-07	**FGFR1OP2**	1.02093	4.33E-06	**SLC30A4**	-1.01233	2.04E-02
CCP110	1.05573	2.10E-11	**LGALSL**	1.02008	1.84E-11	**ECM1**	-1.01238	5.14E-03
DCAF13	1.05527	5.99E-07	**BCL6**	1.01964	9.79E-04	**PRPF6**	-1.01241	2.49E-08
CD164	1.05505	3.48E-16	**HMHA1**	1.01908	7.34E-04	**MBOAT7**	-1.01318	5.44E-10
LYPLA1	1.05465	6.08E-09	**TRAM2**	1.01886	7.72E-11	**CCDC150**	-1.01334	1.23E-03
FER	1.05448	2.18E-07	**KDM6A**	1.01856	1.01E-03	**TTC30B**	-1.01360	1.18E-03
CDYL	1.05325	7.81E-29	**DDX39B**	1.01756	8.91E-13	**B4GALT7**	-1.01405	7.84E-04
MED13L	1.05323	4.01E-11	**NAF1**	1.01693	5.17E-08	**SH3KBP1**	-1.01449	4.72E-06
ARHGEF18	1.05302	1.41E-07	**ALKBH1**	1.01680	7.67E-06	**DTNB**	-1.01449	2.86E-04
YIPF5	1.05268	2.57E-10	**C9orf172**	1.01679	6.18E-04	**ADAM1A**	-1.01480	4.11E-03
SNX30	1.05241	6.02E-11	**C4orf52**	1.01666	1.03E-07	**LPAR1**	-1.01516	2.21E-02
IGF1R	1.05218	1.61E-13	**PRPF38B**	1.01649	8.16E-10	**ASB13**	-1.01525	9.56E-04
CBX4	1.05216	6.33E-05	**DNAJB5**	1.01625	1.77E-04	**LOC254128**	-1.01529	2.99E-02
CCDC58	1.05141	8.90E-08	**BTBD7**	1.01602	3.19E-15	**YLPM1**	-1.01555	1.06E-06
RPL23AP7	1.05136	7.44E-03	**LURAP1L**	1.01599	2.41E-03	**NARFL**	-1.01587	6.56E-08
TMEM159	1.05129	1.17E-11	**STK3**	1.01417	2.73E-07	**HGS**	-1.01618	7.75E-09
SLAIN2	1.05115	3.71E-18	**ABLIM3**	1.01384	1.65E-05	**CBY1**	-1.01620	4.74E-11
TSTD3	1.05075	4.08E-02	**LRRC59**	1.01285	1.65E-14	**PUSL1**	-1.01623	1.69E-05
DEK	1.05051	4.13E-21	**ACVR1**	1.01273	1.52E-12	**RAP2B**	-1.01632	2.77E-07

TMED4	-1.01635	4.72E-05	**CD99P1**	-1.05544	1.24E-02	**RFT1**	-1.08921	5.78E-11
MRPL17	-1.01696	3.00E-11	**TMEM191B**	-1.05569	2.31E-06	**HIST1H3D**	-1.08923	8.39E-05
FKBPL	-1.01697	1.80E-02	**OPA1**	-1.05672	1.61E-08	**PMFBP1**	-1.08940	1.30E-02
PAXIP1	-1.01813	5.58E-11	**GSTO1**	-1.05753	1.48E-09	**PROSAPIP1**	-1.08966	1.02E-04
GSTZ1	-1.01841	3.54E-05	**ZNF18**	-1.05828	2.19E-04	**LRRC8D**	-1.09010	4.74E-12
LRSAM1	-1.01916	1.92E-06	**APEH**	-1.05847	4.65E-08	**LOC728743**	-1.09066	2.50E-04
NAT14	-1.01937	3.63E-05	**PCYOX1L**	-1.05881	1.28E-03	**TAG**	-1.09081	7.84E-07
GNB3	-1.02047	3.73E-02	**ESCO2**	-1.05893	7.22E-04	**LARS2**	-1.09101	4.15E-07
AKR7A3	-1.02049	1.49E-02	**PTRH1**	-1.05900	7.45E-04	**USP46**	-1.09164	8.39E-10
TTC39A	-1.02088	6.92E-05	**IDH3A**	-1.05967	2.35E-06	**BARX2**	-1.09181	9.51E-07
DAG1	-1.02090	6.44E-05	**CABLES2**	-1.06014	2.05E-04	**SERGEF**	-1.09201	2.59E-08
RBM3	-1.02097	5.81E-06	**RNU12**	-1.06051	6.64E-03	**ATP6V0E2**	-1.09240	1.08E-03
WARS2	-1.02153	7.36E-08	**LOC100130673**	-1.06100	2.51E-03	**CCNE2**	-1.09256	3.28E-04
TAF6L	-1.02193	3.48E-07	**HCFC1**	-1.06116	2.59E-07	**PVRIG**	-1.09284	2.10E-06
PQLC3	-1.02235	9.24E-04	**DCTN1**	-1.06121	4.61E-11	**PRRT1**	-1.09308	2.18E-02
FIZ1	-1.02251	2.36E-06	**CDC14B**	-1.06148	2.57E-03	**RMND5B**	-1.09339	1.80E-12
GNPTAB	-1.02339	3.73E-09	**TMEM14E**	-1.06171	4.42E-03	**GRWD1**	-1.09388	7.95E-05
VTI1B	-1.02429	2.04E-13	**NDUFV3**	-1.06235	5.17E-07	**SLC25A15**	-1.09446	1.09E-06
LINC00630	-1.02453	2.30E-06	**HIST1H4C**	-1.06424	3.33E-05	**PSKH1**	-1.09485	3.64E-09
TMEM98	-1.02606	1.91E-02	**HRAS**	-1.06425	9.39E-06	**IGSF9**	-1.09513	2.14E-06
SHC1	-1.02610	8.33E-16	**CHTF18**	-1.06427	1.47E-05	**NFATC3**	-1.09516	3.14E-10
TPX2	-1.02621	3.05E-06	**PLEKHF2**	-1.06515	9.06E-09	**SLC12A9**	-1.09533	1.25E-11
PEF1	-1.02632	3.50E-05	**FAM125B**	-1.06535	2.78E-02	**TIMM13**	-1.09536	3.97E-07
POLR3G	-1.02757	1.26E-02	**ATP5D**	-1.06560	3.97E-06	**NDUFS8**	-1.09610	5.71E-21
PSMB3	-1.02763	7.88E-14	**FRMD4B**	-1.06577	3.81E-04	**ID4**	-1.09789	5.24E-03
POP7	-1.02848	2.84E-06	**TRABD**	-1.06600	3.55E-13	**ZNF513**	-1.09935	1.68E-03
MCTP2	-1.02905	1.01E-02	**ARV1**	-1.06607	2.99E-04	**PMPCB**	-1.10040	8.57E-10
SCARNA2	-1.02922	8.52E-03	**SAAL1**	-1.06608	1.02E-06	**ATOX1**	-1.10111	3.24E-18
TMEM214	-1.02926	2.67E-09	**WDR91**	-1.06634	1.01E-09	**ZNF514**	-1.10173	2.33E-06
MTX1	-1.02958	3.75E-05	**PPIL2**	-1.06679	1.11E-18	**SUCLG1**	-1.10184	6.55E-07
DPF3	-1.02976	1.12E-03	**C15orf59**	-1.06685	2.83E-02	**TRIP13**	-1.10187	2.01E-05
GLE1	-1.03031	7.69E-09	**EIF3K**	-1.06742	3.38E-19	**ADAP2**	-1.10197	3.31E-03
IL11RA	-1.03034	8.46E-03	**LACE1**	-1.06780	8.60E-04	**NUDT4**	-1.10279	1.21E-05
TP53I13	-1.03134	1.82E-06	**TMED9**	-1.06834	3.83E-09	**TMCC1**	-1.10459	6.75E-06
IMPDH1	-1.03245	2.48E-07	**C14orf169**	-1.06840	1.40E-03	**C15orf52**	-1.10489	2.17E-04
LPCAT1	-1.03292	2.26E-11	**TAF10**	-1.06868	9.06E-11	**WBSCR16**	-1.10556	3.41E-06
CD151	-1.03527	3.32E-11	**LOC653501**	-1.06898	4.38E-03	**PKI55**	-1.10635	5.13E-07
IGSF8	-1.03564	4.29E-03	**TSPAN3**	-1.06898	3.91E-11	**C17orf62**	-1.10703	5.52E-08
FAM190A	-1.03636	3.71E-03	**WDHD1**	-1.06935	7.54E-06	**LOC151009**	-1.10711	2.66E-04
LMNB2	-1.03659	3.35E-15	**RUSC1**	-1.06979	2.88E-07	**TRUB2**	-1.10723	1.48E-16
SRD5A3	-1.03730	4.75E-03	**CCNE1**	-1.06986	8.10E-03	**TSEN34**	-1.10826	5.04E-12
FAM83D	-1.03748	9.15E-08	**C20orf96**	-1.07005	1.75E-03	**BNIPL**	-1.10841	4.08E-02
KDELC2	-1.03787	5.12E-08	**OPLAH**	-1.07168	1.26E-05	**ANAPC15**	-1.10868	2.21E-12
C7orf49	-1.03828	1.74E-11	**CACFD1**	-1.07403	1.95E-04	**HIST1H4E**	-1.10933	7.90E-07
ITFG1	-1.03890	2.79E-06	**EXOSC4**	-1.07425	2.43E-13	**SAP25**	-1.10944	3.83E-03
ALPK1	-1.03963	3.11E-06	**VARS2**	-1.07471	3.02E-07	**C1orf122**	-1.10947	1.02E-10
NBN	-1.04074	2.18E-10	**LANCL1**	-1.07542	1.92E-05	**SH3BP5L**	-1.11029	8.18E-07
MTMR11	-1.04114	1.33E-03	**MRPL9**	-1.07549	9.53E-15	**PRPF40B**	-1.11132	1.19E-05
GLA	-1.04115	2.43E-09	**CC2D2A**	-1.07678	4.28E-02	**RANBP10**	-1.11151	2.06E-10
TOMM40	-1.04163	2.40E-07	**STAG1**	-1.07688	1.08E-07	**TBC1D8**	-1.11159	6.73E-05
SCD5	-1.04224	5.60E-07	**SGPP1**	-1.07689	5.86E-10	**C1orf126**	-1.11384	1.26E-04
BUD13	-1.04250	1.16E-09	**PEX10**	-1.07702	1.25E-15	**SERINC2**	-1.11474	1.34E-06
SEPT8	-1.04282	1.01E-08	**MARVELD1**	-1.07704	8.65E-14	**KIF7**	-1.11524	7.99E-04
MPV17L2	-1.04284	5.12E-09	**DPF1**	-1.07769	7.49E-03	**TMX4**	-1.11573	2.92E-05
LOC100128361	-1.04299	2.19E-04	**EML3**	-1.07807	1.15E-09	**ZNF76**	-1.11600	9.15E-03
RNF141	-1.04325	1.85E-09	**ARHGEF9**	-1.07831	4.41E-04	**GEMIN6**	-1.11635	7.54E-05
ATP5E	-1.04392	2.80E-12	**TBCB**	-1.07835	7.11E-09	**SGK196**	-1.11724	6.25E-12
HIST1H3C	-1.04393	1.86E-03	**UNC93B1**	-1.07908	2.03E-06	**ATP13A2**	-1.11738	5.39E-10
RPP38	-1.04437	3.32E-03	**ME3**	-1.07944	2.35E-02	**SIRPA**	-1.11829	2.70E-05
CPNE8	-1.04453	1.19E-02	**TSPYL4**	-1.07949	8.15E-05	**RAB19**	-1.11869	2.92E-02
ZNF444	-1.04588	1.05E-03	**SELO**	-1.07959	3.21E-06	**PANX2**	-1.11871	2.63E-02
CPNE1	-1.04607	1.04E-05	**TPGS2**	-1.08010	2.29E-08	**BAG2**	-1.11897	7.06E-07
FLAD1	-1.04632	3.29E-05	**B4GALNT3**	-1.08016	8.94E-03	**IQCE**	-1.11937	1.13E-08
TRNAU1AP	-1.04659	6.32E-08	**FAN1**	-1.08069	1.85E-06	**IDH1**	-1.11942	1.95E-03
AHSA1	-1.04710	4.20E-08	**ACADSB**	-1.08076	2.11E-03	**CACYBP**	-1.11966	3.82E-12
SGSM2	-1.04736	1.22E-04	**ARPC5L**	-1.08118	6.82E-13	**C17orf97**	-1.12003	4.08E-02
HAGHL	-1.04873	6.47E-04	**PLEKHG5**	-1.08252	1.62E-04	**CMC4**	-1.12143	5.57E-03
COPG2	-1.04936	2.82E-05	**MAVS**	-1.08260	1.13E-09	**PITX1**	-1.12160	2.45E-03
SNF8	-1.05018	9.09E-11	**PANK1**	-1.08311	3.80E-04	**SMARCE1**	-1.12172	8.63E-10
SRSF7	-1.05020	8.22E-08	**FGF12**	-1.08343	1.91E-03	**FAM123B**	-1.12178	8.54E-03
SLC25A42	-1.05034	1.45E-02	**PBXIP1**	-1.08394	6.27E-04	**FAM198B**	-1.12207	3.04E-06
JMJD8	-1.05132	4.94E-10	**ARMC5**	-1.08534	3.16E-05	**IFT43**	-1.12248	1.53E-16
EIF2D	-1.05246	1.01E-05	**MAN2B2**	-1.08654	1.27E-05	**TEX264**	-1.12330	4.99E-09
CMAS	-1.05304	5.97E-07	**TTYH3**	-1.08672	2.22E-04	**ACTL6A**	-1.12338	3.61E-08
FAM217B	-1.05396	2.45E-06	**XRCC6BP1**	-1.08721	1.49E-03	**PTOV1**	-1.12349	2.79E-11
RTN4RL1	-1.05408	4.64E-05	**ZNF704**	-1.08754	7.83E-06	**LINC00094**	-1.12422	1.18E-05
NDUFA2	-1.05411	2.05E-12	**GRHL3**	-1.08775	1.46E-05	**OGFR**	-1.12549	3.72E-06
CPT2	-1.05469	1.29E-04	**DFFA**	-1.08893	2.64E-15	**CAD**	-1.12583	1.62E-07

CDK5RAP2	-1.12645	6.11E-09	**CCT5**	-1.15917	3.45E-15	**POLR2L**	-1.19699	3.06E-13
NEU3	-1.12667	2.05E-09	**TMTC4**	-1.15922	1.58E-04	**IFI30**	-1.19798	5.44E-06
PLK1	-1.12667	1.38E-09	**SIGMAR1**	-1.15946	1.71E-15	**ACLY**	-1.19850	1.08E-09
TALDO1	-1.12682	2.91E-09	**STX17**	-1.15969	9.06E-14	**HSD11B2**	-1.19861	4.88E-02
CEMP1	-1.12731	1.92E-03	**POLR3E**	-1.15973	4.23E-09	**ADM5**	-1.19965	2.53E-03
PRKCSH	-1.12734	1.31E-11	**PNPT1**	-1.16012	1.09E-10	**PXMP2**	-1.20038	1.33E-11
ICT1	-1.12747	3.07E-06	**C8orf33**	-1.16021	2.69E-09	**ALDH4A1**	-1.20084	1.78E-04
MESDC2	-1.12824	4.05E-24	**ASH2L**	-1.16023	1.16E-12	**CTSD**	-1.20357	1.09E-07
DHX58	-1.12981	3.22E-03	**NEB**	-1.16036	6.15E-03	**SLC25A26**	-1.20517	3.92E-06
UMPS	-1.13005	5.65E-06	**MAPK12**	-1.16050	4.34E-13	**RPL13P5**	-1.20526	1.07E-03
NUP133	-1.13062	7.48E-07	**LEPRE1**	-1.16109	2.48E-06	**ARHGAP40**	-1.20583	6.77E-04
NLRP2	-1.13090	1.43E-11	**SMPD4**	-1.16192	7.91E-21	**SAMM50**	-1.20751	7.90E-12
SLC12A2	-1.13110	2.85E-09	**ZNF552**	-1.16192	3.01E-08	**ITFG3**	-1.20776	6.90E-14
MYBBP1A	-1.13117	7.13E-09	**MZT2A**	-1.16309	4.34E-13	**GSDMD**	-1.20785	1.22E-04
KIAA1462	-1.13169	1.93E-06	**RBBP4**	-1.16366	2.39E-20	**ERV3-1**	-1.20787	1.03E-02
GHRLOS2	-1.13242	6.36E-04	**MRM1**	-1.16426	2.29E-05	**ORC3**	-1.20818	1.28E-09
CARD8	-1.13417	1.05E-05	**THADA**	-1.16453	6.11E-06	**COA1**	-1.20843	1.44E-20
DNAJA4	-1.13464	5.02E-11	**DBF4B**	-1.16489	2.82E-08	**NUCB1**	-1.20868	5.59E-09
MSRB2	-1.13471	1.78E-03	**APOOL**	-1.16494	2.04E-05	**ZNF275**	-1.20879	3.16E-03
LOC100093631	-1.13538	1.04E-02	**TCTN1**	-1.16532	9.22E-04	**LOC100130987**	-1.20883	1.06E-02
PLD2	-1.13570	4.00E-06	**HSPA4L**	-1.16533	2.39E-06	**SNORA70D**	-1.20929	3.26E-02
CCNA2	-1.13645	2.46E-05	**SRSF5**	-1.16563	9.75E-09	**MCM6**	-1.20950	1.07E-11
RNASEH2C	-1.13657	1.11E-08	**DNAJC17**	-1.16587	3.22E-04	**C19orf40**	-1.20999	1.37E-03
ANXA8	-1.13662	3.81E-05	**CBX2**	-1.16638	6.19E-07	**SUV420H2**	-1.21078	2.90E-03
ARPC5	-1.13671	1.55E-12	**ZNF74**	-1.16713	5.90E-17	**LRP3**	-1.21163	6.34E-09
KIAA0195	-1.13681	2.08E-08	**PTPRS**	-1.16723	4.55E-09	**RBM38**	-1.21166	2.39E-12
ZNF792	-1.13701	8.79E-03	**AIFM3**	-1.16840	2.26E-03	**TMEM14A**	-1.21183	8.76E-11
FIBP	-1.13736	3.56E-08	**ACACA**	-1.16949	2.14E-11	**MCOLN2**	-1.21241	6.00E-05
DROSHA	-1.13784	1.26E-10	**ANAPC2**	-1.16952	5.47E-06	**NSUN4**	-1.21271	1.98E-07
EXOC4	-1.13869	6.02E-08	**TYW3**	-1.17023	1.04E-06	**FAM86A**	-1.21305	6.47E-05
TXNDC5	-1.13957	8.35E-16	**FAM117B**	-1.17114	1.93E-04	**GALNT11**	-1.21322	8.16E-12
R3HDM1	-1.14100	1.37E-09	**ASMTL**	-1.17133	9.87E-05	**SLC44A1**	-1.21398	1.34E-04
PTGES2	-1.14103	1.73E-12	**GALK1**	-1.17160	5.04E-07	**ZMYND19**	-1.21434	1.70E-10
MKS1	-1.14112	1.26E-08	**NMB**	-1.17259	9.60E-03	**FANCI**	-1.21449	2.49E-05
IQCK	-1.14138	6.51E-04	**BRAT1**	-1.17286	6.72E-19	**KIAA1161**	-1.21461	6.38E-09
FIS1	-1.14150	1.94E-09	**POLD2**	-1.17311	1.73E-11	**HERC2**	-1.21471	4.99E-15
ATF7IP2	-1.14157	3.42E-04	**SLC46A3**	-1.17322	1.57E-03	**TMEM141**	-1.21477	4.14E-06
KIAA1524	-1.14197	7.73E-04	**OXA1L**	-1.17355	2.99E-08	**MRPL55**	-1.21497	2.23E-07
JTB	-1.14207	3.28E-19	**CASP6**	-1.17390	2.11E-06	**RNF26**	-1.21513	1.31E-26
MAD2L1	-1.14210	3.60E-08	**IFT122**	-1.17448	2.13E-11	**ZNF589**	-1.21551	1.38E-04
APOA1BP	-1.14335	5.99E-07	**CLDN7**	-1.17495	3.28E-12	**VPS52**	-1.21606	6.42E-26
UBE4B	-1.14376	6.97E-17	**CLASP1**	-1.17554	9.75E-09	**NUDT6**	-1.21775	3.86E-03
SPATA13	-1.14395	2.36E-05	**RAC3**	-1.17866	1.64E-04	**SAMD10**	-1.21778	2.59E-02
MTSS1L	-1.14410	2.92E-13	**PSMD13**	-1.17872	1.42E-12	**FAM185A**	-1.21803	6.90E-03
PACSIN3	-1.14415	6.01E-12	**HENMT1**	-1.17892	9.00E-06	**MALL**	-1.21848	5.07E-04
COPS7B	-1.14435	6.74E-26	**NUBPL**	-1.17897	1.46E-09	**CENPM**	-1.21884	1.04E-09
SOD1	-1.14457	1.40E-07	**MCF2L**	-1.17963	8.64E-03	**CLSPN**	-1.21897	3.94E-12
CHRNA5	-1.14473	9.98E-06	**DGCR5**	-1.17971	5.77E-03	**EID1**	-1.22083	1.96E-15
PSMD3	-1.14757	6.25E-17	**MORC4**	-1.17999	7.33E-07	**NXPH4**	-1.22085	7.36E-03
DTYMK	-1.14761	2.82E-12	**NPM3**	-1.18000	1.79E-05	**SEPHS1**	-1.22113	1.17E-10
TRAF3IP1	-1.14805	2.01E-10	**KIF1C**	-1.18155	1.61E-20	**PEX19**	-1.22137	3.98E-14
ANAPC4	-1.14820	2.22E-07	**SNX29**	-1.18254	2.40E-10	**METTL1**	-1.22160	7.89E-08
SMC1A	-1.14896	3.07E-21	**PLA2G4B**	-1.18373	2.42E-06	**FKBP1AP1**	-1.22195	2.56E-02
ARHGAP33	-1.14964	8.19E-04	**NUP85**	-1.18394	1.87E-12	**ATPAF2**	-1.22220	5.59E-09
BRIP1	-1.14976	8.51E-06	**GRHPR**	-1.18411	4.82E-15	**TMA16**	-1.22263	9.63E-15
ACP2	-1.15046	1.23E-08	**RPUSD3**	-1.18489	2.46E-13	**COASY**	-1.22334	1.06E-13
SUDS3	-1.15098	2.54E-08	**ERGIC1**	-1.18537	3.15E-11	**ACYP2**	-1.22376	9.09E-07
MED11	-1.15102	4.21E-10	**ALG1**	-1.18611	2.75E-10	**PRPS2**	-1.22556	2.87E-05
CCDC97	-1.15139	3.51E-15	**NCOA2**	-1.18710	1.65E-09	**PNKP**	-1.22580	1.40E-16
PURA	-1.15143	2.45E-02	**PFAS**	-1.18780	1.41E-05	**C15orf41**	-1.22601	6.09E-14
DTWD2	-1.15167	1.18E-06	**WDR83**	-1.18802	5.64E-11	**MRPL32**	-1.22755	3.48E-13
MFSD3	-1.15233	7.79E-07	**NOL6**	-1.18889	5.81E-07	**ZRANB3**	-1.22806	9.03E-06
MCM10	-1.15255	5.24E-06	**UBL5**	-1.18891	9.55E-13	**NDUFA13**	-1.23092	1.82E-12
ZBTB45	-1.15329	2.48E-07	**CNN2**	-1.18902	1.64E-13	**PLCB1**	-1.23136	3.42E-04
CEP68	-1.15413	2.62E-04	**AIFM1**	-1.19016	1.02E-10	**IPO9**	-1.23160	7.23E-10
SRSF6	-1.15451	6.64E-10	**LOC100129917**	-1.19023	1.06E-05	**IFITM2**	-1.23224	1.58E-03
PPIP5K1	-1.15488	4.69E-16	**DLGAP5**	-1.19046	3.69E-13	**HIPK2**	-1.23309	1.26E-11
PRPF31	-1.15508	1.91E-18	**THAP4**	-1.19097	2.99E-11	**TPCN2**	-1.23350	2.33E-08
ATP5J	-1.15578	1.29E-04	**EFNA4**	-1.19216	1.20E-02	**TSEN54**	-1.23376	8.87E-14
COPS6	-1.15579	5.93E-11	**CCS**	-1.19304	5.14E-09	**PPIL1**	-1.23444	4.03E-07
TMCO7	-1.15619	3.18E-05	**FKRP**	-1.19305	3.15E-09	**WWC3**	-1.23480	2.41E-02
FGD3	-1.15656	4.61E-11	**NFU1**	-1.19312	1.10E-10	**ANKRD36B**	-1.23512	5.21E-07
FAM92A1	-1.15673	9.37E-03	**SNORA2B**	-1.19354	1.12E-03	**NCLN**	-1.23643	6.21E-16
MPP7	-1.15799	4.01E-07	**NUDT12**	-1.19414	6.08E-04	**PPP1R12B**	-1.23663	2.18E-05
SUGT1P3	-1.15806	4.52E-02	**FRMD4A**	-1.19427	4.13E-08	**TTC12**	-1.23681	7.89E-07
DDX12P	-1.15820	2.06E-02	**POMT1**	-1.19450	3.85E-10	**C7orf50**	-1.23705	2.89E-21
ZNF184	-1.15856	2.89E-03	**HDAC1**	-1.19493	2.54E-17	**TTC5**	-1.23858	2.30E-08
C14orf93	-1.15915	3.51E-04	**TIMP4**	-1.19665	1.24E-02	**GTF2I**	-1.23907	1.93E-07

SUMF1	-1.24008	2.62E-07	**MLEC**	-1.28111	3.22E-17	**ALG10**	-1.32857	4.09E-08
SVIP	-1.24032	3.78E-08	**MAPKAP1**	-1.28349	4.32E-09	**SLC44A5**	-1.32869	2.55E-09
THOP1	-1.24141	1.38E-18	**KLHDC4**	-1.28364	9.69E-11	**FHL3**	-1.32891	6.10E-07
SOGA1	-1.24156	8.59E-10	**GABPB2**	-1.28380	3.19E-03	**ZNF642**	-1.33002	4.66E-06
CSTF2	-1.24175	3.23E-13	**MYH10**	-1.28395	5.44E-09	**MKRN9P**	-1.33038	1.71E-02
APLP2	-1.24190	5.85E-07	**TSFM**	-1.28482	2.63E-10	**RBX1**	-1.33095	9.47E-14
GLUL	-1.24238	5.43E-07	**ALYREF**	-1.28502	1.69E-14	**HERC6**	-1.33105	1.82E-04
ZNF257	-1.24281	1.26E-04	**ANKRD6**	-1.28520	4.79E-06	**SLC2A8**	-1.33212	1.28E-04
APBB3	-1.24284	2.79E-02	**MOSPD3**	-1.28522	1.17E-04	**SEC61B**	-1.33366	4.92E-09
PSRC1	-1.24530	1.21E-07	**FDXACB1**	-1.28676	2.98E-03	**USP27X**	-1.33465	1.69E-04
PTDSS2	-1.24578	5.27E-11	**CASP2**	-1.28766	6.79E-19	**GYS1**	-1.33545	2.14E-14
CENPH	-1.24614	1.66E-05	**SHMT2**	-1.28897	2.99E-14	**PCDHB16**	-1.33549	2.08E-02
PIGO	-1.24642	4.18E-08	**PCGF2**	-1.28910	8.65E-06	**KAZALD1**	-1.33644	1.66E-03
CLPB	-1.24970	4.42E-02	**CTPS1**	-1.28944	2.12E-09	**LY6G6C**	-1.33671	3.29E-02
CYP2U1	-1.24982	2.30E-02	**TAS2R19**	-1.28958	1.23E-02	**CDC25B**	-1.33711	6.69E-13
LSM6	-1.24997	2.69E-06	**KLHDC5**	-1.29009	2.14E-09	**PYCRL**	-1.33779	1.23E-09
RPUSD2	-1.25038	1.47E-07	**BOLA2B**	-1.29104	2.59E-23	**TM2D3**	-1.33784	4.14E-03
POLR3GL	-1.25060	7.07E-06	**ZNF41**	-1.29169	1.70E-07	**FANCF**	-1.33879	1.98E-11
PPP2R1A	-1.25089	1.28E-28	**MDK**	-1.29259	2.38E-08	**JMJD4**	-1.33902	4.73E-10
CAMKK2	-1.25199	9.94E-10	**PMPCA**	-1.29307	2.03E-10	**C5orf24**	-1.33939	2.01E-14
TPI1P3	-1.25229	9.52E-03	**B3GAT3**	-1.29371	1.87E-07	**WFS1**	-1.33943	3.49E-08
C20orf151	-1.25266	5.14E-03	**C5orf30**	-1.29407	6.01E-03	**ERBB2**	-1.33969	4.40E-15
TMEM208	-1.25277	4.39E-12	**CCDC34**	-1.29565	1.11E-14	**MLST8**	-1.33997	3.70E-13
PPIH	-1.25286	6.69E-03	**HIST1H3B**	-1.29600	3.92E-06	**G6PC3**	-1.34032	2.57E-07
PKN3	-1.25399	6.02E-13	**C22orf39**	-1.29614	6.90E-03	**SMARCA1**	-1.34108	2.10E-05
GJB7	-1.25441	3.36E-04	**HERC2P4**	-1.29761	7.28E-06	**TMEM109**	-1.34222	6.42E-19
PIP5K1B	-1.25523	4.47E-02	**PVRL3**	-1.29814	4.97E-02	**TRIM16**	-1.34237	8.49E-36
SIAE	-1.25548	1.91E-04	**RUVBL2**	-1.29837	2.14E-20	**KCTD17**	-1.34285	1.27E-04
FBXO2	-1.25608	5.73E-06	**RFC4**	-1.29929	2.59E-15	**ARAF**	-1.34294	2.13E-15
GTF2H4	-1.25624	6.53E-12	**SLC35B4**	-1.29956	1.12E-06	**DCLK2**	-1.34373	1.79E-06
TSR1	-1.25674	1.80E-07	**CTU2**	-1.30039	4.67E-05	**RASA3**	-1.34381	7.26E-07
PDF	-1.25682	3.35E-12	**FZD4**	-1.30116	3.55E-02	**PPFIA3**	-1.34409	4.53E-09
MANEA	-1.25698	6.12E-05	**LOC642846**	-1.30194	1.82E-06	**SLC43A2**	-1.34441	1.88E-05
GCA	-1.25714	9.79E-03	**ADAMTSL4**	-1.30251	3.50E-04	**PHB2**	-1.34586	6.27E-15
MSTO1	-1.25751	3.95E-14	**FARP2**	-1.30295	6.02E-05	**LOC81691**	-1.34669	3.73E-05
DEF6	-1.25808	2.97E-05	**NADSYN1**	-1.30333	5.88E-12	**PLK3**	-1.34769	1.89E-08
DCTPP1	-1.25815	7.57E-15	**FUT8**	-1.30408	4.78E-09	**TMEM120A**	-1.35005	5.58E-05
SUMO2	-1.25823	5.31E-19	**TP73**	-1.30480	2.88E-09	**FANCL**	-1.35083	4.44E-18
MAGEA3	-1.25830	4.95E-02	**C3orf33**	-1.30488	2.01E-04	**PPM1F**	-1.35153	1.41E-14
HINT2	-1.25850	3.84E-05	**KRTCAP3**	-1.30536	1.57E-06	**ADSL**	-1.35197	2.09E-14
ABCG2	-1.25869	3.26E-04	**C1orf115**	-1.30550	1.02E-05	**KCNN4**	-1.35200	5.03E-03
PIGU	-1.25885	1.05E-13	**CARHSP1**	-1.30586	1.08E-10	**CCDC74B**	-1.35270	4.15E-02
PCGF3	-1.25986	1.26E-18	**HMGN3**	-1.30605	2.00E-04	**TST**	-1.35461	1.33E-06
PIGM	-1.26008	1.11E-06	**TUBA1B**	-1.30673	2.79E-10	**CHCHD7**	-1.35515	1.09E-02
CEP78	-1.26012	6.16E-08	**USP19**	-1.30724	8.38E-03	**NUDT1**	-1.35525	3.55E-09
PFDN6	-1.26059	1.09E-08	**RFXANK**	-1.30808	2.08E-08	**SEPN1**	-1.35619	6.89E-14
MLF2	-1.26216	8.84E-15	**C15orf23**	-1.30810	6.76E-15	**RNF215**	-1.35666	6.34E-08
CBX5	-1.26278	1.25E-06	**CNP**	-1.30854	1.18E-10	**ZNF750**	-1.35670	1.02E-05
UNK	-1.26372	7.83E-12	**RAVER2**	-1.30897	3.12E-09	**AKAP5**	-1.35699	1.51E-02
BSCL2	-1.26378	5.53E-11	**SYTL1**	-1.30914	7.56E-05	**KRT18**	-1.35722	4.30E-20
VKORC1L1	-1.26433	3.84E-13	**TBCD**	-1.30959	5.31E-13	**PHTF1**	-1.35980	8.76E-11
CFDP1	-1.26440	2.83E-14	**SMIM1**	-1.31068	3.62E-02	**CERCAM**	-1.36078	3.52E-06
LOC283683	-1.26604	6.78E-03	**C7orf43**	-1.31111	9.96E-14	**SLC44A3**	-1.36137	6.74E-08
HMGN2	-1.26678	1.46E-08	**PKMYT1**	-1.31246	9.81E-11	**BFSP1**	-1.36198	2.24E-02
SAPCD2	-1.26770	1.08E-10	**RNASEH2A**	-1.31257	5.65E-27	**MSX1**	-1.36854	3.85E-03
NICN1	-1.26770	2.03E-04	**HRSP12**	-1.31260	1.14E-07	**ARHGAP44**	-1.36896	1.16E-04
CHD1L	-1.26788	1.86E-06	**MRPS9**	-1.31375	2.32E-12	**FAM211B**	-1.36929	4.08E-02
LOC100130298	-1.26812	2.43E-03	**C14orf80**	-1.31397	4.73E-08	**FAM86C2P**	-1.36965	2.42E-02
RUVBL1	-1.26826	7.94E-10	**KCNQ4**	-1.31468	3.85E-05	**MCRS1**	-1.37022	3.56E-21
TMEM143	-1.26877	4.43E-03	**PEBP1**	-1.31508	1.18E-16	**CCNB1**	-1.37133	6.27E-20
GCDH	-1.26965	7.50E-07	**SURF1**	-1.31542	8.88E-11	**ATXN7L2**	-1.37215	5.27E-05
CMTM8	-1.27054	5.58E-08	**EARS2**	-1.31648	6.29E-08	**C1QL1**	-1.37467	1.93E-02
N6AMT2	-1.27060	1.72E-03	**LOC100128531**	-1.31749	2.22E-02	**KANK1**	-1.37475	1.32E-15
FAM171A2	-1.27241	1.55E-03	**PEX11B**	-1.31764	9.16E-06	**CXXC5**	-1.37591	5.88E-05
CPSF1	-1.27261	1.60E-18	**C17orf89**	-1.31835	1.21E-11	**NUP62CL**	-1.37650	1.61E-02
DLX5	-1.27274	2.20E-02	**WDR61**	-1.31873	4.70E-20	**CPNE2**	-1.37687	1.85E-10
TMEM129	-1.27316	1.50E-03	**SDF2L1**	-1.32103	1.45E-09	**CTSL2**	-1.37824	1.11E-09
MCM3	-1.27343	1.96E-14	**EML2**	-1.32116	8.98E-06	**ATRIP**	-1.37841	1.38E-05
SLC9A2	-1.27376	1.41E-05	**LGALS9**	-1.32141	4.77E-03	**LMO7**	-1.37871	1.98E-07
SMCR5	-1.27406	1.29E-02	**SETDB1**	-1.32168	1.06E-09	**NUDT16L1**	-1.37928	2.89E-11
TMEM173	-1.27535	1.43E-05	**CAMK1D**	-1.32296	1.61E-05	**SHC3**	-1.38069	9.02E-04
TOP1MT	-1.27717	1.32E-11	**PXMP4**	-1.32303	9.93E-11	**GPC4**	-1.38090	4.07E-02
RASL11A	-1.27812	2.74E-07	**DMAP1**	-1.32357	1.75E-11	**HSPA1A**	-1.38112	1.19E-07
NDUFB7	-1.27828	2.76E-10	**FAM198A**	-1.32368	4.90E-02	**SFXN5**	-1.38112	1.45E-08
NACC1	-1.27921	8.36E-18	**UQCR10**	-1.32455	4.39E-07	**KEAP1**	-1.38164	3.56E-11
EIF2C1	-1.27974	2.22E-14	**ADAT2**	-1.32699	2.97E-05	**SLC29A2**	-1.38196	3.19E-10
NCAPH2	-1.27986	6.29E-15	**HIST1H2AD**	-1.32709	2.50E-06	**GPS1**	-1.38362	8.53E-27
GABRD	-1.28085	2.87E-02	**PCDH7**	-1.32774	1.30E-05	**C1orf74**	-1.38443	1.95E-05

LOC100134868	-1.38502	1.26E-04	**TIMELESS**	-1.43508	7.26E-11	**FAM96A**	-1.49324	7.73E-15
WNK2	-1.38521	8.79E-09	**A4GALT**	-1.43590	1.62E-09	**MTHFS**	-1.49425	9.60E-11
SHROOM1	-1.38678	3.12E-09	**SETD1B**	-1.43611	5.37E-16	**APEX1**	-1.49630	2.29E-22
C21orf2	-1.38744	2.71E-02	**PRICKLE2**	-1.43695	3.19E-03	**CAPN1**	-1.49690	4.59E-18
FAM188B	-1.38759	6.16E-08	**CENPB**	-1.43833	9.63E-15	**CDC20**	-1.49771	1.33E-11
PLCB3	-1.38769	1.49E-13	**LDB1**	-1.43961	2.03E-13	**SETMAR**	-1.49803	2.91E-04
GPR135	-1.38815	8.43E-03	**SLC5A12**	-1.44147	2.62E-02	**EBPL**	-1.49809	2.11E-09
PLCG2	-1.38837	3.14E-11	**TENM3**	-1.44151	2.12E-14	**PKD2**	-1.49896	3.52E-14
LY6E	-1.38846	3.97E-08	**EEFSEC**	-1.44202	1.14E-08	**TACC3**	-1.49941	5.43E-20
TSPAN33	-1.38862	5.22E-05	**TMEM164**	-1.44258	1.14E-05	**CHID1**	-1.50134	7.04E-13
AGER	-1.38951	1.01E-05	**ZNF689**	-1.44492	1.94E-07	**RPL14**	-1.50181	4.39E-06
RPUSD1	-1.39052	4.86E-14	**ADA**	-1.44662	2.60E-06	**PARP1**	-1.50195	3.28E-12
COX8A	-1.39184	1.90E-25	**L3MBTL1**	-1.44788	3.14E-02	**FBXO41**	-1.50214	3.42E-03
KIAA0664	-1.39240	2.24E-23	**HIGD2A**	-1.44819	7.58E-21	**EIF5**	-1.50338	1.55E-24
CAPS	-1.39242	8.02E-03	**KLK8**	-1.44919	3.33E-02	**MRPS26**	-1.50726	1.20E-13
ACBD7	-1.39394	1.95E-04	**GLI2**	-1.45209	4.24E-11	**NAAA**	-1.50810	2.31E-10
LBH	-1.39561	5.25E-08	**HDHD3**	-1.45261	2.84E-09	**DNMT3A**	-1.50846	1.05E-08
UBA7	-1.39613	1.18E-02	**FAM173A**	-1.45312	1.33E-07	**C2orf54**	-1.50995	5.23E-04
SORD	-1.39721	2.35E-08	**SDCCAG8**	-1.45373	7.65E-06	**ISM2**	-1.50997	3.28E-02
KIAA0825	-1.39731	1.28E-02	**KLK6**	-1.45439	6.71E-03	**PLCE1**	-1.51067	1.84E-03
MTERFD3	-1.39778	1.73E-07	**DUS3L**	-1.45520	8.38E-11	**TOE1**	-1.51376	2.09E-07
C6orf57	-1.39862	1.55E-04	**MRP63**	-1.45556	2.17E-08	**MECR**	-1.51379	5.29E-11
FLJ39051	-1.39863	2.10E-02	**IFT81**	-1.45578	4.90E-04	**ORC1**	-1.51436	1.01E-12
ING5	-1.39937	4.69E-14	**SEPW1**	-1.45595	3.30E-06	**PLAC2**	-1.51666	2.44E-12
MRPL1	-1.39938	3.48E-07	**SLC38A10**	-1.45604	8.78E-18	**TUFM**	-1.51726	1.43E-17
ABCA2	-1.39948	1.44E-04	**ABCD4**	-1.45651	4.77E-10	**GATSL2**	-1.51729	1.07E-05
AGMAT	-1.39957	7.16E-03	**ALKBH6**	-1.45679	5.00E-04	**PMEL**	-1.51789	3.54E-02
TTF2	-1.39959	3.14E-09	**LTBP1**	-1.45746	7.16E-04	**HIST1H4D**	-1.51838	4.61E-11
MRI1	-1.40171	4.04E-23	**SH3RF2**	-1.45893	1.43E-12	**TMEM180**	-1.51949	2.63E-10
C9orf123	-1.40238	8.39E-07	**CCNF**	-1.45931	2.68E-07	**CLDN23**	-1.52079	1.98E-02
MPST	-1.40266	1.04E-08	**RASL11B**	-1.45990	2.34E-05	**ARHGEF39**	-1.52094	6.50E-20
SLC39A11	-1.40479	1.95E-06	**COMTD1**	-1.46128	1.37E-03	**IL17RA**	-1.52179	8.93E-18
CCDC94	-1.40605	2.00E-08	**CALB2**	-1.46257	4.24E-02	**WDR77**	-1.52202	5.77E-20
HIST1H2BC	-1.40681	8.28E-08	**ARSA**	-1.46315	8.69E-04	**PSMD6**	-1.52346	4.87E-19
CASP7	-1.40696	1.56E-04	**WDR37**	-1.46390	1.08E-03	**PSMB5**	-1.52360	7.12E-20
SNORA55	-1.40731	1.08E-07	**NUDC**	-1.46424	7.06E-18	**JPH2**	-1.52401	5.94E-05
ACTRT3	-1.40782	3.06E-03	**NDUFA8**	-1.46454	4.47E-24	**GANAB**	-1.52410	2.98E-20
HEXIM2	-1.40858	1.11E-02	**CDK5RAP3**	-1.46483	2.36E-13	**MRPL38**	-1.52533	4.05E-33
MLLT11	-1.41008	4.60E-07	**RNASEL**	-1.46554	2.10E-07	**CDK2AP1**	-1.52620	1.71E-28
RTF1	-1.41030	7.29E-08	**AKR1C3**	-1.46664	1.96E-03	**PPIC**	-1.52638	2.39E-19
SNPH	-1.41140	4.56E-04	**FBF1**	-1.46696	8.15E-05	**TBX2**	-1.52663	3.10E-03
PLXNB1	-1.41258	9.75E-09	**SNORA69**	-1.46704	4.07E-03	**MYPOP**	-1.52903	9.55E-06
FBXW9	-1.41303	5.03E-11	**LOC84989**	-1.46723	2.80E-06	**DPP3**	-1.52920	8.36E-28
SSBP4	-1.41321	1.28E-13	**CC2D1A**	-1.46781	3.68E-12	**WNT10A**	-1.52981	3.01E-09
MIR600HG	-1.41553	2.05E-08	**PITPNM3**	-1.46833	4.95E-03	**HAUS7**	-1.53040	2.09E-10
CCDC69	-1.41609	8.51E-06	**DTX4**	-1.46898	4.65E-13	**FPGS**	-1.53097	9.68E-09
GTF3C6	-1.41666	2.68E-05	**SPSB2**	-1.46900	7.68E-05	**POLE**	-1.53195	2.46E-24
LAMTOR2	-1.41698	4.60E-08	**PCYOX1**	-1.47071	2.24E-09	**HSD17B4**	-1.53229	2.41E-10
CDK5	-1.41735	5.93E-07	**NDUFA3**	-1.47080	3.00E-26	**PCYT2**	-1.53304	2.62E-08
FAM173B	-1.41829	2.10E-13	**VANGL1**	-1.47254	1.13E-20	**HYAL2**	-1.53399	3.58E-15
NUBP1	-1.41851	5.03E-12	**FGFR4**	-1.47274	4.25E-05	**FN3KRP**	-1.53416	3.95E-13
AKR7A2	-1.41941	1.34E-19	**ALKBH4**	-1.47296	1.03E-09	**HPRT1**	-1.53473	1.03E-09
HNRNPA2B1	-1.41968	2.69E-13	**PRSS27**	-1.47399	9.72E-04	**CTSC**	-1.53496	8.31E-09
MTHFD1	-1.41988	3.06E-19	**FAM89A**	-1.47529	4.97E-07	**PPM1H**	-1.53598	4.85E-11
SP5	-1.42065	8.57E-04	**PTDSS1**	-1.47674	2.04E-09	**HIST1H3I**	-1.53710	3.28E-06
HNRNPUL1	-1.42084	1.87E-28	**PRMT6**	-1.47887	1.33E-14	**PFN2**	-1.53948	2.98E-11
RPS6KA2	-1.42193	1.80E-02	**HMMR**	-1.47902	9.21E-06	**MIS18A**	-1.54276	1.41E-29
MRPL12	-1.42223	6.74E-11	**FZD2**	-1.48147	4.19E-10	**CAT**	-1.54386	3.77E-08
SLC2A13	-1.42313	5.02E-04	**S100A4**	-1.48161	2.73E-02	**PPT2**	-1.54412	2.44E-20
CARKD	-1.42325	7.54E-16	**TRMT2A**	-1.48214	1.40E-22	**EPS8L2**	-1.54541	2.56E-09
DDX54	-1.42376	1.52E-21	**RAB3A**	-1.48248	2.51E-04	**AK3**	-1.54642	2.80E-10
RABL6	-1.42394	2.67E-12	**ASAP3**	-1.48248	3.89E-03	**BAIAP2-AS1**	-1.54680	2.76E-03
KRT14	-1.42462	3.46E-02	**FAM78A**	-1.48344	1.94E-06	**COL9A2**	-1.54863	1.39E-05
TRADD	-1.42580	7.46E-04	**UTP20**	-1.48359	1.42E-06	**TMX1**	-1.55038	5.69E-16
LOC100507299	-1.42680	1.88E-02	**ECH1**	-1.48412	1.92E-19	**MAP4K2**	-1.55059	6.11E-11
TUBA4A	-1.42720	2.47E-06	**NSUN5P1**	-1.48436	6.91E-16	**NFIA**	-1.55279	5.87E-08
C19orf66	-1.42784	1.38E-06	**ZNF576**	-1.48443	3.20E-12	**ENG**	-1.55354	2.78E-13
C19orf60	-1.42855	9.40E-04	**TRIB2**	-1.48473	3.65E-03	**C15orf38**	-1.55359	3.75E-15
FAM171B	-1.42927	3.05E-18	**FLJ33630**	-1.48746	1.47E-02	**SLC2A4RG**	-1.55636	1.65E-11
CROT	-1.42941	3.79E-03	**HDAC10**	-1.48838	8.97E-11	**GADD45G**	-1.55702	1.15E-03
GEMIN4	-1.43023	1.67E-11	**PPCS**	-1.48881	4.10E-22	**ZNF189**	-1.55770	1.86E-02
SHPK	-1.43023	2.47E-11	**PHRF1**	-1.48884	4.58E-08	**ADPRH**	-1.56047	2.00E-02
HTATIP2	-1.43075	4.39E-23	**HDAC11**	-1.49043	1.23E-07	**WDR6**	-1.56056	1.04E-12
ERMAP	-1.43102	1.52E-03	**CPVL**	-1.49117	1.59E-02	**GSTK1**	-1.56104	2.19E-13
NOL12	-1.43135	5.18E-10	**CDK5RAP1**	-1.49130	8.05E-06	**CKAP4**	-1.56163	1.24E-11
TYSND1	-1.43261	1.54E-09	**PCTP**	-1.49152	2.64E-03	**SUCLG2**	-1.56187	8.80E-11
SHCBP1	-1.43428	1.94E-08	**SPEF1**	-1.49164	4.66E-02	**COMMD4**	-1.56238	6.17E-38
PSMA6	-1.43492	1.55E-30	**ACAA1**	-1.49267	1.78E-14	**ALAD**	-1.56413	1.29E-09

RHOBTB2	-1.56422	1.94E-09	**HSD17B11**	-1.62340	4.36E-22	**SLC7A2**	-1.68404	3.67E-04
STUB1	-1.56499	9.20E-19	**ELMO3**	-1.62392	9.70E-10	**FAM64A**	-1.68648	3.09E-14
C8orf82	-1.56558	1.18E-09	**THBS3**	-1.62453	1.69E-02	**RBPMS2**	-1.68772	2.33E-02
USP5	-1.56607	1.66E-16	**PSMD4**	-1.62518	2.08E-21	**ACAD9**	-1.68831	2.04E-21
PDP2	-1.56722	1.56E-06	**CYP8B1**	-1.62579	4.97E-04	**FUZ**	-1.69185	1.25E-07
MCM4	-1.56817	1.98E-42	**AIFM2**	-1.62787	1.63E-09	**TSPAN13**	-1.69216	9.14E-15
HSPE1	-1.56860	6.22E-12	**DSPP**	-1.62958	4.82E-02	**HOOK1**	-1.69241	9.73E-10
CIB2	-1.56869	2.45E-09	**SNED1**	-1.63007	2.03E-03	**L3MBTL2**	-1.69254	3.97E-11
ZAK	-1.56977	1.02E-11	**MMACHC**	-1.63058	1.34E-10	**LPCAT3**	-1.69473	3.09E-15
BRI3BP	-1.57043	2.22E-12	**DHRS1**	-1.63067	4.44E-13	**MRPL4**	-1.69503	6.91E-12
SLC25A1	-1.57135	1.50E-14	**INCA1**	-1.63219	2.86E-04	**CRTAP**	-1.69613	2.15E-16
ZNF503	-1.57314	1.24E-13	**ERCC6L**	-1.63250	5.56E-13	**DEPDC4**	-1.69806	9.36E-05
PPM1L	-1.57328	2.79E-06	**ARHGEF26**	-1.63309	1.97E-07	**PCDHA11**	-1.69998	2.03E-03
USB1	-1.57341	5.77E-15	**PAQR4**	-1.63417	3.39E-12	**MYL9**	-1.70067	1.03E-02
SALL4	-1.57435	1.48E-02	**WDR85**	-1.63453	3.06E-05	**C12orf43**	-1.70071	1.50E-13
MAD1L1	-1.57503	8.81E-40	**B3GALTL**	-1.63705	1.45E-10	**LRRC20**	-1.70289	2.91E-02
LINC00518	-1.57613	2.26E-02	**ALG10B**	-1.63880	5.12E-14	**ODF2**	-1.70465	1.09E-11
COMMD9	-1.57735	7.09E-07	**PLCG1**	-1.63939	1.92E-20	**PCDHGA12**	-1.70477	4.25E-07
GTPBP6	-1.57782	9.35E-24	**PNPO**	-1.64046	3.48E-10	**COL18A1**	-1.70487	3.37E-11
HSP90AA1	-1.57833	9.81E-24	**CBR1**	-1.64067	3.27E-15	**SPC24**	-1.70504	1.05E-18
APOBEC3F	-1.57837	4.44E-08	**LOC344595**	-1.64272	8.14E-07	**UBAC1**	-1.70696	5.20E-19
AP1G2	-1.57843	3.48E-21	**OMP**	-1.64285	2.91E-02	**GJB5**	-1.70696	7.40E-09
IQSEC1	-1.57887	3.88E-04	**ISOC1**	-1.64421	4.57E-09	**ATP7B**	-1.71000	2.74E-02
FTX	-1.58022	1.93E-11	**EPHX1**	-1.64431	3.01E-11	**ATAD3A**	-1.71009	1.83E-12
EME1	-1.58126	8.30E-08	**ALDH5A1**	-1.64505	4.19E-11	**APBA1**	-1.71075	1.15E-02
NHP2	-1.58164	4.66E-11	**TSPAN1**	-1.64633	7.46E-03	**APOBEC3C**	-1.71079	6.69E-08
ENGASE	-1.58189	1.71E-12	**GAS6**	-1.64782	2.24E-08	**ABHD16B**	-1.71166	3.13E-04
DGCR6L	-1.58363	1.99E-26	**LOC100289230**	-1.64784	1.51E-04	**UROD**	-1.71287	1.61E-37
METAP1D	-1.58424	8.11E-09	**C7orf31**	-1.64811	5.47E-03	**CCDC19**	-1.71310	1.70E-05
MSL3	-1.58436	2.47E-15	**LRPAP1**	-1.64898	1.77E-12	**CTBS**	-1.71575	2.91E-14
GLB1L2	-1.58465	9.84E-09	**AMT**	-1.64902	3.54E-02	**PLXND1**	-1.71629	4.27E-12
TELO2	-1.58471	3.87E-19	**GPR21**	-1.64909	1.84E-05	**SNAPC5**	-1.71742	9.36E-06
HIBCH	-1.58532	2.16E-10	**MRPL23**	-1.64926	1.57E-15	**CLTA**	-1.72004	8.28E-04
HIST1H2BB	-1.58571	6.61E-07	**DCXR**	-1.64937	4.07E-18	**GARNL3**	-1.72201	8.88E-05
PABPC4	-1.58726	2.36E-13	**DNAJA1**	-1.64948	3.96E-20	**DPP4**	-1.72206	7.94E-06
WIBG	-1.58815	1.27E-12	**KDM1A**	-1.65097	1.57E-21	**TNS1**	-1.72280	7.05E-04
EPHA1	-1.59132	2.56E-15	**LOC100133669**	-1.65181	2.68E-02	**SSSCA1**	-1.72294	3.54E-10
CRYL1	-1.59163	4.01E-05	**AP1S1**	-1.65195	2.15E-19	**ENPP1**	-1.72346	3.73E-02
HYLS1	-1.59298	4.53E-04	**PTPRU**	-1.65256	3.01E-12	**NFKBID**	-1.72444	9.44E-11
ZBED2	-1.59323	3.85E-02	**C8orf31**	-1.65301	1.23E-11	**ARL17A**	-1.72855	4.14E-22
SPAG5	-1.59639	1.11E-11	**STAT6**	-1.65332	3.36E-27	**ZNF32**	-1.73029	1.01E-04
LAMB1	-1.59786	1.35E-21	**LOC100287042**	-1.65364	6.58E-03	**KIAA0930**	-1.73057	1.05E-18
PPAP2B	-1.59840	2.99E-14	**CEP128**	-1.65445	9.07E-12	**PSMD1**	-1.73066	1.67E-31
CCDC14	-1.60015	6.40E-10	**ACO2**	-1.65446	1.77E-27	**HIST1H4H**	-1.73071	7.29E-18
CDH24	-1.60067	2.80E-08	**NAT6**	-1.65690	3.60E-02	**FECH**	-1.73322	2.45E-06
TMEM161A	-1.60184	4.12E-15	**MAPK15**	-1.65709	8.34E-13	**FOXO4**	-1.73324	1.13E-04
TRIM62	-1.60259	1.77E-08	**HS6ST1**	-1.65832	3.87E-22	**HPSE**	-1.73474	6.74E-03
MAP3K6	-1.60294	5.76E-25	**ERVK13-1**	-1.65890	8.67E-05	**LRP4**	-1.73531	5.43E-04
UNC5B	-1.60298	1.40E-04	**TESC**	-1.66201	2.36E-02	**ETFB**	-1.73574	1.01E-17
CPNE3	-1.60399	4.55E-14	**ARID5B**	-1.66255	2.44E-07	**HRCT1**	-1.74100	1.80E-02
MPPE1	-1.60498	2.67E-08	**LSM10**	-1.66319	2.40E-17	**STEAP3**	-1.74224	1.71E-25
CES2	-1.60504	2.91E-12	**B4GALNT1**	-1.66476	1.01E-09	**FHOD1**	-1.74282	3.59E-12
DUSP9	-1.60647	9.27E-03	**FANK1**	-1.66575	3.56E-05	**SPON2**	-1.74357	1.43E-06
ALDH1A3	-1.60650	1.58E-07	**ZC3HC1**	-1.66763	1.16E-18	**ERCC2**	-1.74419	1.20E-17
KDM8	-1.60677	4.06E-03	**CYB561**	-1.66772	3.53E-04	**KIFC2**	-1.74510	7.25E-11
CFD	-1.60715	1.73E-11	**NPEPL1**	-1.66802	2.35E-29	**MAGEA6**	-1.74706	1.74E-03
MRPS21	-1.60883	1.66E-07	**USPL1**	-1.66807	7.54E-13	**ATP9A**	-1.74945	2.06E-08
RTKN2	-1.61010	9.76E-11	**B3GALT4**	-1.66876	1.44E-04	**RAB26**	-1.75179	2.79E-04
HAUS1	-1.61050	7.94E-12	**MYO1C**	-1.66950	4.19E-28	**SSH3**	-1.75516	4.21E-08
FBXO4	-1.61057	3.33E-02	**SEMA3F**	-1.66986	1.96E-06	**SUOX**	-1.75516	7.05E-14
EEF2K	-1.61147	6.86E-20	**GPR161**	-1.66995	1.05E-02	**HIST2H2BE**	-1.75538	4.21E-13
CYBASC3	-1.61198	6.88E-12	**PCDHB3**	-1.67015	5.82E-04	**CYP24A1**	-1.75585	1.30E-10
ACOT7	-1.61223	3.54E-24	**ABHD14A**	-1.67122	4.46E-03	**USP13**	-1.75838	1.10E-15
EHMT2	-1.61275	5.62E-24	**TMEM53**	-1.67128	2.29E-06	**PCDHB8**	-1.75845	2.47E-02
NOP9	-1.61342	2.68E-22	**MON1A**	-1.67182	1.57E-10	**UHRF1**	-1.75899	1.80E-34
RPS26	-1.61361	3.95E-07	**WDR96**	-1.67232	3.66E-02	**SLC39A6**	-1.76024	9.51E-08
HMGB3	-1.61567	1.34E-19	**FCGRT**	-1.67394	1.06E-07	**NDUFAF3**	-1.76093	1.42E-21
C16orf59	-1.61577	7.80E-06	**PLOD1**	-1.67484	8.68E-15	**EPS8**	-1.76170	5.07E-08
RAB15	-1.61604	9.61E-09	**MICALL2**	-1.67538	2.45E-10	**TNFAIP8L1**	-1.76354	1.42E-05
TIMM8B	-1.61700	5.30E-21	**DFFB**	-1.67540	1.07E-16	**MGMT**	-1.76464	4.00E-13
RPP40	-1.61744	7.89E-08	**CLU**	-1.67661	3.20E-24	**LOC113230**	-1.76552	1.22E-02
MSX2	-1.61845	2.93E-17	**HIST1H3H**	-1.67935	1.01E-02	**MYO18A**	-1.76605	4.77E-12
ZBED3	-1.61977	7.83E-07	**ACCS**	-1.67979	9.14E-03	**ISOC2**	-1.76747	3.39E-12
RXRA	-1.62089	4.31E-14	**SUMO3**	-1.67982	2.34E-49	**POMGNT1**	-1.76767	2.31E-20
BEND3	-1.62110	1.74E-12	**MRPL52**	-1.68084	2.36E-19	**DPRXP4**	-1.76834	2.36E-02
LOC283070	-1.62113	1.37E-07	**CLCN2**	-1.68172	2.98E-10	**CHURC1**	-1.76846	2.05E-04
PYROXD2	-1.62114	8.28E-04	**PCDHA10**	-1.68297	3.34E-03	**D2HGDH**	-1.76934	1.93E-05
SRPX2	-1.62226	1.50E-02	**RARG**	-1.68402	1.40E-12	**FGFRL1**	-1.77147	3.63E-08

RNASET2	-1.77177	2.59E-11	**C11orf31**	-1.85649	1.80E-25	**DSCC1**	-1.96021	6.99E-15
UBE2Q2	-1.77226	1.62E-14	**MED12**	-1.85698	2.43E-32	**FRK**	-1.96119	5.33E-13
TAF9B	-1.77287	3.26E-14	**AURKA**	-1.85788	2.03E-16	**LINC00085**	-1.96231	4.40E-10
KIAA1737	-1.77561	4.59E-23	**SUSD2**	-1.85842	4.08E-05	**MCM5**	-1.96471	6.21E-27
B4GALT6	-1.77951	1.90E-17	**NEIL1**	-1.85861	6.84E-03	**KIAA0101**	-1.96646	1.80E-15
MYCBP	-1.78050	8.87E-14	**SCRN2**	-1.85971	5.33E-09	**ITPKB**	-1.96870	7.63E-17
CMTM7	-1.78150	6.73E-13	**KATNB1**	-1.86048	1.41E-08	**TRAP1**	-1.96954	1.63E-25
PSMA3	-1.78566	7.83E-20	**FABP5**	-1.86100	3.12E-10	**LOC100507266**	-1.96980	4.86E-02
MOV10	-1.78593	1.24E-32	**CHAF1B**	-1.86340	1.10E-25	**SWSAP1**	-1.97070	1.02E-11
TNFAIP8	-1.78607	2.98E-13	**ZNF414**	-1.86560	3.19E-13	**TCF7**	-1.97133	1.96E-02
ALG1L	-1.78616	1.58E-09	**RBFA**	-1.86761	1.87E-13	**C9orf116**	-1.97355	2.10E-10
CDK10	-1.78660	2.58E-13	**TM7SF2**	-1.86834	6.35E-10	**ATHL1**	-1.97467	1.80E-12
EXTL3	-1.78769	1.59E-11	**PVRL1**	-1.87166	1.11E-12	**SPC25**	-1.97843	2.78E-09
CRISPLD2	-1.78785	2.55E-12	**NUDT16**	-1.87286	5.18E-05	**SGK3**	-1.98106	2.87E-14
FAM102B	-1.78786	3.12E-12	**NUP155**	-1.87301	7.21E-40	**SMARCA2**	-1.98138	1.76E-09
TMEM160	-1.78790	8.82E-11	**SLC7A7**	-1.87681	1.23E-02	**SHMT1**	-1.98160	5.58E-11
PIR	-1.78793	1.69E-16	**HIST1H2AM**	-1.87946	3.53E-11	**HIST1H4B**	-1.98190	2.37E-14
MEX3A	-1.78971	1.05E-07	**TREX1**	-1.87966	4.85E-03	**GALT**	-1.98689	7.31E-16
PROCR	-1.78991	6.60E-08	**HIST1H2AG**	-1.88041	9.89E-06	**GPLD1**	-1.98695	1.69E-05
PXN-AS1	-1.79118	5.73E-05	**PDIK1L**	-1.88104	3.80E-14	**SULT1A1**	-1.98906	3.40E-02
KIF20A	-1.79269	1.41E-14	**PCSK9**	-1.88194	2.24E-02	**HSP90AB1**	-1.99164	2.61E-26
LINC00673	-1.79413	3.10E-05	**EMP2**	-1.88244	1.40E-11	**RNF144A**	-1.99170	3.02E-02
FARS2	-1.79423	4.18E-13	**NECAB3**	-1.88373	2.83E-10	**JAKMIP3**	-1.99256	5.53E-08
CDX2	-1.79464	5.91E-12	**ATAD3B**	-1.88543	1.06E-07	**MBOAT1**	-1.99442	4.45E-08
SRRT	-1.79494	4.06E-19	**PLLP**	-1.88603	2.85E-03	**BCAM**	-1.99494	6.51E-10
GLI3	-1.79673	5.08E-03	**PTGES**	-1.88709	1.91E-10	**SLC2A11**	-1.99576	1.29E-11
FAM109A	-1.79683	1.13E-03	**THYN1**	-1.88839	6.69E-08	**EFR3B**	-1.99695	4.42E-02
PTS	-1.79761	3.49E-15	**HAUS5**	-1.88939	1.50E-19	**SRM**	-1.99828	7.33E-23
ANGPTL7	-1.79894	2.57E-02	**FAM156A**	-1.89216	2.73E-02	**TFR2**	-1.99886	1.90E-08
CAMK2G	-1.80333	3.89E-13	**NDUFS5**	-1.89232	5.52E-45	**POP1**	-2.00091	1.82E-09
CRYZ	-1.80385	1.67E-15	**FAAH**	-1.89290	8.62E-04	**HIST1H2BG**	-2.00199	5.14E-18
CISD3	-1.80386	5.41E-30	**ZMYM3**	-1.89422	1.13E-10	**SARS2**	-2.00538	3.03E-15
QTRT1	-1.80424	3.34E-20	**VPS26B**	-1.89675	2.59E-22	**UROS**	-2.00663	1.64E-08
MUC20	-1.80458	9.94E-03	**PPDPF**	-1.89686	1.93E-09	**CEBPA-AS1**	-2.00664	1.46E-05
RAPGEF5	-1.80743	3.45E-04	**MAP3K7**	-1.89723	1.39E-21	**TSHZ2**	-2.00762	2.30E-02
DCAKD	-1.80802	4.55E-07	**RAB27B**	-1.90032	2.33E-04	**FERMT1**	-2.01007	4.70E-20
MAP3K8	-1.80951	8.70E-04	**IRX4**	-1.90263	2.70E-02	**MEIS2**	-2.01260	9.26E-21
SLC52A3	-1.80991	1.18E-11	**GXYLT2**	-1.90269	2.12E-03	**NME3**	-2.01340	3.95E-10
ECHDC2	-1.81041	2.00E-10	**SPG20**	-1.90415	1.80E-03	**KISS1R**	-2.01436	1.60E-02
PMVK	-1.81053	5.40E-09	**CKMT1B**	-1.90552	4.96E-16	**MAP6D1**	-2.01674	1.06E-06
LOC730101	-1.81134	1.10E-05	**CORO1A**	-1.91165	2.39E-08	**SYNM**	-2.01788	5.75E-06
OAZ2	-1.81209	8.48E-06	**NME4**	-1.91374	7.07E-17	**C10orf57**	-2.01831	3.07E-11
ARHGDIB	-1.81232	1.72E-33	**SLC19A1**	-1.91378	2.45E-10	**GATSL3**	-2.01915	1.13E-06
ZDHHC12	-1.81261	1.94E-12	**TRPV6**	-1.91504	6.07E-04	**HIST1H2AJ**	-2.01935	3.30E-11
MMP14	-1.81403	1.32E-08	**CD86**	-1.91631	2.11E-02	**MYCL1**	-2.02044	3.55E-05
HBA2	-1.81630	4.92E-02	**MRAS**	-1.91776	2.01E-05	**TTC31**	-2.02062	1.13E-38
ERMP1	-1.81755	3.90E-19	**RGS19**	-1.91862	7.10E-04	**ARHGAP18**	-2.02144	5.96E-19
PDIA4	-1.81787	1.51E-19	**ZNF385A**	-1.91967	3.65E-13	**CHST4**	-2.02374	4.77E-02
CNIH2	-1.82205	1.39E-12	**FASN**	-1.92053	1.29E-35	**POLE2**	-2.02491	5.49E-11
PMF1	-1.82312	4.77E-20	**AIF1L**	-1.92109	5.62E-10	**FAM222A**	-2.02519	1.68E-04
LZTS2	-1.82549	1.38E-19	**ISYNA1**	-1.92500	9.19E-16	**BMP4**	-2.02524	1.99E-13
CHST14	-1.82668	1.54E-13	**PECR**	-1.92646	2.71E-02	**ZFP36L2**	-2.02552	9.87E-55
LOC338799	-1.82692	1.21E-02	**LRRC28**	-1.92915	3.03E-15	**TYMS**	-2.02600	1.21E-18
FOXRED2	-1.82782	1.26E-23	**COA3**	-1.93072	7.45E-26	**PIF1**	-2.02608	7.63E-09
HIST2H2AB	-1.82798	7.62E-27	**HOOK2**	-1.93182	4.77E-22	**HIST1H2BN**	-2.03039	2.30E-17
FAM98B	-1.83025	6.10E-19	**ANKRD5**	-1.93339	1.31E-07	**XRCC1**	-2.03520	2.29E-49
NSMCE1	-1.83234	9.45E-23	**STRA13**	-1.93471	6.56E-26	**DCPS**	-2.03546	2.41E-13
ARHGAP28	-1.83277	9.01E-03	**IFT74**	-1.93515	1.92E-17	**H2AFX**	-2.03660	2.07E-15
CRABP2	-1.83652	5.35E-05	**FOXM1**	-1.93602	6.23E-35	**MPND**	-2.03949	1.84E-03
CHCHD10	-1.83946	5.61E-13	**BDH2**	-1.93633	4.72E-09	**CLCF1**	-2.03967	2.23E-16
RFC5	-1.84096	1.52E-10	**GAMT**	-1.93637	6.69E-04	**CEBPA**	-2.04287	1.79E-08
BTBD6	-1.84122	1.85E-15	**PPP5C**	-1.93821	2.82E-26	**LOC148696**	-2.04364	1.12E-03
TMCO6	-1.84205	2.87E-15	**LHX4**	-1.94019	6.69E-07	**FUT10**	-2.04428	5.77E-20
STK36	-1.84222	6.13E-12	**ZNF362**	-1.94079	5.71E-13	**ALDH3B1**	-2.04502	1.49E-04
GLB1L	-1.84332	9.33E-04	**CACNG4**	-1.94205	7.21E-05	**C8orf73**	-2.05091	7.76E-09
LRRC4	-1.84540	4.45E-02	**CUEDC2**	-1.94676	1.35E-04	**CROCC**	-2.05382	4.05E-06
CADM4	-1.84694	4.54E-12	**PIK3AP1**	-1.94748	2.05E-03	**MCIN**	-2.05600	5.97E-06
WWOX	-1.84699	7.36E-05	**SLC9A3R1**	-1.94766	2.43E-28	**AZI1**	-2.05653	2.52E-15
RAB43	-1.84943	2.35E-08	**CDC45**	-1.94811	6.02E-11	**BST2**	-2.05733	1.56E-06
CTSH	-1.84984	6.66E-11	**HIST1H2BO**	-1.94906	8.16E-04	**RTEL1**	-2.05795	4.11E-10
GYG2	-1.85064	3.07E-06	**METTL25**	-1.94909	3.78E-02	**SPINK5**	-2.05863	7.44E-08
POLR3K	-1.85082	1.15E-25	**SLC39A4**	-1.95370	2.92E-27	**SNCG**	-2.05977	1.34E-07
LPHN3	-1.85188	2.50E-04	**SKP2**	-1.95438	3.34E-30	**KIAA1211L**	-2.06098	2.50E-04
DAGLA	-1.85189	1.11E-07	**GBAP1**	-1.95462	8.66E-10	**GSTM3**	-2.06277	2.74E-04
CD99L2	-1.85327	1.80E-12	**MYBL2**	-1.95660	1.61E-23	**PASK**	-2.06322	5.16E-14
SPAG7	-1.85501	4.16E-22	**HIST1H2AH**	-1.95735	1.20E-17	**ADAM11**	-2.06380	2.13E-07
IKZF2	-1.85555	1.33E-06	**RAB11FIP4**	-1.95878	4.71E-18	**MPP1**	-2.06535	1.98E-07
DHTKD1	-1.85634	4.07E-09	**CTDSPL**	-1.95998	9.39E-18	**ADK**	-2.06582	8.24E-30

MAGEA2B	-2.06618	2.37E-02	**QPRT**	-2.21198	7.12E-14	**MYLIP**	-2.41079	1.56E-10
ROGDI	-2.06674	2.57E-09	**SAYSD1**	-2.21245	6.32E-16	**TRPM4**	-2.41137	1.16E-16
LOC100133315	-2.06733	4.56E-07	**MANSC1**	-2.21477	5.92E-12	**TMEM107**	-2.41347	8.64E-16
IFI6	-2.06739	1.93E-02	**CLEC7A**	-2.21814	4.05E-02	**HIST1H3G**	-2.41483	2.12E-08
SLC35C1	-2.06751	3.89E-18	**XPA**	-2.21902	3.23E-25	**WDR4**	-2.42151	4.07E-04
GPER	-2.06820	6.64E-10	**KRT8**	-2.21994	2.55E-35	**TTC22**	-2.42157	6.07E-10
CX3CL1	-2.07054	2.32E-02	**TPM3P9**	-2.22191	9.64E-24	**RBM45**	-2.42518	4.69E-19
BCL11A	-2.07333	8.12E-10	**HIST1H2AI**	-2.22342	6.60E-16	**HES2**	-2.43069	5.72E-06
FAM210B	-2.07360	1.58E-08	**CCDC171**	-2.22380	6.29E-03	**ABR**	-2.43143	4.67E-08
UBL7	-2.07467	5.82E-13	**C1QTNF6**	-2.22566	4.22E-10	**TROAP**	-2.43238	6.11E-27
CAB39L	-2.07619	1.35E-10	**HNRNPA3P1**	-2.22614	4.36E-04	**LOXL4**	-2.43487	3.74E-11
LOC100507547	-2.07725	3.73E-05	**CDK18**	-2.22835	7.18E-13	**SLC16A9**	-2.45205	1.92E-02
DUSP13	-2.07732	5.21E-03	**TOMM40L**	-2.23039	1.95E-22	**ITGA2B**	-2.45280	4.82E-05
NR1H3	-2.07833	8.94E-04	**FUT8-AS1**	-2.23370	3.74E-06	**U2AF1L4**	-2.45369	1.24E-02
PIN1	-2.08178	8.94E-33	**IL22RA1**	-2.23388	2.78E-03	**NIPSNAP3A**	-2.45592	7.37E-11
FOXQ1	-2.08211	1.57E-05	**PCDHB4**	-2.23600	1.09E-02	**GALM**	-2.45786	1.14E-11
MANEAL	-2.08382	2.21E-16	**CALCOCO2**	-2.23757	1.50E-03	**HIST1H3A**	-2.46033	9.59E-08
RIMBP3B	-2.08549	2.02E-02	**CPNE7**	-2.24016	1.73E-07	**RNF182**	-2.46320	6.11E-04
MNF1	-2.08587	1.93E-43	**FAM122B**	-2.24025	6.13E-33	**ADCK1**	-2.46376	3.72E-11
PCSK4	-2.08708	3.00E-02	**ANKMY2**	-2.24069	6.15E-40	**MXD3**	-2.47259	2.34E-12
OBSL1	-2.08809	2.17E-10	**OSBPL7**	-2.24663	3.34E-08	**NTHL1**	-2.47291	6.94E-09
ENOSF1	-2.09216	7.05E-24	**RPL3L**	-2.24902	1.95E-04	**FGFBP1**	-2.47994	3.86E-02
HNRNPA3	-2.09223	4.87E-19	**CPLX1**	-2.25040	1.10E-02	**SPTBN2**	-2.48055	2.25E-27
MOCOS	-2.10013	1.77E-06	**NIPSNAP1**	-2.25161	4.29E-12	**CD46**	-2.48192	3.84E-04
MEOX1	-2.10079	2.54E-04	**PLA2G4A**	-2.26677	4.75E-07	**KCNK5**	-2.48242	3.85E-08
HOXA11	-2.10115	3.00E-02	**FDXR**	-2.26793	1.46E-18	**ALDH3A2**	-2.48403	1.38E-03
GGCT	-2.10803	1.46E-39	**SHISA2**	-2.26901	2.07E-03	**MUC16**	-2.48414	5.18E-06
TMEM52B	-2.10933	1.19E-17	**GCAT**	-2.26964	3.06E-13	**ALDH7A1**	-2.48560	1.49E-38
KIF20B	-2.11312	6.80E-35	**HMBS**	-2.27597	1.04E-28	**LRRC10B**	-2.48838	1.08E-04
NSFL1C	-2.11348	7.30E-41	**PATZ1**	-2.28012	1.29E-17	**CLEC17A**	-2.49559	1.80E-02
RNF113B	-2.11485	2.44E-04	**FKBP4**	-2.28142	1.07E-30	**JMJD7**	-2.49570	3.24E-11
LOC283335	-2.11581	5.87E-03	**LMTK3**	-2.28154	2.95E-02	**G6PD**	-2.49657	1.27E-30
IFRD2	-2.11675	4.40E-21	**NKD1**	-2.28318	4.22E-12	**GINS2**	-2.50141	6.64E-24
STMN3	-2.12217	4.46E-12	**HIST2H3D**	-2.28321	7.21E-11	**NAALADL2**	-2.50165	8.85E-07
ZWINT	-2.12458	7.77E-29	**NDUFB10**	-2.28534	1.83E-20	**PEMT**	-2.50688	7.60E-35
TMEM117	-2.12498	2.49E-13	**IL17RE**	-2.29118	4.37E-11	**ENDOD1**	-2.51366	7.39E-17
CRELD2	-2.12780	1.08E-40	**GDPD3**	-2.29412	6.78E-09	**ZNRF3**	-2.51710	1.97E-31
TRIM45	-2.13127	5.03E-13	**EPHX2**	-2.29619	1.52E-02	**B3GNT1**	-2.52055	3.44E-10
PRR19	-2.13199	3.43E-04	**HIST1H2AB**	-2.29676	2.38E-14	**RASSF2**	-2.52162	4.88E-19
LIPE	-2.13303	1.76E-03	**CTTN**	-2.29887	6.68E-45	**LOC149086**	-2.52212	2.74E-02
PRODH	-2.13440	2.11E-07	**DYNC1I1**	-2.30187	7.97E-06	**COCH**	-2.52455	1.37E-06
RECQL4	-2.13596	7.71E-38	**ASIC1**	-2.30523	1.38E-09	**FIBCD1**	-2.52537	1.25E-07
FLJ13224	-2.13718	8.00E-03	**TRIM34**	-2.31206	3.73E-12	**STS**	-2.52817	2.88E-03
OSGEP	-2.13736	6.14E-23	**ANKRD39**	-2.32055	8.70E-16	**ACACB**	-2.53147	4.45E-04
WDR34	-2.14042	1.48E-34	**AKNAD1**	-2.32184	7.16E-03	**KLK7**	-2.53243	3.78E-05
PRSS12	-2.14101	2.08E-08	**TEAD2**	-2.32191	1.04E-05	**PCDHB2**	-2.53265	4.13E-24
SPR	-2.14415	3.77E-27	**TBC1D16**	-2.32236	4.84E-08	**GNGT1**	-2.53346	2.65E-02
LRRK1	-2.14748	2.49E-24	**STMN1**	-2.32950	3.98E-03	**DPYSL4**	-2.53794	6.14E-07
FUT2	-2.14922	9.06E-05	**ZSCAN4**	-2.33485	4.36E-02	**APOBEC3G**	-2.53849	4.41E-06
FUOM	-2.15006	3.79E-05	**VWA1**	-2.33750	9.98E-19	**RAD54L**	-2.53951	1.18E-17
PAFAH1B3	-2.15646	1.15E-34	**ALDH16A1**	-2.33839	7.37E-50	**SERHL2**	-2.54972	1.25E-07
TONSL	-2.15713	1.27E-34	**HEXIM1**	-2.33853	5.94E-30	**SIGLEC6**	-2.55227	1.58E-02
KREMEN1	-2.15751	3.38E-13	**NDRG2**	-2.34368	9.91E-15	**CDCA3**	-2.55385	2.32E-25
PROM2	-2.15769	3.17E-03	**EPN3**	-2.34561	1.88E-11	**DOK4**	-2.55450	2.28E-16
HSPH1	-2.15873	1.41E-40	**SFXN2**	-2.34620	1.51E-15	**SLC25A10**	-2.55593	1.80E-17
BANK1	-2.16268	1.55E-02	**FAM114A1**	-2.35148	1.15E-11	**KAT2A**	-2.56634	1.34E-28
GUSBP1	-2.16728	1.83E-02	**LEPREL2**	-2.35340	3.32E-15	**GPR162**	-2.56739	2.26E-02
RARRES3	-2.16737	6.40E-04	**RABEP2**	-2.35965	3.67E-16	**CRIP2**	-2.57233	7.92E-12
CHCHD5	-2.16975	2.26E-19	**OGFOD3**	-2.36059	1.74E-20	**HIST1H1D**	-2.57541	1.10E-07
SEPT6	-2.16984	3.48E-08	**NAGPA**	-2.36111	4.10E-13	**SMAD6**	-2.57771	1.78E-09
CHDH	-2.17471	9.30E-07	**SESTD1**	-2.36467	1.45E-03	**RIMS3**	-2.57846	1.88E-06
SLC22A18	-2.18190	1.62E-02	**HIST1H3J**	-2.36499	5.71E-13	**MYCN**	-2.58059	1.21E-05
ARRB1	-2.18204	3.33E-18	**CYP1B1**	-2.36772	1.92E-05	**EMID1**	-2.58135	6.15E-03
MUTYH	-2.18466	2.16E-05	**HIST1H2BI**	-2.37100	1.17E-14	**SLC4A11**	-2.58321	3.56E-09
FGFR3	-2.18969	6.65E-04	**ZNF784**	-2.37136	1.71E-03	**MBLAC1**	-2.58377	2.77E-02
MSRB1	-2.19149	2.55E-17	**UBXN8**	-2.37303	6.10E-04	**TNNC1**	-2.58633	7.87E-04
SOX4	-2.19494	1.47E-12	**UNG**	-2.37513	6.59E-25	**VASH1**	-2.58696	2.01E-03
OPA3	-2.19618	2.42E-04	**CERS4**	-2.37551	6.46E-06	**HCAR1**	-2.58975	1.15E-24
CISH	-2.19872	1.72E-06	**RARRES2**	-2.38141	3.31E-12	**LRRC8A**	-2.58998	4.48E-07
SLC7A4	-2.20081	3.18E-02	**PSD4**	-2.38802	5.26E-06	**MTHFD2L**	-2.59317	4.22E-06
UPK2	-2.20183	5.11E-04	**TNS4**	-2.39012	5.16E-04	**KREMEN2**	-2.59831	5.57E-12
CCDC159	-2.20312	5.10E-04	**ILDR1**	-2.39050	1.04E-02	**BMP7**	-2.59923	2.89E-43
PACSIN1	-2.20322	5.21E-03	**HIST1H2BF**	-2.39090	4.10E-13	**SERPINH1**	-2.60061	6.17E-56
PIDD	-2.20404	2.41E-18	**PPAP2C**	-2.40064	5.87E-11	**LIG1**	-2.60430	2.02E-08
LRRC45	-2.20529	2.89E-11	**MMP17**	-2.40089	1.36E-04	**GPD1L**	-2.60512	5.27E-13
REPIN1	-2.20650	1.77E-31	**GINS4**	-2.40227	2.30E-26	**SCAMP5**	-2.60604	6.70E-23
SH3TC2	-2.21006	1.95E-10	**B3GNTL1**	-2.40400	7.76E-08	**TMEM18**	-2.60701	4.95E-27
LEF1	-2.21116	3.47E-09	**PPIE**	-2.40801	2.04E-02	**HIST1H4L**	-2.60876	4.77E-22

HIST1H2BH	-2.61018	1.30E-21	**KRT6A**	-3.05478	4.24E-04	**KRT5**	-3.71243	2.18E-03
SRGAP3	-2.61999	4.74E-02	**NT5DC2**	-3.05687	4.92E-17	**FAM47E**	-3.72957	1.30E-02
NRGN	-2.62958	3.08E-03	**ST6GALNAC4**	-3.05687	2.52E-12	**AQP3**	-3.73162	2.47E-08
HIST1H2BL	-2.63133	1.51E-06	**PDE4D**	-3.05961	2.87E-05	**HIST1H4A**	-3.74851	1.80E-32
PAGR1	-2.63452	2.99E-34	**ID2**	-3.06219	1.11E-23	**PRSS36**	-3.76523	3.39E-02
P2RY2	-2.64907	7.54E-10	**GYLTL1B**	-3.06309	1.73E-30	**RASAL1**	-3.76867	1.73E-03
SYTL4	-2.65028	4.42E-10	**BCL2L15**	-3.06554	4.04E-03	**GJA5**	-3.78223	3.16E-12
SLC25A35	-2.65758	5.43E-09	**PRSS35**	-3.06737	2.34E-02	**MYOZ1**	-3.78349	2.00E-02
LMNB1	-2.65932	3.77E-39	**HMCN1**	-3.08251	3.30E-03	**CD52**	-3.80111	1.81E-02
EGFL8	-2.65944	2.05E-19	**FAM69B**	-3.10142	9.29E-06	**EFS**	-3.80575	2.79E-03
RAB40B	-2.66129	2.11E-05	**SELENBP1**	-3.10855	4.56E-02	**LOC145783**	-3.80787	4.66E-02
CSRNP3	-2.66747	2.06E-02	**DLGAP4**	-3.11552	3.70E-03	**GRIN1**	-3.80868	1.31E-02
SAMD15	-2.67381	4.45E-04	**LOC284751**	-3.11576	2.16E-02	**MATN2**	-3.81023	2.55E-21
HSPA2	-2.67405	4.23E-14	**HSD17B6**	-3.12074	2.89E-02	**ABCG1**	-3.81410	1.65E-02
PRKCDBP	-2.67744	2.02E-04	**NES**	-3.12074	1.71E-12	**ALPPL2**	-3.83836	1.00E-02
PGP	-2.69344	8.94E-21	**IVL**	-3.12666	2.24E-02	**TNFRSF13C**	-3.85079	2.56E-02
LOC283299	-2.69933	2.85E-07	**BLNK**	-3.13485	2.94E-12	**METTL7A**	-3.89038	5.69E-16
MAB21L2	-2.70106	2.47E-05	**IDH2**	-3.13939	2.06E-24	**PCDHGA4**	-3.92093	2.02E-02
GABRA3	-2.70302	1.89E-15	**SLC37A4**	-3.14872	7.34E-04	**ABCA1**	-3.93154	3.19E-02
CBR3	-2.70904	2.98E-05	**SPTB**	-3.15596	2.04E-02	**HOXA2**	-3.94716	9.92E-03
SECTM1	-2.71475	2.03E-17	**DNMT3B**	-3.16019	1.45E-10	**HOXA13**	-3.94780	3.44E-02
DLX3	-2.71810	1.67E-08	**EPHB6**	-3.16804	1.98E-04	**KIF2A**	-3.95058	7.83E-05
SELL	-2.72294	8.86E-03	**DOCK8**	-3.19971	8.44E-30	**ATP6V1B1**	-3.95412	3.23E-06
USH1G	-2.72535	7.99E-04	**GATS**	-3.20142	7.45E-04	**LOC401109**	-3.96621	2.84E-02
PYCARD	-2.72807	2.81E-10	**TNFSF10**	-3.20836	1.65E-02	**CRLF1**	-3.97257	9.47E-03
HIST1H2AK	-2.73241	1.55E-24	**NME2**	-3.22082	1.61E-02	**MGAT3**	-3.99795	1.82E-02
MIR205HG	-2.74804	5.60E-06	**ZNF703**	-3.22589	4.38E-35	**ACPP**	-4.00184	7.65E-12
IMPA2	-2.74900	3.28E-23	**PARM1**	-3.22985	4.27E-03	**MARC1**	-4.02281	2.53E-04
SPIN2B	-2.75055	9.41E-06	**CCL2**	-3.23167	1.49E-03	**PCDHGB2**	-4.02308	5.88E-03
SCARA3	-2.75296	2.17E-42	**C1orf186**	-3.23584	5.03E-03	**OASL**	-4.03935	1.05E-04
HADH	-2.75829	9.36E-42	**SLC6A4**	-3.25161	6.49E-04	**HIST1H1B**	-4.04346	1.52E-16
HIST1H2AL	-2.76554	2.37E-10	**KLHL31**	-3.25950	4.10E-02	**PKP1**	-4.06323	1.70E-02
C1orf53	-2.78338	3.22E-05	**DMBX1**	-3.26341	7.55E-08	**RASSF9**	-4.06766	8.21E-03
FBN3	-2.78406	2.01E-06	**COL9A3**	-3.27436	1.09E-18	**ECI2**	-4.07596	1.69E-02
FAH	-2.78558	9.53E-13	**SRSF2**	-3.27930	1.10E-33	**SPTSSB**	-4.07978	1.14E-03
ACTL10	-2.79794	1.97E-12	**LCN12**	-3.29562	3.52E-02	**COL4A5**	-4.10469	4.99E-02
DNAJC22	-2.79797	2.69E-02	**ANKRD65**	-3.30268	7.23E-06	**FOXN4**	-4.11081	2.20E-02
CAPN5	-2.79961	6.91E-07	**CKMT1A**	-3.32279	3.39E-05	**ALPP**	-4.14293	1.11E-07
PHF15	-2.80163	1.57E-08	**TNNT3**	-3.32607	5.73E-08	**NUDT8**	-4.15290	6.32E-03
TAGLN	-2.80221	4.10E-02	**SLC16A10**	-3.33283	1.90E-06	**IGF2BP1**	-4.17009	1.01E-02
HIST1H2BM	-2.82104	1.29E-18	**GMPR**	-3.34783	1.06E-02	**ID3**	-4.17860	4.53E-05
CYP3A5	-2.82116	9.77E-04	**CYP2W1**	-3.37927	3.33E-08	**MYO7A**	-4.17864	4.21E-15
LOC219347	-2.82911	9.39E-03	**EOMES**	-3.38210	2.85E-04	**LOC730102**	-4.19706	4.05E-03
ANXA9	-2.82982	3.49E-05	**JRK**	-3.39310	4.45E-02	**PALM3**	-4.22409	8.51E-09
NMU	-2.84050	5.18E-03	**SERPINF1**	-3.39575	4.77E-03	**PP14571**	-4.22574	3.06E-03
HIPK4	-2.84173	1.08E-03	**ROR2**	-3.40350	4.64E-02	**CSF2RB**	-4.22922	5.64E-04
FAM149A	-2.85261	1.07E-06	**CPZ**	-3.40362	1.55E-03	**KRT13**	-4.23203	1.09E-06
SPTLC3	-2.86584	3.69E-05	**SLC16A14**	-3.43400	7.05E-11	**SULT2B1**	-4.24376	1.28E-02
IQGAP2	-2.86652	4.62E-13	**ZNF618**	-3.46115	7.55E-23	**ADAM22**	-4.25333	6.79E-03
ABHD11	-2.87134	2.72E-22	**STOX2**	-3.46589	2.24E-03	**PRR15L**	-4.25783	3.42E-12
ACSM3	-2.88010	1.48E-04	**SUSD3**	-3.47291	1.33E-11	**REEP6**	-4.26206	6.85E-04
IGFL2	-2.88088	5.13E-08	**C19orf57**	-3.48222	1.24E-08	**FAM50B**	-4.27342	2.57E-03
CLIC3	-2.88264	8.60E-09	**GCHFR**	-3.48755	4.83E-02	**WNT11**	-4.30740	1.65E-10
CXXC1	-2.89867	1.64E-07	**IL17RB**	-3.49493	3.73E-13	**KRT3**	-4.30770	2.18E-02
CARD9	-2.90086	2.03E-15	**FOLR1**	-3.50321	2.60E-02	**HFE**	-4.31899	5.00E-22
HIST1H4I	-2.90784	2.33E-07	**HR**	-3.50448	7.17E-04	**NPNT**	-4.35475	1.74E-02
MNS1	-2.92585	2.19E-05	**PRR9**	-3.51357	4.29E-03	**PLEKHB1**	-4.37697	1.67E-04
DOC2A	-2.92923	3.32E-02	**PCDHA5**	-3.52611	1.64E-06	**HSPA8**	-4.38375	1.56E-69
FLJ30403	-2.92972	5.25E-03	**HPGD**	-3.54343	1.21E-08	**HSPB1**	-4.38467	8.97E-74
PSCA	-2.93199	6.61E-06	**ZNF488**	-3.54861	4.76E-14	**VMAC**	-4.42188	2.75E-03
AXIN2	-2.94478	3.95E-16	**TMEM150C**	-3.54940	8.60E-04	**ZSCAN10**	-4.46475	1.45E-02
NOTUM	-2.94801	5.37E-18	**NCF4**	-3.55893	1.05E-02	**PLA2G4F**	-4.47994	5.45E-08
ABCA4	-2.94969	3.23E-05	**KHK**	-3.56086	1.07E-11	**RHOBTB1**	-4.48255	3.07E-30
POLD1	-2.95695	1.97E-32	**SLC22A11**	-3.56551	1.09E-04	**LFNG**	-4.50189	3.05E-11
IGFL4	-2.97607	1.62E-26	**SOWAHA**	-3.57702	2.49E-02	**KRI1**	-4.50801	2.94E-03
LRRIQ3	-2.97826	8.54E-03	**LOC100131347**	-3.59254	4.90E-02	**LOC153684**	-4.50875	1.76E-03
HSPA1B	-2.98368	1.56E-27	**SYNC**	-3.59448	3.63E-02	**PCSK2**	-4.52989	5.41E-07
STAB1	-2.99712	3.41E-03	**WNT6**	-3.60162	4.16E-27	**THBS4**	-4.53570	3.31E-03
SNRNP25	-2.99976	8.17E-23	**ID1**	-3.60920	3.56E-09	**P2RY6**	-4.57799	8.41E-03
LOC100130275	-3.00478	7.36E-04	**SPP1**	-3.63039	1.20E-07	**FAM213A**	-4.58223	1.12E-03
SLC40A1	-3.00839	4.06E-06	**IQSEC2**	-3.63144	3.75E-04	**LSP1**	-4.60949	1.30E-02
GALNT12	-3.02216	4.01E-08	**MRVI1**	-3.63633	2.66E-02	**PRRT4**	-4.64186	3.91E-03
HIST2H2BC	-3.03061	8.10E-08	**NYNRIN**	-3.66407	3.50E-25	**BZRAP1-AS1**	-4.64340	1.29E-03
MGST2	-3.04139	1.48E-27	**C2CD4A**	-3.67104	2.77E-16	**ZBTB7C**	-4.66669	1.67E-19
RHPN1	-3.04171	2.49E-12	**TMSB4Y**	-3.68067	1.80E-02	**SIX1**	-4.71793	1.23E-03
LRP8	-3.04398	4.56E-38	**KRT71**	-3.68220	3.75E-02	**TNFRSF19**	-4.74565	3.07E-22
ITIH5	-3.04398	1.30E-06	**PBX1**	-3.70894	1.69E-18	**FREM2**	-4.79490	8.88E-04
PRSS23	-3.04788	1.01E-40	**ANK1**	-3.71213	3.22E-16	**SMTNL2**	-4.81239	5.79E-09

VTCN1	-4.83008	1.11E-07	**APCDD1**	-5.08289	2.07E-17	**VSNL1**	-5.88024	5.77E-05
PCDHA2	-4.84222	9.15E-03	**OVCH2**	-5.19953	2.64E-04	**LOC100506810**	-5.90929	5.00E-05
MAP2K6	-4.85016	3.22E-06	**EDNRB**	-5.20729	5.46E-06	**ALDH3B2**	-6.23157	3.22E-05
SIGLEC5	-4.87445	2.66E-04	**NTS**	-5.37467	2.08E-04	**BCAS1**	-6.39098	8.05E-06
GLRA3	-4.89604	8.60E-04	**PCDHGB1**	-5.49498	2.29E-04	**ARHGEF35**	-6.48643	6.09E-07
BTBD11	-4.96618	4.25E-03	**GABRP**	-5.55762	3.11E-04	**SGK2**	-6.59338	5.14E-25
PCDHA4	-5.01443	5.50E-07	**HNMT**	-5.71465	7.82E-05	**EDAR**	-7.98747	3.82E-09
MANSC4	-5.02914	2.46E-03	**LHX1**	-5.74348	2.21E-04	**CSNK1G1**	-10.16950	2.15E-16
SPARC	-5.07163	2.01E-03						

Supplementary Table 4. Cell cycle-related gene expression in MKN74 cells challenged with *H. pylori* OMVs or with *H. pylori*, when compared to the control cells. The Table displays fold changes and adjusted *p* values of the expressed genes.

	OMVs			*H. pylori*		
Gene ID	**log_2-FC**	**lfcSE**	***p*adj**	**log_2-FC**	**lfcSE**	***p*adj**
ABL1	-0.123	0.145	0.556	0.685	0.168	0.000
ANAPC1	-0.393	0.132	0.011	-0.181	0.155	0.338
ANAPC10	0.477	0.125	0.001	-0.057	0.152	0.778
ANAPC11	0.690	0.469	0.258	1.490	0.545	0.015
ANAPC13	0.826	0.178	0.000	1.176	0.206	0.000
ANAPC2	-0.077	0.198	0.805	-1.170	0.240	0.000
ANAPC4	-0.569	0.166	0.003	-1.148	0.209	0.000
ANAPC5	-0.362	0.106	0.003	-0.525	0.126	0.000
ANAPC7	-0.344	0.093	0.001	-0.081	0.110	0.561
ATR	-0.442	0.140	0.006	-0.191	0.168	0.353
BUB1	-0.758	0.145	0.000	0.823	0.167	0.000
BUB1B	-1.038	0.143	0.000	-0.586	0.166	0.001
BUB3	-0.393	0.124	0.006	0.686	0.143	0.000
CCNA2	-1.031	0.215	0.000	-1.136	0.251	0.000
CCNB1	-1.110	0.122	0.000	-1.371	0.144	0.000
CCNB2	-0.473	0.135	0.002	-0.636	0.157	0.000
CCND2	1.200	0.337	0.002	0.621	0.399	0.189
CCND3	-0.861	0.119	0.000	-0.905	0.140	0.000
CCNE1	-1.836	0.301	0.000	-1.070	0.363	0.008
CCNE2	-2.309	0.237	0.000	-1.093	0.280	0.000
CCNH	0.288	0.176	0.203	1.819	0.202	0.000
CDC14A	-0.363	0.192	0.131	1.113	0.221	0.000
CDC14B	-0.408	0.238	0.179	-1.061	0.319	0.003
CDC20	-1.099	0.180	0.000	-1.498	0.211	0.000
CDC23	-0.395	0.130	0.009	-0.255	0.155	0.163
CDC25A	-1.023	0.255	0.000	-0.968	0.307	0.004
CDC25B	-0.107	0.150	0.632	-1.337	0.178	0.000
CDC26	0.324	0.142	0.060	0.617	0.166	0.001
CDC27	-0.113	0.140	0.577	0.410	0.163	0.026
CDC45	-1.555	0.242	0.000	-1.948	0.283	0.000
CDC6	-0.975	0.171	0.000	-0.264	0.198	0.270
CDC7	-0.730	0.128	0.000	-0.386	0.151	0.023
CDK1	-0.664	0.133	0.000	0.537	0.154	0.002
CDK2	-0.381	0.143	0.025	-0.522	0.167	0.005
CDK6	0.412	0.155	0.025	1.683	0.179	0.000
CDK7	0.670	0.150	0.000	0.868	0.174	0.000
CDKN1A	1.881	0.129	0.000	2.504	0.149	0.000
CDKN1B	-0.389	0.156	0.037	-0.768	0.186	0.000
CDKN1C	0.419	0.280	0.248	1.467	0.323	0.000
CDKN2B	1.961	0.183	0.000	2.370	0.210	0.000
CDKN2C	-1.918	0.209	0.000	0.087	0.238	0.785
CDKN2D	-0.200	0.166	0.373	0.567	0.195	0.009
CHEK1	-0.190	0.194	0.484	-0.793	0.245	0.003
CHEK2	-0.488	0.222	0.071	-0.771	0.299	0.022
CREBBP	0.803	0.138	0.000	1.444	0.159	0.000
CUL1	-0.172	0.134	0.336	0.586	0.155	0.001
DBF4	-0.559	0.135	0.000	-0.574	0.161	0.001
E2F1	-1.405	0.220	0.000	-0.839	0.256	0.003
E2F2	-1.694	0.252	0.000	-0.482	0.297	0.169
E2F3	-0.380	0.150	0.034	0.662	0.174	0.000
E2F4	0.534	0.130	0.000	1.139	0.150	0.000
E2F5	0.206	0.179	0.398	0.902	0.208	0.000
ESPL1	-0.443	0.154	0.014	-0.465	0.180	0.022
GADD45A	2.709	0.366	0.000	3.105	0.423	0.000
GADD45B	1.233	0.147	0.000	2.630	0.168	0.000
GADD45G	-1.913	0.346	0.000	-1.557	0.437	0.001
GSK3B	0.586	0.120	0.000	1.289	0.139	0.000
HDAC1	-0.689	0.115	0.000	-1.195	0.136	0.000
MAD1L1	0.036	0.095	0.815	-1.575	0.116	0.000
MAD2L1	-1.091	0.167	0.000	-1.142	0.196	0.000
MCM2	-0.926	0.140	0.000	-0.663	0.167	0.000
MCM3	-0.898	0.136	0.000	-1.273	0.159	0.000
MCM4	-1.329	0.095	0.000	-1.568	0.112	0.000
MCM5	-1.629	0.150	0.000	-1.965	0.177	0.000
MCM6	-1.164	0.146	0.000	-1.210	0.170	0.000
MCM7	-0.590	0.187	0.006	-0.812	0.217	0.001
MDM2	-0.210	0.196	0.436	0.923	0.226	0.000
MYC	0.333	0.449	0.613	1.309	0.518	0.025

ORC1	-1.882	0.166	0.000	-1.514	0.203	0.000
ORC2	0.056	0.125	0.774	0.709	0.147	0.000
ORC3	-0.407	0.149	0.021	-1.208	0.189	0.000
ORC5	0.229	0.184	0.353	0.696	0.217	0.004
ORC6	-0.934	0.182	0.000	-0.327	0.212	0.193
PCNA	-1.116	0.180	0.000	-0.374	0.208	0.122
PKMYT1	-0.729	0.157	0.000	-1.312	0.193	0.000
PLK1	-0.717	0.151	0.000	-1.127	0.176	0.000
PRKDC	-0.245	0.146	0.190	-0.483	0.169	0.011
PTTG1	-0.774	0.186	0.000	-0.739	0.225	0.003
PTTG2	-2.052	0.758	0.022	-2.089	1.065	0.090
RAD21	-0.618	0.114	0.000	0.775	0.132	0.000
RB1	0.134	0.105	0.339	0.949	0.122	0.000
RBL1	-0.295	0.134	0.071	0.361	0.157	0.044
RBL2	-0.639	0.160	0.000	-0.512	0.191	0.017
RBX1	-0.485	0.147	0.004	-1.331	0.171	0.000
SKP2	-0.962	0.137	0.000	-1.954	0.166	0.000
SMAD2	0.052	0.104	0.750	0.554	0.123	0.000
SMAD3	-0.104	0.169	0.685	0.641	0.195	0.003
SMC1A	-0.435	0.098	0.000	-1.149	0.117	0.000
SMC3	-0.341	0.170	0.104	0.576	0.196	0.009
STAG1	-0.683	0.154	0.000	-1.077	0.191	0.000
TFDP1	-0.742	0.134	0.000	-0.885	0.157	0.000
TFDP2	-0.208	0.174	0.374	0.570	0.204	0.013
TGFB1	-0.498	0.124	0.000	1.117	0.143	0.000
TGFB2	0.342	0.534	0.669	2.076	0.588	0.001
TP53	0.467	0.127	0.001	0.343	0.148	0.041
TTK	-1.045	0.153	0.000	0.245	0.177	0.249
WEE1	-0.514	0.136	0.001	0.540	0.158	0.002
YWHAB	-0.377	0.135	0.017	0.585	0.156	0.001
YWHAE	-0.221	0.131	0.186	0.835	0.152	0.000
YWHAH	-0.184	0.146	0.347	0.510	0.169	0.007
YWHAQ	-0.071	0.112	0.674	0.598	0.130	0.000
YWHAZ	0.158	0.217	0.620	0.800	0.251	0.004
ZBTB17	0.547	0.119	0.000	0.537	0.139	0.000

Supplementary Table 5. DNA repair-related gene expression in MKN74 cells challenged with *H. pylori* OMVs or with *H. pylori*, when compared to the control cells. The Table displays fold changes and adjusted *p* values of the expressed genes.

	OMVs			*H. pylori*		
Gene ID	**log_2-FC**	**lfcSE**	***p*adj**	**log_2-FC**	**lfcSE**	***p*adj**
APEX1	0.413	0.125	0.004	-1.496	0.148	0.000
ATR	-0.442	0.140	0.006	-0.191	0.168	0.353
BABAM1	-0.343	0.126	0.021	-0.634	0.149	0.000
BARD1	-0.503	0.162	0.007	-0.759	0.194	0.000
BLM	-1.039	0.179	0.000	-0.489	0.210	0.041
BRCA1	-0.614	0.118	0.000	-0.872	0.147	0.000
BRCA2	-0.258	0.182	0.280	0.647	0.212	0.006
BRIP1	-1.690	0.190	0.000	-1.150	0.241	0.000
EME1	-0.580	0.198	0.012	-1.581	0.278	0.000
EXO1	-1.167	0.265	0.000	0.032	0.308	0.942
FEN1	-0.832	0.133	0.000	-0.854	0.155	0.000
HMGB1	-0.445	0.147	0.010	-0.466	0.170	0.015
LIG1	-2.004	0.377	0.000	-2.604	0.439	0.000
LIG3	-0.002	0.131	0.994	-0.727	0.160	0.000
MBD4	-0.379	0.131	0.014	-0.235	0.157	0.210
MLH1	0.080	0.174	0.768	-0.598	0.217	0.014
MLH3	0.679	0.135	0.000	0.298	0.165	0.121
MPG	0.125	0.169	0.614	-0.617	0.200	0.005
MSH2	-1.034	0.115	0.000	-0.661	0.135	0.000
MSH6	-1.054	0.091	0.000	-0.958	0.109	0.000
MUTYH	0.703	0.279	0.035	-2.185	0.478	0.000
NBN	-0.458	0.132	0.002	-1.041	0.156	0.000
NEIL1	-0.017	0.407	0.982	-1.859	0.618	0.007
NEIL3	-0.971	0.180	0.000	-0.614	0.216	0.011
NTHL1	-1.101	0.300	0.001	-2.473	0.404	0.000
OGG1	0.342	0.183	0.135	-0.602	0.223	0.016
PARP1	-1.102	0.177	0.000	-1.502	0.206	0.000
PARP2	-0.672	0.144	0.000	-0.838	0.177	0.000
PARP3	0.613	0.221	0.018	0.295	0.275	0.384
PARP4	-0.091	0.091	0.475	0.293	0.109	0.016
PCNA	-1.116	0.180	0.000	-0.374	0.208	0.122
PMS2	0.306	0.146	0.088	-0.766	0.178	0.000
POLD1	-1.312	0.200	0.000	-2.957	0.242	0.000
POLD2	-0.358	0.143	0.036	-1.173	0.166	0.000
POLD3	-0.488	0.117	0.000	-0.687	0.143	0.000
POLD4	0.999	0.202	0.000	0.966	0.237	0.000
POLE	-1.191	0.120	0.000	-1.532	0.145	0.000
POLE2	-1.595	0.229	0.000	-2.025	0.294	0.000
POLE3	-0.120	0.175	0.646	-0.500	0.203	0.029
POLL	1.099	0.159	0.000	0.610	0.196	0.005
RAD50	0.549	0.129	0.000	1.471	0.149	0.000
RAD51C	-0.034	0.167	0.906	0.827	0.194	0.000
RAD52	0.514	0.195	0.026	-0.157	0.250	0.625
RAD54B	-1.253	0.115	0.000	0.337	0.132	0.024
RAD54L	-1.798	0.228	0.000	-2.540	0.285	0.000
RFC1	-0.568	0.136	0.000	-0.183	0.158	0.345
RFC2	-0.468	0.141	0.004	-0.904	0.170	0.000
RFC3	-1.461	0.179	0.000	-0.327	0.208	0.184
RFC4	-0.519	0.126	0.000	-1.299	0.157	0.000
RFC5	-1.336	0.221	0.000	-1.841	0.273	0.000
RPA1	-0.906	0.130	0.000	-0.762	0.151	0.000
RPA2	-0.487	0.159	0.009	-0.723	0.189	0.000
RPA4	0.273	0.597	0.769	1.534	0.682	0.049
SMUG1	-0.006	0.175	0.985	-0.685	0.214	0.004
SSBP1	0.424	0.172	0.040	0.048	0.200	0.861
TDG	-0.199	0.176	0.408	0.686	0.204	0.002
TOP3B	0.094	0.262	0.823	-0.879	0.359	0.031
TOPBP1	-0.769	0.135	0.000	-0.168	0.158	0.389
UIMC1	0.600	0.157	0.001	-0.022	0.194	0.937
UNG	-1.596	0.186	0.000	-2.375	0.223	0.000
XRCC1	-0.325	0.106	0.008	-2.035	0.134	0.000
XRCC3	-0.478	0.164	0.013	0.059	0.193	0.822